Fate maps and gene expression in normal and abnormal facial primordia of chick embryos

Imelda Mary McGonnell

A thesis submitted for the degree of

Doctor of Philosophy

in the

Faculty of Life Science

Department of Anatomy and Developmental Biology

University College London

February 1998

ProQuest Number: U643717

All rights reserved

INFORMATION TO ALL USERS
The quality of this reproduction is dependent upon the quality of the copy submitted.

In the unlikely event that the author did not send a complete manuscript
and there are missing pages, these will be noted. Also, if material had to be removed,
a note will indicate the deletion.

To my parents

Abstract

This thesis investigates the cellular and molecular basis of shaping of facial primordia during normal and abnormal primary palate formation in chick embryos. DiI fate maps of facial primordia indicate that local differences in expansion between cell populations and directed expansion of cell populations shape the face and mediate outgrowth. Examination of patterns of cell proliferation, cell death and cell intercalation showed that these cell activities make important contributions to expansion. Application of retinoic acid to chick embryos results in primary palate clefting. Fate maps showed this is due to decreased expansion and proliferation in cell populations contributing directly to primary palate formation. However, other cell populations in the upper face expanded more uniformly, apparently due to loss of tension normally created by primary palate formation. Thus changes in behaviour in a few cell populations lead to global changes in facial shape.

Cellular behaviour is coordinated by signalling molecules. Connexins 43 and 32, gap junction proteins mediating cell-cell signalling, were found to be expressed in regions of greatest mesenchymal expansion in the face. Retinoic acid treatment reduces expression of connexin 43 in cell populations forming the primary palate. Application of connexin 43 antisense oligodeoxynucleotides to the chick face results in facial clefting. Signalling via epithelial-mesenchymal interactions are also necessary for shaping. Removal of ectoderm from maxillary primordia *in ovo* resulted in reduced outgrowth. FGF, an ectodermal signal, rescues outgrowth, but does not maintain mesenchymal *Msx-1* expression. BMP, another ectodermal signal, does not increase outgrowth but maintains *Msx-1* expression. *Eph4A*, expressed in overlapping domains with *Msx-1* in the face, is also dependent on an ectodermal signal, FGF, for maintained expression. These results are consistent with the idea that cell signalling via gap junctions and between epithelium and mesenchyme control cell behaviour that lead to primary palate formation.

Acknowledgements

I would like to thank my supervisor Prof Cheryll Tickle for her excellent tuition, support, constant enthusiasm for my project and for always having an open door. I would also like to thank her for critical reading of this thesis and having the remarkable ability to return comments the next day. Without this, it would have taken me much longer!

I would also like to thank my "Glaxo supervisor" Dr. Derek Newall, not only for his guidance throughout this project but also during my undergraduate degree and for introducing me to embryology in the first place. I am also grateful for the financial support provided by Glaxo-Wellcome Research and Development.

I would like to extend my gratitude to Drs. Jon Clarke, David Becker and Ketan Patel for collaborations that led to work in chapters 3, 4 and 5 respectively. I am also grateful to Drs. Jon Clarke and David Becker for critical reading of chapters 3 and 4 respectively.

I am grateful to many members of the lab and department, past and present, for intellectual discussion, technical advice and moral support. They are too numerous to name but include Anne Sheasby, for showing me how to do most things, Mark Turmaine for SEM tuition, Paris Ataliotis for showing me how to "do molecular biology" and for putting up with yet another PhD student writing up in the departure lounge. In particular I am grateful to Neil Vargesson and Lynda Erskine for moral support and being true friends.

I would like to thank my family for their encouragement and love. In particular I would like to thank my parents for instilling in me the value of education. Finally I would like to thank my husband Duncan for putting up with me while writing this thesis, for helping me print it out and most of all for believing in me.

Contents

8

List of figures

List of tables and graphs

Abbreviations

A	Anterior
A-P	Anteroposterior
AER	Apical ectodermal ridge
BMP	Bone Morphogenetic Protein
BrdU	Bromodeoxyuridine
Cek-8	Chick embryo kinase - 8
CHAPS	3-((3-cholamidopropryl)-dimethyl-ammonio)-1-propane sulphonate
Cx	Connexin
D	Distal
DiI	1,1 dioctadecyl-3,3,3',3'-tetramethylindo-carbocyanine perchloride
Eph4A	Eph tyrosine kinase receptor 4A
FGF	Fibroblast growth factor
FGFR	Fibroblast growth factor receptor
FNM	Frontonasal mass
L	Lateral
LNP	Lateral nasal process
M	Medial
M-L	Mediolateral
Mn	Mandibular primordium
Msx-1	Mucle segmentation homeobox-class homeobox gene
Mx	Maxillary primordium
NP	Nasal pit

17

ODNs	Oligodeoxynucleotides
P-D	Proximodistal
PBS	Phosphate buffered saline
PBT	Phosphate buffered saline + Triton X-100
PFA	Paraformaldehyde
Po	Posterior
Pr	Proximal
RA	Retinoic acid
RAR	Retinoic acid receptor
SEM	Scanning electron microscopy
TUNEL	Terminal transferase nick end labelling

Chapter One - General Introduction

The question of how a complex system such as the head develops has been the focus much research. This is not only due to its complexity but also because of the large number of abnormalities and teratologies seen in the craniofacial system. The avian embryo has proved particularly useful for studying the development of the head and has allowed many key questions to be answered, such as how and where do the tissues of the head arise? It is the aim of this introduction to indicate how some of these questions have been answered and to highlight some that remain unanswered.

1.1 The origins of the head and facial primordia - neural crest and non-neural crest derived structures.

The vertebrate head consists of diverse interacting tissues with two main developmental origins, neural crest derived and mesoderm derived. Cranial neural crest is ectodermal in origin. It has been shown in chick embryos that neural crest arises from an inductive interaction between presumptive dorsal ectoderm and dorsal neural plate (Bronner-Fraser 1995). At very early stages of development, the neural tube is straight and unsegmented. Between stages 8 and 10 in chick embryos (Hamburger and Hamilton 1951), three segments arise rostrally to caudally (head to tail). The prosencephalon (forebrain) is situated most rostrally followed by the mesencephalon (midbrain), with the rhombencephalon (hindbrain) situated most caudally. Further segmentation divides the prosencephalon into telencephalon and diencephalon and the rhombencephalon into metencephalon and mylencephalon. At the time of dorsal neural tube closure, approximately stages 8 to 9 in the chick, the crest cell populations begin to migrate subectodermally, in a ventral direction (Johnston, 1966, Noden, 1975). Migration starts at the mesencephalic region in the chick embryo at stage 9-, where the neural tube begins fusing, and then occurs caudally and rostrally (Noden 1975). However, no migratory

crest arises from the telencephalic region of the neural tube (Johnston 1966, Noden 1975) and very small amounts from the regions of the rhombencephalon corresponding to rhombomeres 3 and 5 (Lumsden et. al., 1991, Sechrist et. al., 1992, Birgbauer et. al., 1995). In the mammalian embryo, neural crest migration occurs at a time when the neural tube is open, therefore it does not begin at the point of neural tube fusion. Migration begins in the mesencephalic (midbrain) region closely followed by the rostral then caudal rhombencephalic crest (Tan and Morris-Kay 1985). Thus there are some subtle differences in early avian and mammalian head development.

Neural crest cell populations migrate in streams, following distinct pathways (Noden 1975). There is no mixing between streams. Pathways of migration and the sites in which cranial neural crest cells localise have been the subject of much investigation for some time using labelling techniques such as ^{3}H-thymidine and DiI. It has been shown that pathways of migration are not random and are in fact region specific. The routes differ with axial level of origin of the crest populations and this is influenced by the environment they migrate through (Johnston 1966, Noden 1975). However, these labels become diluted with successive cell division and fate can only be followed for a few days. The differentiated fates of neural crest populations have been investigated, through more permanent markers. Chick/quail chimeras have been extensively used as quail cells have a large nucleolus with associated heterochromatin which can readily be identified by Feulgen reagent. This heterochromatin is not present in the chick nucleolus (Le Douarin, 1973). More recently, monoclonal antibodies to quail cells have become available (Pardanaud et. al., 1987). Studies using these chimeras have shown that once the neural crest cells have reached their target site they differentiate into a variety of tissues. The majority of the skeletal elements of the head and face are neural crest in origin. This includes the frontal and parietal bones of the skull vault which were previously thought to be of mesodermal origin (Couly et. al., 1993, Le Douarin et. al., 1993). Other tissues formed by the neural crest include cartilage, dermis, tendons, skeletomuscular connections, connective tissue, pigment cells, sensory and autonomic nerves and Schwann cells (Le Lièvre and Le Douarin 1975, Noden 1978b, Noden 1983a, Couly et. al., 1992, Köntges and Lumsden 1996).

It had been thought that migratory cranial neural crest is initially pluripotent and that the environment encountered during migration and after settling of the cells dictates the tissues that the cells form (Noden 1978a, b). These experiments involved grafting quail derived forebrain and hindbrain cranial neural crest into orthotopic and heterotopic regions of presumptive cranial neural crest of chick embryos. Both sets of experiments resulted in normal embryos, with no misplacement of head structures or abnormal differentiation of tissues (Noden 1978a). Pluripotency has also been demonstrated by clonal analysis of pre-migratory cephalic neural crest populations (Baroffio *et. al.,* 1991). The homogeneity of premigratory and subsequent heterogeneity of migrating cranial crest i.e. division into subpopulations, has also been demonstrated by antibody labelling. For example, Heath *et. al.,* (1992) showed that in stage 8-9 quail embryos, individual cranial neural crest populations were initially homogenous, although there were differences between populations, and that subpopulations appeared very early in crest migration. However other experiments appear to contradict these findings, indicating that there may be some prepatterning of cranial neural crest cell populations. For example, experiments in which stage 9+ mesencephalic neural crest was transplanted to myencephalic regions resulted in ectopic beak structures and auditory meatus forming in the neck region (Noden 1983b) suggesting some prepatterning.

Non - neural crest derived tissues in the chick head include muscles which have been shown, by chick/quail chimeras to be derived from mesoderm lateral to the neural tube (Noden 1983a b, Couly *et. al.,* 1992) and endothelial cells which are derived from paraxial head mesoderm (Noden 1988). Mesodermal cells also contribute, with the neural crest, to the orbitosphenoid and corpus sphenoidalis bones and the otic capsule (Couly *et. al.,* 1992).

1.2 Development of facial primordia

Once neural crest migration has finished, at approximately stage 12 in chick embryos, the facial primordia begin to appear. The first branchial arch becomes visible at stage 14 (Hamburger and Hamilton 1951) followed by the nasal placode, a region of thickened epithelium overlying the forebrain between stages 15 and 16 (Yee and Abbott 1978). The

first branchial arch splits at stage 18, the anterior portion forming the maxillary primordium and the posterior portion the mandibular primordium (Yee and Abbott 1978). By stage 20 the primordia which form the basic pattern of the face are clearly defined and are arranged symmetrically around the stomodeal (oral) cavity. The frontonasal mass (which is not thought of as a pair of primordia in the chick embryo, but is in mammalian embryos) and lateral nasal process lie above the oral cavity and are separated by the nasal pits. Lateral to the oral cavity, on each side, lie the maxillary primordia, which are joined to the lateral nasal processes in the region of the presumptive lacrimal groove. Beneath lie the paired mandibular primordium. Each consists of a bud of undifferentiated mesenchyme surrounded by epithelia. (see Fig. 1.1a)

1.3 Cranial neural crest populations in facial primordia

Each facial primordium is populated by a specific set of cranial neural crest populations. The mesenchyme of the chick frontonasal mass is mainly derived from neural crest cells originating at the posterior prosencephalic level, which migrate rostrally then laterally. Some contribution is also thought to be made by crest cells from the anterior mesencephalon, although the exact location of this population in the frontonasal mass is not clear (Le Lièvre 1978, Noden 1978a, Couly and Le Douarin 1985). These crest populations also contribute to frontonasal mass primordia in mammalian embryos (Osumi-Yamashita et. al., 1994). The chick lateral nasal process consists of crest cells arising from both the prosencephalic and mesencephalic regions of the neural tube (Le Lièvre 1978) although it is not clear if these populations remain separate. There also appears to be two cranial neural crest populations in the maxillary primordium. The most rostral (anterior) region consists prosencephalic and mesencephalic crest while only mesencephalic crest migrates into the caudal regions of this primordium (Le Lièvre 1978, Lumsden et. al., 1991). In the mandibular primordium, studies suggest that tissues are derived from posterior mesencephalic and metencephalic (rhombencephalic) neural crest (Le Douarin and Le Lièvre 1975, Noden 1978). DiI labelling studies indicate that crest cells of mesencephalic and rhombomeric regions (specifically at the level of rhombomere 1) migrate into the rostral mandibular primordium while crest cells from the level of

rhombomere 2 populate the caudal mandibular primordia (Lumsden *et. al.,* 1991). Thus it appears that each primordium is derived from more than one cranial neural crest population.

The origin of the ectoderm overlying the facial primordia has been extensively investigated by Couly and Le Douarin (1985, 1987, 1990). The ectoderm overlying the frontonasal mass is derived from the anterior neural folds at the level of the prosencephalon. This is also true in mammalian embryos (Osiumi-Yamashita *et. al.,* 1994). The ectoderm of the lateral nasal processes, maxillary and mandibular primordia are all derived from ectoderm lateral to the neural folds.

1.4 Shaping of the facial primordia and development of the primary palate

In chick embryos, between stages 20 and 28, each primordium undergoes considerable enlargement and also changes shape, compare Figs. 1.1a and 1.1b. The frontonasal mass lengthens and the nasal pits elongate and deepen into slits (Yee and Abbott 1978). The frontonasal mass also widens at the edge abutting the oral cavity, forming two globular processes, jutting out laterally. The lateral nasal processes lengthen, in concert with the frontonasal mass, and broaden, becoming more square in appearance. The maxillary primordia expands, jutting out into the oral cavity. By stage 26, it is in close apposition to the globular processes of the frontonasal mass. Also, a stage 26, the lateral nasal process and maxillary primordia, which are already joined, merge to form the lacrimal groove. Merging has been described as the process attaching adjacent primordia and the smoothening of contours between them (Minkoff 1980). The mandibular primordia extend into a peak at the midline of the paired primordium and fuse to form a single primordium. The face at stage 28 appears flat as all primordia have grown forward to a similar extent (Yee and Abbott 1978). However, the cellular processes that underlie these changes in morphology have not been thoroughly investigated.

The formation of the chick primary palate begins between stages 26 and 28 when the maxillary primordium, lateral nasal process and frontonasal mass grow together and appose. This phase is marked by a brief period of changed cell morphology in opposing

epithelia at prospective fusion points. This includes the appearance of filopodia and numerous junctional complexes such as desmosomes and gap junctions, which, presumably aid cell adhesion (Yee and Abbott 1978, Kosaka *et. al.,* 1985, Kosaka and Eto 1986). At stage 28, the fusion of the maxillary primordium, frontonasal mass and lateral nasal process occurs, forming the primary palate (Yee and Abbott 1978, Will and Meller 1981, Tamarin *et. al.,* 1984). Breakdown of apposed epithelial at fusion points, which in mammals may involve apoptotic cell death (Pellier and Astic 1994), begins the fusion process and continuity of mesenchyme, known in mammals as the mesenchymal bridge (Wang *et. al.,* 1995) completes the process. These fused tissues separate the stomodeal and nasal cavities. However, in the chick embryo, the processes that control breakdown of the epithelial seams to allow mesenchymal merging in the primary palate have not been investigated.

Following primary palate fusion is a period of growth and differentiation, including outgrowth of the primordia to form, by stage 35, the characteristic beak of the chick face (Fig. 1.1c). The frontonasal mass gives rise to most of the upper beak structures in the adult chick face including the nasal septum and premaxillae bone. The remaining upper beak structures are contributed by lateral nasal process and maxillary primordia. The lateral nasal processes form the chonchae which jut into the nasal cavity, some of which are lined with olfactory epithelium. The maxillary primordia form the lip of the upper beak known as the tomium and also the palatal shelves which elevate and fuse in the oral cavity (with the premaxillae) to form the secondary palate. In chick embryos, fusion of the secondary palate only occurs distally, proximal regions remain open. The paired mandibular primordium give rise to all lower beak structures.

1.5 Clefting of the primary palate

Failure of primary palate fusion leads to cleft lip. This indicates the importance of primary palate fusion in establishing the basic shape of the upper face. The aetiology and mechanisms of primary palate clefting are, in most cases, unknown as there has been surprisingly little experimental work performed on the developing primary palate. Other fusion and clefting processes in the developing oro-facial region have been characterised

in far more detail. One example is fusion of the secondary palate. In this case, it is known that palatal shelves arise from the oral aspect of the maxillary primordia grow down, alongside the tongue, then elevate above it. The two palate shelves then appose, fuse and differentiate. Disruption of any of these processes, growth of palatal shelves, elevation of shelves, apposition, fusion and mesenchymal merging, leads to secondary palate clefting (Ferguson 1988). By analogy with we can propose that similar mechanisms are involved in the formation of the primary palate and that disruption of some of these processes may cause primary palate clefting. Thus, reduced growth of primordia, lack of apposition of primordia and failure of the fusion process itself could all result in primary palate clefting.

Disruptions in outgrowth have been identified in animal models where clefting of the primary palate has been induced with chemical and pharmaceutical compounds. Phenytoin (Dilantin), an antiepileptic compound, has been shown to cause cleft primary palate in mammalian embryos by leading to changes in size in the lateral nasal process (Sulik *et. al.*, 1979). Primary palate clefting has also been reported in human embryos exposed to this compound *in utero* (Hanson and Smith, 1975). Retinoic acid (Acutane) is also teratogenic, causing various developmental defects, including primary palate clefting in avian and mammalian embryos (Morris 1972, Jelenik and Kistler 1981, Tamarin *et. al.*, 1984) and craniofacial defects in human embryos (Lammer *et. al.*, 1985). In chick embryos, retinoic acid-induced clefting of the primary palate appears to be due to reduced outgrowth of the frontonasal mass (Tamarin *et. al.*, 1984, Wedden 1987) Figs. 1.1d, e, f. Thus such experimental systems may lead to further understanding of the mechanisms of human primary palate clefting.

1.6 The function of retinoic acid in the normal embryo and retinoic acid embryopathy

As indicated above, administration of retinoic acid to avian, mammalian and human embryos results in severe teratogenic effects. However, retinoic acid has also been implicated as a natural signalling molecule in the developing embryo. For example, experiments indicate that retinoic acid may be involved in the initial specification of the main anteroposterior body axis as treatment with retinoic acid reduces forebrain (anterior)

but increases hindbrain (posterior) in *Xenopus* embryos (Durston *et. al.*, 1989). In the mouse, retinoic acid treatment also respecifies anterior axial skeleton to more posterior elements (Marshall *et. al.*, 1994). HPLC investigations have indicated that there is a higher level of retinoic acid in the posterior (trunk) of the mouse embryo than the anterior (Horton and Maden 1995). Retinoic acid has also been implicated in patterning of the skeletal structures in the limb, as application of retinoic acid to anterior limb buds results in digit duplications thus mimicking the endogenous polarising signal in the posterior region of the limb bud (Tickle *et. al.*, 1982).

Retinoic acid is one of the retinoids synthesised from dietary vitamin A (all - trans retinol). Metabolism of vitamin A to retinoic acid requires binding to cellular retinol binding proteins (CRBPs). CRBPs also sequester and protect retinol from other digestive enzymes in the circulation and in cells (reviewed in Napoli *et. al.*, 1996). Retinoic acid signals by binding to nuclear steroid hormone type receptors - retinoic acid receptors RAR's and RXR's. All - trans retinoic acid and 9-cis retinoic acid bind to RAR's of which there are three types - α, β, γ each with several isoforms. RXR's bind only 9-cis retinoic acid and also have 3 types α, β, γ and isoforms. (Lohnes *et. al.*, 1994). Cellular retinoic acid binding proteins (CRABPs), bind retinoic acid and sequester it in the cytosol, thus reducing the nuclear concentration. They also aid metabolism of retinoic acid, which again reduces potency (Napoli *et. al.*, 1996). It is not clear if they also transport retinoic acid to the nucleus. The binding of retinoic acid to the receptor induces receptor dimerisation such that RARs heterodimerise with RXRs (Leid *et. al.*, 1992), which it has been suggested may also be liganded (Lu *et. al.*, 1997). This heterodimeric complex binds to particular sequence motifs, known as retinoic acid response elements (RARE's) (Chambon 1996), in target genes. Many genes are known to contain RAREs, such as some of the Hox genes (Marshall *et. al.*, 1996). RXRs can also form homodimers and heterodimers with other steroid hormone receptors such as thyroid hormone receptors and vitamin D receptors which also bind to DNA (Chambon 1996)

The requirement for retinoic acid during development is demonstrated by defects in mammalian embryos deprived of vitamin A *in utero* (Wilson *et. al.*, 1953) and avian

embryos *in ovo* (Thompson *et. al.,* 1969, Heine *et. al.,* 1985, Dersch and Zile 1993). Vitamin A deficiency syndrome (VAD) in mammals results numerous defects, including heart and lung defects, male sterility, limb truncation and cleft secondary palate, (Wilson *et. al.,* 1953, Howell *et. al.,* 1964, Morris Kay 1993). Administration of retinoic acid can prevent these defects (Howell *et. al.,* 1964). There are also reports of facial clefting in VAD mice (Morris - Kay and Sokolova 1996, Dickman *et. al.,* 1997) however, these embryos do not survive to full term. Avian embryos deprived of Vitamin A also die at early stages of development due to abnormal heart development and this also can be rescued with retinoic acid treatment (Dersch and Zile 1993).

The importance of vitamin A in development is also indicated by functional inactivation of retinoic acid receptor genes. Most single receptor isoform knockouts and some isotype knockouts resulted in normal mice, for example *RARα1* (Li *et. al.,* 1993, Lufkin *et. al.,* 1993) and *RARβ* (Luo *et. al.,* 1995), presumably due to functional redundancy. Some isotype knockouts resulted in mice displaying some of the defects of mammalian VAD syndrome, for example male RARα knockout mice are sterile (Lufkin *et. al.,* 1993). Functional inactivation of two or more RAR receptor types resulted in mice with most defects found in VAD syndrome, for example αγ knockout mice display secondary palate clefts (Lohnes *et. al.,* 1994, Mendelsohn *et. al.,* 1994, see Kastner *et. al.,* 1995 for review). They also exhibited defects not reported in mammalian VAD syndrome such as malformed or missing craniofacial skeletal elements such as missing nasal and frontal bones in the αγ mutant (Lohnes *et. al.,* 1994). This is possibly due to more complete removal of retinoic acid signalling in this system compared to VAD syndrome. Thus the requirement for retinoic acid throughout development is maybe even more widespread than the VAD syndrome has indicated.

A further interesting result was found from these functional inactivation studies. Mice deficient in RXRα show resistance to retinoic aid induced limb defects (Sucov *et. al.,* 1995) while RARγ deficient mice are resistant to retinoic acid induced axial skeleton

defects (Lohnes *et. al.,* 1993). Thus teratogenic effects of retinoic acid in different tissues are mediated via different receptor types.

Administration of excess vitamin-A or retinoids during development also results in various developmental defects depending on the time of administration and dose (Morris 1973). This includes craniofacial defects in humans (Lammer *et. al.,* 1985). In addition, clefting of the primary palate also occurs in mammalian (Goulding and Pratt 1986, Morris-Kay 1993) and chick embryos (Jelenick and Kistler 1981, Tamarin *et. al.,* 1984). Some retinoic acid - induced craniofacial defects are thought to be due to disruption of formation or migration cranial neural crest. Retinoic acid is thought to normally have a role in patterning the hindbrain, through interaction with RAREs, associated with Hox genes, which are thought to confer segmental identity on rhombomeres and also their neural crest populations (Krumlauff et. al., 1993). Excess vitamin A / retinoid at pre neural crest migration stages has been shown to disrupt the segmentation of the hindbrain with an associated loss of segmental gene expression. For example, there is rostral extension of HoxB gene expression in retinoic acid treated mice (Morris-Kay *et. al.,* 1991, Conlon and Rossant 1992, Marshall *et. al.,* 1992, Wood *et. al.,* 1994) producing an apparent change in rostral neural crest identity and thus, a subsequent loss of some rostral head structures. Retinoic acid has also been shown to interfere with neural crest migration (Thorogood *et. al.,* 1982, Pratt *et. al.,* 1987) which could result in small or even absent facial primordia. However, facial development can also be disrupted by retinoic acid applied at post neural crest migration stages and clefts of the primary palate are produced (Tamarin *et. al.,* 1984, Goulding and Pratt, 1986). Further investigations have shown that the frontonasal mass mesenchyme is the primary target at these stages of development, the effect being a reduction of outgrowth of which results in clefting (Wedden 1987), see also Fig. 1.1d, e, f. More recent studies have indicated that retinoic acid reduces the expression of particular genes in the region of primary palate formation such as *Msx-1* and *Msx-2* (Brown *et. al.,* 1997) while others such as *FGFRs* and *FGFs* are unaffected (Richman and Delgado 1995, Helms *et. al.,* 1997). Transcripts of RARβ have also been reported to be more widespread in the maxillary primordium upon retinoic acid treatment (Rowe *et. al.,* 1992). Further investigation of patterns of gene expression

in this region and their response to retinoic acid may enable us to more fully understand the mechanisms of normal and abnormal primary palate development.

1.7 Signalling mechanisms involved in control of chick embryo facial development

The cellular processes that control shaping and fusion of the facial primordia and result in primary palate formation are largely unknown. It seems likely that cell proliferation, cell death and cell intercalation may, in some way, play a role in facial shaping. The co-ordination of such cell behaviour and cell interactions will be essential for normal development of the face and will be under the control of genes expressed in facial primordia. Such interactions may include epithelial-mesenchymal interactions mediated by signalling molecules and direct cell-cell signalling which can be mediated by gap junctions.

1.7.1 Epithelial-mesechymal interactions

Epithelial-mesenchymal interactions have already been shown to be important in promoting and co-ordinating outgrowth of facial primordia (Wedden 1987, Richman and Tickle 1989, 1992). In other parts of the embryo, such as the developing limb and tooth, signalling molecules, such as growth factors, are known to mediate epithelial-mesenchymal interactions (see, for example, Thesleff *et. al.,* 1995).

Members of one group of signalling molecules - the Fibroblast Growth Factor family (FGFs), are expressed in the ectodem of the developing face between stages 20 and 28, the period during which facial primordia expand and fuse. FGFs are small peptide molecules with a conserved signalling sequence. Their proliferation promoting activities were first discovered in cultures of NIH3T3 cells (Gospodarowicz 1974) but FGFs are now known to have a wide variety of roles, both in the adult and developing embryo.

Three members of the FGF family have been found to be expressed in the developing avian or mammalian face, namely FGF-2 in chick embryos (Richman *et. al.,* 1997), *Fgf-4* in the mouse at E 9.5 (Niswander and Martin 1992) and in the chick (Barlow and Francis-West 1997) and *Fgf-8* in both mouse and chick embryos (Heikinheimo *et. al.,*

1994, Ohuchi *et. al.,* 1994, Crossley and Martin 1995, Wall and Hogan 1995, Vogel *et. al.,* 1996).

FGFs signal by interacting with receptors (FGFRs) which are encoded by four distinct genes and alternative mRNA splicing has lead to multiple receptor isoforms (Ornitz *et. al.,* 1996). This interaction is also known to require cell surface heparin sulphate proteoglycans for maximum binding affinity (Yanyon *et. al.,* 1991). FGFRs are all transmembrane tyrosine kinase receptors which dimerise upon ligand binding. This allows autophosphorylation of tyrosine residues which triggers subsequent intracellular signalling cascades. Different receptor types bind different FGFs with different affinity and specificity (Ornitz *et. al.,* 1996).

Various human syndromes have been linked to mutations in the FGF signalling pathway. A remarkable number of syndromes linked to mutations in FGF receptors display craniofacial abnormalities, such as Crouzon syndrome (*FGFR2* Reardon *et. al.,* 1994) and some also have limb abnormalities such as Pfeiffers syndrome (*FGFR1*, Muenke *et. al.,* 1994). FGF-2, FGF-4 and FGF-8 are also expressed at high levels in the AER of the developing limb bud (Savage *et. al.,* 1993, Niswander and Martin 1992, Heikinheimo *et. al.,* 1994, Ohuchi *et. al,* 1994, Crossley and Martin 1995, Mahmood *et. al.,* 1995, Crossley *et. al.,* 1996, Vogel *et. al.,* 1996). Studies have shown that these can maintain outgrowth of the limb bud after removal of the AER (Fallon *et. al.,* 1994, Niswander *et. al.,* 1993, Crossley *et. al.,* 1996), strongly suggesting that FGFs from the AER mediate limb outgrowth. However, the role of FGFs in the control of outgrowth of facial primordia has not been fully investigated.

A second group of signalling molecules has been associated with epithelial-mesenchymal controlled outgrowth in the developing face and limb. The Bone Morphogenetic Proteins (BMPs) were first identified as cartilage and bone inducing activity in demineralised bone matrix (Urist 1965). There are at least 13 members of this family of secreted peptide growth factors. *Bmp-2* and *Bmp-4*, in particular, are expressed in regions of epithelial - mesenchymal interactions in the developing embryo (Lyons *et. al.,* 1990, Jones *et. al.,* 1991). BMPs bind to serine/threonine kinase transmembrane receptors of which there are types I and II. Ligand binding to type II receptors provokes

dimerisation to type I receptors to form a receptor-ligand complex (Ebner *et. al.*, 1993). Type II receptor subsequent phosphorylates type I receptor and triggers an intracellular signalling cascade which is now well identified (Wrana *et. al.*, 1994, see also Baker and Harland 1997 for review).

In chick embryos, BMPs are expressed both in ectoderm and mesenchyme of facial primordia between stages 20 and 28. *Bmp-4* is mainly expressed in the ectoderm, only appearing in the mesenchyme at stage 28 while *Bmp-2* is expressed in both ectoderm and mesenchyme (Francis-West *et. al.*, 1994, Barlow and Francis-West 1997). In the limb, *Bmp-2* and *Bmp-4* are both expressed in the apical ectodermal ridge (AER) (Lyons *et. al.*, 1990, Jones *et. al.*, 1991, Francis *et. al.*, 1994) but act in an antagonistic manner to FGF, inhibiting outgrowth (Niswander and Martin 1993). Functional inactivation of *Bmp-2* in mice leads to embryonic lethality due to disruption of heart development (Zhang and Bradley 1996) thus we cannot conclude from this experiment if *Bmps* are important in controlling outgrowth of facial primordia. However, recently, Chondrodysplasia Grebe type has been linked to a mutation that disrupts BMP signalling in humans. This syndrome is characterised by limb shortening and dysmorphogenesis (Thomas *et. al.*, 1997). This indicates that BMPs have an important role in the control of outgrowth, at least in the limb.

The homeobox containing gene, *Msx-1* is expressed at sites of epithelial - mesenchymal interaction in the face (Mackenzie *et. al.*, 1991 a, b, Suzuki *et. al.*, 1991, Brown *et. al.*, 1993, 1997, Satokata and Maas 1994, Nishikawa *et. al.*, 1994, Mina *et. al.*, 1995, Foerst-Potts and Sadler 1997), the limb (Davidson and Hill 1991, Davidson *et. al.*, 1991, Robert *et. al.*, 1991, Brown *et. al.*, 1993) and the tooth (Mackenzie *et. al.*, 1991 a, b,).

Msx-1 is homologous to Drosophila msh (muscle segment homeobox) and has been isolated in both mouse (Hill *et. al.*, 1989, Robert *et. al.*, 1989) and chick (Yokouchi *et. al.*, 1991, Suzuki *et. al.*, 1991, Robert *et. al.*, 1991). Genes which contain homeoboxes encode proteins which bind to DNA in a sequence specific manner, thus regulating expression of particular genes . Homeobox genes are divided into families on the basis of

conservation within the homeodomain (Burglin 1994). There are currently three members of the vertebrate *Msx* family (*Msx-1 - 3*).

Strong evidence for the importance of *Msx-1* in outgrowth and patterning of the face has come from functional inactivation studies in the mouse. These mice display clefts of the secondary palate, absence of teeth and surrounding alveolar bone in the mandibular and maxillary primordia, shortening of the mandibular primordium and abnormalities in the shaping of frontal, parietal and nasal bones (Satokata and Maas 1994). Functional inactivation of both Msx-1 and Msx-2 (Dr. R. Maas, Boston, pers comm) results in additional clefting of the primary palate. Interestingly, over expression or gain of function mutation in murine *Msx-2* or human MSX-2, known as Boston - type craniosynostosis, also leads to very similar craniofacial defects (Jabs *et. al.*, 1993, Winograd *et. al.*, 1997), indicating the importance of correct levels of *Msx* gene expression during facial development.

1.7.2 Direct cell-cell interactions

Direct cell-cell interactions can be mediated by gap junctions. Freeze fracture preparation of maxillary primordium mesenchyme has indicated that gap junctions are present in this primordia in restricted pattern (Minkoff 1983). Furthermore, the presence of connexin 32 protein in gap junction plaques in the chick upper beak primordia have been shown (Minkoff *et. al.*, 1991).

Gap junctions form between two adjacent cells, by the docking of two subunits, known as hemichannels or connexons, one contributed from each cell. This forms a continuous pore of 1-2nm in size between the cells which allows for the diffusion of ions, metabolites and second messengers such as cAMP, up to 1kD molecular weight. Individual connexons consist of six protein subunits known as connexins (Goodenough 1974). There is a large family of connexin genes, each encoding an individual protein named after its molecular weight, for example, connexin 43 has molecular weight 43 kD (Beyer *et. al.*, 1987). The exact role of gap junctions in development is not well understood. It is thought that they allow the establishment of communication compartments between tissues that may allow for the co-ordination of such processes as

cell proliferation or specification of lineage compartments (Warner *et. al.*, 1984, Guthrie, 1984, Lo *et. al.*, 1979).

Human diseases have also been linked to mutations in connexin genes. Visceroatrial heterotaxia has been linked to mutations in *connexin 43* (Britz-Cunningham *et. al.*, 1995) which is very similar to the heart phenotype seen in mice in which *connexin 43* has been functionally inactivated (Reaume *et. al.*, 1995). Mutations in *connexin 32* have been linked to X-linked Charcot-Marie-Tooth disease, a peripheral neuropathy (Bergoffen *et. al.*, 1993). Late onset peripheral neuropathy also occurs in mice with connexin 32 functionally inactivated (Anzini *et. al.*, 1997). More recently mutations in *connexin 26* have been linked to congenital deafness and skin hyperplasia (Kelsell *et. al.*, 1997) however functional inactivation of this gene in mice is an embryonic lethal (H.D. Gabriel and K. Willecke, pers. comm. in Nicholson and Bruzzone 1997).

1.8 Specific aims of this thesis

The long term aim is to understanding the cellular and molecular basis of shaping of normal facial primordia and the changes in these mechanisms that occur after retinoic acid treatment. This may give new insights into how some types of primary palate clefting may occur.

This thesis investigates the behaviour of cell populations in the chick embryonic facial primordia between stages 20 and 28. During this period of development, the primordia enlarge and undergo considerable changes in shape. In order to understand changes in shape, I made detailed fate maps of cells in different regions of facial primordia to understand how cells behave locally, within primordia. I determined patterns of cell proliferation and cell death in facial primordia and related this to the fate maps. I also related the fate maps to previous descriptions of gene expression in the chick face. Fate maps also allow one to follow cells in regions of fusion, particularly in the primary palate. Facial clefting can be induced by chemical compounds such as retinoic acid but the changes in cell behaviour that produce this clefting are not fully understood. I treated embryos with retinoic acid to produce clefting and then constructed a similar fate map to examine how behaviour of cell populations was affected.

Cell behaviour in the face may be coordinated by direct cell-cell signalling via gap junctions. I describe my experiments to examine expression of connexin proteins that are expressed in gap junctions and how connexin expression is affected after retinoic acid treatment. I then directly tested the role of connexin 43 containing gap junctions in facial shaping and fusion by disruption of connexin 43 protein expression with antisense oligodeoxynucleotides. Finally, I examined the role two signalling molecules expressed in the ectoderm, FGF and BMP, on mesenchymal expression of *Msx-1* and other genes expressed in the maxillary mesenchyme to begin to dissect the potential role of epithelial-mesenchymal interactions in formation of the primary palate.

Figure 1.1 Changes in morphology of chick facial primordia between stages 20 and 28 and changes in induced by treatment with retinoic acid

a. SEM of stage 20 chick embryo head. Above the stomodeal cavity lies the frontonasal mass and nasal pits. Either side of the stomodeal cavity lie maxillary primordia and beneath lie paired mandibular primordia. Each consists of a bud of mesenchyme surrounded by ectodermal. Note the lateral nasal processes are not obvious in this picture.

b. SEM of stage 28 chick embryo head. The frontonasal mass and lateral nasal processes have elongated and broadened. The maxillary primordia jut out to meet the frontonasal mass. The mandibular primordium juts under the frontonasal mass at this stage.

c. SEM of stage 36 chick embryo head. The upper beak forms from the frontonasal mass, lateral nasal process and maxillary primordium. The lower beak is formed by the paired mandibular primordia. The egg tooth is an epithelial thickening on the upper beak.

d. SEM of stage 24 chick embryo head, 24 hours after retinoic application at stage 20. The bead soaked in retinoic acid is in the left nasal pit (black arrow). The nasal pit and maxillary primordium on the left side of the face are shortened.

e. SEM of stage 29 embryo head, 48 hours after retinoic acid treatment. This embryo is affected on both sides of the face. The frontonasal mass is shortened, as are the maxillary primordia and nasal pits. Bilateral clefting of the primary palate is seen (white arrows).

f. Whole mount of stage 36 chick embryo head after treatment with retinoic acid at stage 20. The whole of the upper beak is clearly missing in this embryo (black arrow). The lower beak has not been affected.

Figure labels:

FNM: Frontonasal mass	NP: Nasal pit
Mx: Maxillary primordium	Mn: Mandibular primordium
Sc: Stomodeal cavity	LNP: Lateral nasal process
UB: Upper beak	LB: Lower beak

Axes labels:

D: Distal	Pr: Proximal
M: Medial	L: Lateral
Po: Posterior	A: Anterior

Figure 1.1

35
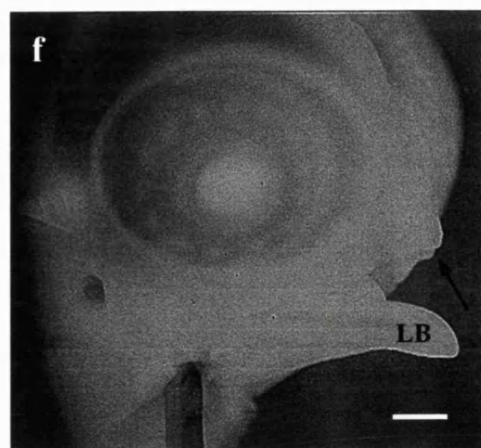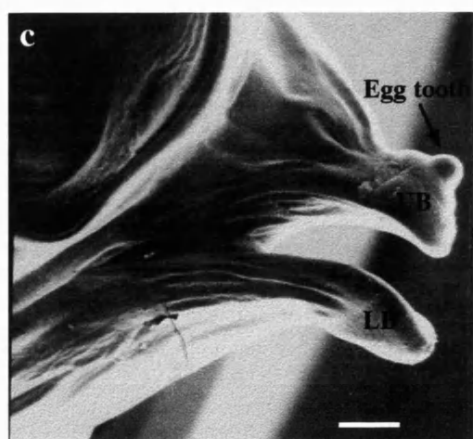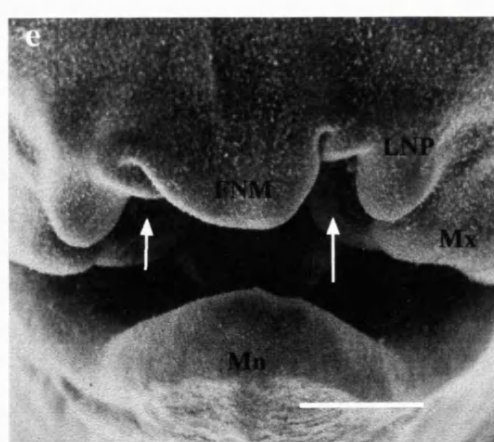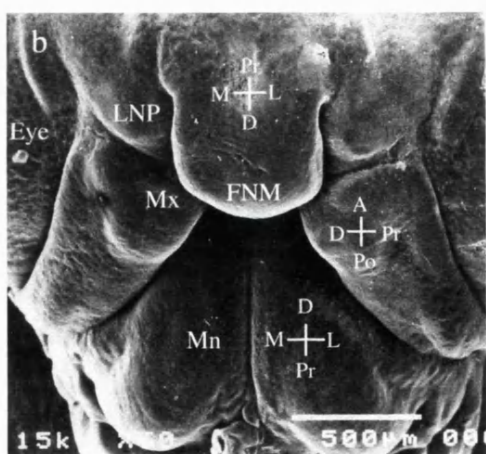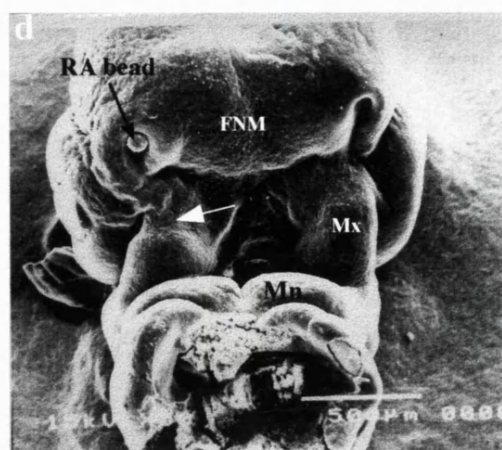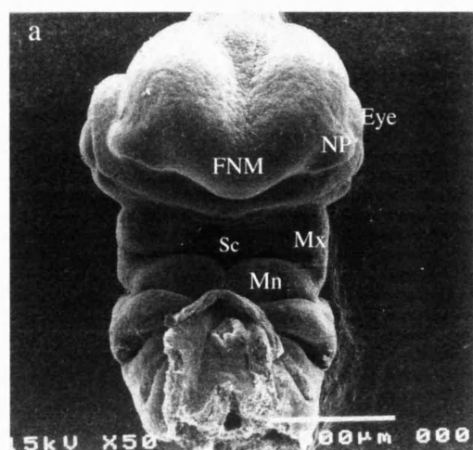
Chapter Two - General Materials and Methods

The experimental procedures listed in this chapter are used in two or more experimental chapters. More specific methods, used in one chapter only, are listed within that chapter.

2.1 Manipulation of chick embryos

Fertilized White Leghorn chicken eggs were obtained from Poyndon Farm, Waltham Cross, Hertfordshire, U.K. Eggs were incubated at 38 ± 1°C and windowed on day 2 or 3 of incubation. Briefly, eggs were swabbed with tissue soaked in 70% alcohol and rotated 90° to ensure that the embryo had not stuck to the inside of the shell. The blunt end of the egg was pierced with forceps, followed by the upper surface. Tape was placed over this hole and a "window" cut from the shell using scissors, thus exposing the embryo. Embryos were staged according to the method of Hamburger and Hamilton (1951). For manipulation, the embryo was revealed by carefully opening the vitelline and amniotic membranes around the head region of the embryo.

2.2 Treatment of embryos with retinoic acid.

Retinoic acid stock solution, 10mg/ml, was prepared from All-trans retinoic acid (Sigma) dissolved in sterile dimethylsulphoxide (DMSO, Sigma). This stock solution was aliquoted and stored at -20°C, in the dark as retinoic acid is light sensitive.

AG1-X2 formate beads (BioRad) were sized using an eyepiece graticule and beads of 100μm diameter selected. They were placed in a small diameter, non coated, petri-dish and soaked in either 10, 5 or 1mg/ml retinoic acid in DMSO (Sigma) for 20 minutes, at room temperature, in the dark. Control beads were soaked in DMSO only. Beads were washed for 5 minutes in two changes of serum containing "Growth Medium" (see below)

at room temperature and subsequently incubated in growth medium, at 37°C, for 20 minutes (see also Eichele *et. al.,* 1984, Richman and Delgado 1995). Growth medium contains phenol red, thus beads soaked in it become red.

Beads were then pushed into the right nasal pit of stage 20 embryos, using fine forceps. The eggs were re-sealed and incubated for various times.

2.3 Preparation of growth medium

Minimal Essential Medium (MEM, Gibco) was supplemented with 10% Foetal Calf Serum (FCS, Gibco), 2% 100x (200mM) L-glutamine (Gibco) and 1% 100x antibiotic/antimycotic (Gibco), in sterile conditions. This solution was then filtered using millipore syringe filter, pore size 0.2μm, and stored for up to 3 days at 4°C.

2.4 Fixation of embryos in paraformaldehyde

Sterile 10x phosphate buffered saline (PBS, Gibco) was diluted 1:10 with sterile distilled water. 4% (w/v) paraformaldehyde powder (Sigma) was dissolved in PBS by heating gently. Aliquots of PFA were stored at -20°C.

2.5 scanning electron microscopy

For fixation, a modified Tyrodes solution was prepared as follows.

5.5g NaCl

0.2g KCl

0.2g $CaCl_2$

0.1g $MgCl_2$

1.0g sucrose

1.0g $NaHCO_3$

0.5g $NaH_2PO_4.H_2O$

40mls 25% gluteraldehyde (EM grade)

Make up to 1l with distilled water .

Chick embryos were removed from the shell into PBS. Membranes were removed and heads were removed with forceps or scissors (older embryos). They were fixed in modified Tyrodes solution for at least 24 hours at 4°C. The heads were then washed in 5-6 changes of distilled water over a 24 hour period and in 5-6 changes of 100% ethanol (Analar grade) over the subsequent 24 hour period.

Prior to critical point drying, the heads were soaked in iso-amyl acetate for 20 minutes. Critical point drying was carried out with CO_2 for 90 minutes at approximately 15-20°C and the drying chamber evacuated for 60 minutes at 35°C. Heads were then mounted onto stubs,

coated with Electrodag 1415M high conductivity paint and allowed to dry for 20 minutes and sputter-coated with gold by emscope sc500 sputtercoater. Heads were scanned with a Jeol JSM5410LV scanning electron microscope. Photographs were taken on Ilford FP4 film.

2.6 Whole mount in situ hybridisation

2.6.1 Preparation of linear DNA from plasmid DNA

Plasmid (circular) DNA is cut with restriction enzymes to produce linear DNA. Linear DNA is required to produce riboprobes. The details of the plasmids and restriction enzymes required to linearise them, for each probe used in this thesis, will be listed in this or subsequent chapters.

(A) To cut the plasmid:

Total digestion volume = 200μl

20μl enzyme buffer (x10) - this value is always 10% of the total volume

10μl restriction enzyme

20μg plasmid DNA

Make up to 200μl with sterile water. Mix, centrifuge briefly and incubate for 2 hours at 37°C.

(B) To ensure plasmid DNA has linearised

Run on a 1% agarose gel made as follows:

Melt 1% low melting point agarose (Sigma) in 1x Tris acetate with EDTA (TAE). Add 0.002% 10mg/ml Ethidium Bromide.

Load 1-2μl cut or uncut DNA with 1μl loading buffer. Run against a DNA ladder to estimate the size of the cut DNA. The cut DNA will appear as a single band, the uncut DNA as a streak of bands.

(C) Precipitate DNA

Once cut, precipitate by adding an equal volume (200μl) of phenol:chloroform (Gibco). Vortex, centrifuge 14000 rpm for 5 minutes. Remove the top layer (100μl) and add an equal volume of phenol:chloroform, vortex and centrifuge as before. Remove the top layer (100μl). To this add 1/4 volume 10M ammonium acetate and 2.5x volume of ethanol. Freeze at -20°C for 30 minutes to precipitate. Centrifuge at 14000rpm for 10 minutes to produce a pellet and tip the supernatant off. Resuspend in 70% ethanol to clean, centrifuge and remove the supernatant. Air dry. Resuspend in 20ul of water.

2.6.2 Synthesis of riboprobes for whole mount in situ hybridisation

Riboprobes are synthesised from linearised plasmid DNA. The method of linearisation of each plasmid will be listed separately either in this or subsequent methods chapters.

For all steps of the *in situ* protocol, sterile, RNase free water was produced by treating distilled water with 0.05% diethylpyrocarbonate (DEPC) for several hours before autoclaving.

The following were mixed at room temperature in a sterile eppendorf tube:

10μl   sterile distilled water

4μl	5x transcription buffer (Promega)
2μl	0.1M DTT (Dithiothretol, Promega)
2μl	DIG 10x nucleotide mix (Digoxigenin labelled nucleotides, Boheringer)
1.5μl	Linearised plasmid (1μg/1ml)
0.5μl	RNAsin ribonuclease inhibitor (Promega)
1.5μl	RNA polymerase (SP6, T7 or T3) (Promega)

Incubate in a water bath at 37°C for 2-3 hours. Run 1μl of labelled probe on a 1%

agarose gel against a DNA ladder to estimate size. Labelled probe will appears as an

intense band and there will also be a faint, larger DNA band. Add 2μl DNAse I, to digest

DNA, at 37°C for 15 minutes. Add the following ice cold: 50μl water, 1μl glycogen

(20ug/ul, from mussels, Boheringer), 25μl ammonium acetate and 200μl ethanol. Mix,

place on dry ice for 30 minutes or overnight at 70°C. Centrifuge at 14000rpm for 20

minutes at 4°C. Remove supernatant, wash with 70% ethanol, centrifuge for 5 minutes.

Remove supernatant, air dry. Resuspend in 50μl sterile water and aliquot.

2.6.3 Preparation of embryos for hybridisation

Remove embryos from egg. Wash in PBT (PBS + 0.1% Triton 100), fix in 4% PFA

in PBT (w/v) overnight. Wash twice in PBT. (If embryos are to be stored, dehydrate in

ascending series of methanol (Analar grade) in PBT - 25%, 50%, 2x 100% and store for

up to 2 months at 20°C. Rehydrate in descending series of methanol in PBT - 50%, 25%,

2x PBT). Digest embryos with 20ug/ml proteinase K (Sigma) in PBT. Embryos stage 20-

24 were digested for 20 minutes, stages 25-30 for 25 minutes. Wash in PBT, 5 minutes.

Refix in 4% PFA, 0.25% gluteraldehyde (Sigma, tissue culture grade), 20 minutes. Wash

in PBT, 5 minutes. Incubate in preheated hybridisation mix (see below) at 60°C overnight.

Hybridisation mix is as follows:

25ml formamide (Fluka)

3.25ml 20xSSC (3M NaCl, 0.3M Na Citrate, pH to 4.5 with citric acid)

0.5ml 0.5M EDTA pH 8

250µl 20mg/ml Yeast tRNA (Bakers yeast, Boheringer).

100µl Triton 100

2.5ml 10% CHAPS (Boheringer)

100µl 50mg/ml heparin (Sigma)

1g blocking powder (Boheringer)

Make up to 50ml with sterile water. Store at -20°C.

2.6.4 Hybidisation, post hybridisation washes and visualisation of signal

Wash embryos in pre-warmed hybridisation mix. Incubate in pre-warmed hybridisation mix with 1µl/ml labelled probe overnight at 60°C.

Wash twice in 2xSSC, 0.1% CHAPS, 20 minutes at 60°C. Wash twice in 0.2%SSC, 0.1% CHAPS, 20 minutes at 60°C. Wash once in KTBT (50mM Tris pH7.5, 150mM NaCl, 10mM KCl, 1% Triton), 5 minutes, room temperature.

Incubate in 50% lambs serum (Gibco) in KTBT for 4 hours at room temperature. Meanwhile, prepare 50% lambs serum in KTBT plus 1/1000 anti-DIG antibody (Boheringer) and rock on ice for 4 hours. Incubate in this antibody solution at 4°C overnight.

Wash with KTBT at room temperature for 1 hour 5-6 times and then overnight at 4 °C. Wash in Alkaline phosphatase buffer, NTMT, (1ml 5M NaCl, 2.5ml 2M Tris-HCl pH9.5, 1.25 ml 2M $MgCl_2$, 500µl Tween-20 (Sigma), make up to 50ml with sterile

water), 10 minutes, room temperature. Prepare colour reagent as follows, keep dark:

NTMT + 4.5µl NBT (4-Nitrobluetetrazolium) /ml + 3.5µl BCIP (5-Bromo-4-chloro-3-indolyl-phosphate) /ml. Incubate embryos in colour reagent, in dark, until purple stain appears to sufficient strength. Wash for 1 hour, x2, in NTMT at room temperature. Re-fix in 4% PFA.

2.7 Preparation of *Msx-1* riboprobe from plasmid DNA.

Msx-1 DNA Bluescript SK2 plasmid, obtained from S. Wedden, University of Edinburgh, was linearised with BamHI and Buffer A (Boheringer) as in section 2.6.2. Antisense RNA was produced by transcribing with T7, as in section 2.6.2. and stored in 5µl aliquots at -70°C. Embryos were hybridised with 1µl/ml Msx-1 riboprobe as described in section 2.6.4 and 2.6.5, see also Brown *et. al.,* 1993).

2.8 Frozen sectioning of embryos

Embryo heads were fixed in 4% PFA overnight. They were then sunk in 30% sucrose solutions. Embryo heads were then processed into OCT compound (Tissue Tek) for 1 hour to allow infiltration and then frozen in fresh OTC with liquid nitrogen.

Chapter Three - Expansion of Cell Populations in Chick Facial Primordia between stages 20 and 28

3.1 Introduction

During development, the embryo undergoes extensive changes in shape. Such changes occur locally and on a well defined schedule. We are particularly interested in the processes underlying shaping of the developing chick face, which is comprised of four types of primordia which lie symmetrically around the stomodeal (oral) cavity. Below the cavity, paired mandibular primordia form the lower beak. Laterally, on either side of the cavity, lie maxillary primordia which together with the frontonasal mass and lateral nasal processes (which are separated by the nasal pits) give rise to the upper beak. All of these primordia are formed by settling of mesenchyme derived from specific cell populations of cranial neural crest which migrate from the neural folds. A critical phase of facial development is the formation of the primary palate which establishes the basic plan of the face. At this stage, the appearance of the face is rather similar in all vertebrates and subsequently diverges.

Previous fate maps employed to investigate morphogenesis of the face have concentrated on contributions of neural crest to facial development. Pathways of migration of cranial neural crest cells into developing facial primordia have been elucidated with techniques such as grafting labelled tissue (Johnson 1966; Noden 1975) and more recently DiI labelling (Lumsden *et . al.,* 1991; Morris-Kay *et. al.,* 1993). This has shown, for example, that the mesencephalic (midbrain) neural crest commences migration first, followed by posterior diencephelic (forebrain) crest and that both migrate ventrally, from the neural folds, beneath the head ectoderm (Noden 1975). The extent to which different cranial neural crest cell populations (forming connective tissues) and also mesoderm populations (forming muscle tissues) contribute to each of the tissues and

structures of the adult face has been investigated through the use of chick/quail chimeras (for example Le Douarin 1973; Le Lièvre and Le Douarin 1975; Le Lièvre 1978, Noden 1988; Köntges and Lumsden 1996). These studies show that mesenchyme of the frontonasal mass in the avian embryo is derived from crest populations migrating from the posterior diencephalon and anterior mesencephalon (Le Lièvre, 1978), maxillary mesenchyme comes from posterior diencephalon and mesencephalic crest (Le Lièvre 1978) whilst mandibular mesenchyme is formed by mesencephalic (Le Douarin and Le Lièvre 1975, Noden 1978a) and rhombencephalic (hindbrain) crest (Lumsden *et. al.,* 1991). However, none of these studies addressed the issue of how individual primordia are moulded after neural crest migration but before cell differentiation, during the crucial stages when the primary palate is formed and the face acquires its initial shape.

We have investigated how cells contribute to growth and fusion processes in each primordium by constructing an expansion map of facial primordia around the time of primary palate formation using DiI, a lipophilic cell autonomous marker. This has provided data on expansion of discrete populations of cells within each primordium and we relate this to patterns of cell proliferation and cell death. Retinoic acid treatment of embryos causes clefting of the primary palate and truncation of the upper beak (Jelinek and Kistler 1981, Tamarin *et. al.,* 1984; Wedden and Tickle 1986; Richman and Delgado 1995) and we have analysed how expansion of cell populations, cell proliferation and cell death contribute to the changes in shape of the face.

3.2 Materials and methods

3.2.1 DiI labelling of facial primordia

Vitelline and amniotic membranes were opened to expose the head region of stage 20 chick embryos, staged according to Hamburger and Hamilton 1951. A single injection of DiI (Molecular Probes) 3mg/ml in dimethylformamide (DMF) was pressure injected into the mesenchyme of the face of each embryo, using a micropipette and a General Valve Picospritzer II with a single 5-9 ms pulse at a pressure of 50-55 psi. The site of injection was selected from a grid constructed for the stage 20 embryonic face (Fig. 3.1). Embryos

were harvested immediately or resealed and incubated for 48 hours (up to stage 28 of development). Upon harvesting they were fixed in 4% PFA.

3.2.2 Fluorescence microscopy

Stage 20 and 28 DiI labelled heads were removed, using forceps, and mounted face up in citifluor antifade agent. DiI labelled cells were viewed under fluorescence using a rhodamine filter on a Nikon Opitphot 2 microscope. Dimensions of each primordium and the spread of DiI labelled cell populations, in 2 dimensions, were measured using a graticule and micrometer. Samples were photographed on Kodak EPY 64T colour film.

3.2.3 Analysis of data

For each cell population at least three embryos were examined. Embryos examined at stage 20 were analysed for accuracy of site of injection. Embryos incubated up to stage 28 were examined for the maximum spread of DiI labelled cell populations and the maximum dimensions of the primordium concerned, in two axes. The percentage spread was calculated along each axis, e.g.(spread in proximodistal axis (μm)/total proximodistal length of primordium (μm))x100. These results were averaged for each individual grid point and plotted onto a standard camera lucida drawing of each primordium at stage 28, thus showing the relative size and shape of the labelled population in a primordium (Fig. 3.2). The percentage of primordium area comprised of DiI labelled cells was calculated for each embryo and averaged for each grid point as before. This value indicated the relative total expansion of each labelled cell population (Fig. 3.6 d, e).

To assess changes in shape of labelled cell populations after retinoic acid treatment, the ratio of the mean length : mean width for each grid point was calculated for upper beak primordia of normal and retinoic acid treated embryos. This gave a measure of uniformity of shape of labelled cell populations (1 = uniform expansion) enabling a comparison of the shape of treated and untreated cell populations (Table 3.2).

3.2.4 Sectioning and analysis of DiI labelled embryos

Fixed embryos were frozen in OCT compound (Tissue Tek) as described in section

2.8. Embryos were sectioned at 15μm on a Leica CM1900 cryostat and examined by

fluorescence microscopy as before. In stage 20 embryos, the total number of cells initially

labelled was estimated by adding together the number of labelled cells in every section. In

stage 28 embryos, the extent of expansion of the labelled cell population in the

dorsoventral axis of the maxillary primordium was estimated by counting the number of

sections in which labelled cells appeared.

3.2.5 Examination of cell death in facial primordia

Embryos at stage 24 and 28 were fixed in 4% PFA and processed for frozen sectioning

as before. 7μm sections were permeabilised with 0.1% Triton X-100 in 0.1% sodium

citrate for 2 minutes at 4°C. Slides were rinsed in PBS and incubated with TUNEL

labelling mix (1 part terminal deoxynucleotidyl transferase (TdT) x 10 conc : 9 parts

nucleotide mixture in reaction buffer x 10 conc, In situ Fluorescent Cell Death Detection

Kit, Boehringer Mannheim) for 60 minutes in a humidified chamber at 37°C. Negative

controls were incubated without TdT. Positive controls were treated with DNase I after

permeabilisation to induce DNA strand breaks and then incubated with TUNEL labelling

mix. Slides were rinsed 3x in PBS, mounted in citifluor. and viewed under a Leica

confocal microscope.

3.2.6 Cell proliferation assay

Stage 24 embryos were incubated with 100μl of 0.5mg/ml BrdU (Sigma), applied on

top of the embryo for 1 hour. Embryos were fixed in 4% PFA, and processed into wax as

follows:

Heads were fixed in 4% PFA overnight, then transferred into each of the following

solutions for 1 hour. 50% alcohol in PBS, 70% alcohol in PBS, 95% alcohol in PBS, 2 x

absolute alcohol, 2 x Toluene, 2 x melted paraffin 1 hour. The embryos were then

embedded in a final change of melted paraffin. Blocks were sectioned at 7μm and then

sections de-waxed in histoclear for 10 minutes. Sections were subsequently rehydrated for 2 minutes in each of the following solutions : absolute alcohol, 95% alcohol in PBS, 85% alcohol in PBS, 70% alcohol in PBS, 50% alcohol in PBS, 3 x PBS. Incorporation of BrdU was determined with the BrdU Labelling and Detection Kit II (Boheringer Mannheim) as follows. The sections were incubated with anti-BrdU mouse monoclonal antibody IgG + nuclease for 30 minutes at 37°C in a humidified chamber, then washed 3 x PBS. The sections were then incubated with anti-mouse Ig-AP for 30 minutes at 37°C in a humidified chamber then washed 3 x PBS. Labelling was visualised by reacting with NBT/X-phosphate. Slides were mounted in permamount. For estimating the percentage of labelled cells in each region, the facial primordia were measured and divided into the same grid system used to label stage 20 embryos (Fig. 3.1). BrdU labelled and total number of cells, lying within a 60 x 60μm ocular square, were counted in 3 populations of each primordia in a total of three embryos. 16-18 sections, each three sections apart, were analysed for each region in total. Percentage of labelled cells in each region was calculated.

3.2.7 Araldite embedding of facial primordia and semi-thin sectioning.

Facial primordia were individually dissected from the face with fine forceps, then fixed in 1/2 strength Karnovskys fixative (see below). Primordia were then washed in 0.1M cacodylate buffer, 5 minutes, 50% alcohol 15 minutes and 70% alcohol 10 minutes. Primordia were then stained in alcian green for 30 minutes and washed in 90% alcohol for 15 minutes. They were then washed for 15 minutes 3 x in absolute alcohol. They were then processed into propylene oxide for 30 minutes, then 50:50 propylene oxide:araldite solution (see below) for 30 minutes and finally into araldite overnight at room temperature. They were processed in fresh araldite for the next 24 hours and baked overnight. Sections were cut at 1μm and stained with toluidine blue. Sections were photographed either on Kodak EPY64T colour film or Ilford PANF50 black and white film.

1/2 stength Karnovskys fixative

25mls distilled water + 1g paraformaldehyde + 3 drops 1M NaOH, heated gently until dissolved, cool and add 5 mls gluteraldehyde, 18 mls 0.2M cacodylate buffer.

To make up 0.2M cacodylate buffer:

25mls 0.2M sodium cacodylate + 1.4 mls 1.7% HCl in distilled water, pH 7.4.

Araldite solution

10g Araldite

10g DDSA

0.8g dibutylpthalate (DBP)

mix on heated stirrer, for 30 minutes, then add

0.4mls BDMA

3.2.8 Fgf-8 riboprobe

800bp chick Fgf-8 cDNA, cloned into Bluescript was obtained from Prof. Gail Martin, UCSF. The plasmid was linearised with EcoRI and the antisense riboprobe was transcribed with T7 RNA polymerase (see also Crossley *et. al.,* 1996).

3.3 RESULTS

3.3.1 Expansion of DiI labelled cell populations in facial primordia between stages 20 and 28.

To understand how cells within individual primordia at stage 20 contribute to the emerging face, 31 separate mesenchymal populations were defined in the facial primordia, assigned a grid reference according to their position (Fig. 3.1) and injected with DiI. Three or more embryos were examined for each data and time point. Injections labelled a small cluster of cells approximately 25µm in diameter (Fig. 3.3A). The average number of cells labelled by the injection was 257 (± 110) (n=19). Some embryos were fixed immediately and analysed for accuracy of injection of DiI. This confirmed the ability to distinguish between injection points *in ovo*. Remaining embryos were incubated for 48 hours to examine how labelled cell populations contributed to facial structures. Results were expressed in terms of direction and amount of expansion of DiI labelled cell populations (see appendic es 1, 2, 3). The axes of each primordium were defined as

follows: the distal tip abuts the stomodeal (oral) cavity, medial edges are closer to middle/midline of a primordium and anterior edges are those closer to the top of the head (Fig. 3.1). The axes, as defined here, are used throughout this thesis

3.3.1.1 Mandibular primordia

DiI was injected into a series of embryos in the right mandibular primordium, marking cell populations in a lateral to medial direction (labelled 1 to 4 respectively) and a proximal to distal direction (labelled A to C respectively, Figs. 3.1d, 3.2b).

Groups of cells marked near the distal midline of the paired primordia (C4 and C3, Figs. 3.1d, 3.2b) expanded more in a proximodistal direction (Fig. 3.2c, e) giving rise to streaks of labelled cells extending down the midline from the tip (Fig. 3.3B). Cells marked proximal to the tip (B4, Figs. 3.1d, 3.2b) expanded to a similar extent both mediolaterally and proximodistally (Fig. 3.2c) while at the proximal edge of the midline (A4 Fig. 3.1d) mediolateral spread predominated (Figs. 3.2c, 3.3C). Cell populations in central and proximal midline regions made the greatest contribution to the primordium (Fig. 3.6d). Laterally, cell populations showed a general reduction in proximodistal expansion and an increase in mediolateral expansion (C1-C3, A1-A3, B1-B3 Figs. 3.1d, 3.2d, d, e). Total overall expansion of the lateral cell populations was much less than that of medial cell populations (Fig. 3.6d).

Cells labelled near the proximal midline (A3 and 4) in the right mandibular primordium sometimes crossed into the adjacent left mandibular primordium. This was never seen to occur with cells situated more distally along the midline (at C4 and B4). Semi-thin sections of mandibular primordia were examined at stage 23 and 28 to see if an epithelial seam was present, which may have prevented this cell movement. This showed that epithelia was present only in the most distal regions of the primordia even at stage 23 (Fig. 3.4), suggesting that epithelia was not preventing movement of cells more distally along the midline at stages later than 23. Proximal midline cells (A4) were also occasionally seen to cross into the second branchial arch below. Cells marked at the point where mandibular and maxillary primordia join (D1 Figs. 3.1d, 3.2b) extend into both primordia (Figs. 3.2c, 3.3D) forming a continuous "v" shaped streak of cells parallel to

Figure 3.1 Diagram of stage 20 chick embryo indicating grid points at which DiI was injected into facial primordia.

a. Drawing of a side view of the head of a stage 20 chick embryo, as seen *in ovo*.

b. Enlarged view of the frontonasal mass, lateral nasal process and nasal pit of a stage 20 chick embryo with grid points corresponding to points at which DiI was injected. Axes as indicated on the figure.

c. Enlarged view of stage 20 maxillary primordium with grid points indicating regions in which DiI was injected. Note that grid point I1 is shown on both this and the above diagram. Axis as shown on the diagram.

d. Enlarged view of the mandibular primordia with grid points corresponding to points at which spots of DiI were injected. Axes as on figure.

Figure labels

Mx:	Maxillary Primordium	Mn:	Mandibular Primordium
LNP:	Lateral Nasal process	FNM:	Frontonasal Mass
NP:	Nasal pit		

Axes labels

Po:	Posterior	A:	Anterior
Pr:	Proximal	D:	Distal
M:	Medial.	L:	Lateral.

Figure 3.1
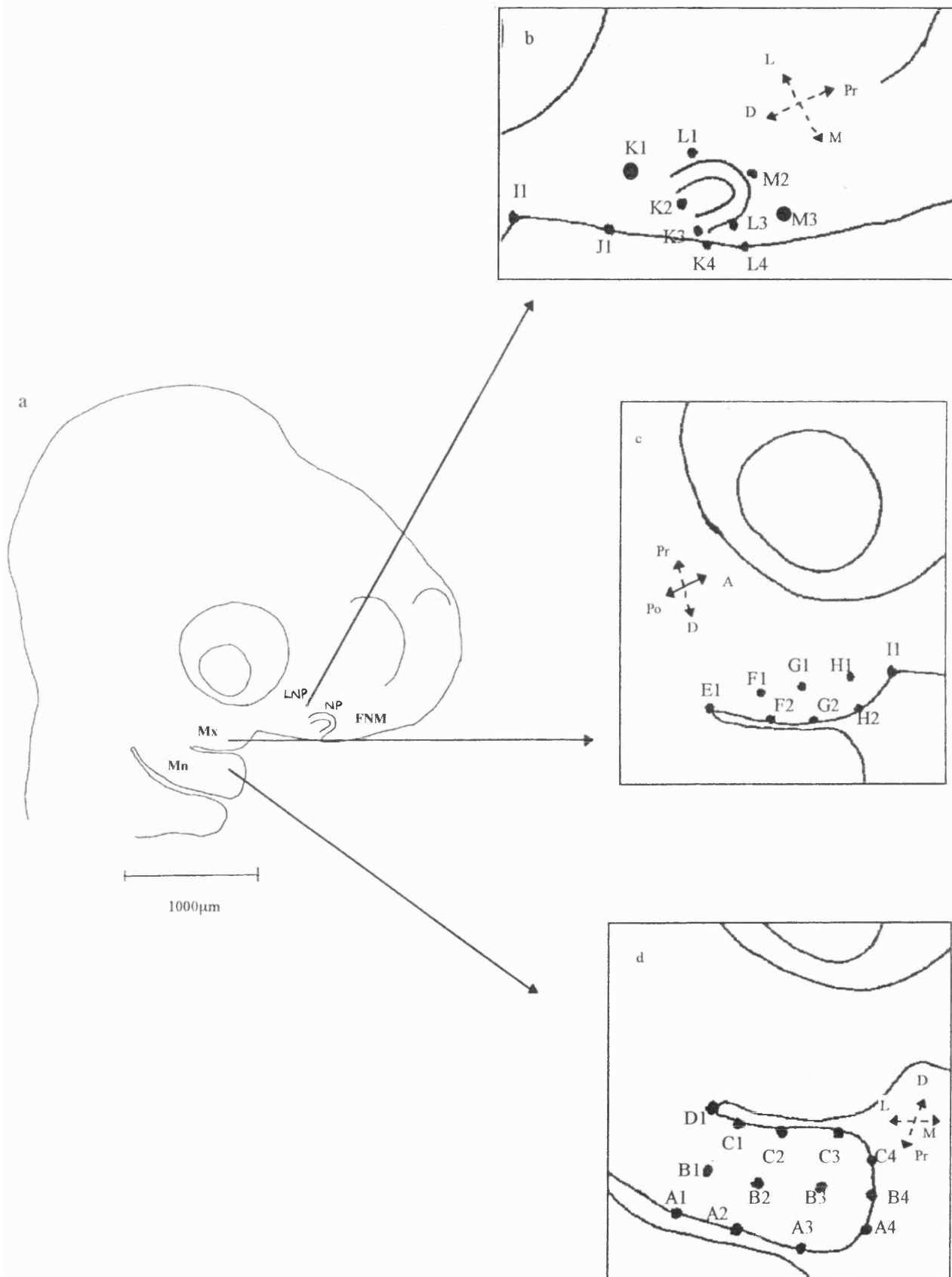
Figure 3.2 Expansion of labelled cell populations in the face between stages 20 and 28.

a. Frontal view of a stage 28 chick embryo head, showing mandibular primordium, maxillary primordium, frontonasal mass and lateral nasal process to aid identification of accompanying diagrams showing expansion.

b. Frontal view of stage 20 head indicating grid points at which DiI was initially injected in the mandibular primordium (see also figure 3.1).

c., d., e. Enlarged view of stage 28 mandibular primordium. Spread and shape of DiI labelled cell populations is drawn schematically as boxes. Note larger boxes are situated towards the midline. Boxes in mid-distal regions of the midline expand proximodistally. Those situated laterally expand mediolaterally. Note, populations A3, A2, A1 are drawn staggered rather than superimposed for clarity. Axes as indicated on the figures.

f. Frontal view of a stage 20 head indicating grid points at which DiI was initially injected in the maxillary primordium (see also figure 3.1).

g., h. Expansion and shape of DiI labelled cell populations in maxillary primordium at stage 28. Note difference in shape of boxes. Proximodistal expansion predominates at the tip (g), anteroposterior expansion predominates at the base (h). Larger boxes are also at the tips.

i. Frontal view of a stage 20 head indicating grid points at which DiI was initially injected in the lateral nasal process and frontonasal mass (see also figure 3.1).

j., k. Expansion and shape of DiI labelled cell populations in lateral nasal process and frontonasal mass at stage 28. Larger boxes are near the nasal slits. Cell populations proximally (j) expanded predominantly proximodistally while cell populations distally (k) expand mainly mediolaterally. Axes as indicated on figure.

Figure labels

Mx:	Maxillary Primordium	Mn:	Mandibular Primordium
LNP:	Lateral Nasal process	FNM:	Frontonasal Mass
Sc:	Stomodeal Cavity	NP:	Nasal pit

Axes labels as figure 3.1

Figure 3.2
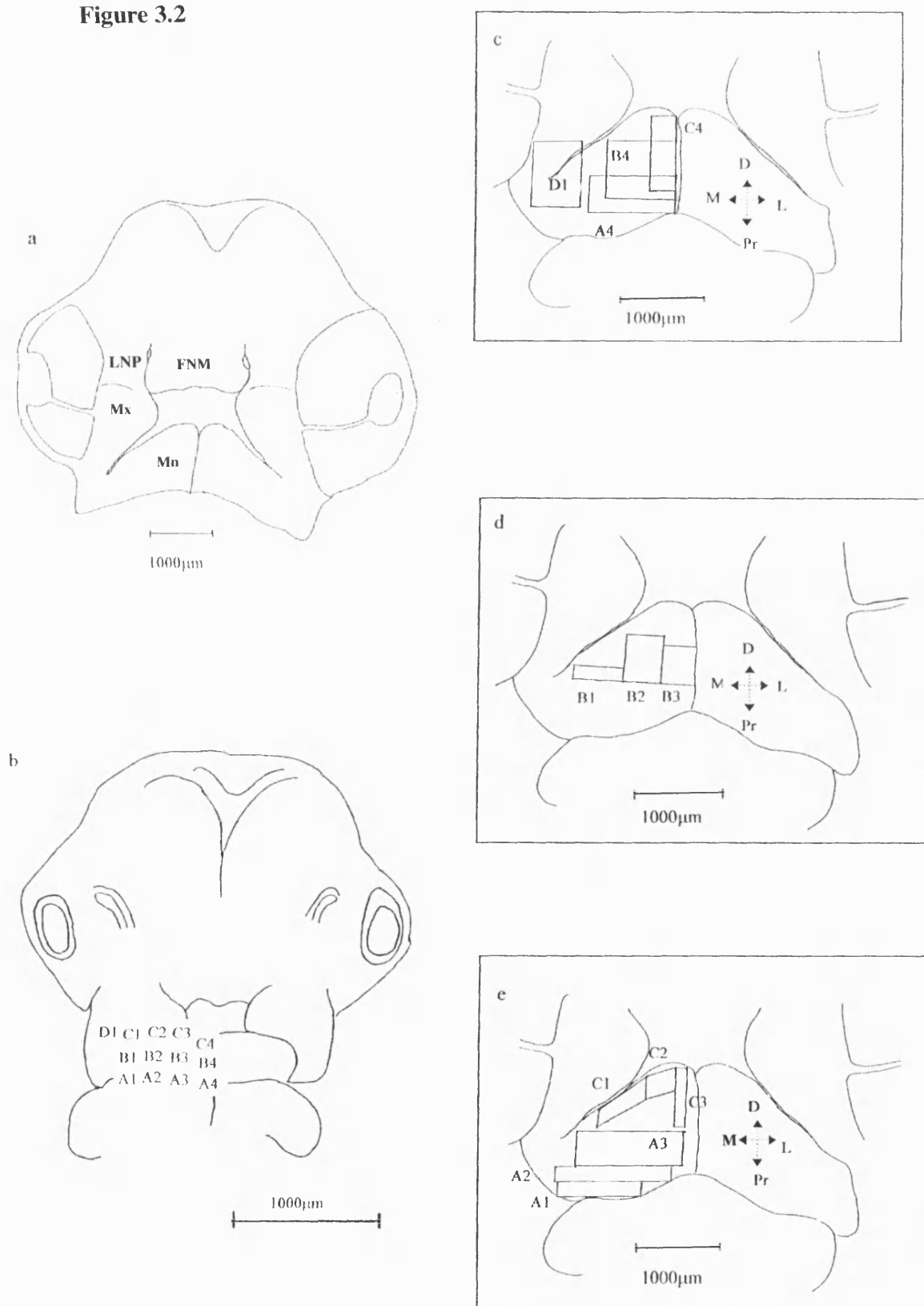
Figure 3.2

52
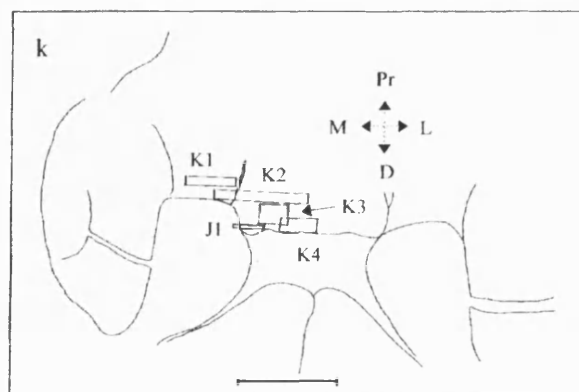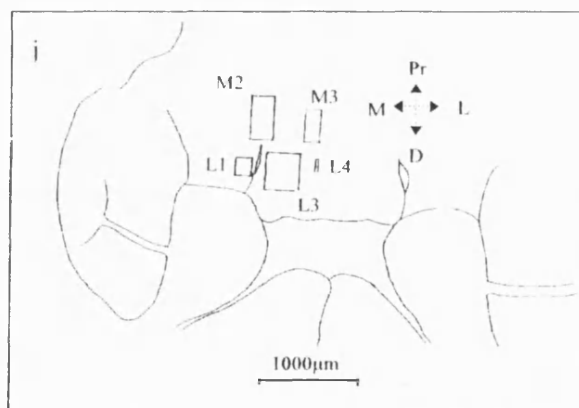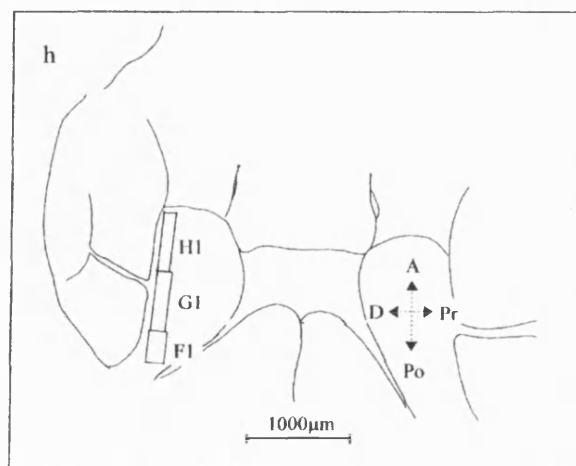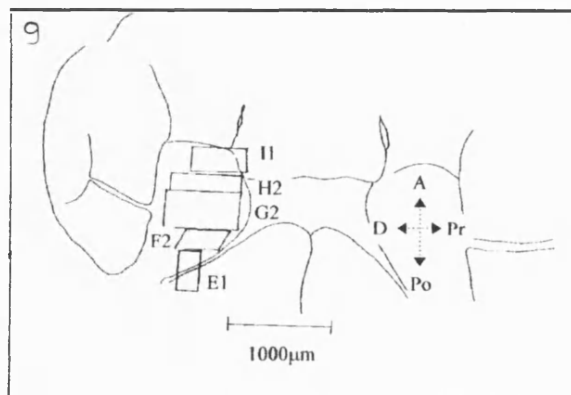
Figure 3.3 Photographs and diagrams of frontal views of chick embryo heads 48 hours after labelling with DiI at stage 20.

Dashed lines on diagrams Ai-Ji indicate area represented in photograph.

A and A(i) - DiI injected at position I1 and fixed immediately. Symmetrical spot of DiI in distal maxillary primordium, below the nasal pit.

B and B(i) - DiI injected at position C4 in mandibular primordium, fixed at 48 hrs. Streak of labelled cells extending from tip of primordium.

C and C(i) - DiI injected at position A4 in mandibular primordium, fixed at 48hrs. Streak of labelled cells extends laterally, from the midline, across the primordium.

D and D(i) - DiI injected at position D1 in mandibular primordium, fixed at 48hrs. Labelled populations extending as a "v" shaped streak into both maxillary and mandibular primordia.

E and E(i) - DiI injected at position G1 in the maxillary primordium, fixed at 48hrs. Streak of labelled cells runs parallel to the eye.

F and F(i) - DiI injected at position I1 in mandibular primordium, fixed at 48hrs. Indicates fate of labelled cell population shown in A/A(i). Cells, initially labelled in anterior distal maxillary primordium, move into the frontonasal mass as the primary palate forms.

G and G(i) - DiI injected at position L3 in the frontonasal mass, fixed at 48hrs. Streak of cells runs parallel to the nasal slit.

H and H(i) - DiI injected at position K3 in the frontonasal mass, fixed at 48hrs. Labelled cells extend mediolaterally, parallel to distal edge of the primordium, near the stomodeal cavity. Compare with J/J(i).

I and I(i) - DiI injected at position I1 in the maxillary primordium, treated with retinoic acid, fixed at 48hrs. Population expands but is unable to move into the frontonasal mass due to failure of fusion of primary palate. Compare with A and F, which show initial point of labelling and normal expansion of this population respectively.

J and J(i) - DiI injected at position K3 in the frontonasal mass, treated with retinoic acid, fixed at 48hrs. Population expands but has changed shape. Compare with H which indicates the normal direction of expansion of this population.

Figure 3.3

Figure 3.3

E

E(i)

G1

F

F(i)

I1

G

G(i)

L3

H

H(i)

K3

54
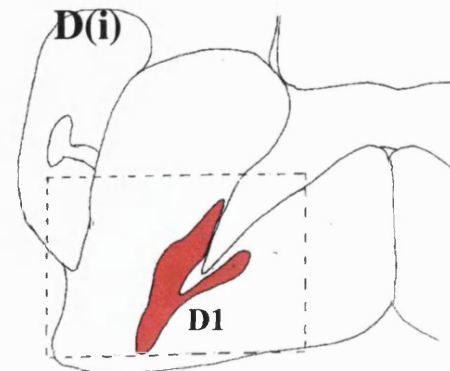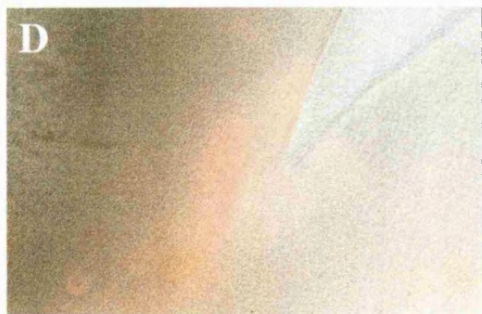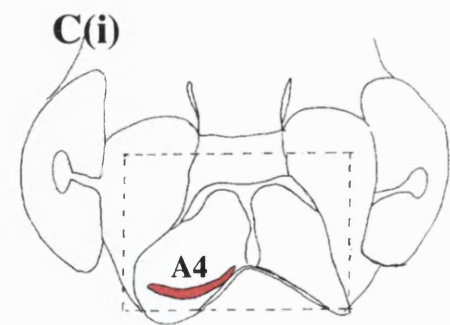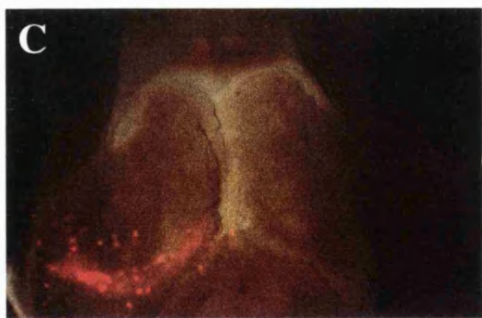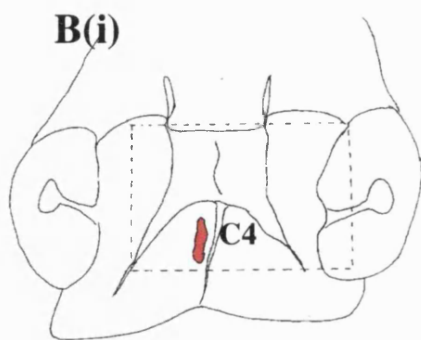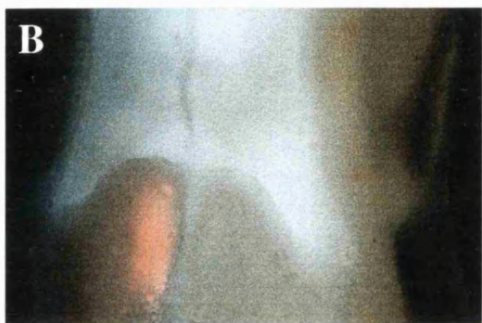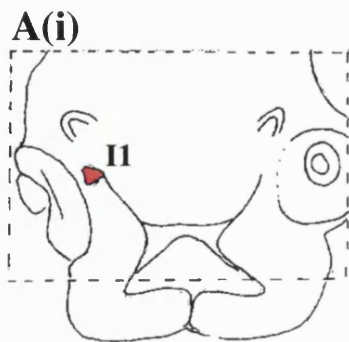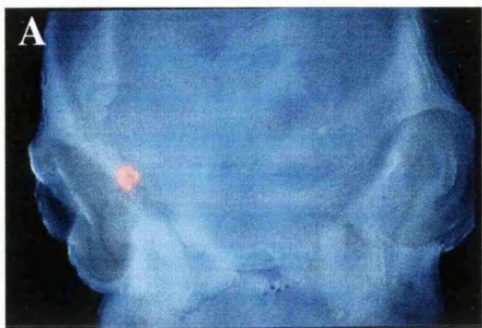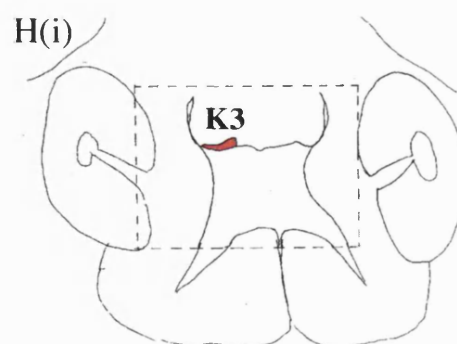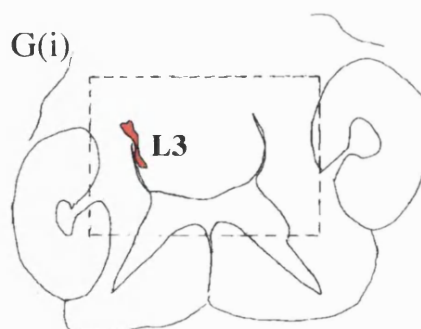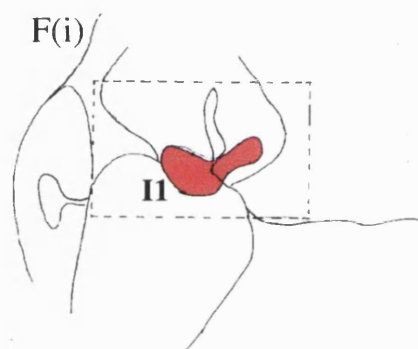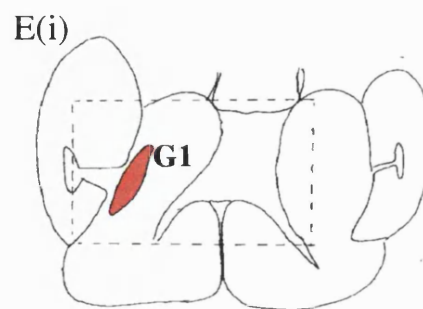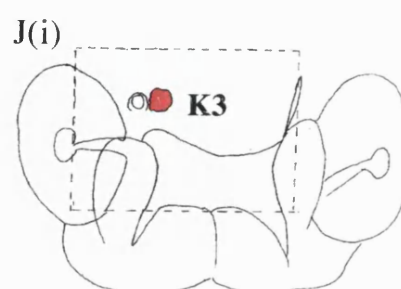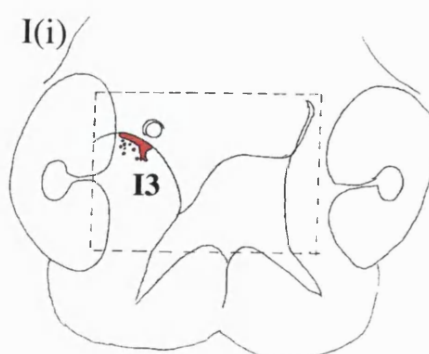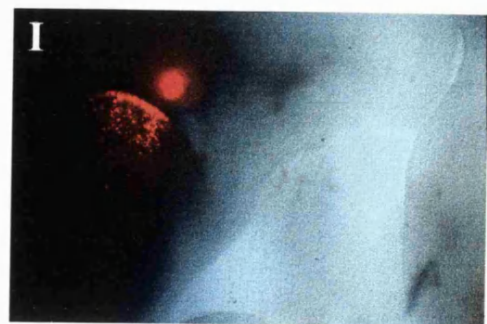
Figure 3.3

Figure 3.4 Semi-thin sections of stage 23 mandibular primordia

Sections are cut in the dorsoventral plane.

a. Diagram of frontal view of stage 23 chick embryo head, indicating facial primordia. Box indicates region of the mandibular primordium shown in b.

b. Enlarged view of stage 23 chick embryo mandibular primordium indicating the levels at which the sections in the accompanying figures were cut (black lines).

c. Low power view of section of mandibular primordium cut close to the distal tip. The paired primordia meet however, there is a clear epithelial seam between them, indicated by black arrow.

d. High power view of the same section as in d. This shows clearly the epithelia which separates the mesenchyme of the two paired mandibular primordia, black arrow.

e. High power view of section of stage 23 chick mandibular primordium, cut close to the proximal edge. There is no continuous epithelial seam extending between the paired mandibular primordia proximally. Epithelia are indicated by black arrows.

f. Low power view of section of stage 23 chick mandibular primordium, cut close to the proximal edge. This indicates that the mesenchyme of the two primordia are continuous, indicated by black arrow.

Figure 3.4
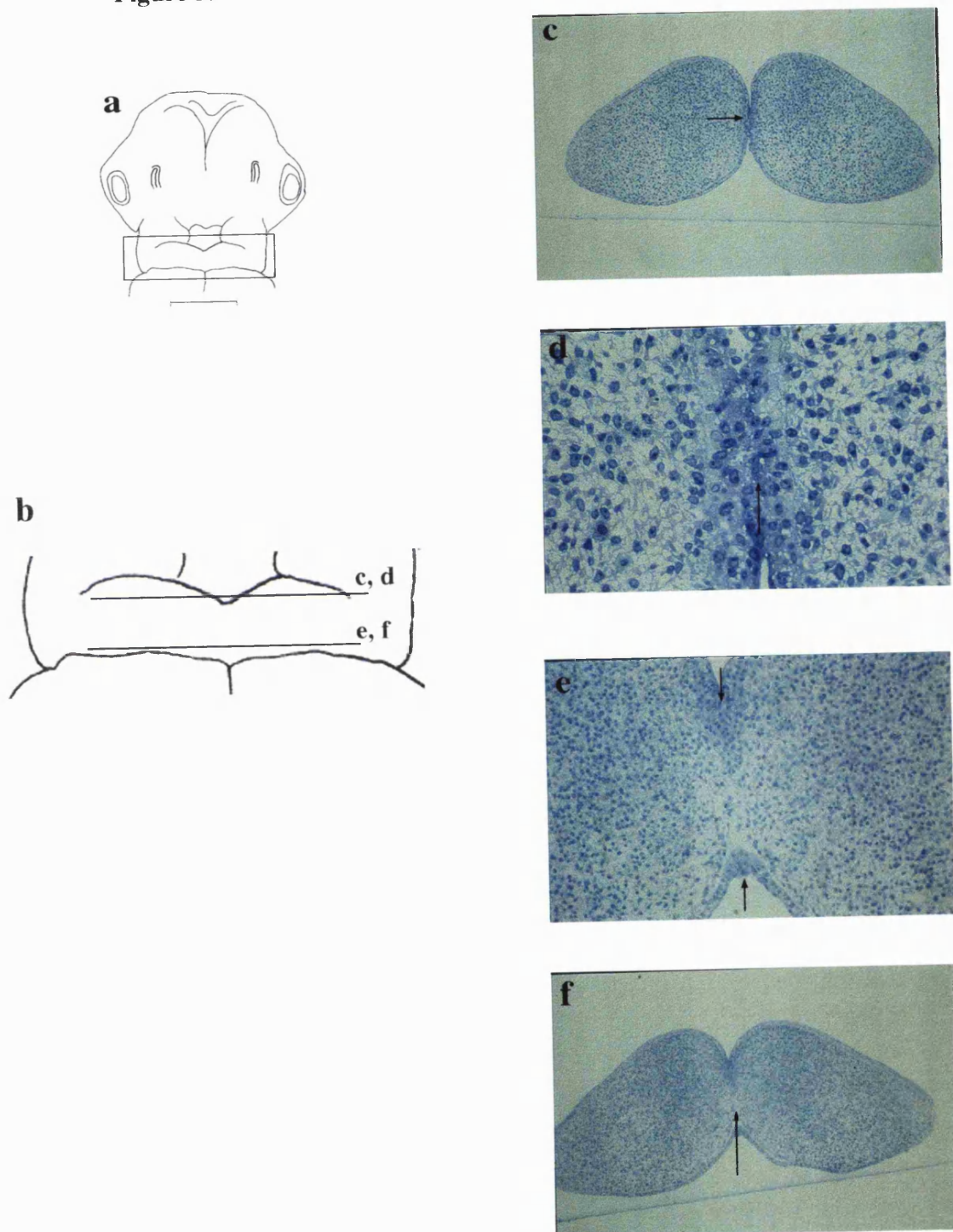
Figure 3.5 Frontal semi-thin sections of stage 26 and stage 28 chick embryo facial primordia

A. Diagram of stage 28 chick embryo facial primordium. This is to show the regions of the facial primordia shown in accompanying figures (black box).

B. Frontal section of the region where maxillary primordium and lateral nasal process join. There is a thick epithelial seam extending between the two primordia, indicated by black arrows. The frontonasal mass can be seen at the edge of the figure, right.

C. High power view of the join between maxillary primordium and lateral nasal process, clearly indicating an epithelial seam, black arrow.

D. Frontal section of stage 28 chick embryo facial primordia. This is a shallow section. The frontonasal mass and lateral nasal process are continuous, there is no epithelial seam separating them, indicated by white arrowhead. There is, however, an epithelial seam between the maxillary primordium and the lateral nasal process, indicated by black arrow.

E. Frontal section of stage 28/9 chick facial primordia, a deeper section than in D. In this section, the frontonasal mass, lateral nasal process and maxillary primordium have fused to form the primary palate, indicated by white arrowhead. The epithelial seam between the maxillary primordium and lateral nasal process has regressed in the region of the primary palate, but is still present more laterally, indicated by black arrow. Thus at this stage, deeper mesenchymal cells of the maxillary primordium and lateral nasal process merge.

Figure labels

Mx:	Maxillary Primordium	Mn:	Mandibular Primordium
LNP:	Lateral Nasal process	FNM:	Frontonasal Mass
NP:	Nasal pit		

Figure 3.5
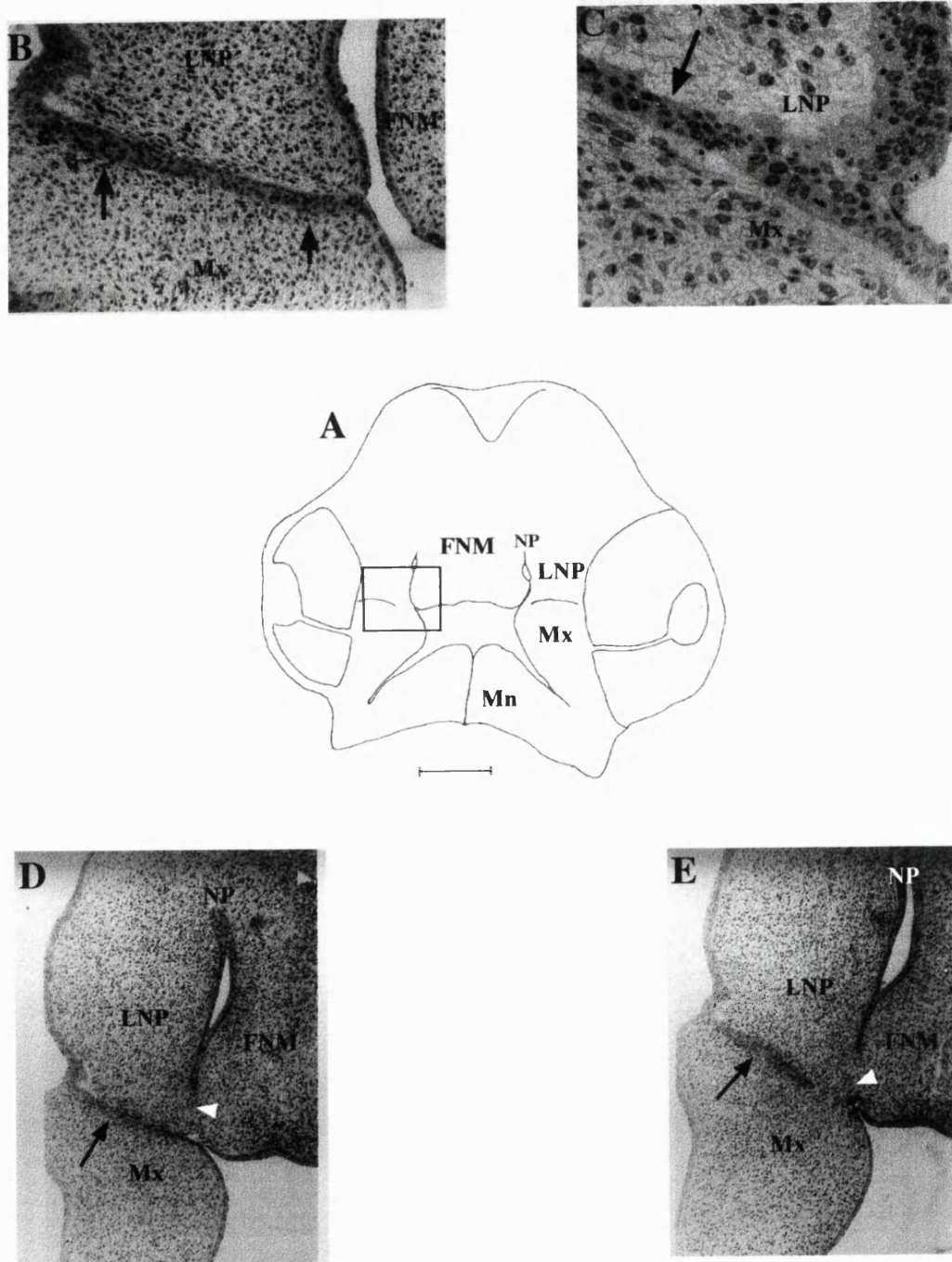
the jaw line. Spread of DiI labelled cell populations at these fusion points was extensive and much higher than that seen in neighbouring populations of both primordia.

3.3.1.2 Maxillary primordia

Expansion of marked cells in the maxillary primordium was considered in relation to anteroposterior axis (from the junction with the lateral nasal process to the junction with the mandibular primordium) and proximodistal axis (from base to distal tip of the primordium). Cells were marked at a series of positions proximally (F1, G1, H1) and along the distal tip (F2, G2 H2, Figs. 3.1c, 3.2f).

Cell populations marked in the proximal anterior part of the primordium, near to the developing eye (H1, G1, Figs. 3.1c, 3.2f) show marked anteroposterior expansion (Fig. 3.2h) giving rise to long streaks of labelled cells along the proximal edge of the primordium (Fig. 3.3E). Cells in the distal portion of the primordium (H2, G2, F2, Fig. 3.1c) exhibited predominant proximodistal expansion (Fig. 3.2g). Cell populations at the distal midpoint (G2) showed most expansion and those marked in the most posterior distal position (F2, Figs. 3.1d, 3.2g) less. In contrast, posterior proximal cell populations (F1) expanded least (Figs. 3.2h, 3.6d). Thus the maxillary primordium does not enlarge evenly, mid/anterior regions contribute more than posterior regions.

The maxillary primordium fuses with the median nasal process to form the primary palate and also merges with the mandibular primordium. Labelled cells at the anterior end of the primordium (I1 Figs. 3.1c, 3.2f) were found in the frontonasal mass (Fig. 3.3F) but cell populations marked further posteriorly along the distal edge (H2) were not. This suggests that fusion between maxillary primordium and frontonasal mass initially begins near the nasal slits and spreads posteriorly around the distal edge of the maxillary primordium. Maxillary cell populations labelled at the point of fusion with the mandibular primordium (E1) expanded into the mandibular primordia (Fig. 3.2g). The maxillary primordium also borders the lateral nasal process but mixing of these neighbouring cell populations (I1 and K2) was not observed. Frontal semi-thin sections of this border indicate that there is a deep epithelial seam between the maxillary primordia and the lateral nasal process at stage 28 (Fig. 3.5), which may prevent mixing in these regions.

Expansion of labelled cell populations in the third, dorsoventral, axis was examined. DiI labelled embryos were sectioned at stage 28 and five different points in the maxillary primordia (I1, G1, G2, H2 and F1) examined in a total of 16 embryos. The maximum depth of labelled cells was, on average, 285µm ± 75.7 and did not vary between different areas of the primordium. This shows that expansion in two dimensions truly reflects total expansion of labelled populations.

3.3.1.3 Frontonasal mass and lateral nasal processes

Proximally, cell populations were labelled above (M2) and medial to the top of the nasal slits (M3). More distally, lateral and medial points were marked on either side of the nasal pit (L1, L3 and L4). At the distal edge, cells were marked laterally (K1), at the open end of the nasal pit (K2) and medially (K3 and 4 Figs. 3.1b, 3.2i).

Cell populations marked above the nasal pits (M2, Figs. 3.1b; 3.2i) expanded proximodistally as the nasal pit lengthened, as did those more medially (M3) but to a lesser extent. The distal edge of both these cell populations remained level with the top of the nasal slits (Fig. 3.2j) indicating that deepening of the slits did not involve slit extension proximally. Labelled cell populations halfway along the proximodistal axis of the nasal pit (L1 and L3, Figs. 3.1b, 3.2i) gave rise to streaks running parallel to the nasal slits (Fig. 3.3G). Expansion on the lateral side of the nasal pit (L1, Fig. 3.2j) was more restricted than on the medial side (L3, Fig. 3.2j). In the centre of the frontonasal mass (L4 Figs. 3.1b, 3.2i), cell populations displayed little expansion (Fig. 3.2j) remaining as a small spot of labelled cells. Bordering the oral cavity, (K1 and K2, Figs. 3.1b, 3.2i) cell populations expanded mediolaterally, producing streaks running parallel to the distal edge of the presumptive upper beak (Fig. 3.2k). Labelled populations lateral to and directly underneath the nasal pit experienced greater total expansion than medial populations (K1 and 2 Fig. 3.6d).

Labelled cells from the median nasal process (K2 and 3) expanded into the lateral nasal process as the primary palate formed, but labelled cells from the lateral nasal process (K1) were not seen in the frontonasal mass (Fig. 3.2k). Cell populations marked directly below

Figure 3.6 Summary diagrams of direction and amount of expansion of DiI labelled cell populations in the stage 28 chick facial primordia compared to patterns of gene expression.

a. Summary of direction of expansion of cell populations in the stage 28 facial primordia. Blue arrows indicate predominant direction of expansion in different regions of each primordium.

b. Whole mount stage 25 chick face hybridised with chick *Msx-1* riboprobe. Transcripts are expressed in the distal tips of the mandibular primordium, the anterior maxillary primordium and in the lateral nasal process and frontonasal close to the nasal pits.

c. Stage 26 chick facial primordium hybridised with chick *Fgf-8* riboprobe. Transcripts are expressed around the nasal pits but are more abundant in the frontonasal mass than lateral nasal process. Expression is also seen at the join between mandibular and maxillary primordia.

d. Summary of total expansion of DiI labelled cell populations in the chick face. Populations coloured darker shades of green indicate greater expansion of cell populations 48 hours after labelling than those coloured lighter shades of green. Clusters of darker green populations are seen around the nasal pit and tip of the maxillary primordia in the upper face and at the proximal midline of the mandibular primordia in the lower face. Compare with b and c.

e. Summary of total expansion of DiI labelled cell populations in the chick upper beak primordia after retinoic acid treatment. This can be compared directly with d. Expansion is decreased in populations lateral to and underneath the nasal pit while expansion in most other populations is slightly increased or unchanged. Insert shows a retinoid treated face stage 28. Note the shorter, wider maxillary primordium and clefting of the primary palate on the right hand side of the face.

Mx:	Maxillary Primordium	Mn:	Mandibular Primordium
LNP:	Lateral Nasal process	FNM:	Frontonasal Mass

a

1000μm

b

LNP   FNM

Mx

Mn

c

LNP   FNM

Mx

Mn

d

M2   M3

L1   L3   L4
K1   K2   K3   K4

J1

I1
I2
H1   G5
G1
F1
E1   C3   C4
D1   C2   C1   C4
B1   B2   B3   B4
A1   A2   A3   A4

KEY: Spread of DiI as %
of area of primordium

20.1%-22%
10.1%-20%
5.1%-10%
3.1%-5%
0.3%-3%

1000μm

e

M2   M3

L1   L3   L4
K1   K2   K3   K4

J1

H1   H2
G1   G5
F1   F3

KEY: Spread of DiI as %
of area of primordium

20.1%-27%
10.1%-20%
5.1%-10%
3.1%-5%
0.3%-3%

1000μm

1000μm
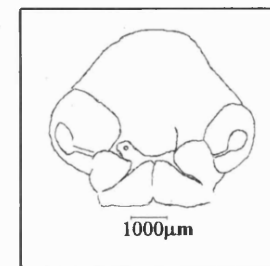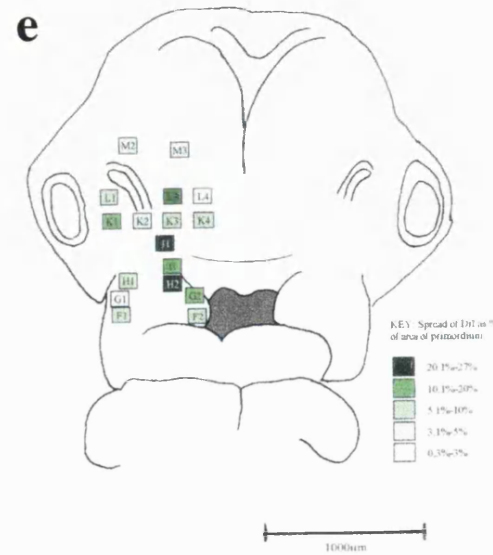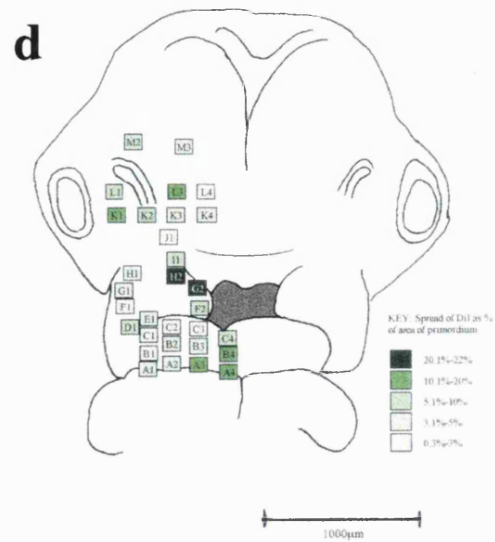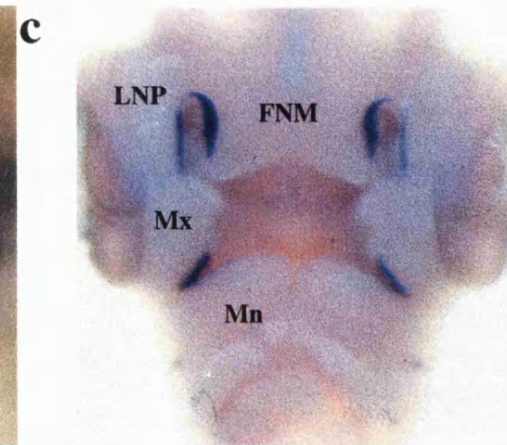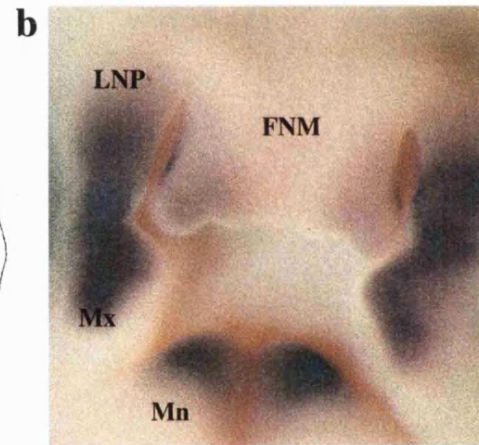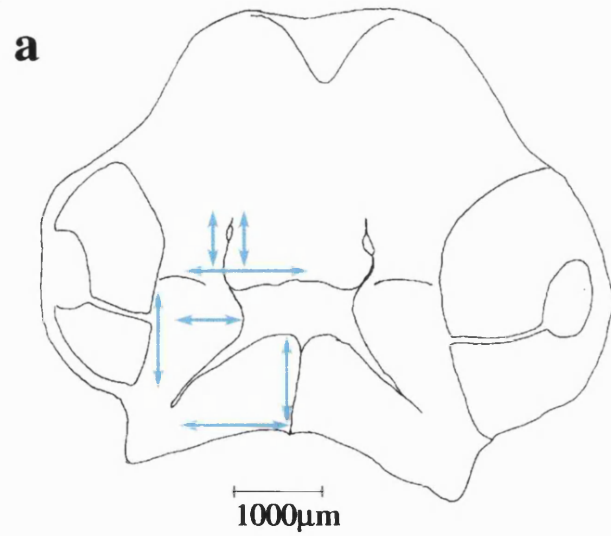
the open end of the nasal pit (J1) expanded mediolaterally to give a streak (Fig. 3.2k) with cells appearing in both maxillary primordium and frontonasal mass.

3.3.2 Expansion of facial primordia and patterns of gene expression

To further understand these results, we compared overall expansion of the facial primordia (Fig. 3.6d) with patterns of some genes that are known to be expressed in the developing face. Figure 3.6a summarises the predominant direction of expansion of regions in facial primordia and Figure 3.6d summarises the amount of expansion of cell populations in each primordium. We compared these summary diagrams with patterns of expression of *Msx-1*, a homeobox-containing gene expressed in the mesenchyme of chick facial primordia, and *Fgf-8*, a member of the Fibroblast Growth Factor Family, expressed in the facial ectoderm. *Msx-1* transcripts are found in many regions where mesenchymal expansion is substantial, for instance, the tips of maxillary and mandibular primordia and in tissues around the nasal pits (Fig. 3.6b). *Fgf-8* transcripts are found in the ectoderm overlying some regions of high mesenchymal expansion, for example, around the nasal pits (Fig. 3.6c). However, *Fgf-8* is not expressed, for example, in the midline ectoderm where the mandibular primordia join and considerable expansion takes place. Thus *Msx-1* expression correlates with all regions of greatest mesenchymal expansion, while *Fgf-8* is expressed in ectoderm overlying some, but not all, of these regions.

3.3.3 Analysis of cell proliferation in facial primordia at stage 24.

Cell proliferation was assessed in regions showing the highest and lowest expansion, as revealed by DiI labelling. Table 3.1 shows % cells in S phase which ranged from 15% to 35% in 16 different regions of the face. In the mandibular primordium, cell proliferation was found to be substantially higher in the medial proximal region (34.7%, A4) than in central (26.1%, B3) and lateral distal regions (19.7%, C2). In the maxillary primordium, cells in the mid distal region (33.8%, G2) proliferate more than in the proximal posterior region (28.7%, F1). The central region in the mid frontonasal mass, which hardly expanded at all, showed only slightly less proliferation (18%, L4) than most other populations examined in the frontonasal mass. The rate of cell proliferation either side of the nasal pit was similar (23.6%, L3 and 26.8%, L1) even though the medial

Table 3.1

Primordia	Grid Position	CONTROL		RA TREATED		% Change expansion	% change prolif.
		% Expansion	% Proliferation ± S.D.	% Expansion	% Proliferation ± S.D.		
Mandibular Primordium	A4	11.0 ± 4.9	34.7 ± 6.8	N/A	N/A	N/A	N/A
	B3	4.0 ± 1.2	26.1± 8.2	N/A	N/A	N/A	N/A
	C2	2.0 ± 0.7	19.7 ± 6.1	N/A	N/A	N/A	N/A
Lateral Nasal Process	K1	14.0 ± 3.0	23.7 ± 8.6	11.0 ± 5.0	18.6 ± 7.6	-3.0	-5.1
	L1	10.0 ± 1.4	26.8 ± 12.4	10.0 ± 1.4	N/A	0	N/A
Fronto Nasal Mass	K2	8.0 ± 4.5	20.4 ± 7.2	4.0 ± 0.2	17.4 ± 8.3	-4..0	-3.0
	K3	4.0 ± 0.2	19.0 ± 9.9	9.0 ± 2.8	19.8 ± 4.0	+ 5.0	+ 0.8
	K4	4.0 ± 1.7	18.2 ± 5.9	10.0 ± 2.1	19.6 ± 5.3	+ 6.0	+1.4
	L3	12.0 ± 2.8	23.6 ± 12.3	12.0 ± 0.7	N/A	0	N/A
	L4	18.0 ± 8.2	0.3 ± 0.03	3.0 ±0.7	N/A	+2.7	N/A
	M2	8.0 ± 1.7	19.3 ± 10.9	5.0 ± 0.1	17.3 ± 6.0	-3.0	-2.0
	J1	1.2 ± 0.2	14.5 ± 7.4	20 ± 5.6	21.3 ± 4.9	+18.8	+6.8
Maxillary Primordia	I1	9.0 ± 2.0	30.3 ± 9.6	17.0 ± 4.9	30.3 ± 7.1	+8.0	0
	G2	21.0 ± 1.4	33.8 ± 10.6	13.0 ± 4.0	17.4 ± 4.7	+8.0	-16.4
	G1	5.0 ± 2.1	22.5 ± 5.9	3.0 ± 0.6	20.4 ± 3.5	-2.0	-2.1
	F1	2.0 ± 0.7	28.7 ± 7.4	6.0 ± 2.6	27.8 ± 5.5	+4.0	-0.9

Comparison between the total expansion of cell populations and the % cells in S-phase in different regions of the normal face and in the face of retinoic acid treated embryos.

population expanded more than the lateral. In all cases, regions of highest proliferation correlate with regions of greatest expansion (compare data in Table 3.1 with Fig. 3.6d) but differences between populations was less than might have been predicted from the results of DiI labelling experiments .

3.3.4 Patterns of cell death in facial primordia

Cell death was examined at stages 24 and 28 in frontal frozen sections through the developing facial primordia. Results from both stages are summarised on the left in Figure 3.7A with black dots indicating mesenchymal cell death and grey dots epithelial cell death.

At both stages in the mandibular primordium, there was a central region of apoptotic mesenchymal cells (black dots), extending to the lateral edge (Fig. 3.7C) while in the maxillary primordium, little mesenchymal apoptosis was seen at either stages 24 or 28. In the upper face, at stage 24, mesenchymal apoptosis is seen in distal lateral nasal process bordering the maxillary primordium and also in the frontonasal mass running parallel to the nasal slits (Fig. 3.7B). By stage 28, mesenchymal apoptotic cells were observed at the top of the nasal pit in deeper sections and also at the centre of the frontonasal mass, away from the distal edge (Fig. 3.7A). This central region of the frontonasal mass exhibits very low expansion (Fig. 3.6d).

Epithelial apoptosis (grey dots, Fig. 3.7A, left side) was seen laterally in the mandibular primordium, in the anterior region of the maxillary primordium, bordering the lateral nasal process, and in the distal lateral nasal process at stage 24 (Fig. 3.7B). At stage 28, apoptosis was noted in epithelia where the mandibular and maxillary primordia join and also in the epithelia at the distal edges of frontonasal mass, at the edges of the lateral nasal process and distal anterior maxillary primordium (Fig. 3.7A) where fusion to form the primary palate occurs.

3.3.5 Behaviour of cells in embryos treated with retinoic acid.

In order to investigate the cellular basis of the shape changes that lead to facial clefting, stage 20 embryos were treated with retinoic acid and immediately injected with DiI as before. Only embryos displaying the characteristic defect at stage 28 were evaluated.

Figure 3.7 Patterns of cell death in stage 24 and stage 28 facial primordia.

A. Diagram of frontal view of stage 28 embryo face. Black dots indicate areas of mesenchymal apoptosis found at stages 24 and 28 and grey dots indicate epithelial apoptosis found at stages 24 and 28. The left side of the diagram indicates the pattern of apoptosis found in the normal chick embryo facial primordia while the right side indicates the pattern of apoptosis seen after application of retinoic acid.

B. Apoptotic cells in frozen sections of the normal chick face. Mesenchymal apoptosis is seen in the frontonasal mass whilst both mesenchymal and epithelial apoptosis occurs in the lateral nasal process. Only epithelial apoptosis is seen in the maxillary primordium at stage 24.

C. Apoptotic cells in frozen sections of the normal chick face. Mesenchymal apoptosis is seen in the centre of the mandibular primordium at stage 28.

D. Apoptotic cells in frontonasal mass treated with retinoic acid. Mesenchymal apoptosis is seen in the centre of the frontonasal mass, as in the normal stage 28 embryo. However, unlike the normal pattern, apoptotic cells are situated laterally, towards the nasal pit. White arrowhead indicates the edge of the bead soaked in retinoic acid placed in the nasal pit.

E. Apoptotic cells in chick facial primordia treated with retinoic acid. Mesenchymal and epithelial apoptosis is induced in the anterior proximal region (Pr) of the maxillary primordium at stage 24. There is comparatively little apoptosis distally (D), as in the normal embryo.

Figure labels

Mx:	Maxillary Primordium	Mn:	Mandibular Primordium
LNP:	Lateral Nasal process	FNM:	Frontonasal Mass
NP:	Nasal pit		

Figure 3.7
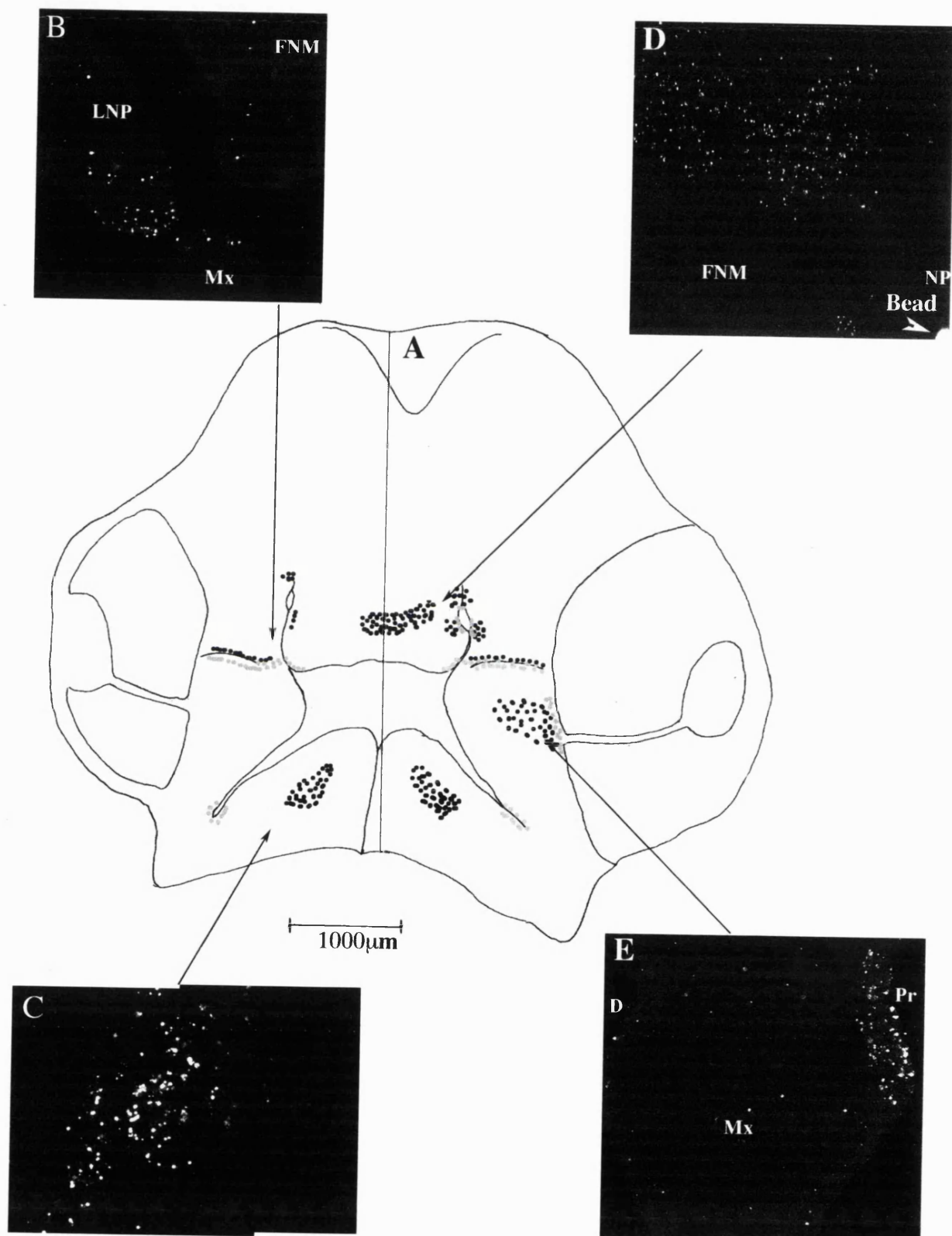
Expansion of DiI labelled populations on the treated side of the face is expressed as a percentage of normal dimensions to enable a direct comparison between these data and those for normal facial development (above) see also appendicies 4, 5. These data were also analysed to assess uniformity in the shape of labelled cell populations (Table 3.2). Patterns of cell proliferation (Table 3.1) and cell death (Fig. 3.7A) were also examined.

A few populations made a reduced contribution to expansion of the face, particularly those lateral to and underneath the nasal pit (K1 and K2) and in the central maxillary primordium (G1 and G2 Table 3.2, Fig. 3.6e, table 3.2). Reduction in expansion in lateral nasal process and beneath the nasal pit was associated with a slight decrease in cell proliferation and in maxillary primordium, also with ectopic cell death (Table 3.1; Fig. 3.7E). At the most anterior distal point of the maxillary primordia (I1) cells were prevented from moving into the frontonasal mass by failure of frontonasal mass and maxillary primordium to appose (Fig. 3.3I). Here, expansion of labelled populations appeared to have increased at the open end of the gaping nasal slits. It is interesting to note, however, that epithelial cell death still occurs at the edges of the frontonasal mass maxillary primordium, lateral nasal process even though apposition does not occur.

Generally, other cell populations of the upper beak primordia which are further away from the source of retinoic acid, expansion more uniform than directed. Most of these cell populations also increased their total expansion slightly, thus covering a larger area of the primordia than in the normal embryo (Table 3.2 and Fig. 3.6e). The population at the distal midline of the frontonasal mass even changed its predominant direction of expansion from mediolateral to proximodistal (K4 Table 3.2). Thus both primordia became shorter, wider, and more spherical upon retinoic acid treatment (Fig. 3.6e insert) but patterns of cell proliferation and cell death were generally little changed (Table 3.1, Fig.3.7A).

Table 3.2 Comparison of characteristics of DiI labelled cell populations in the upper beak primordia between normal embryos and embryos treated with retinoic acid (RA) in the nasal pit at stage 20.

POSITION OF DiI LABEL	COMPARATIVE SIZE AND SHAPE OF DiI LABELLED CELL POPULATIONS		#	SPREAD OF DiI AS % OF AREA OF PRIMORDIUM		RATIO OF LENGTH:WIDTH OF DiI LABELLED CELL POPULATION (* indicates an increased uniformity in shape).	
	NORMAL	RA		NORMAL	RA	NORMAL	RA
I1			+++	9	17	0.25	0.46*
H1			+	5	8	2.70	0.70*
G1			-	5	3	2.33	1.00*
F1			++	2	6	1.29	0.85*
H2			+	24	27	0.43	0.23
G2			- - -	21	13	0.32	0.28
F2			+	6	7	0.35	0.50*
M2			-	8	5	3.80	0.96*
M3			=	4	4	3.7	1.28*
L1			=	10	10	1.54	1.10*
L3			=	12	12	2.08	1.33*
L4			+	0.3	3	8.00	0.78*
K1			-	14	11	0.23	0.73*
K2			—	8	4	0.17	1.16*
K3			++	4	9	1.32	1.30*
K4			++	4	10	0.83	2.74*
J1			++++	1.2	20	0.19	0.64*

#
+/-   increase/decrease by 0.1-3% in area of population after 10mg/ml retinoic acid treatment.
++/--   increase/decrease by 4-6% in area of population after 10mg/ml retinoic acid treatment.
+++/---   increase/decrease by 7-9% in area of population after 10mg/ml retinoic acid treatment.
++++   increase by 9+% in area of population after 10mg/ml retinoic acid treatment.

3.4 DISCUSSION

3.4.1 Patterns of expansion within facial primordia

Shaping of facial primordia is dependent on local differences in expansion. During the period studied, the mandibular primordium changes from a rounded mass to a larger, elongated triangular shaped structure. My DiI labelling study shows that medial cell populations, particularly proximally, contribute much more to enlargement of the primordium than lateral populations. Cell populations labelled distally, in the mandibular primordium, expanded predominantly in a proximodistal direction. The maxillary primordium elongates and broadens between stages 20 and 28. Unexpectedly, the anterior half of the primordium contributes much more to total expansion than the posterior regions. Distal maxillary populations exhibited predominant expansion along the proximodistal axis which suggests that, as in the mandibular primordia, outgrowth involves cell populations at tips of this primordium. However, in the frontonasal mass and lateral nasal process, in contrast to maxillary and mandibular primordia, distal populations are not involved in proximodistal expansion. Instead distal populations showed predominant mediolateral expansion, causing jutting out laterally of the frontonasal mass, leading to broadening of this primordium. Lengthening of the frontonasal mass accompanies elongation of the nasal pits into slits. Cell populations marked midway along the proximodistal axis of the slits expanded predominantly in this direction. Therefore outgrowth along the proximodistal axis of the frontonasal mass and lateral nasal process involves cell populations that lie at a distance from the distal tips. Cell populations bordering the nasal pits dominated total expansion, while the midline cell populations of the frontonasal mass expanded very little.

3.4.2 Contribution of cell proliferation and apoptosis to shaping of facial primordia

Several processes may influence shaping of primordia including cell proliferation, cell death (apoptosis), and cell rearrangements. Changes in cell proliferation have been shown to be involved in limb budding, where proliferation is maintained in presumptive limb

regions but decreases in interlimb regions (Searls and Janners, 1971). Cell death is known to play a role in shaping of many parts of the embryo, such as the limb (Fallon and Saunders, 1968, Ganan *et. al.*, 1996) where, for example, it leads to regression of soft tissues between the digits. Cell rearrangements are important in convergence and extension movements that take place during gastrulation (Keller and Danilchick, 1988).

My analysis shows that cells throughout the face at stage 24 are undergoing proliferation. My data on S phase labelling are similar to those reported for chick stage 24 maxillary primordia (Minkoff, 1980) and mandibular primordia (Barlow and Francis-West, 1997). Rather surprisingly, however, although we found that proliferation is highest in regions of greatest expansion e.g. proximal medial edge of the mandibular primordium, anterior maxillary primordium and regions around the nasal pits, the difference between levels of proliferation here and those seen in regions of the face which expand least were not very great. In some regions of low expansion, such as central regions of frontonasal mass and mandibular primordium, mesenchymal apoptosis was also detected and this could magnify small differences in proliferation. It is not clear whether these minor differences in cell proliferation and cell death, even taken together, could account for the large differences in expansion we observed in different facial regions.

My results suggest that cell intercalation and rearrangements could also contribute to expansion of the face because expanding cell populations clearly overlap and intermingling is seen between labelled and non-labelled cells. Cell intercalation could either drive or be driven by stretching of the primordium and many of the cell populations that undergo greatest expansion are those which expand most non-uniformly. It has been hypothesised that the frontonasal mass could be stretched by the enlargement of the underlying forebrain (Patterson and Minkoff, 1985) which allows for intercalation to occur.

3.4.3 Fusion of facial primordia

A major feature of facial morphogenesis is the fusion of neighbouring primordia, initially involving epithelial interactions followed, in some cases, by merging of

mesenchymal cell populations. Cell populations near points of fusion generally showed greater expansion compared with neighbouring cell populations. Observations on shaping of facial prominences in human embryos suggested that merging of two adjacent primordia involved regions of high proliferation while neighbouring cell populations proliferated less (Streeter, 1948, Patten, 1961). More recently, Minkoff (1980) found higher rates of proliferation in areas of the chick face where primordia attach to each other.

Three patterns of mesenchymal cell behaviour were observed at points of fusion or merging. Unidirectional migration of cells was observed from frontonasal mass into lateral nasal process but not vice versa. Patterson et. al., (1984) also observed lateral movement of mesenchyme into lateral nasal process and suggested that it played a role in reorientation of the invaginating nasal pits and in producing a more prominent lateral nasal process. Bi-directional cell mixing was observed between anterior maxillary primordium and distal frontonasal mass and between mandibular and maxillary primordia. This mixing indicates that these mesenchymal cell populations do not represent separate lineage restricted compartments and has implications for understanding maintenance of discrete patterns of gene expression in cells of different primordia. Cells were also seen to cross the midline at the junction between the paired mandibular primordia. Finally, no mixing of cell populations between lateral nasal process and maxillary primordium was detected. A lack of mixing between these two populations was also noted by Patterson et. al., (1984). I have shown, in semi-thin sections, that there is an epithelial seam between these two primordia which may be preventing mixing of mesenchymal cell populations.

Traffic of cells at the junction of the paired mandibular primordia was restricted to proximal regions. Histological examination shows that an epithelial seam is present only very distally at stage 23, implying that this does not prevent movement of mesenchyme in this region up to stage 28. Movement of proximal cell populations appears to reflect the fact that fusion begins proximally and proceeds in a proximal to distal direction. During primary palate fusion, mixing of cell populations was also seen only in proximal regions. This suggests, by analogy with the mandibular primordium, that fusion again proceeds proximally to distally, away from the open end of the nasal pit. However scanning

electron microscopy studies suggested that fusion to form the primary palate occurs in the opposite direction in the mouse (Kosaka *et. al.,* 1985, Kosaka and Eto 1986). It would be of interest to carry out DiI labelling experiments in mice to test whether cells mix distally.

Epithelial cell death in the chick face appears to occur in regions where primordia fuse and may be part of the mechanism by which epithelial seams break down. I observed epithelial apoptosis in the anterior maxillary primordium and the lateral edge of the frontonasal mass, which fuse to form the primary palate and where bi-directional cell movement occurs. This pattern of epithelial cell death is similar to that previously reported in the fusing rat primary palate (Pellier and Astic, 1994). Epithelial apoptosis also occurs prior to and during fusion of the secondary palate (Ferguson 1988; Mori *et. al.,* 1994). Fusion of the paired mandibular primordia in the mouse is thought to occur by epithelial cell migration alone (Chai *et. al.,* 1997) and it is therefore interesting that we failed to detected any epithelial apoptosis in this region of the chick.

3.4.4 Signalling molecules and control of expansion

Local availability of molecules such as growth factors and ability of cells to respond to them are key factors which may underlie differences in growth within and between facial primordia. It is therefore of interest to compare my fate map with patterns of expression of growth factors, their receptors and other signalling molecules.

Transcripts of a fibroblast growth factor *Fgf-8* are expressed in ectoderm overlying facial primordia, specifically in the ectoderm at the posterior distal edge of the maxillary primordium and in ectoderm overlying the nasal pit (Ohuchi *et. al.,* 1994, Heikinheimo *et. al.,* 1994, Crossley and Martin 1995, Wall and Hogan, 1995). This pattern of expression correlates with some, but not all, of the areas found by our study to undergo greatest expansion, suggesting a role for *Fgf-8* in maintenance of mesenchymal cell proliferation. Expression of *Fgf-8* is greater on the medial side of the nasal pit than the lateral and my data suggest that the expansion is greater medially than laterally. Members of the Bone Morphogenetic family of signalling molecules may modulate cell proliferation during development (Niswander and Martin 1993). Genes encoding BMP-2, BMP-4 and BMP-7 are expressed in the developing chick face between stages 18-28 (Francis-West

et. al., 1994, Wall and Hogan 1995) in regions of high expansion. Application of BMP s to the face increases cell proliferation and induces expression of *Msx-1* (Barlow and Francis West 1997). The pattern of expression of *Msx*-1 (and the related *Msx-2*) in the mesenchyme of the face closely correlates with areas that, from this study, expand most. It is also interesting to note that *Msx-1* is expressed in the anterior maxillary primordium rather than the posterior since my study has shown that the anterior portion makes a greater contribution to the face.

Another type of signalling found in the embryos is direct cell-cell signalling, for example, through gap junctions. Distribution of gap junctions has been reported to be restricted in the maxillary primordium (Minkoff, 1983) and are found mainly in regions that were found to expand the most by DiI labelling. This may indicate an important role for gap junctions in maintaining local differences in expansion of facial primordia.

3.4.5 Alteration in patterns of facial expansion, by retinoic acid, suggests that shaping forces may be due to interaction of primordia.

Local application of retinoic acid to the chick embryonic face produced marked changes in expansion of labelled cell populations in the three primordia that form the upper beak. Expansion was reduced in cell populations near the retinoid source (anterior distal maxillary primordium and those populations immediately below and lateral to the open end of the nasal pit). No additional cell death was detected in these regions but cell proliferation was reduced. The regions that are affected are those that express the retinoic acid receptor RARβ (Rowe *et. al.,* 1992) and retinoic acid treatment also results in reduced levels of *Msx-1* and *Msx-2* in these regions (Brown *et. al.,* 1997). Transgenic mice in which both *Msx-1* and *Msx-2* are functionally inactivated display clefts of the primary palate (R. Mass, Boston, pers comm). Taken together, this suggests that outgrowth of facial primordia to form the primary palate is dependent on *Msx* gene expression in cell populations at the distal anterior maxillary primordium and at the open end of the nasal pit. A recent study has also proposed that changes in *sonic hedgehog* (*shh*) expression in the endoderm may also play a role in facial clefting (Helms *et. al.,* 1997).

I found changes in behaviour of cell populations at some distance away from the retinoic acid soaked beads. Cell populations lying between the open end of the nasal slit and maxillary primordium unexpectedly showed increased expansion. Also instead of directed expansion, more uniform, or in a few cases expansion in the opposite direction, occurred in distal regions of the upper face. The maxillary primordium has no intrinsic shape (Richman and Tickle 1992) and tends to become a uniform ball of tissue when isolated from the face. Thus the more uniform expansion of the individual cell populations and overall expansion of the primordium seen upon retinoic acid treatment may be due to reduced tension forces in the primordium as a result of failure of primary palate fusion and lack of normal anchoring to the frontonasal mass. This is consistent with the idea that face shape is dependent on global forces generated between neighbouring tissues.

Chapter Four - The role of Connexin 43 and Connexin 32 in shaping and fusion of chick facial primordia.

4.1 INTRODUCTION

In chapter 3, I mapped the expansion of cell populations in different regions of the face. As discussed, local expansion could be mediated by spatially and temporally restricted expression of molecules that control cell behaviour in either mesenchymal or ectodermal cells, or both. These molecules could control cell proliferation, cell death and cell rearrangements and these cellular activities would have to be locally co-ordinated. There are many different methods of signalling which are utilised in the developing embryo to coordinate cell activities. One method of signalling is direct cell-cell signalling which only occurs between neighbouring cells in contact and one such type of cell-cell signalling occurs via gap junctions.

4.1.1 The structure of gap junctions

Gap junctions are made from protein subunits called connexins which are inserted into the cell membrane. All connexin proteins in cell membranes consist of four transmembrane domains, two extracellular loops, one intracellular loop and intracellular amino and carboxyl terminals (Milks et. al., 1988, Kumar and Gilula 1996), illustrated in Figure 4.1a. The majority of the protein is highly conserved between vertebrate species with the exception of the cytoplasmic loop and carboxy terminal (Bennett et. al., 1991).

Connexins aggregate symmetrically into units comprised of six proteins, forming a hemichannel hexameric connexon, Fig. 4.1b (Unwin and Zampighi 1980). These connexons are generally thought to be formed from a single connexin protein type (homomeric connexons). Heteromeric connexons, containing more than one type of connexin protein have been found rarely in vivo (Jiang and Goodenough 1996).

Figure 4.1a. Structure of a connexin protein in the cell membrane.

All connexin proteins form this structure in the membrane. There are two extracellular loops, which are the sites of docking with other connexins from adjacent cells, and one intracellular loop. Both the N and C terminals are intracellular. All connexin types share highly conserved amino acid sequence, differing only in the cytoplasmic loop and C-terminal region. The diagram also shows the regions of the protein against which the two antibodies used in this chapter, Gap 15 (connexin 43) and Des 5 (connexin 32), were raised.

Figure 4.1b. Formation of gap junctions between two adjacent cells.

This diagram illustrates the relationship between connexins, connexons and gap junctions. Connexons are formed by the aggregation of six connexin proteins. Connexons from two neighbouring cells dock in the extracellular space to form a continuous channel between the cells known as a gap junction.

Figure 4.1

a Structure of a connexin protein in the cell membrane

Extracellular space

Cell membrane

Des 5

Cytoplasm

NH2

Gap 15

COOH

b Formation of gap junctions between two cells

Cell Membranes

Connexon
pore

Two connexons 'dock'
together to form a channel
between cells
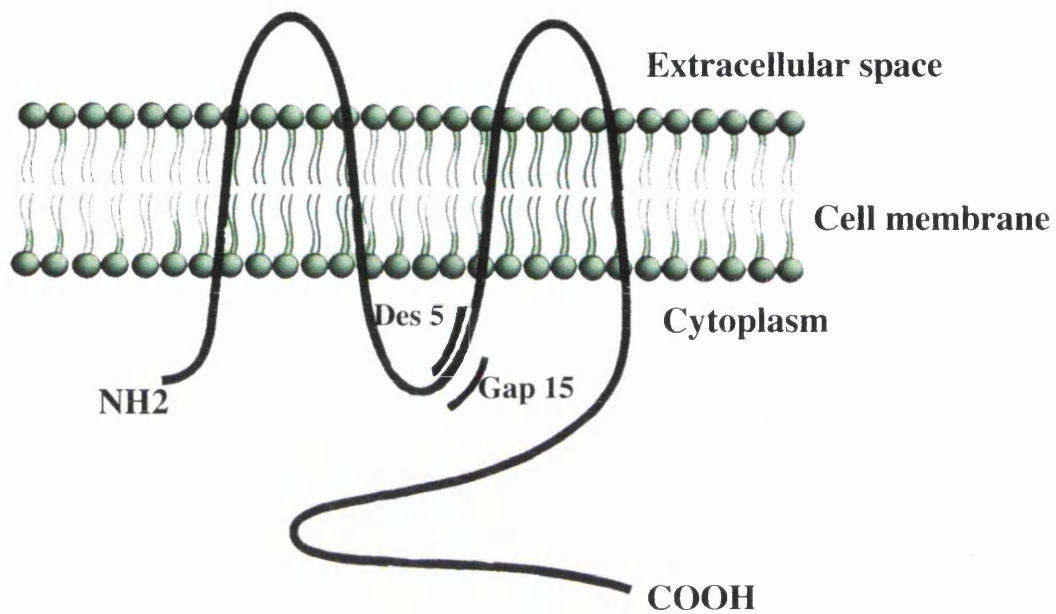
Connexon
comprised from
six subunits
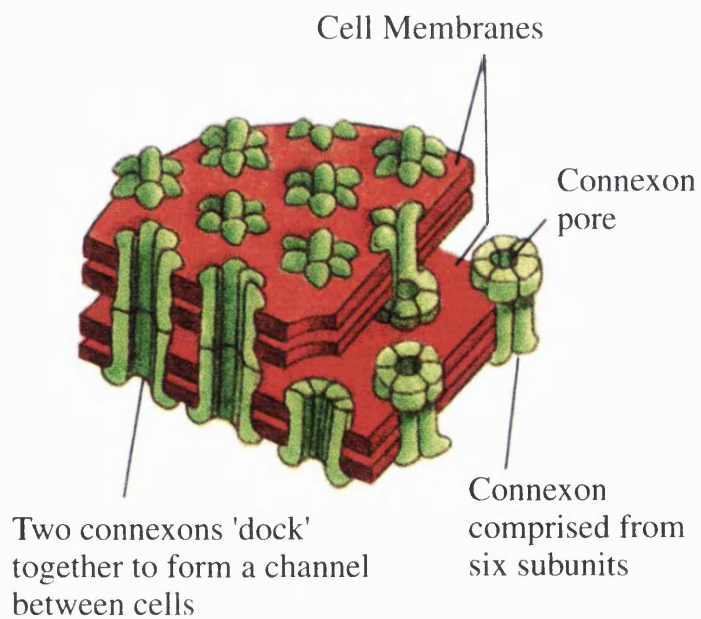
Two connexons dock by their extracellular portions (Dahl *et. al.*, 1994, Warner *et. al.*, 1995) to form a gap junction pore between two cells.

Gap junctions can be formed by two connexons containing the same connexin protein type known as homotypic gap junctions, or by two connexons from different connexin proteins known as heterotypic gap junctions. There is also the possibility that heteromeric connexons from each cell could form a heteromeric gap junction channel (White and Bruzzone 1996). However, not all types of connexins can interact to form functional channels *in vitro* (for review of connexin compatibility see Bruzzone *et. al.*, 1996, White and Bruzzone 1996). This variation in compatibility between connexins may allow the establishment of communication compartments in tissues without the presence of a physical barrier (Warner *et. al.*, 1984, Guthrie, 1984, Warner 1985, Lo and Gilula, 1979). These compartments may have important functions during development such as in co-ordination of cell proliferation within a population or specification of lineage compartments.

4.1.2 Gap junction communication

The result of the docking of two connexons is the formation of pore between the two cells which allows the diffusion of ions, metabolites and second messengers such as cAMP and IP_3 up to 1kD molecular weight between cells (Simpson *et. al.*, 1977, Flagg-Newton *et. al.*, 1979). The presence of gap junctions and passage of such molecules between cells is thought to be important in many processes such as the control of cell proliferation and differentiation (Lowenstein, 1981). Experiments have also shown that they may play a role in patterning and induction during development (Warner *et. al.*, 1984, Guthrie and Gilula 1989).

The function of each type gap junction channel is measured in two ways. The conductance is measured by electrophysiological methods and the permeability is assessed by the transfer of non-membrane permeable low molecular weight fluorescent dyes. The unitary conductance or flux of ions (in picosiemens, pS) across a single gap junction, has been found to range from 30-300pS depending on the connexin types forming the channel, suggesting wide variation in diameter of the channel pore (Veenestra 1996). It

has also recently been shown that gap junctions can have different selective permeability for a molecule, depending on the size and charge of that molecule (Elfgang *et. al.*, 1995). This selectivity again is related to the types of connexin forming the channel. Unexpectedly, permeability is not related to the unitary conductance/channel diameter suggesting that the charge of the molecule is important for selectivity (White and Bruzzone 1996, Vennestra 1996). Unidirectional coupling has also been observed between different types of oligodendrocytes in the retina, indicating a further refinement in the level of communication between different cell types (Robinson *et. al.*, 1993). Thus, expression of gap junction in a cell can confer restrictions on communication depending on the functional characteristics of the homotypic and/or heterotypic channels that they can form with their neighbouring cells and the direction of conductance between them.

4.1.3 Regulation of gap junction formation and channel function

Gap junctions are not static and their conductance can change in response to a variety of external factors. Many factors affect the rate of formation of gap junctions such as the presence of adhesion molecules, such as E-cadherin and CAMs, which increase coupling (Mège *et. al.*, 1988, Jongen *et. al.*, 1991). Extracellular calcium levels were shown to either increase or decrease the rate of channel formation depending on the cell type (Jongen *et. al.*, 1991, Dahl *et. al.*, 1992). A second level of control of signalling through gap junctions occurs after channels have formed, through gating or closing of the channel. Increased cytoplasmic calcium levels decreases conductance (Lowenstein, 1981, Bennett *et. al.*, 1991). Decreased pH can also decrease gap junction coupling in early *Xenopus* embryos (Turin and Warner 1977, 1980). Closure of most gap junction channels is voltage dependent (see for example Harris *et. al.*, 1981) and heterotypic channels have unique voltage gating properties compared to homotypic channels formed by single connexin types (see for example Barrio *et. al.*, 1991, Hennemann *et. al.*, 1992). Phosphorylation of the connexin protein also modulates the activity of gap junction channels. In some cell types, such as hepatocytes which express connexins 26 and 32, phosphorylation by cAMP dependent protein kinase results in increased conductance (Säez *et. al.*, 1986). In other tissues, such as uterine muscle, which expresses connexin

43, phosphorylation by cAMP dependent protein kinase inhibits conductance (Cole and Garfield 1986). Thus the response to phosphorylation is connexin and tissue specific (see also Bennett *et. al.*, 1991 for review). In all cases of regulation of gap junction activity, the sensitivity depends on the type of connexin forming the gap junction. It must be noted, however, that many of the experiments described above have been performed in artificial systems, such as expression in *Xenopus* oocytes, and we cannot be sure that they reflect the physiological state. However, the formation, function and gating of gap junction channels is a highly complicated, regulated system, allowing restricted passage of information between cell populations which is dependent not only on the types of connexins that they express but the cellular environment as well.

4.1.4 Techniques for studying roles of genes and gene products

Assigning exact functions to particular connexins and gap junctions that they form during development has proved difficult due as to the widespread and overlapping expression of many connexin proteins and the complex nature of gap junction communication and regulation. Recent advances in molecular biology techniques have allowed the exact roles of genes and their products during development to be defined by removal or inactivation of the gene or gene product in the developing embryo. Several different approaches can be made to remove or inactivate molecules in a developing system at the DNA level or the protein level.

4.1.4.1 Functional inactivation.

Achieving complete removal of a molecule from a developing system requires inactivation at the DNA level in the very initial stages of development. This technique, functional inactivation or "knockout" of a gene has inherent problems such as lethality if the gene is essential in early development. Often, the complete function of the gene is not always fully revealed which is presumably due to compensation between related gene products. This has been indicated in experiments where disruptions of single genes have little or even no effect on development but disruption of two (or more) related genes - "double knockouts" - produces a more severe phenotypic effect. A good example of this is seen when paralogous group 11 members of two Hox gene clusters, *Hoxa11* and

Hoxd11, are inactivated singly or in combination. These genes are expressed in mesenchyme of the developing limb during specification of the cartilage elements which later form the bones of the limb. Functional inactivation of *Hoxa11* results in misshapen ulna and radius and fused carpal bones in the forelimb with homeotic transformations also seen in the thoracic and sacral regions of the vertebrae (Small and Potter 1993). Functional inactivation of *Hox d11* also resulted in fusion of carpal bones and distal defects in radius and ulna and abnormalities in length and structure of metacarpals and phalanges were also seen (Davis and Capechi 1994). Functional inactivation of both *Hoxa11* and *Hoxd11*, however, results in virtual elimination of the radius and ulna, more severe homeotic transformations of vertebrae and an additional kidney defect (Davis *et. al.*, 1995). This indicates that there is functional redundancy between *Hoxa11* and *Hoxd11* in specification of the radius and ulna, some vertebrae and in the kidney.

Several connexin genes have been functionally inactivated. The results suggest roles for connexins in such diverse processes as oocyte maturation (Cx 37, Simon *et. al.*, 1997) and development of the heart (Cx 43, Reaume *et. al.*, 1995) (see Nichols and Bruzzone 1997 for recent review of connexin knockouts). However in many cases the phenotype is less severe than would have been predicted from the expression patterns. Compensation by co-expressed connexin proteins is thought to be the reason for this. As yet, the functional inactivation of two connexin genes together has not been reported.

4.1.4.2 Blocking antibodies

Another method which has been used to define the functions of certain proteins is application of blocking antibodies. These have been used successfully to block the gap junction channel during development, albeit transiently, thus preventing communication. Blocking communication in 8-cell stage *Xenopus* resulted in absence of structures such as the eye (Warner *et. al.*, 1984) indicating the importance of gap junction communication in patterning. Blocking gap junction communication in the 8 cell stage mouse embryo resulted in decompaction of the embryo which is incompatible with survival (Lee *et. al.*, 1987, Becker *et. al.*, 1992, 1995). However, with older embryos it may be difficult to

load sufficient blocking antibody to reveal an effect, limiting the usefulness of this technique.

4.1.4.3 Antisense oligodeoxynucleotides - mechanism of action

Another approach to reducing the level of a protein in the developing embryo is the application of antisense oligodeoxynucleotides (ODNs). Antisense ODN's are thought to act by binding to mRNA, thus forming DNA/mRNA hybrids. This has been shown to physically block the transcription of mRNA into protein (Ch'ng *et. al.*, 1989). In some cases the double stranded DNA/mRNA hybrid is a substrate for endogenous RNase H, which cleaves the mRNA, thus reducing both mRNA and protein level (Shuttleworth and Coleman 1988) prolonging the effectiveness of the treatment. The rate of cleavage by RNase H increases when the antisense ODN sequence is an exact match for the target RNA (Woolf *et. al.*, 1992).

Confirmation of the effectiveness of antisense treatment is usually by investigation of the presence of protein, by immunohistochemistry or western blot, as a change in phenotype does not always occur. Assaying for mRNA levels is not useful as this may remain intact (Wagner 1994). It is also recommended to check that the antisense ODNs enter into cells, for example by using fluorescently labelled antisense ODNs and that they do not affect the expression of other proteins. This method of interfering with expression of proteins during embryonic development is attractive as it is generally not lethal and as the effect is transient, it can be used in a stage specific manner to investigate the role of a gene in several different developmental events.

4.1.5 Design of antisense ODN's and appropriate controls

The design of antisense ODN's must meet certain criteria. The antisense ODN sequence must bind with specificity to the target mRNA. It is thought that the shortest sequence that will confer specificity within the in-frame coding sequence of a typical vertebrate genome is 13 nucleotides (13mer) (Woolf *et. al.*, 1992) although most studies use around 20 nucleotides. However increasing length also decreases specificity (Milligan *et. al.*, 1993). Binding efficiency can be predicted by melting temperature of the DNA/mRNA hybrid, higher melting points indicate more stable hybrids (Wagner *et. al.*,

1993). The actual sequence itself may also cause non-specific effects, for example four G nucleotides in a row have been shown to be non-specifically antiproliferative (Milligan *et. al.*, 1993). Although antisense ODN's are generally designed to hybridise to the region containing the translation initiation codon (Weiss *et. al.*, 1997), evidence shows that they can effectively bind to most regions in the reading frame (Wagner 1994), thus such sequence non specific effects may often be avoided. The secondary structure of the antisense ODN sequence must also be determined to ensure that they do not form hairpin loops or heterodimers with each other, which prevents binding to target mRNA (Blake *et. al.*, 1985).

Appropriate controls must be employed in studies using antisense oligonucleotides to confirm that the resulting phenotype is specific (Stein and Chang 1993). Sense ODN's and missense ODN's containing the same base composition but not in the same sequence as the antisense ODN's are the most commonly used controls. They indicate if any effects occur due to administration and breakdown of nuclotides that are not related to the sequence.

4.1.6 Entry of antisense ODN's into cells

Antisense ODN's enter cells by binding to cell surface receptors which are internalised by endocytosis (Loke *et. al.*, 1989). Use of labelled antisense ODN's have shown that entry into cells is highly inefficient *in vitro* and that also ODNs then tend to accumulate in cytoplasmic organelles (Milligan 1993). Increased effectiveness has been shown when antisense ODN's are administered with cationic lipids (Colige *et. al.*, 1993) which increase uptake into the cell and nucleus. Conjugation of molecules with antisense ODN's have been made to enhance uptake into the cell. Poly(L)lysine (Stevenson *et. al.*, 1989) and cholesterol (Stein *et. al.*, 1991) enhance uptake of antisense ODN's but it is thought that in some cases, conjugates may increase non specific effects.

4.1.7 Modification of antisense ODNs

The effects of antisense ODN's are transient as phosphodiester linkages are susceptible to rapid intracellular degradation. Phosphodiester antisense ODN's have a typical half life of 20 minutes (Wagner, 1994) thus high doses are required. High doses of antisense

ODN's have been shown to have a non specific toxic effect (Woolf *et. al.,* 1990) and the rapid accumulation of their breakdown products (nucleotides/nucleosides) is also very toxic to the cell (Rathbone *et. al.,* 1992).

To protect antisense ODNs from nuclease digestion, chemical modifications can be made to the structure. The most common modification of antisense ODN's is a replacement of an oxygen atom in the phosphodiester bond with sulphur to form a phosphorothioate. This modification reduces exo- and endonuclease digestion and increases the half life to hours (Fisher *et. al.,* 1993). Modification allows for the use of much lower doses of antisense ODN's with fewer or no non-specific toxic effect and few breakdown products. However modified antisense ODN's have a reduced affinity for target mRNA and in general the resulting hybrid has a lower melting temperature than unmodified ODN's indicating reduced stability (Hoke *et. al.,* 1991). Modified antisense ODN's are also less efficient at entering cells (Stein *et. al.,* 1988). Compared with unmodified phosphodiester ODN's, modified antisense ODNs can cause non specific effects by binding to essential proteins (Perez *et. al.,* 1994)

4.1.8 The role of gap junction communication in facial expansion and fusion

The presence of gap junctions in the primordia of the upper face as reported in TEM studies (Minkoff, 1983) indicated that there were regional differences in the density of gap junctions which correlated with regions of high cell proliferation. Later studies indicated that connexin 32 containing gap junctions were present between cells in facial primordia, but were distributed relatively evenly (Minkoff *et. al.,* 1991).

The regional distribution of gap junctions in the upper face (Minkoff 1983) correlated well with my analysis of facial expansion in the chick face, suggesting that gap junction proteins were expressed in regions that displayed greater expansion and thus gap junctional communication may be important for facial shaping and fusion. In this chapter, I aim to amplify the knowledge of expression of particular gap junction proteins, in particular connexin 43 which, at the onset of this study, had not been reported. In addition, there are well documented effects of retinoic acid decreasing gap junctional

expression and communication between cells (Pitts *et. al.,* 1986, Mehta *et. al.,* 1989). However, changes in gap junction expression have not been investigated in retinoic acid - induced clefting of the avian primary palate. In this study, expression of connexins after retinoic acid treatment have been investigated, in this study, to see if they alter when facial clefting is induced.

Finally, to define possible roles for connexin 43 during chick facial development, unmodified antisense ODN's have been designed to disrupt expression of connexin 43. As just outlined, unmodified antisense oligonucleotides have higher affinity for target mRNA, are more efficient at entering the cell and have less non specific binding than modified antisense ODN's but rapid degradation and toxicity problems related to this make them difficult to use. I have developed, in collaboration with D. Becker, University College London, and C. Green, University of Auckland, a novel technique of applying unmodified antisense ODN's to chick embryos. This involves mixing the antisense ODNs with carrier gel that acts as a slow, sustained release system with mild surfactant properties. These studies indicate an essential role for connexin 43 protein in facial fusion.

4.2 Materials and methods

4.2.1 Whole mount antibody labelling of chick embryos

Embryos were staged according to Hamburger and Hamilton (1951) and fixed in 4% PFA (w/v) at 4°C, see also chapter 2, section 2.1 and 2.4. Embryos stage 12-18 were fixed for 2 hours. Older embryos were fixed for up to 6 hours. Embryos were washed briefly in PBS and then placed in "antibody block" solution, at 4°C over night. This solution consisted 1% Lysine (Sigma), 0.5% Triton x - 100 (Sigma) in PBS. This solution blocks the tissue prior to antibody labelling and also permeabilised the embryos to aid penetration of the antibody.

Embryos were washed for 1 hour, 3 times, with PBS and then incubated overnight, at 4°C, with a polyclonal primary antibody, raised against either connexin 43 or connexin

32, diluted 1:100 in PBS. See below for information on characterisation of antibodies. Embryos were washed again for 1 hour, 3 times, with PBS and then incubated overnight with fluorescent secondary antibody at 4°C in the dark. For both connexin 43 and connexin 32 antibodies, the secondary antibody used was mouse anti-rabbit FITC (DAKO) diluted 1:20 with PBS. Embryos were washed for 1 hour, 3 times. The heads were mounted on cavity slides (BDH) in Citifluor antifade mounting solution.

4.2.1.1 Characterisation of connexin 43 and connexin 32 antibodies

The characterisation of these antibodies can be found in Becker *et. al.,* 1995. For connexin 43 the primary antibody used was the rabbit polyclonal antibody Gap 15 raised against connexin 43 specific peptides at the C-terminal end of the cytoplasmic loop, see also figure 4.1a. Briefly, western blots indicate that this antibody recognises connexin in heart tissue, which contains only connexin 43 and does not recognise connexins in liver tissue, which contains only connexin 32. Immunolabelling with this antibody was found in heart tissue but not in liver tissue. For connexin 32, the primary antibody used was the rabbit polyclonal antibody Des 5 raised against connexin 32 specific peptides at the C - terminal end of the cytoplasmic loop, see also Figure 4.1a. Briefly, western blots recognised liver tissue, containing connexin 32 but not heart tissue, containing connexin 43. Immunostaining with the antibody was seen in liver tissue but not heart tissue. See also Makarenkova *et. al.,* 1997

4.2.2 Visualisation of immunolabelled connexins in chick facial primordia

Whole mount chick embryo heads labelled with connexin antibodies were viewed under a Leica TCS 4D laser scanning confocal microscope. The heads were optically sectioned and 3D recombination software was used to indicate the distribution of staining throughout the facial primordia.

4.2.3 Design of unmodified connexin 43 antisense oligodeoxynucleotides

The 30 base connexin 43 antisense ODN (DB1) was designed by Dr. D. Becker and obtained from British Biotech (Abingdon) at a concentration of 2M. The sequence, complementary to bases 1094-1123 of the mouse *connexin 43* gene, is as follows :

GTA aTT gCG gCA GGA GGA ATT GTT tCT GTC

There are 4 mismatches with the chick connexin 43 sequence and these are indicated in lowercase. A chick sequence corresponding to bases 954-983 of the chick connexin 43 gene was designed but analysis showed a high probability of forming stem loops (G = -7.0 kcal/mol, Loop Tm =92°) and homodimerisation (Tm = 1.5°)

The 30 base connexin 43 sense ODN was also obtained from British Biotec (Abingdon) at a concentration of 2M. The sequence is as follows:

GAC AGA AAC AAT TCC TCC TGC CGC AAT TAC

A chick *connexin 43* antisense ODN sequence (CG1), complementary to bases 720-749, was also designed by Dr C. Green, University of Auckland. This was found to produce the same phenotype as the mouse sequence DB1 (Becker, Lorimer, Makarenkova, McGonnell, Tickle and Green, 1998 submitted).

4.2.4 Preparation and application of connexin 43 antisense ODNS to chick embryos

Pluronic gel F-127 (BASF Corp) was diluted to 30% in PBS made with molecular grade water and kept at 4°C. Preliminary dose response experiments with ODN concentrations between 0.05µM and 50µM, indicated that toxic effects were seen above 10µM final concentration. A final concentration of 0.5-1.0µM ODN in 30% pluronic gel was used in all experiments in this chapter. Both antisense and sense solutions were made fresh for each experiment. Pluronic gel is a liquid between 0-4°C but sets at higher temperatures. It has the added advantage of being a mild surfactant, thus aiding penetration of the antisense oligonucleotides into cells, a step which has previously been shown to be limiting the effectiveness of antisense treatment (Wagner 1994).

The ODN/pluronic gel solution was kept on ice at all time after preparation. Embryos were exposed *in ovo*, as in chapter 2 section 2.1 and 10μl of ODN solution were pipetted onto the embryo using a Gilson pipette. The solution sets on contact with the warm embryo and stays in place. Experiments with dyed pluronic gel show that the gel stays in place, on the embryo, for up to 24 hours. This gel provides continuous, slow release of the ODNs. The eggs were re-sealed with tape and reincubated at $38 \pm 1°C$. In preliminary experiments, antisense ODNs were applied to embryos with sense ODNs, mismatch base ODNs and mixtures of antisense and sense ODNs and PBS as controls (Becker, Lorimer, Makarenkova, McGonnell, Tickle and Green, 1998 submitted). None of the control groups produced facial defects. Antisense ODNs, sense ODNs and pluronic gel alone were applied to embryos in these experiments.

4.2.5 Assessment of embryos after treatment with ODNs

Embryos were removed from the egg, washed in PBS and immediately viewed under a light microscope to assess changes in morphology. Embryos were then fixed in 4% PFA for storage or processing for whole mount *in situ* hybridisation with the *Msx-1* riboprobe (see chapter 2 section 2.6.3-4 for method). Alternatively, some were fixed in modified Tyrodes solution and processed for scanning electron microscopy (see chapter 2, section 2.5).

4.3 Results

4.3.1 Expression patterns of Connexin 43 in chick facial primordia between stages 20 and 28.

Localisation of connexin 43 gap junction protein in chick facial primordia was investigated between stages 20 and 28. Connexin 43 was visualised by immunohistochemical methods in whole mounts of chick facial primordia using laser scanning confocal microscopy. Gap junction plaques containing connexin 43 protein appeared as puncta (or dots) of fluorescent staining. Connexin 43 was found to be expressed in both epithelia and mesenchyme in all stages examined and patterns of

expression in both tissues are summarised in figure 4.2. Black dots represent areas where plaques containing connexin 43 were very abundant in the mesenchyme and red lines indicate areas of abundance in the ectoderm.

4.3.1.1 Epithelial connexin 43 expression

Epithelial labelling was intense in surface nasal epithelium at all stages (summarised in Fig. 4.2 and shown in Figs. 4.3B, 4.4B, C, 4.6B, at stage 20, 24, 28 respectively) but no expression was seen deeper in the invaginating epithelium of the pit. In general, other epithelia were evenly labelled , i.e. had moderate intensity of labelled plaques. However, a few regions of facial epithelia transiently displayed a higher level of connexin expression. At stage 20, connexin 43 was expressed at high levels in epithelial cells at midline and proximal and distal edges of the mandibular primordium (Figs. 4.2, 4.3D). At stage 24, the epithelium at the distal anterior edge of the maxillary primordium expressed high levels of connexin 43 (Figs. 4.2, 4.5B) and, at stage 28, the epithelium at the proximal edge of the mandibular primordium was seen to display abundant connexin 43 containing plaques (Fig 4.2, 4.7 F).

4.3.1.2 Mesenchymal connexin 43 expression

In contrast to the epithelia, the abundance of gap junctions containing connexin 43 between mesenchymal cells was much more variable within different primordia. Use of confocal microscopy allowed examination of the mesenchyme in whole mount preparations without interference from epithelial expression.

Expression of connexin 43 gap junction protein was high in mesenchyme surrounding the nasal pit at all three stages examined, summarised in Fig. 4.2 and shown in Figs. 4.3B, 4.4B and C, 4.6B. Mesenchyme at the distal (open) end of the nasal pit expressed particularly high levels of protein at stages 20 and 24 (Figs. 4.2, 4.3B) while regions above (or proximal to) the nasal pit generally expressed lower levels (Figs. 4.2, 4.3B, 4.4B).

Figure 4.2 A summary diagram of the patterns of connexin 43 protein expression in chick facial primordia between stages 20 and 28.

Connexin 43 protein was localised by immunohistochemical methods. Regions of abundant mesenchymal expression are indicated by black dots, regions of abundant epithelial expression are indicated by red lines.

At stage 20, mesenchymal expression is restricted in all facial primordia. Expression is found at the open end of the nasal pits, at the distal edge of the maxillary primordium, bordering the oral cavity, and at the midline of the paired mandibular primordia. By stage 24 expression has spread towards the top of the nasal pits, across the anterior part of the maxillary primordium and across the proximal edge of the mandibular primordium. At stage 28, connexin 43 protein is expressed at the midline of the frontonasal mass, extends across the anterior of the maxillary primordium and remains restricted to the midline and proximal edge of the mandibular primordium.

Epithelial expression is more widespread, but some regions show transient increases in the level of connexin 43 containing gap junctions. At stage 20, epithelia of the nasal pits and at the midline of the paired mandibular primordium express high levels of connexin 43. At stage 24, epithelia of the nasal pit and at the distal edges of the maxillary primordia transiently express high levels of connexin 43. At stage 28, again the epithelia of the nasal pit expresses abundant connexin 43, as does the epithelia at the proximal edge of the mandibular primordium, near to the midline.

FNM: Frontonasal mass.   NP: Nasal pit.

LNP: Lateral nasal process.   Mx: Maxillary primordium.

Mn: Mandibular primordium.

Figure 4.2

Stage 20
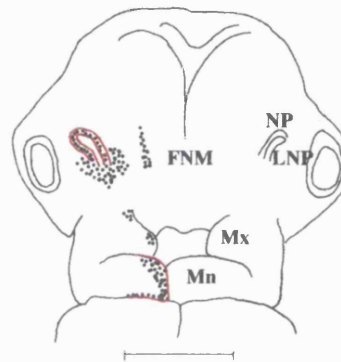
Stage 24
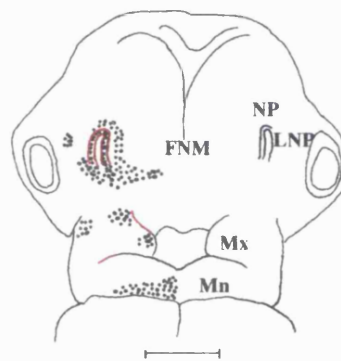
Stage 28
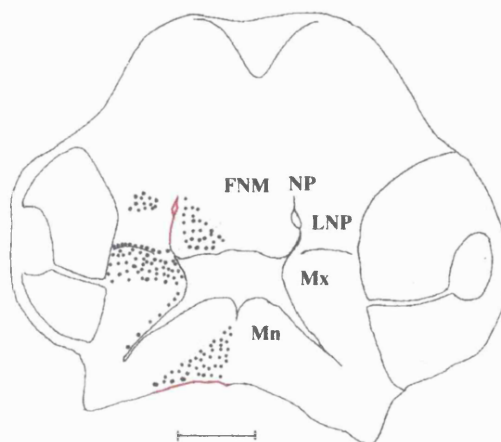
⋮⋮⋮ Mesenchymal expression

— Epithelial expression

Figure 4.3 Connexin 43 protein expression in stage 20 facial primordia

A. Diagram of chick embryo facial primordia at stage 20. Boxes indicate regions of the face shown B-D, while black dots summarise regions of abundant connexin 43 containing gap junctions shown in B, C, D. Scale bar = 1000 μm.

B. Connexin 43 containing gap junctions (white dots) in the nasal pit region, the lateral nasal process and frontonasal mass of the chick embryo at stage 20. Expression is abundant in epithelia of the nasal pit. Abundant mesenchymal expression is seen at the distal end of the nasal pit, indicated by *, and in distal regions of the frontonasal mass adjacent to the nasal pit, indicated by a white arrowhead. Axes indicated to the left of the figure. Scale bar = 100μm.

C. Connexin 43 expression in mid and anterior regions of maxillary primordium at stage 20. Expression is seen in anterior distal regions (white arrowhead) and also in mid distal mesenchyme. Posterior proximal regions, indicated by *, have fewer connexin 43 containing gap junctions. Axes indicated to left of the figure. Scale bar = 100μm.

D. Connexin 43 localisation in the mandibular primordium at stage 20. Expression is seen in the distal regions and near the midline, indicated by white arrowhead, while more lateral regions have fewer connexin 43 containing gap junctions. Axes indicated to the right of the figure. Scale bar = 100μm.

Figure labels:

FNM: Frontonasal mass.	NP: Nasal pit.
LNP: Lateral nasal process.	Mx: Maxillary primordium.
Mn: Mandibular primordium.	

Axes:

D: Distal	Pr: Proximal
A: Anterior	Po: Posterior
M: medial	L: Lateral.

Figure 4.3
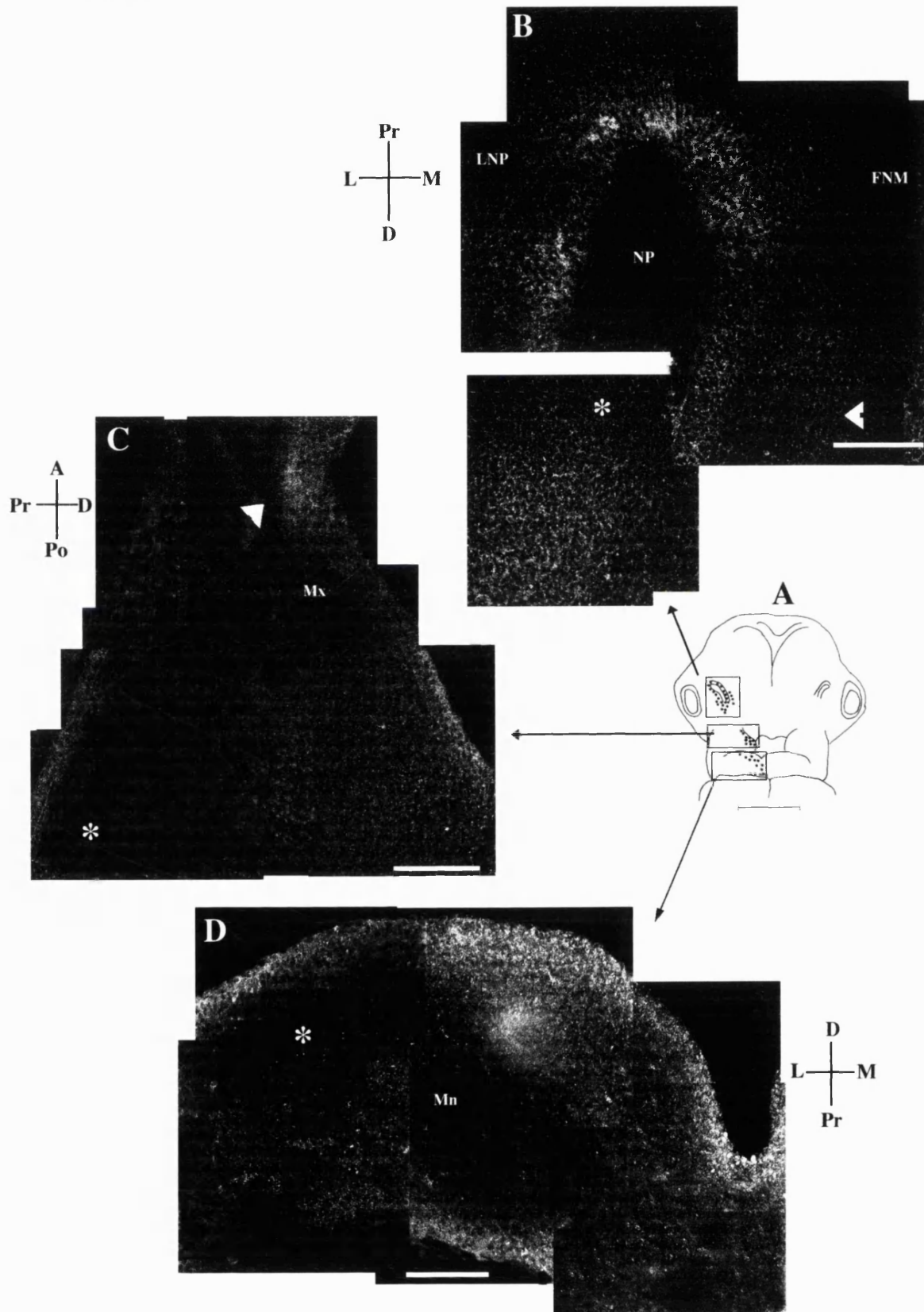
Figure 4.4 Connexin 43 expression in stage 24 frontonasal mass and lateral nasal process

A. Diagram of chick embryo facial primordia at stage 24. Box indicates area in centre of frontonasal mass shown in D, while black dots summarise regions of abundant connexin 43 containing gap junctions close to the nasal pit, as indicated in B, C, D. Scale bar = 1000μm.

B. Pattern of connexin 43 containing gap junctions in the lateral nasal process and nasal pit of stage 24 chick embryos. Expression is abundant in nasal pit tissues and distal lateral nasal process, as at stage 20. Expression is seen proximally, away from the nasal pit also, as indicated by *. Axes indicated to the right of the picture. Scale bar = 100μm.

C. Connexin 43 containing gap junction expression in the nasal pit and frontonasal mass at stage 24. Gap junctions are abundant in epithelia of the nasal pit and in frontonasal mass mesenchyme close to the nasal pit. There is a region devoid of gap junctions immediately adjacent to the nasal pit, as indicated by white arrowhead. Scale bar = 100μm.

Figure labels:

FNM: Frontonasal mass.   NP: Nasal pit.

LNP: Lateral nasal process.

Axes:

D: Distal   Pr: Proximal

M: medial   L: Lateral.

Figure 4.4
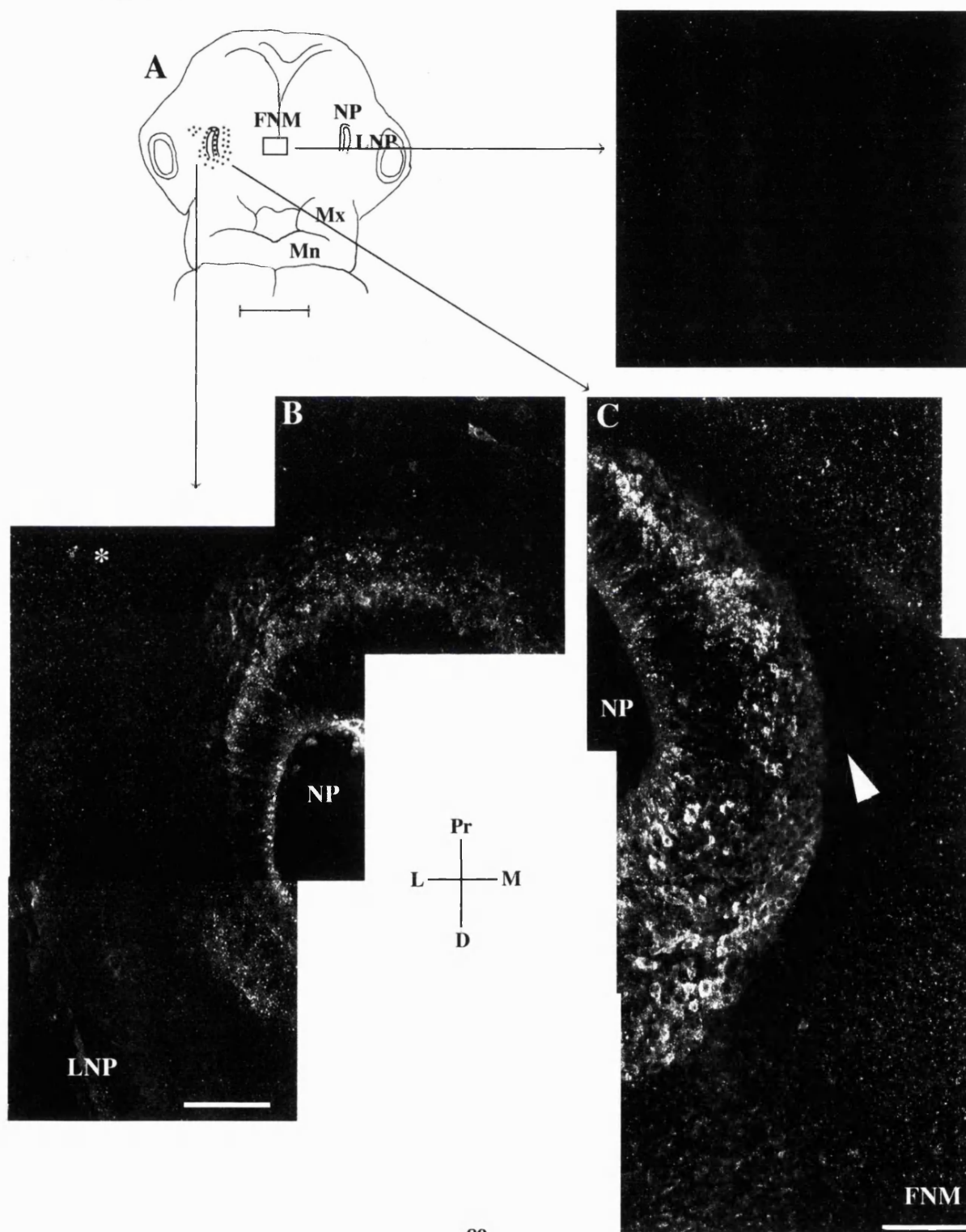
Figure 4.5 Connexin 43 expression in stage 24 maxillary primordium.

A. Diagram of chick embryo facial primordia at stage 24. Box indicates region of maxillary primordium shown in B. Black dots summarise pattern of labelling as seen in B. Scale bar = 1000 μm.

B. Pattern of connexin 43 containing gap junctions in maxillary primordium at stage 24. Abundant epithelial expression is seen at the distal edge of the primordium, particularly in anterior regions, indicated by white arrowhead, top right. Abundant mesenchymal expression is seen in anterior lateral regions, white arrowhead top left, and in mid distal regions, white arrowhead in white box. White boxes indicate regions of the primordium shown in C, D, E, at a higher magnification. Scale bar = 100μm.

C. Gap junction distribution in anterior distal regions of maxillary primordium. Abundant gap junctions are seen in both epithelia and mesenchyme. Scale bar = 100μm.

D. Gap junction distribution in mid - distal regions of maxillary primordium. Abundant gap junctions seen in both epithelia and mesenchyme. Scale bar = 100μm.

E. Gap junction distribution in posterior distal regions of maxillary primordium at stage 24. Gap junctions are seen in epithelia but few in the mesenchyme. Scale bar = 100μm.

Figure labels

FNM: Frontonasal mass.   Mn: Mandibular primordium.

Mx: Maxillary primordium.

Axes:

D: Distal   Pr: Proximal

A: Anterior   Po: Posterior

Figure 4.5
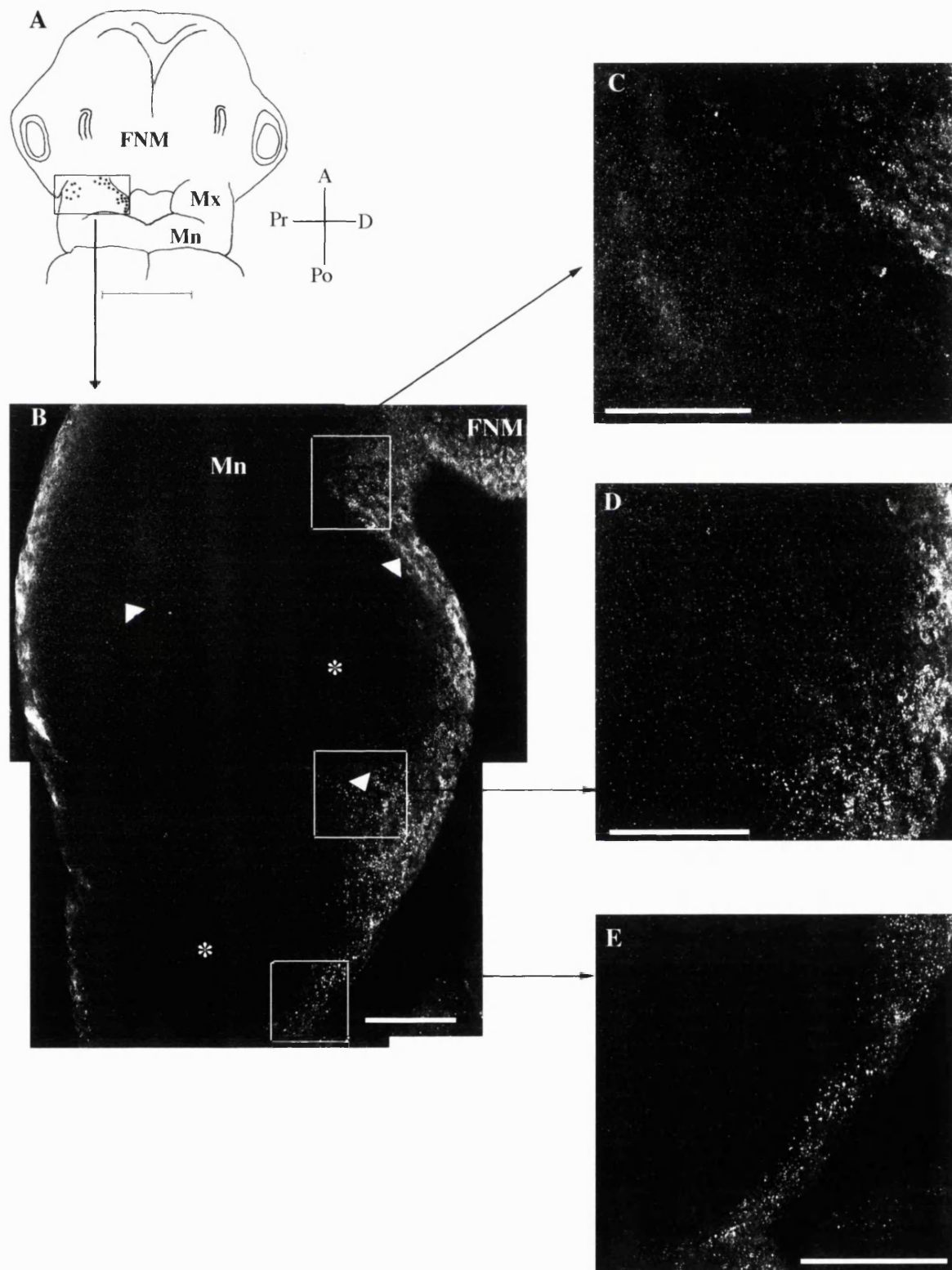
Figure 4.6 Connexin 43 expression in stage 28 frontonasal mass and lateral nasal process.

A. Diagram of chick embryo facial primordia at stage 28. Boxes indicate regions of facial primordia shown in accompanying pictures, B and C. Black dots summarise connexin 43 containing gap junction distribution in those areas as shown in B and C. Scale bar = 1000μm.

B. Expression of connexin 43 containing gap junctions in the lateral nasal process and nasal pit at stage 28. Expression is abundant in proximal regions, away from the nasal pit, as indicated by *. Scale bar = 100μm.

C. Expression of connexin 43 containing gap junctions in the stage 28 frontonasal mass. Abundant expression is seen in mesenchyme near the nasal pit. A mesenchymal region with few gap junctions can be seen immediately adjacent to the nasal pit, as indicated by white arrow heads. Scale bar = 100μm.

Figure labels:

FNM: Frontonasal mass.   NP: Nasal pit.

LNP: Lateral nasal process.

Axes:

D: Distal   Pr: Proximal

M: medial   L: Lateral.

Figure 4.6
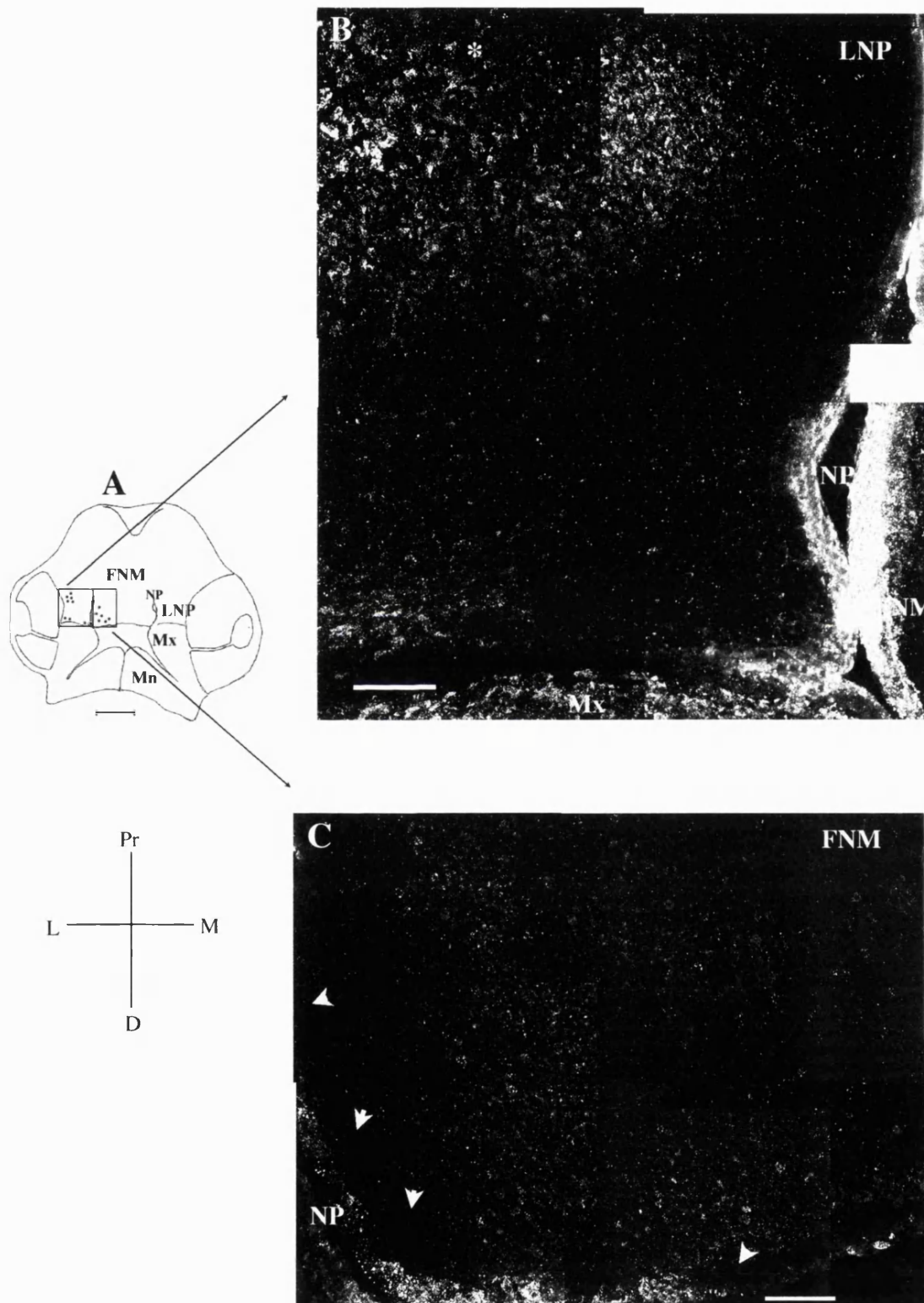
Figure 4.7 Expression of connexin 43 in stage 28 maxillary and mandibular primordia.

A. Diagram of chick embryo facial primordia at stage 28. Boxes indicate regions of maxillary and mandibular primordia as shown in B-F. Black dots summarise patterns of connexin 43 containing gap junctions shown in B-F. Scale bar = 1000μm.

B. Expression of connexin 43 containing gap junctions in the anterior maxillary primordium. Epithelial expression is abundant in anterior distal regions, (white arrowhead). Expression is seen throughout the mesenchyme. Axes right of the picture. Scale bar = 100μm.

C. Gap junction distribution in posterior lateral mesenchyme of stage 28 maxillary primordium. Very few gap junctions are expressed in this region, indicated by *. Axes to right of the figure. Scale bar as in D.

D. Connexin 43 expression in posterior distal regions of the maxillary primordium. Connexin 43 gap junctions are seen in the distal epithelia as shown by white arrowhead. The mesenchyme, as indicated by *, has few gap junctions. Axes to the right of the figure. Scale bar = 100μm.

E. Gap junction distribution in lateral regions of mandibular primordium. Abundant epithelial and mesenchymal expression is seen in proximal regions (arrowhead). Few gap junctions are observed in distal epithelia and mesenchyme, indicated by *. Axes indicated to the right of F. Scale bar = 100μm.

F. Gap junction distribution in midline regions of the paired mandibular primordia. Abundant mesenchymal expression is seen proximally (white arrowhead) but there are less distally, indicated by *. White arrows indicate region with few or no connexin 43 containing gap junctions immediately underneath distal tip epithelia. M denotes the midline between the paired mandibular primordia, which also has few connexin 43 containing gap junctions. Axes indicated to right of picture. Scale bar = 100μm.

Figure labels:

FNM: Frontonasal mass.   LNP: Lateral nasal process.

Mx: Maxillary primordium   Mn: Mandibular primordium.

Axes as in Figure 4.3

Figure 4.7
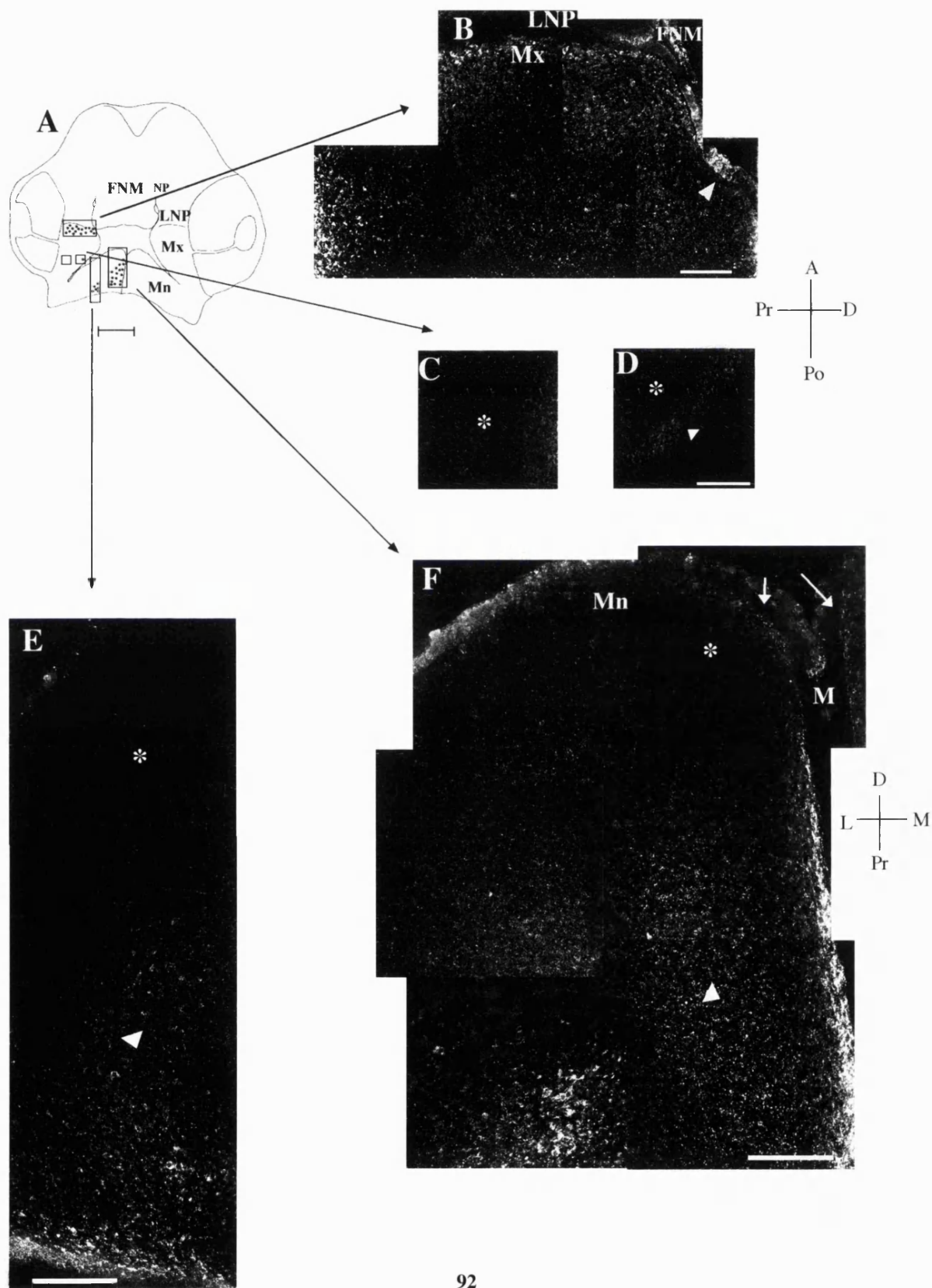
Initially, expression in the lateral nasal process was more intense in distal medial regions, close to the nasal pit (Fig 4.2, 4.3B). At stage 24, a patch of expression appeared proximally, away from the nasal pit (Fig. 4.2, 4.4B indicated by white astenx) and expression was still intense in this region at stage 28 (Fig. 4.6B, indicated by white asterix). At stage 28 connexin 43 protein was also expressed distally in the lateral nasal process, close to maxillary primordium and nasal pit (Fig. 4.6B).

In the frontonasal mass, mesenchymal expression was higher distally next to the nasal pit at stage 20 (Figs. 4.2, 4.3B indicated by arrow head). By stage 24, moderate expression was also found proximally next to the nasal pit (Fig. 4.4C) and this persisted until at least stage 28 (Fig 4.2, 4.6C). In contrast, central regions of the frontonasal mass expressed very little connexin 43 protein (Fig. 4.4D) until stage 28 when some staining was seen in central distal regions. At stage 24 and 28, a clear region of non -expressing mesenchymal cells was also seen in the frontonasal mass, immediately next to the nasal pit (Fig 4.4C and 4.6C, indicated by arrowheads).

In stage 20 maxillary primordium, connexin 43 expression was abundant in mid - distal regions and also in the anterior region, adjoining the lateral nasal process (Figs. 4.2, 4.3C indicated by arrowhead) but there was very little mesenchymal expression in posterior proximal regions (Fig. 4.3C, *). This pattern was similar at stage 24 but a region of expression was also seen in anterior proximal regions, near to the eye (Fig. 4.5B, top left arrowhead) and also at the join between maxillary and mandibular primordium (Figs. 4.5B and E). At stage 28, expression was seen to extend the whole way across the proximodistal axis in the anterior part of the primordium (Figs. 4.2, 4.7B) while expression posteriorly remained low (Fig 4.7C and D, arrowhead indicates some epithelial labelling, * low mesenchymal labelling).

Connexin 43 expression in the mandibular primordium was high in proximal midline regions at all stages examined (Figs. 4.2, 4.3D, 4.7 E, F). At stage 20, connexin 43 protein was also expressed distally in the mesenchyme as well as at the proximal midline, but this did not persist (Fig. 4.3D). Expression of connexin 43 protein in lateral regions

of the mandibular primordium was very low at all stages (Figs. 4.2, 4.3D, 4.7E, indicated by *).

4.3.2 Expression patterns of Connexin 32 in chick facial primordia between stages 20 and 28.

Connexin 32 is often found co-expressed with connexin 43 in developing organs such as the limb (Makarenkova *et. al.*, 1997) and rat tooth (Fried *et. al.*, 1996). Therefore, patterns of connexin 32 expression in chick facial primordia between stages 20 and 28 were also examined using immunohistochemistry and confocal microscopy and compared to the patterns of connexin 43 just described (see also Minkoff *et. al.*, 1991). Gap junction plaques containing connexin 32 gap junction protein were found between both epithelial cells and mesenchymal cells and patterns of expression are summarised in Figure 4.8.

4.3.2.1 Epithelial connexin 32 expression

Expression of connexin 32 in epithelia of the nasal pit was particularly intense at all three stages (Figs. 4.8. 4.9 B, C, 4.10B, 4.11B) as found for connexin 43. The distribution of connexin 32 containing plaques was generally uniform in other epithelia of other facial primordia. However, like connexin 43, there were transient regions of higher expression. In particular, gap junction plaques containing connexin 32 protein were abundant between epithelial cells of the distal maxillary primordium at stage 20 (Figs. 4.8, 4.9F) and between epithelial cells at the mandibular / maxillary primordium join at stage 24 (Fig. 4.10E, arrowhead). These regions of connexin 32 epithelial expression do not overlap with regions of high connexin 43 epithelial expression (compare summary Figs. 4.2 and 4.8).

4.3.2.2 Mesenchymal connexin 32 expression

Levels of mesenchymal connexin 32 expression varied in each primordium. It was noted that, in general, the level of expression of connexin 32 was more uniform than connexin 43.

Figure 4.8 Summary diagram of the patterns of connexin 32 protein expression in chick facial primordia between stages 20 and 28.

Connexin 32 protein was localised by immunohistochemical methods. Regions of abundant mesenchymal expression are indicated by black dots, regions of abundant epithelial expression are indicated by red lines.

At stage 20, abundant connexin 32 expression was observed in the epithelia of the nasal pits and at the distal edge of the maxillary primordium, next to the oral cavity. Abundant mesenchymal expression was seen at the top of the nasal pit in both lateral nasal process and frontonasal mass. Anterior and distal mesenchyme in maxillary primordia also expressed high levels of connexin 32 protein, as did the distal and proximal mesenchyme of mandibular primordia, particularly near the midline. At stage 24, epithelial expression was again abundant in the nasal pit and at the join between maxillary and mandibular primordia. High levels of mesenchymal connexin 32 expression were widespread, being found throughout the frontonasal mass and lateral nasal process, in the anterior region of maxillary primordia and throughout most of the mandibular primordia. At stage 28, expression was more restricted. Epithelial expression was abundant in the nasal pits and at the proximal edge of the mandibular primordium. Mesenchymal expression was most abundant in lateral regions of the lateral nasal process, away from the nasal pits and throughout most of the frontonasal mass. Distal and lateral maxillary mesenchyme expressed higher levels of connexin 32 protein, while central regions expressed much less. Midline and proximal regions expressed the highest levels of connexin 32 in the stage 28 mandibular primordia.

Figure 4.8

Stage 20
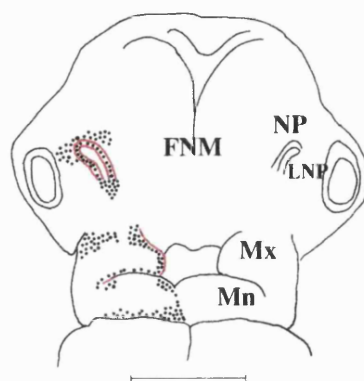
Stage 24
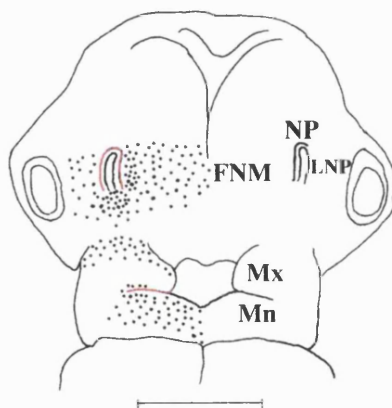
Stage 28
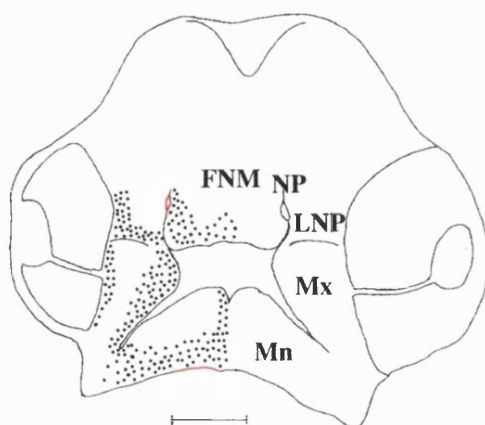
Mesenchymal expression
Epithelial expression

Figure 4.9 Expression of connexin 32 in the stage 20 facial primordia.

A. Diagram of chick embryo facial primordia at stage 20. Black dots summarise expression of connexin 32 protein in B-H. Pr and D refer to proximal and distal regions of the nasal pit, as marked in B, C and D. Scale bar = 1000µm.

B. Connexin 32 expression in lateral nasal process and nasal pit. Labelling is seen in nasal pit epithelia and proximal lateral nasal process mesenchyme (white arrowhead). Few gap junctions are seen distally, indicated by *. Scale bar = 100µm. Axes top right.

C. Connexin 32 labelling in the proximal nasal pit. Expression is seen in nasal pit epithelia. Mesenchymal expression is observed in proximal regions of the frontonasal mass, next to the nasal pit, (white arrowhead). Scale bar = 100µm. Axes top right.

D. Connexin 32 labelling in distal nasal pit. Mesenchymal expression streaks out in a wide band from the base of the pit (white arrowhead). Regions either side are relatively gap junction free, indicated by *. Scale bar = 100µm. Axes top right.

E. Connexin 32 in proximal frontonasal mass, near to the nasal pit. Mesenchymal expression is concentrated proximally, (white arrowhead), while there is little expression distally, indicated by *. Scale bar = 100µm. Axes top right.

F. Connexin 32 expression in maxillary primordium. Epithelial and mesenchymal expression is seen at the distal edge, (white arrowheads to right and bottom of figure). Mesenchymal expression is also seen in anterior proximal regions, (white arrowhead top left of figure). There is little connexin 32 expression centrally, indicated by *. Axes to the left of the picture. Scale bar = 100µm.

G. Connexin 32 expression in lateral mandibular primordia. Abundant mesenchymal expression in central proximal regions (white arrowhead), less expression distally (*). Epithelial staining is seen at the distal edge. Axes to the right of H. Scale bar = 100µm.

H. Connexin 32 in midline (M) regions of mandibular primordium. Expression is seen distally, (white arrowhead top of figure), extending down the midline and at the proximal edge of the primordium, (white arrowhead bottom of figure). Mesenchyme adjacent to the midline have few gap junctions (*). Axes to the right of the picture. Scale bar = 100µm.

Figure and axes labels as in Figure 4.3.

Figure 4.9
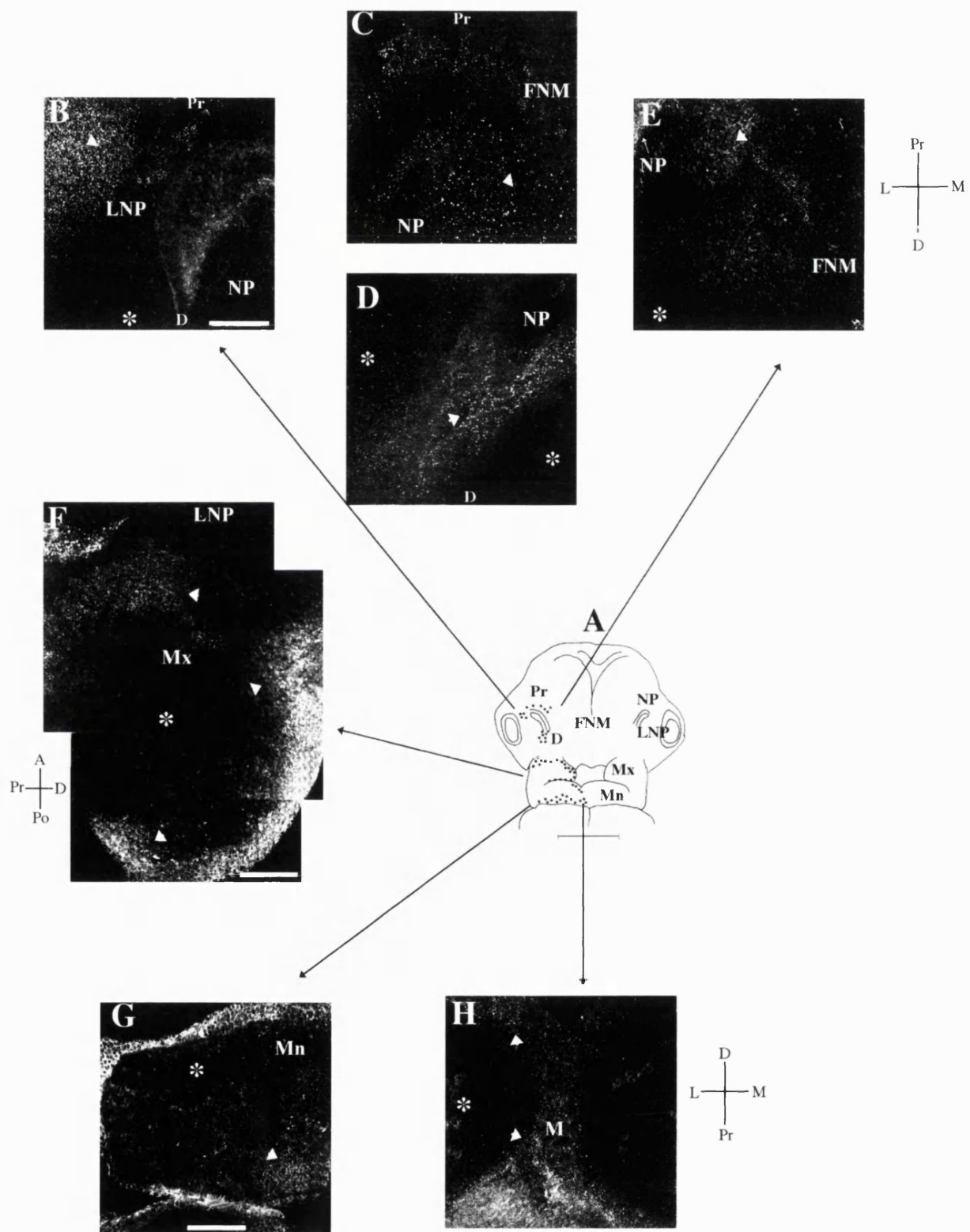
Figure 4.10 Expression of connexin 32 in stage 24 facial primordia

A. Diagram of chick embryo facial primordia at stage 24. Boxes indicate regions shown in B-G. Black dots summarise expression of connexin 32 in facial primordia as shown in B-G. Scale bar = 1000μm.

B. Connexin 32 in nasal pit, lateral nasal process and frontonasal mass. Connexin 32 containing gap junctions are distributed evenly in the primordia with slightly heavier expression in the distal nasal pit. Scale bar = 100μm. Axes to right of figure.

C. Connexin 32 expression in central frontonasal mass. Connexin 32 containing gap junctions are again visible throughout this region. Axes as in B. Scale bar = 100μm

D. Connexin 32 in maxillary primordium. Connexin 32 containing gap junctions are concentrated in the anterior regions (white arrowhead) while fewer gap junctions are seen proximally, indicated by *. Axes to right of figure. Scale bar = 100μm.

E. Connexin 32 in mandibular primordium. Connexin 32 containing gap junctions are distributed throughout most of the mandibular primordium particularly at the proximal midline (white arrowhead right of figure). Less expression is found in the lateral proximal edge, indicated by *. Intense labelling can also be seen at the merging point of mandibular and maxillary primordia (white arrowhead top left). Spots on this picture are background. Axes to right of figure. Scale bar = 100μm.

F. High power view of the distal edge of the mandibular primordium. Connexin 32 containing gap junctions can be seen throughout this region. Axes to left of figure. Scale bar = 100μm.

G. High power view of the proximal midline region of the mandibular primordium. High levels of expression can be seen close to the midline, (white arrowhead), while few connexin 32 containing gap junctions are seen laterally, indicated by *. Axes to the left of the figure. Scale bar = 100μm.

Figure and axes labels as in figure 5.3.

Figure 4.10
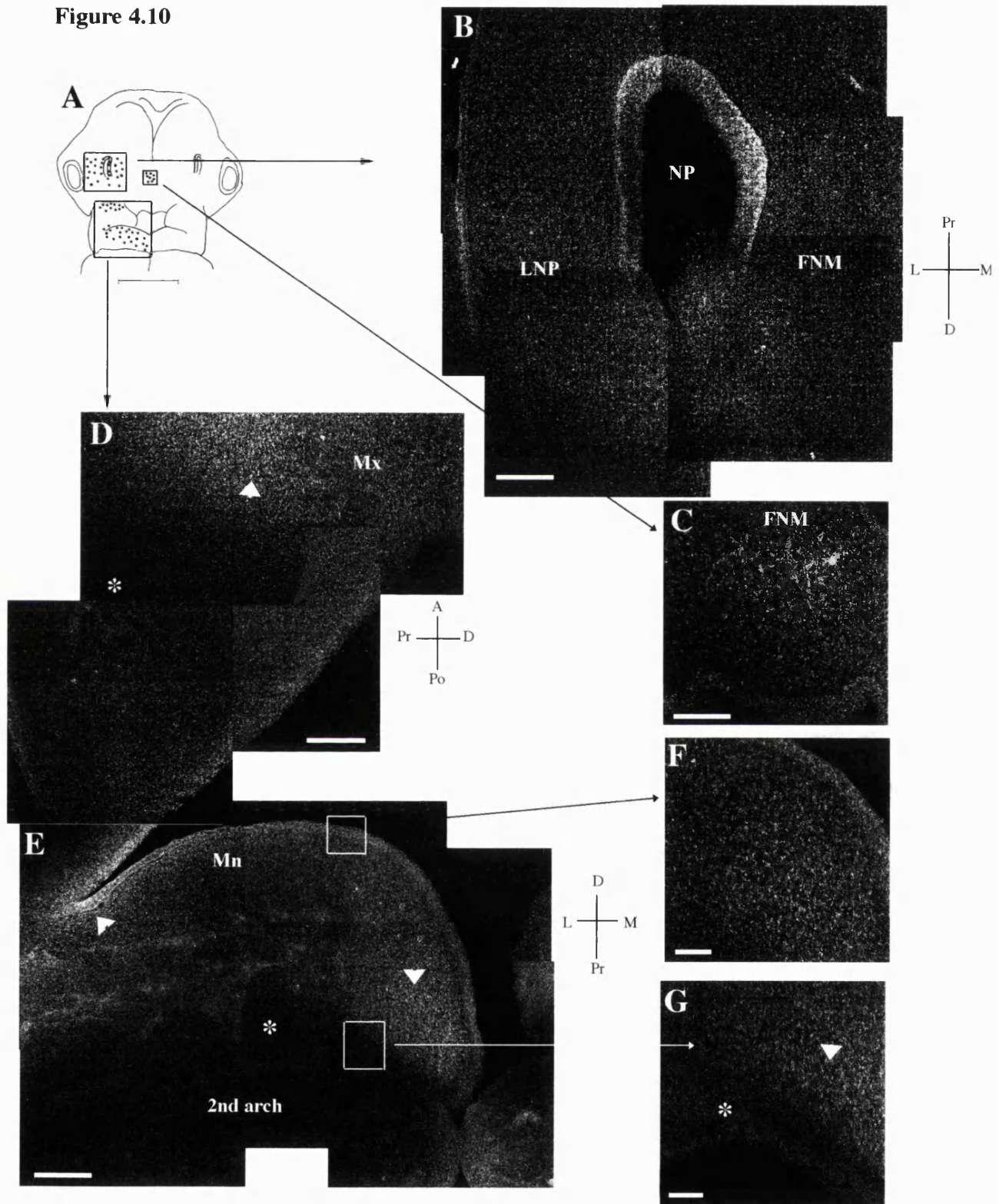
Figure 4.11 Connexin 32 expression in stage 28 lateral nasal process and frontonasal mass.

A. Diagram of chick embryo facial primordia at stage 28. Boxes represent regions shown in B and C. Black dots summarise connexin 32 expression as shown in B and C. Scale bar = 1000μm.

B. Connexin 32 in the stage 28 lateral nasal process and nasal pit. Connexin 32 expression is seen in lateral regions, indicated by white arrowhead. Less expression is observed closer to the nasal pits (*). Axes to the right of the figure. Scale bar = 100μm.

C. Connexin 32 in the frontonasal mass (FNM) at stage 28. High levels of connexin 32 can be seen particularly at the lateral distal edge, close to the nasal pit, indicated by white arrowhead. Fewer connexin 32 containing gap junctions are seen in central regions, as indicated by *. Axes above figure. Scale bar = 100μm.

Figure labels:

FNM: Frontonasal mass.   NP: Nasal pit.

LNP: Lateral nasal process.   Mx: Maxillary primordium.

Mn: Mandibular primordium.

Axes:

D: Distal   Pr: Proximal

M: medial   L: Lateral.

Figure 4.11
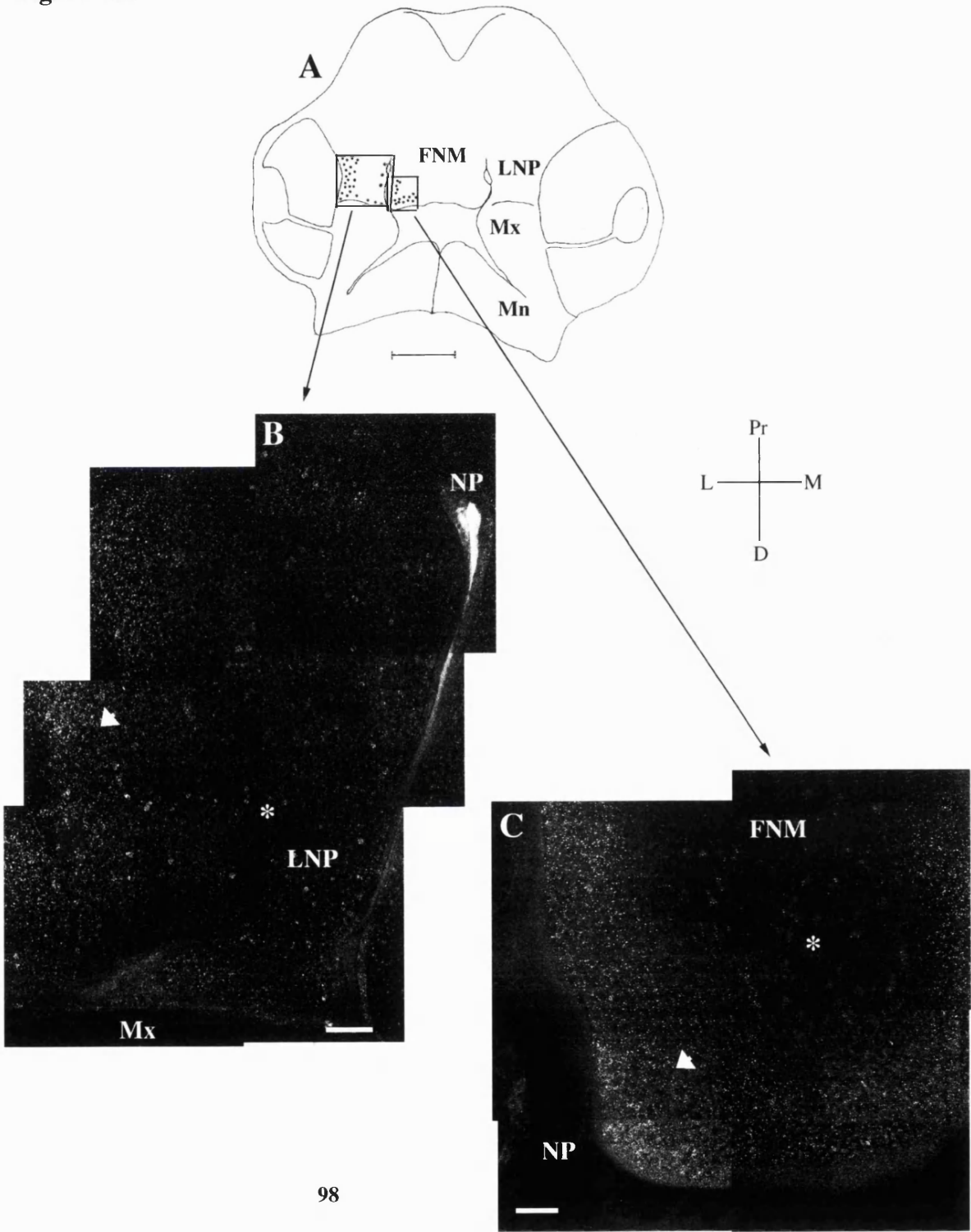
Figure 4.12 Connexin 32 expression in stage 28 maxillary and mandibular primordia.

A. Diagram of chick embryo facial primordia at stage 28. Boxes indicate regions shown in B and C. Black dots summarise connexin 32 expression shown in B and C. Scale bar = 1000μm.

B Connexin 32 expression in stage 28 maxillary primordium. Connexin 32 containing gap junctions are observed in distal regions, indicated by white arrowhead to the right of the figure and in anterior proximal regions, indicated by white arrowhead on the left of the picture. Expression can also be seen in the region where maxillary and mandibular primordia (Mn) join. Less expression is seen centrally and posteriorly, indicated by *. Axes top right of the figure. Scale bar = 100μm.

C. Connexin 32 in the stage 28 mandibular primordium. High levels of connexin 32 containing gap junctions can be seen in lateral regions, indicated by white arrowhead. Fewer gap junctions are observed in distal regions, indicated by *. Axes below the figure. Scale bar = 100μm.

Figure labels:

FNM: Frontonasal mass.   LNP: Lateral nasal process.

Mx: Maxillary primordium.   Mn: Mandibular primordium.

Axes:

D: Distal   Pr: Proximal

A: Anterior   Po: Posterior

M: medial   L: Lateral.

Figure 4.12
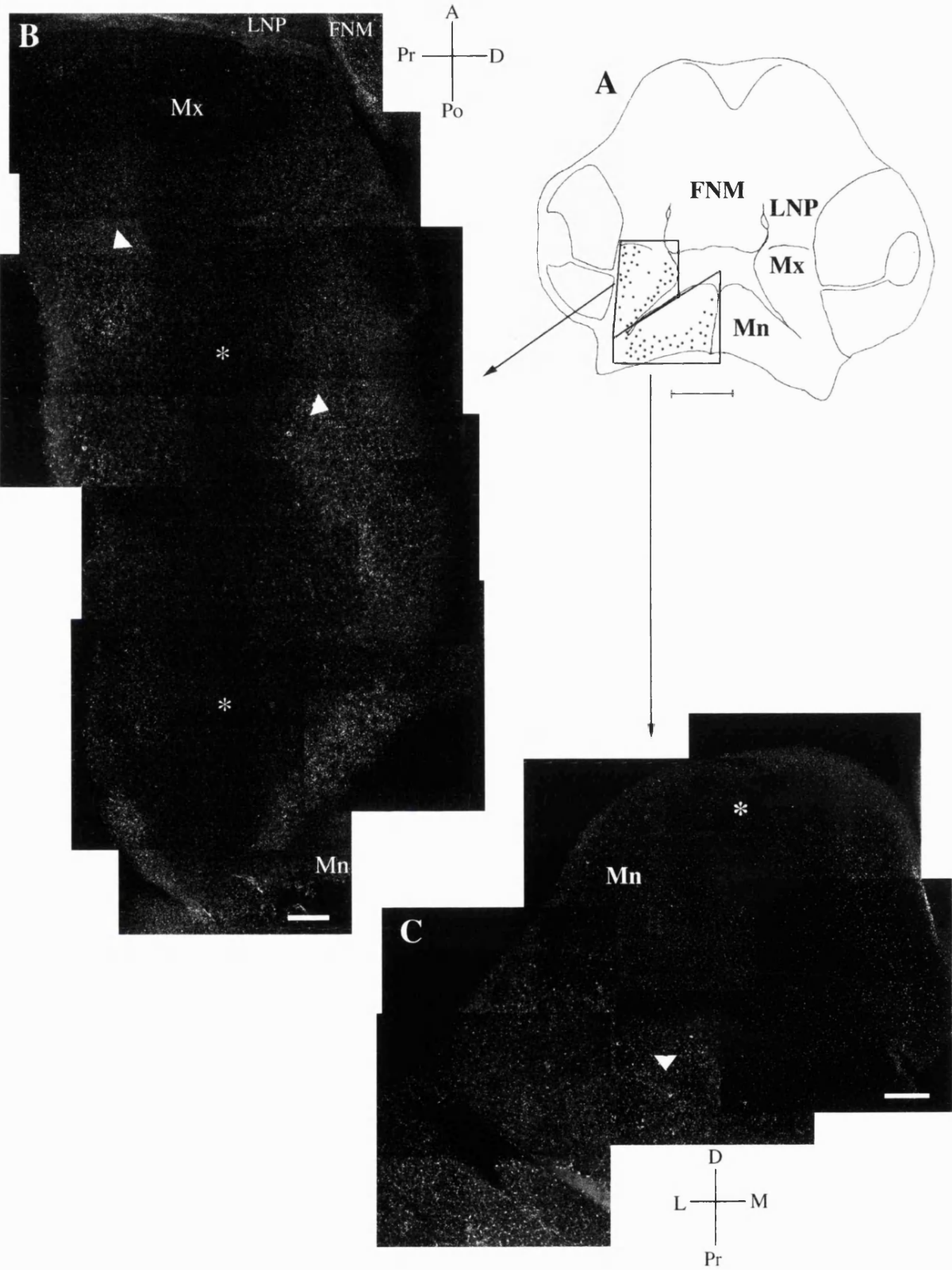
At stages 20 and 24 expression of connexin 32 was abundant in mesenchyme at the open end of the nasal pits (Figs. 4.8, 4.9D arrowhead), similar to connexin 43. In the lateral nasal process, however, patterns of connexin 43 and 32 expression were very different. Initially, high levels of connexin 32 staining were seen in proximal regions, away from the nasal pit (Figs. 4.8, 4.9B). By stage 24, numerous connexin 32 gap junction proteins were seen throughout the lateral nasal process (Fig. 4.10B), which is in direct contrast to connexin 43 where high levels were initially expressed distally and then more proximally at later stages (compare summary Figs. 4.2 and 4.8). At stage 28, connexin 32 protein was restricted laterally, near the eye, and distally near the maxillary primordium (Fig. 4.11B). Thus domains of expression of connexin 43 and 32 protein in the lateral nasal process do not overlap between stages 20 and 28.

In the frontonasal mass, high expression of connexin 32 was seen proximally near the nasal pit at stage 20 (Fig. 4.8, 4.9 C, E) then, at stage 24, throughout the primordium, even in central regions (Fig. 4.10C). Later, at stage 28, expression was quite widespread throughout the primordium even in central regions, however a small region of mesenchyme near the nasal pit expressed fewer connexin 32 containing gap junctions (Fig. 4.11C). This pattern has some similarities to that of connexin 43, which is initially expressed distally at high levels, then both proximally and distally next to the nasal pit but is not found in central regions of the frontonasal mass. Thus, at earlier stages, overlap is found in mesenchyme immediately distal to the nasal pit only. At later stages, the overlap is more substantial next to the nasal pit and along the distal edge of the frontonasal mass (compare Figs. 4.2 and 4.8).

In the maxillary primordium at stage 20, connexin 32 was abundant between cells in anterior regions, near the lateral nasal process (Figs. 4.8, 4.9F, arrowheads) but was more sparse posteriorly (Fig. 4.9 *) rather similar to the pattern seen with connexin 43 protein. At stage 24, expression was again particularly high anteriorly compared to posterior proximal regions (Fig. 4.10D arrowhead indicates abundant expression, * indicates less expression). Mesenchyme at the join between the maxillary primordium and mandibular primordium also expressed abundant connexin 32 protein (Fig. 4.10E arrowhead). At stage 28, there was distinct expression at the distal edge and in anterior

proximal regions, while there was little expression centrally (Fig. 4.12B). Thus at all three stages, anterior distal cells, near the join with the lateral nasal process expressed high levels of both connexins whereas posterior proximal cells did not express high levels of either connexin. At later stages, cells at fusion points, particularly between maxillary and mandibular primordia also express high levels of both connexin proteins.

In mandibular primordia, expression of connexin 32 was intense at the midline at early stages, similar to the pattern of connexin 43 (Figs. 4.8, 4.9H). At stage 24, high levels of connexin 32 expression were found almost throughout, with the exception of the very proximal lateral edge (Fig. 4.10E). At stage 28, expression became more restricted to midline and proximal edges and was also seen at the border between the mandibular and maxillary primordia (Figs. 4.8, 4.12C). Thus there seems to be a substantial amount of overlap of high levels of connexin 32 and 43 protein expression in proximal midline of mandibular primordium and regions of fusion between the paired primordium and with the maxillary primordium.

4.3.3 Expression of connexins 43 and 32 in upper beak primordia after treatment with retinoic acid.

Connexins 43 and 32 are expressed in gap junction plaques between epithelial cells and mesenchymal cells of facial primordia as just described (see also Minkoff *et. al.,* 1991, 1997). Retinoic acid has previously been shown to decrease levels of gap junction expression and communication (Pitts *et. al.,* 1986, Mehta *et. al.,* 1989). In order to examine whether retinoid induced facial defects are associated with changes in gap junction expression, the distribution of connexins 43 and 32 containing plaques in upper beak primordia were examined after retinoic acid treatment at stage 20 (n=3 in each group at each time point). These results are summarised in Figure 4.13.

4.3.3.1 Effect of retinoic acid on connexin 43 expression

The expression of connexin 43 expression in epithelia of upper beak facial primordia was substantially reduced but not abolished within 24 hours of retinoic acid treatment. Expression was slightly reduced in distal epithelium of the nasal pit 12 hours after treatment (Fig. 4.14B, *). By 24 hours, when the nasal pit was notably shortened, very

Figure 4.13 Summary diagrams of the patterns of connexin 43 and connexin 32 expression in the upper beak primordia of the chick face after treatment with retinoic acid.

Patterns of expression are shown at time points after treatment at stage 20.

12 hours after treatment (stage 22), patterns of connexin 43 expression are little changed, with only slight reduction lateral to the nasal pit as shown in 1st figure, top left. 24 hours after treatment (stage 24) expression of connexin 43 is much reduced in regions lateral to and underneath the nasal pit and in the anterior maxillary primordium (middle figure, left panel). 48 hours after treatment, expression is still reduced in lateral nasal process and maxillary primordium, while it has returned to the normal pattern of expression in the frontonasal mass (bottom figure, left panel).

12 hours after treatment, the expression of connexin 32 is as normal, top figure, right panel. Expression of connexin 32 was also normal at 24 and 48 hours after retinoic acid treatment, shown in middle and bottom figures, right panel respectively.

Figure 4.13

Connexin 43   Connexin 32

Stage 22
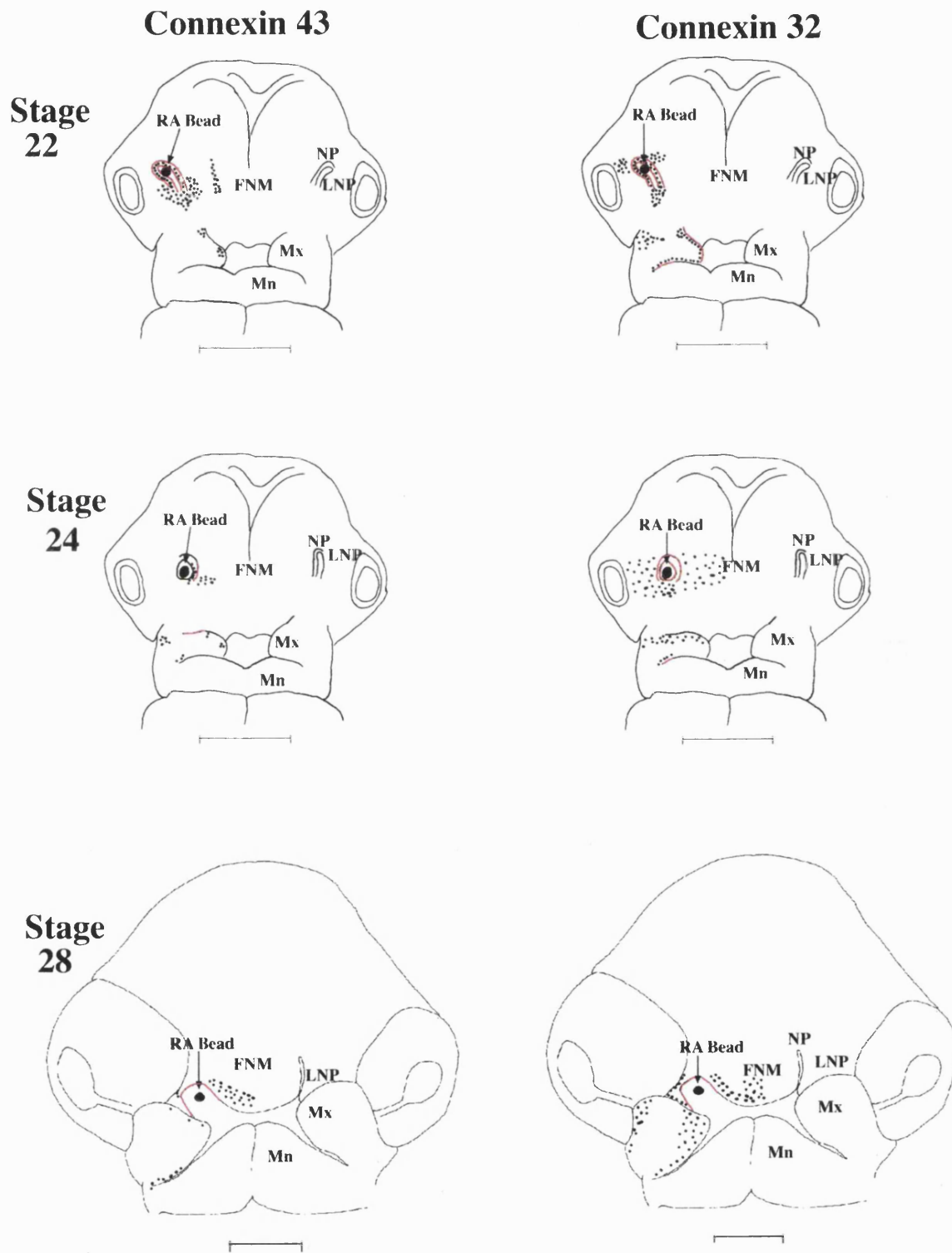
Stage 24

Stage 28

Figure 4.14 Expression of connexin 43 in upper beak primordia after treatment with retinoic acid.

A. Diagram of chick embryo facial primordia at stage 24, 24 hours after treatment with retinoic acid. Right hand side of the diagram indicates a retinoic acid soaked bead in the nasal pit, with characteristic abnormalities seen upon retinoid treatment, i.e. shortened nasal pit and a shortened maxillary primordium. Boxes indicate regions shown in B-E. Scale bar = 1000μm.

B. Connexin 43 in the nasal pit region, lateral nasal process and frontonasal mass 12 hours after a retinoic acid treatment. Expression can be seen throughout most of the region. However, reduced expression can be seen in distal lateral nasal process and frontonasal mass adjacent to the nasal pit, indicated by *. Scale bar = 100μm.

C. Connexin 43 expression in lateral nasal process and nasal pit 24 hours after retinoic acid treatment. Labelling can be seen in the lateral nasal process, but is much reduced. Scale bar = 100μm.

D. Connexin 43 in the nasal pit and frontonasal mass 24 hours after retinoic acid treatment. Expression of connexin 43 is reduced in the frontonasal mass, but not quite as severely as in the lateral nasal process, indicated by *. Scale bar = 100μm.

E. Connexin 43 in the maxillary primordium 24 hours after retinoic acid treatment. A small patch of epithelial expression can be seen at the top of the picture. Little mesenchymal expression can be seen, especially distally (D) indicated by *. Scale bar = 100μm.

Figure labels:

FNM: Frontonasal mass.   LNP: Lateral nasal process.

Mx: Maxillary primordium.   Mn: Mandibular primordium.

NP: Nasal pit

Axes:

D: Distal   Pr: Proximal

A: Anterior   Po: Posterior

M: Medial   L: Lateral.

Figure 4.14
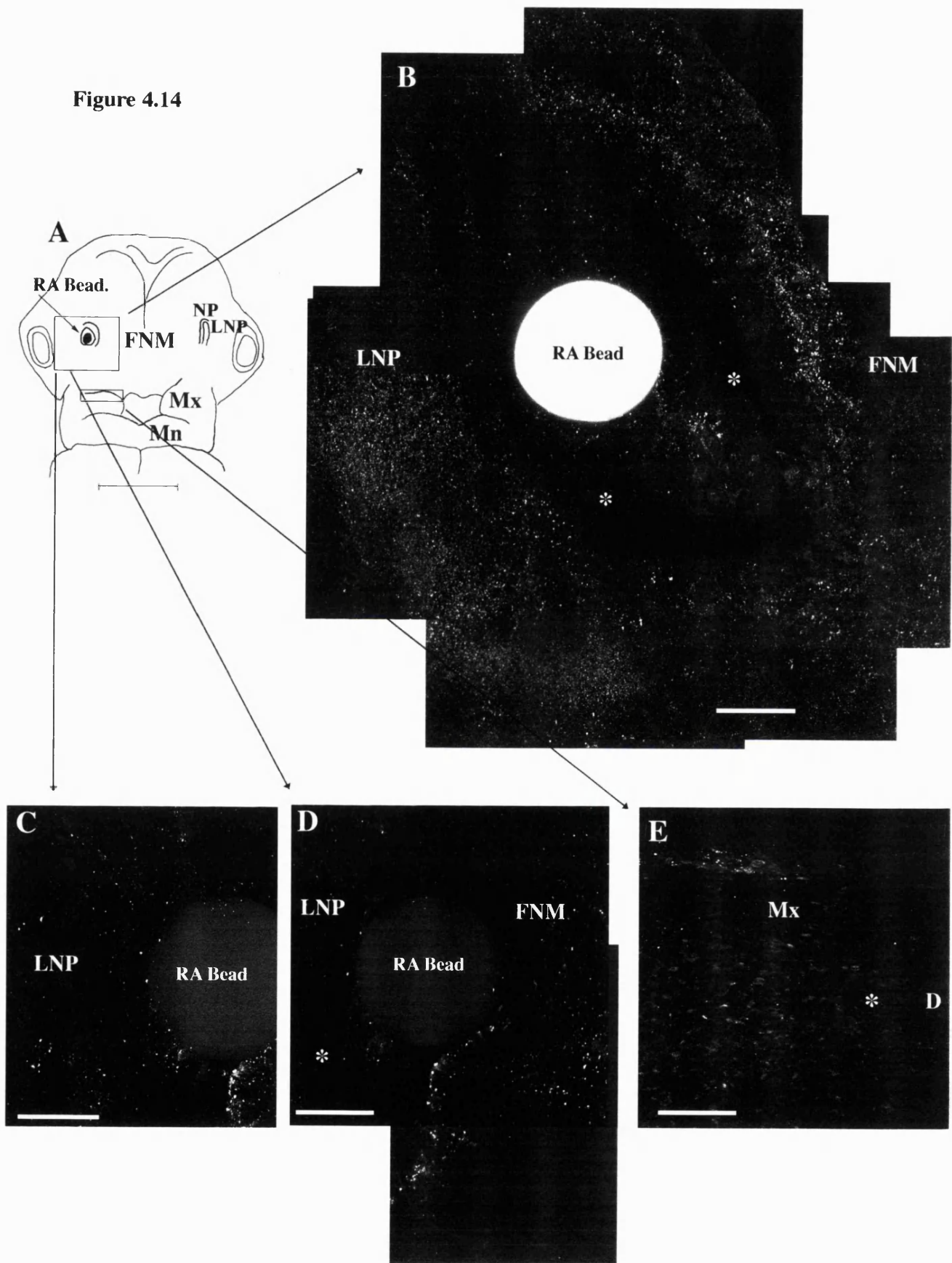
little expression was detected in the lateral edge, next to the nasal pit, although some expression was still seen in the medial epithelium (Figs. 4.14C, D). In epithelium of maxillary primordia, labelling was somewhat reduced in distal anterior regions 24 hours after treatment (Fig. 4.14E, *). However, epithelial expression had returned to normal in all primordia 48 hours after treatment with retinoic acid (Fig. 4.15 B, C, D).

Mesenchymal expression of connexin 43 protein was also reduced considerably within 24 hours of treatment. Embryos were examined for expression of connexin 43, 12 hours after treatment (approximately stage 22), and patterns of mesenchymal staining in the medial and lateral nasal process (Figs. 4.13, 4.14B) and maxillary primordium were normal (compare Figs. 4.2 and 4.13). However, 24 hours after the retinoic acid bead had been placed in the nasal pit, the number of plaques containing connexin 43 gap junction protein was greatly reduced in the mesenchyme immediately distal and lateral to the nasal pit (Figs. 4.14C, D, *). Expression in frontonasal mass and anterior distal mesenchyme of maxillary primordia (at the join with the lateral nasal process, labelled D in figure) was also reduced (Figs. 4.14D, E). After 48 hours, the number of connexin 43 positive plaques was still reduced distally in lateral nasal process mesenchyme (Fig. 4.15C) and in anterior maxillary primordium (Fig. 4.15D). The distribution and abundance of connexin 43 containing plaques appeared normal in the frontonasal mass despite the large cleft that skewed this primordium (Fig. 4.15B).

4.3.3.2 Effect of retinoic acid on connexin 32 expression

In contrast to these substantial reductions in the level of connexin 43 containing gap junctions, both epithelial and mesenchymal expression of connexin 32 seemed to be relatively unaffected by retinoid treatment. At 12 hours (Fig 4.16A), 24 hours (Fig 4.16B, C) and 48 hours (Fig 4.16D) after treatment with retinoic acid, connexin 32 containing gap junctions were found as in normal embryos (also compare Fig. 4.8 with Fig. 4.13). These results show that a marked reduction in connexin 43 expression, in mesenchyme, accompanies retinoid induced clefting of the primary palate in chick embryos whereas there is no effect on expression of connexin 32 containing gap junctions.

Figure 4.15 Expression of connexin 43 in upper beak primordia 48 hours after retinoic acid treatment.

A. Diagram of retinoic acid treated chick embryo facial primordia at stage 28. The right hand side of the diagram indicates a retinoic acid soaked bead in the nasal pit, a shortened nasal pit, a shortened maxillary primordium and a skewed frontonasal mass. Boxes indicate regions shown in the B-D. Scale bar = 1000μm.

B. Connexin 43 expression in frontonasal mass 48 hours after retinoic acid treatment. Expression can be seen in the lateral distal region, near the nasal pit (white arrowhead), and extending along the distal edge of the primordium. In mesenchyme immediately underneath the epithelia, there are few gap junctions, (white arrows). This expression pattern is similar to that in normal embryos at this stage. Scale bar = 100μm.

C. Connexin 43 expression in the lateral nasal process 48 hours after retinoic acid treatment. Labelling can be seen in the epithelia at the edge of the nasal pit and some labelling is also seen laterally. Expression is still reduced compared to normal. Scale bar = 100 μm.

D. Connexin 43 expression in maxillary primordium 48 hours after retinoic acid treatment. Gap junctions are seen in the epithelia of the lateral nasal process and maxillary primordium, however mesenchymal expression is sparse. Expression is reduced compared to normal. Scale bar = 100μm.

Figure labels:

FNM: Frontonasal mass.   LNP: Lateral nasal process.

Mx: Maxillary primordium.   NP: Nasal pit

Figure 4.15
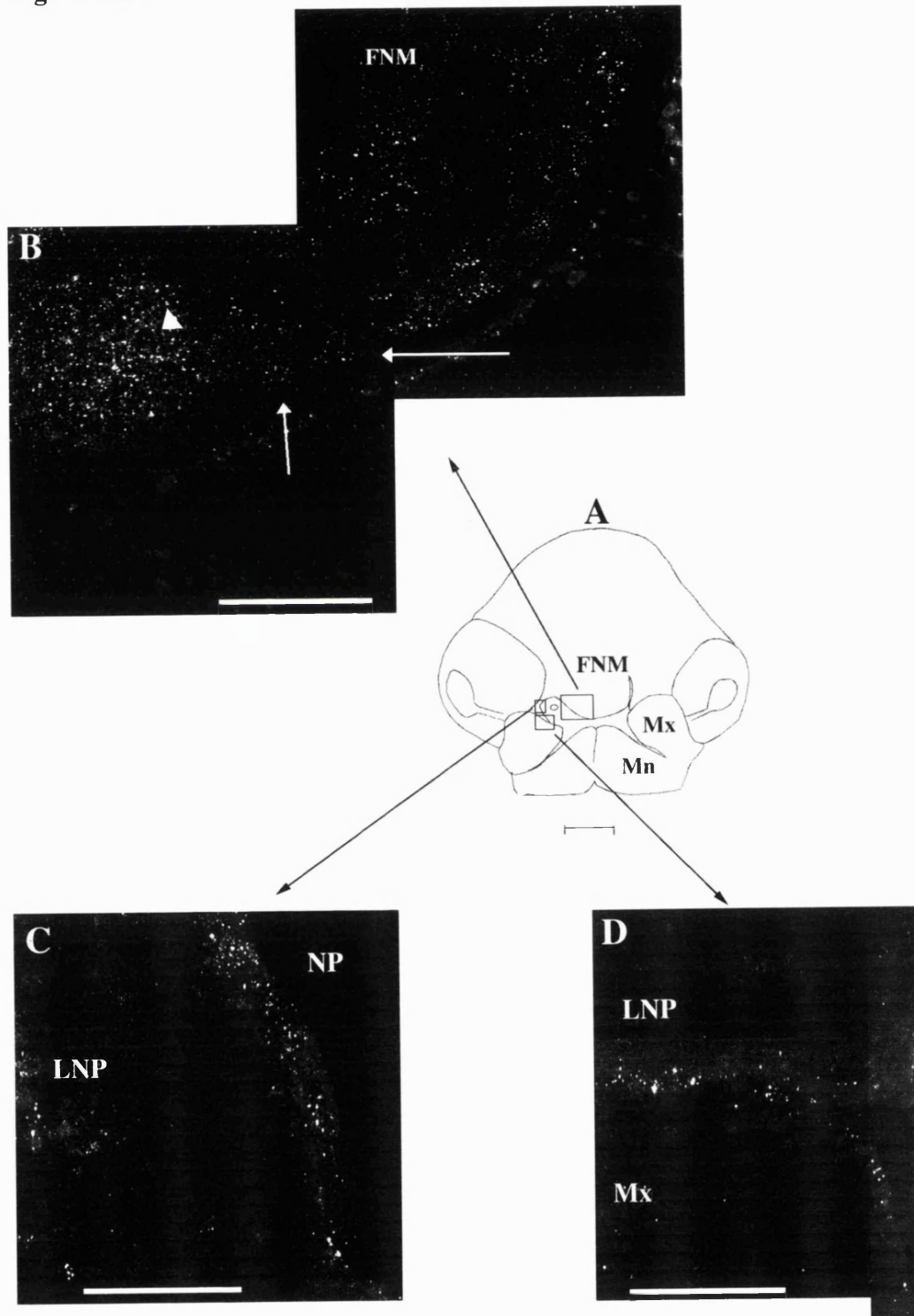
Figure 4.16 Expression of connexin 32 in upper beak primordia after retinoic acid treatment.

A. Connexin 32 expression in the nasal pit region 12 hours after retinoic acid treatment. Abundant expression can be seen in the lateral nasal process, in the region at the base of the nasal pit (bnp) and in the frontonasal mass. Scale bar = 100μm.

B. Connexin 32 expression in the nasal pit region 24 hours after retinoic acid treatment. Again abundant expression can be seen both in the nasal pit epithelia, in mesenchyme beneath the nasal pit and in lateral nasal process.

C. Connexin 32 expression in anterior distal maxillary primordium 24 hours after retinoic acid treatment. Expression can be seen in epithelia at the edge of the primordium and in mesenchyme throughout this region.

D. Connexin 32 expression in frontonasal mass and maxillary primordium 48 hours after retinoic acid treatment. Expression can be seen in epithelia and mesenchyme of both primordia even though they are separated by a large cleft.

Figure labels:

FNM: Frontonasal mass.   LNP: Lateral nasal process.

Mx: Maxillary primordium.   NP: Nasal pit

Figure 4.16
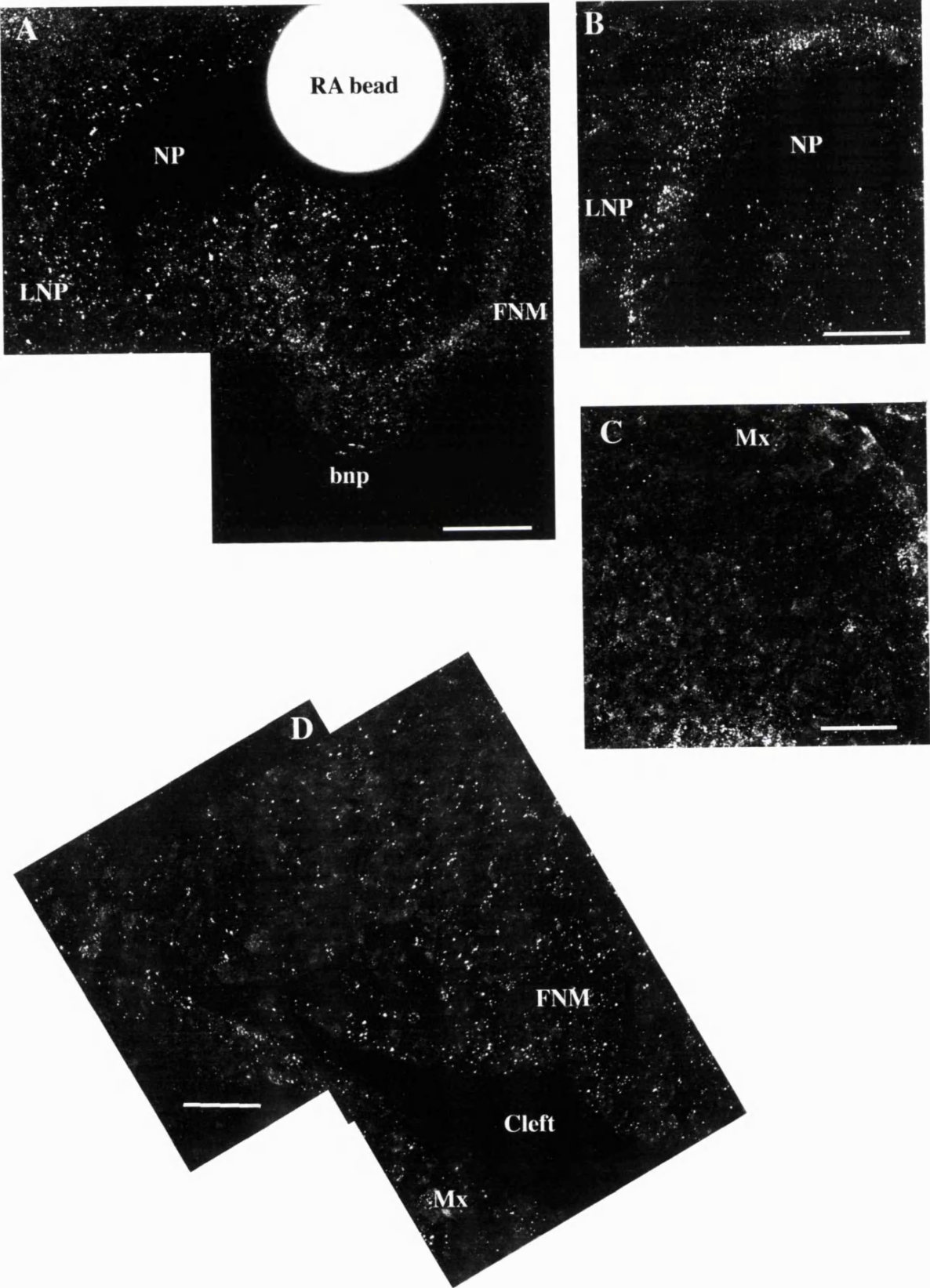
4.3.4 Application of connexin 43 unmodified antisense and sense deoxyoligonucleotides to chick facial primordia *in ovo*.

Application of retinoic acid to the chick face results in clefting of the primary palate and, as we have shown above, this is accompanied by a reduction in expression of connexin 43 gap junction proteins. This implies that reduction of connexin 43 expression may either be causally related to primary palate clefting or be a consequence of failure of primary palate morphogenesis. To test directly the role of connexin 43 expression in primary palate formation and in facial fusion in general, we applied antisense oligonucleotides against connexin 43 protein. These oligonucleotides prevented specifically the translation of mRNA transcripts encoding connexin 43 into protein, thus lowering connexin 43 protein levels. Unmodified antisense and sense deoxyoligonucleotides (ODN's) against connexin 43 were applied to chick embryos *in ovo*, at various stages of development, between stages 7 and 25, suspended in a 30% solution of pluronic gel F-127 (BASF Corp).

4.3.5 Connexin 43 antisense ODNs enter cells and reduce the level of connexin 43 protein in facial primordia.

Two of the criteria required to indicate that antisense ODNs are effective are entry of the ODNs into cells and specific reduction in the level of protein. Connexin 43 antisense ODNs tagged with FITC, suspended in pluronic gel, were applied to chick embryos as before and assessed at 2 and 4 hours after application for the presence of FITC staining in cells. FITC fluorescent labelling was found to be concentrated in the nucleus of mesenchymal cells by 2 hours, although there was some cytoplasmic staining. Intense fluorescent staining was still found at 4 hours (Fig. 4.17). This indicates that these ODNs are able to rapidly penetrate the cell and reach the nucleus.

The effectiveness of antisense oligonucleotide in preventing connexin 43 gap junction protein translation was assessed by immunohistochemistry in embryos dosed at stage 10 or 11 (n=3 for each time point). Embryos were examined at 2 and 4 hours after application of antisense oligonucleotides but no changes in protein expression were detected. In other tissues of the embryo, such as the limb bud and spinal cord, expression

Figure 4.17 FITC-labelled connexin 43 antisense ODNs in mesenchymal cells 4 hours after administration.

Fluorescent labelling is concentrated in the nucleus of the cells. Some labelling, though not as intense, is also found in the cytoplasm. This indicates that these ODNs are able to enter cells rapidly and concentrate in the nucleus.

Figure 4.17

FITC-labelled antisense ODNs
localised in cytoplasm
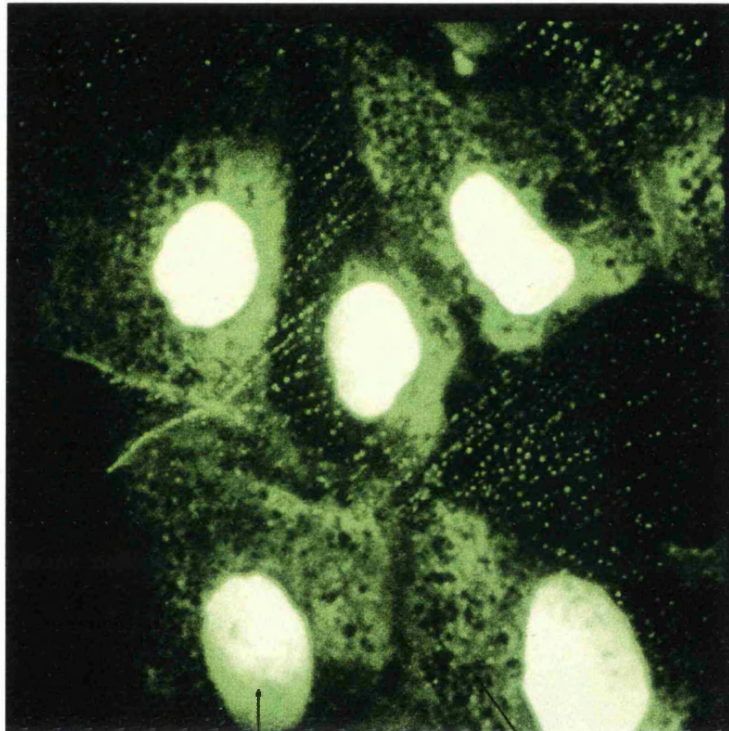
FITC-labelled antisense ODNs
localised in nucleus

of connexin 43 protein was notably reduced at 4 hours (Becker et. al., 1998, submitted). Reduced levels of connexin 43 protein expression were noted 8 hours after application of connexin 43 antisense ODNs. At this stage (approximately stage 12/3), no facial primordia are discernible but the neural crest, which later forms the majority of facial tissue, is still migrating laterally from the dorsal neural tube (Fig. 4.18A). Control embryos (control, sense and pluronic gel treated) at this stage show abundant connexin 43 staining in neural tube and neural crest regions as well as the ectoderm (Fig. 4.18B). Embryos have not turned at stage 12 and therefore tended to show a bilateral reduction in connexin 43 staining across the head region (4.18C). This could account for the occasional bilateral defects in embryos that were treated at these early stages (see section 4.3.6 below and Fig. 4.22A). Embryos that were slightly more advanced (stage 13+) were turning and tended to show reduction of connexin 43 staining predominantly on one side - the side uppermost in the egg, nearest to the pluronic gel.

At stages 17/8 (24 hours after treatment with antisense oligonucleotides), expression of connexin 43 gap junction protein in mesenchyme of the frontonasal mass and 1st branchial arch was still very reduced. There was, however, more abundant expression in epithelia of these treated primordia (Figs. 4.18 G, H, note that this is a side view of the face). Normal embryos at this stage of development show abundant connexin 43 protein in both epithelia and mesenchyme of developing facial primordia (Fig. 4.18F). 48 hours after treatment, approximately stage 22/3, expression of connexin 43 gap junction protein had returned to normal levels in mandibular primordium (Fig. 4.19E) and were beginning to be expressed in distal lateral nasal process (Fig. 4.19B) and distal frontonasal mass (Fig. 4.19C). However the maxillary primordium still had little or no expression (Fig. 4.19D). This suggests that there is a difference in turnover rate of connexin 43 in different facial primordia.

These data show that up to 8 hours of antisense oligonucleotide treatment is required for a significant reduction of connexin 43 gap junction protein production and degradation of existing protein. The reduction of connexin 43 protein expression lasts up to 40 hours. Expression of connexin 43 in the mesenchyme of maxillary primordium was affected for

Figure 4.18 Connexin 43 expression in head and facial primordia after treatment with connexin 43 antisense ODNs

A. Diagram of dorsal anterior (head) regions of stage 11-12 chick embryos. The neural tube (DNT) runs along the A-P axis of the embryo. Neural crest (NC) migrates laterally from edges of neural tube, into the ventral side of the head. Optic cups (OC) also indicated in this figure. Scale bar = 1000 μm.

B. Expression of connexin 43 in dorsal stage 11 chick head. Expression is seen in the dorsal neural tube (DNT), at the edges of the neural tube and in tissue lateral to this (NC). Little expression is seen in the developing eye (OC). Scale bar = 100 μm.

C. Expression of connexin 43 in stage 12 chick head, 8 hours after application of connexin 43 antisense ODNs. Little expression is seen in either mesenchyme or epithelia. Box indicates region shown in enlarged view, D. Scale bar = 100 μm.

D. Lateral dorsal edge of stage 12 embryo as in C. Labelling at epithelial edge is likely to be background staining as not punctate (arrowhead). A few gap junctions can be seen in the mesenchyme at this magnification. Scale bar = 100 μm.

E. Diagram of stage 17 chick embryo head and facial primordia. The frontonasal mass (FNM) and developing nasal pit are seen at this stage. The 1st branchial arch (1st arch) later splits to form both maxillary and mandibular primordia. The heart (Ht) protrudes from between 1st and 2nd branchial arches. Scale bar = 1000 μm.

F. Connexin 43 expression in stage 16/17 chick facial primordia. Abundant connexin 43 containing gap junctions can be seen in 1st arch, (white arrowhead). Some expression is also seen in frontonasal mass (FNM). Gap junctions are also observed in the heart (Ht). Scale bar = 100 μm.

G. Expression of connexin 43 containing gap junctions in the facial primordia at stage 17, 24 hours after application of connexin 43 antisense ODNs. Some expression can be seen in the epithelia of frontonasal mass and 1st arch primordia, (white arrowheads). Little mesenchymal expression is seen in this region. Scale bar = 100 μm.

H. Expression of connexin 43 in stage 17 facial primordia, 24 hours after treatment with connexin 43 antisense ODNs. Again there is very little expression in the frontonasal mass or first arch primordia. Scale bar = 100 μm.
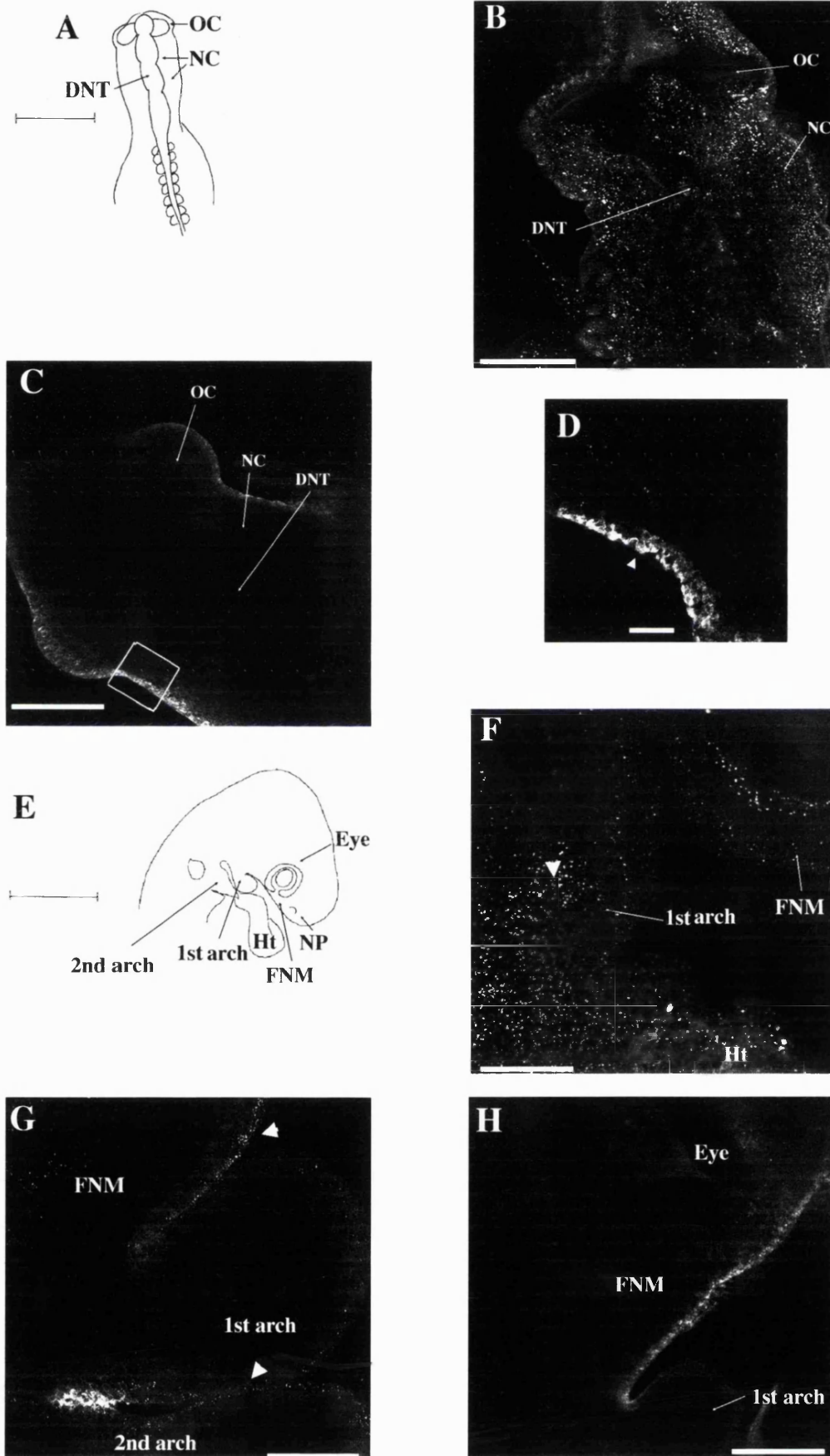
Figure 4.18

Figure 4.19 Expression of connexin 43 in facial primordia 48 hours after treatment with connexin 43 antisense ODNs.

A. Diagram of chick facial primordia at stage 22/3. Boxes indicate regions shown in B-E and black dots summarise patterns of connexin 43 expression in these figures. Scale bar = 1000 μm.

B. Connexin 43 expression in lateral nasal process and nasal pit at stage 23, 48 hours after treatment with connexin 43 antisense ODNs. Patches of gap junction labelling can be seen in lateral and distal edges, as indicated by white arrowheads. This indicates expression of connexin 43 protein is returning. Scale bar = 100μm.

C. Connexin 43 expression in the frontonasal mass 48 hours after application of connexin 43 antisense ODNs. Expression is observed in distal regions, in particular at the base of the nasal pit as indicated by white arrowhead. This is similar to the pattern observed in untreated stage 23 frontonasal mass. Scale bar = 100 μm.

D. Connexin 43 expression in stage 23 maxillary primordium, 48 hours after application of connexin 43 antisense ODNs. Only a few gap junction plaques are observed in the region close to where the maxillary primordium joins to the mandibular primordium, indicated by white arrowhead. Scale bar = 100 μm.

E. Connexin 43 expression in stage 22 mandibular primordium, 48 hours after application of connexin 43 antisense ODNs. Expression can be seen throughout the primordium, particularly in mesenchyme close to the midline, as indicated by white arrowhead. This pattern is similar to that seen in the untreated stage 22 mandibular primordium. Scale bar = 100 μm.

Figure labels:

FNM: Frontonasal mass.	NP: Nasal pit.
LNP: Lateral nasal process.	Mx: Maxillary primordium.
Mn: Mandibular primordium.	

Figure 4.19
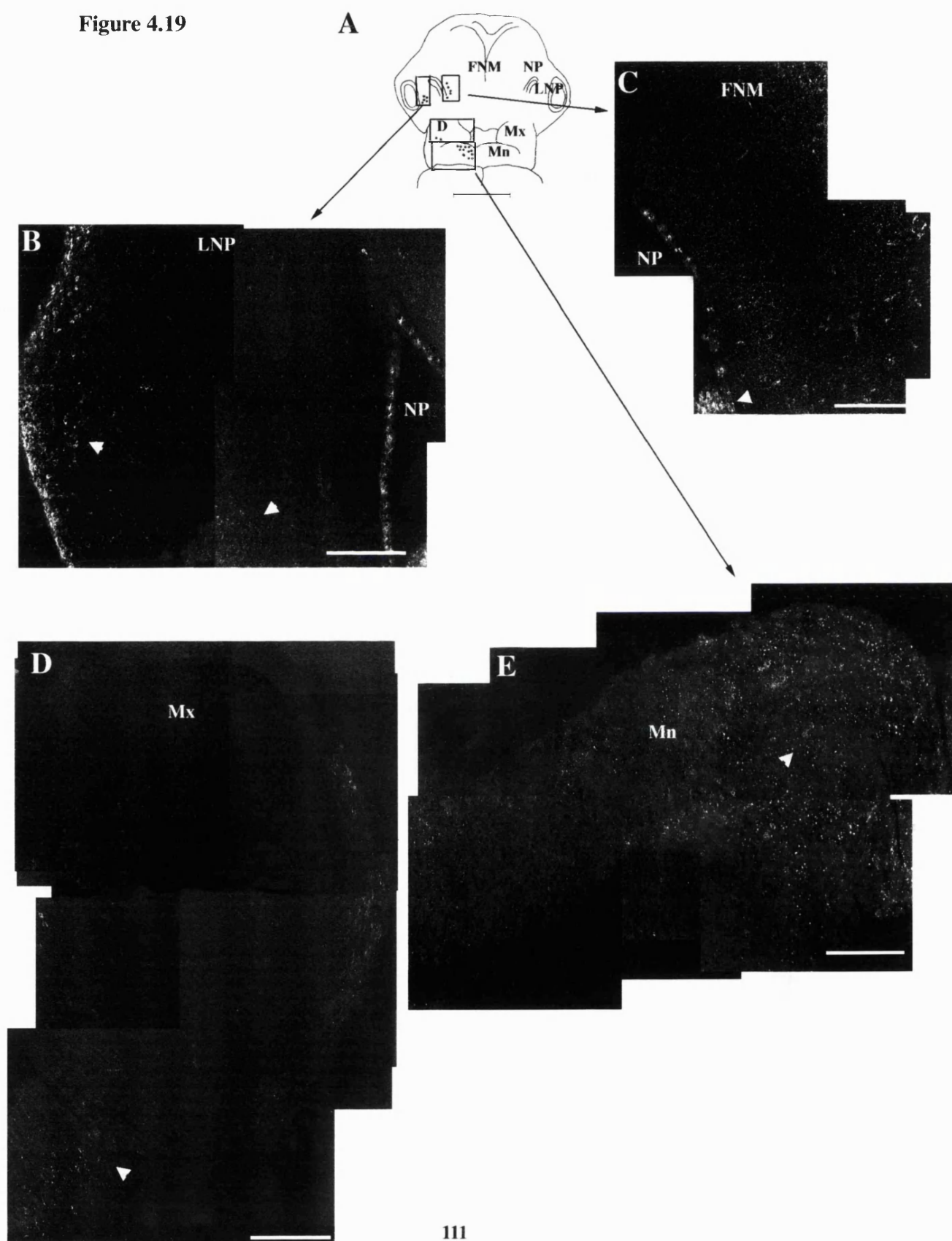
Figure 4.20 Expression of connexin 32 in facial primordia after treatment with connexin 43 antisense ODNs.

A. Diagram of stage 17 chick embryo head. The frontonasal mass (FNM) and developing nasal pit are obvious structures at this stage. The 1st branchial arch (1st arch on the diagram) later splits to form both maxillary and mandibular primordia. The heart (Ht) protrudes between 1st and 2nd branchial arches. Scale bar = 1000 μm.

B. Connexin 32 expression in the developing facial primordia of an untreated stage 17 chick embryo. Expression is observed in mesenchyme (indicated by top white arrowhead) and epithelia of the frontonasal mass (FNM). 1st arch primordia also express abundant epithelial and mesenchymal connexin 32, the latter indicated by bottom white arrowhead. Scale bar =100 μm.

C. Connexin 32 expression in the developing facial primordia of stage 17 chick embryo, 24 hours after treatment with connexin 43 antisense ODNs. Abundant expression is seen in the frontonasal mass (FNM) and 1st arch primordia, both indicated by arrowheads. This pattern of labelling is similar to that seen in controls. Scale bar = 100μm.

D. Diagram of facial primordia at stage 22/3. Box indicates region of face shown in E and F. Black dots summarise expression of connexin 32 seen in those figures. Scale bar = 1000 μm.

E. Connexin 32 expression in the untreated stage 23 chick head, in the region where maxillary (Mx) and mandibular (Mn) primordia join. Abundant expression can be seen throughout this region, particularly in mesenchyme close to the join indicated by white arrowheads. Scale bar = 100 μm.

F. Connexin 32 expression in stage 23 facial primordia, 48 hours after application of connexin 43 antisense ODNs. This picture shows the same region as E. As in the untreated embryo, expression is abundant in both maxillary (Mx) and mandibular (Mn) primordia, particularly close to the join between primordia, as indicated by white arrowheads. Scale bar = 100 μm.

Figure 4.20
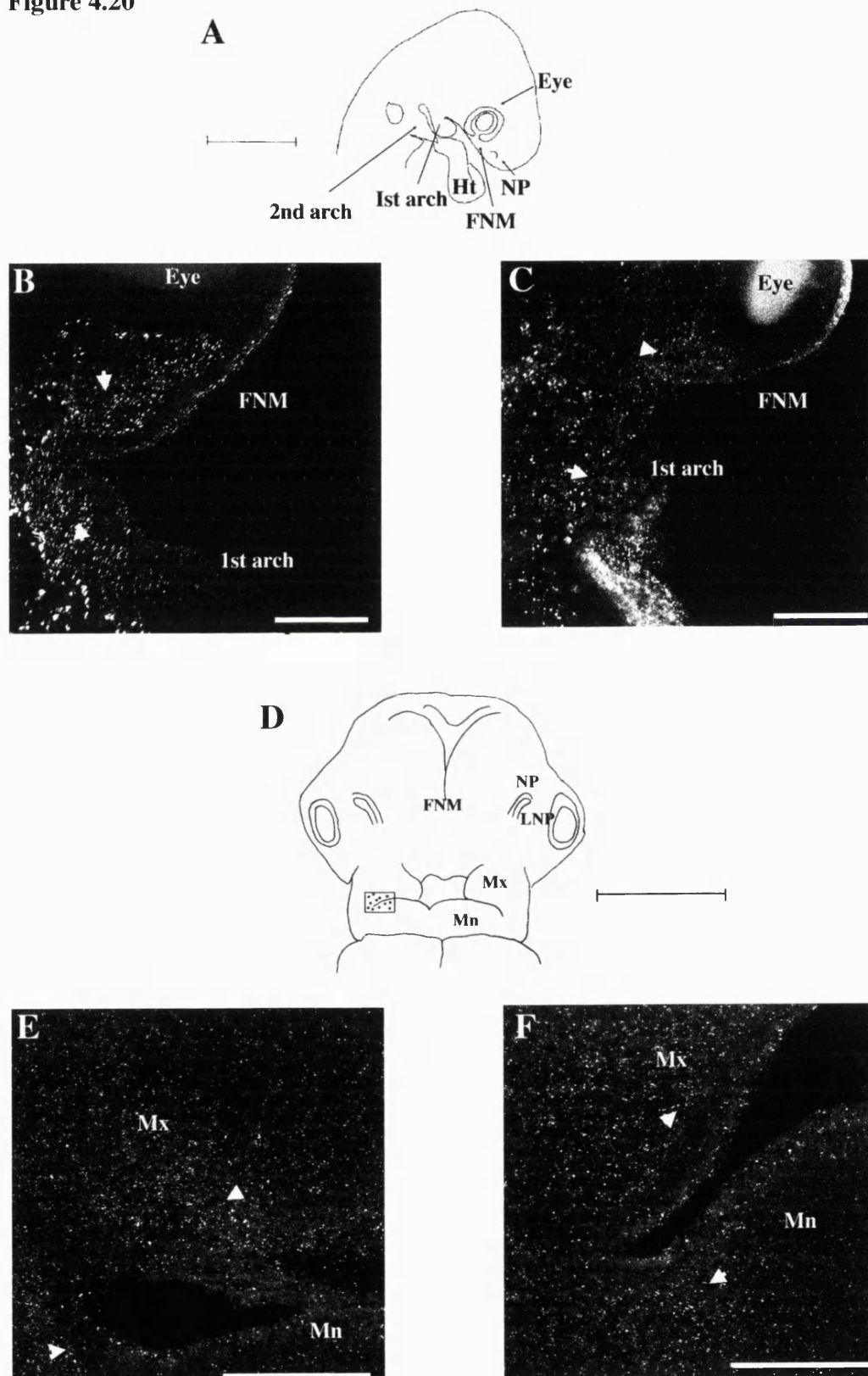
a longer period of time than that in other facial mesenchyme and ectoderm of all facial primordia, in general, seemed less affected than mesenchyme.

The specificity of connexin 43 antisense oligonucleotide treatment was assessed by examining connexin 32 expression in facial primordia by immunohistochemistry at 2, 4, 8, 24, (Fig. 4.20 B, C) and 48 hours (Fig. 4.20 E, F) after application of connexin 43 antisense oligonucleotides (n=3 for each time point). Expression of connexin 32 was similar to that in control embryos at all time points examined, indicating that the antisense oligonucleotides used had a specific effect on connexin 43 expression.

4.3.6 Effect of connexin 43 antisense ODNs on development of facial primordia

Embryos were incubated for 48 hours and assessed for normal facial development by light and scanning electron microscopy (stage 21/2 for embryos treated at stages 10/11). Some embryos were also incubated up to day 10 of development (stage 33/4) to assess the final shape of the face. Sense oligonucletides against connexin 43 suspended in pluronic gel and pluronic gel alone were applied as controls. At early stages of application (stages 7-12) the embryo is "face down" in the egg, thus gel was applied evenly over the dorsal part of the head. At later stages (13-25), the embryo turns, so that the right side of the head and face is uppermost in the egg and is turned into the gel. Thus at these stages, it seems likely that right and left sides of the face will be differentially treated.

Normal stage 22 embryos show symmetry in growth and shape of facial primordia around the oral cavity (Fig. 4.21A) (n=3 examined). Embryos treated with sense oligonucleotides in pluronic gel (Fig. 4.21B) and pluronic gel only (Fig. 4.21C) also showed symmetrical development of facial primordia at all stages of dosing. In contrast, defects in shape and growth of facial primordia were seen in embryos at treated with antisense connexin 43 between stages 7 and 18. Three types of defects were seen - retardation of nasal pit development (shorter and wider pits) with associated flattening of the lateral nasal process and frontonasal mass near the nasal pit (Figs. 4.21D, H), retardation of maxillary primordium development (shorter and less outgrowth) (Figs. 4.21 E, F) and retardation of mandibular primordium outgrowth (Fig 4.21D). Defects

113

were, in most cases, unilateral presumably due to asymmetry of treatment but in a few notable exceptions, defects were found on both sides of the face (as in Figs. 4.21D and Fig. 4.23A). These bilateral defects were found in embryos treated at early stages (stage 9/10) when treatment would be even over the whole head. Unilateral defects were found either on the right or left sides of the face. In total, 60% of affected embryos had defects on the right side of the face and 40% on the left. The incidence of embryos turning to the left is low in chick embryos. This result suggests that this treatment affects direction of turning, however this is probably due to the weight of the pluronic gel. Embryos treated with antisense ODN's between stages 20 and 24 had no detectable facial defects. The numbers of deaths in sense, antisense and pluronic gel treated groups were similar at each stage (Table 4.1). Only embryos that survived were included for analysis.

Embryos treated at stages 7-9 had a poor survival rate, both with antisense (79% deaths) sense oligonucleotide (92% deaths) and pluronic gel (80%) treatments (Table 4.1). Embryos at this stage are very delicate and also susceptible to damage when opening the embryonic membranes. The three surviving embryos treated with antisense ODN's showed defects in facial development (100% of surviving embryos, Table 4.1, graph 4.1). All three embryos had smaller, wider nasal pits than normal and shorter mandibular primordia (Fig. 4.21D) and 2 out of the 3 had shorter maxillary primordia (Table 4.2, Graph 4.2).

47%, nine out of 19 surviving embryos, treated with antisense oligonucleotides at stages 10 and 11 showed defects in maxillary primordia development (Table 4.2, Graph 4.2, Figs. 4.21E, F) whilst almost half the affected embryos had nasal pit defects and/or mandibular primordium defects (Table 4.2, Graph 4.2).

Embryos dosed between stages 12 and 14 also showed a high incidence of defects with 59%, 10 out of 17 surviving embryos, with defective facial development (Table 4.2, Graph 4.2). Again all affected embryos had defects in maxillary primordium development but fewer mandibular defects (Table 4.2, Graph 4.2). After stage 14, the incidence of defects decreases with only one out of 5 surviving embryos, 20%, with defects in all three primordia (Table 4.2 and Graph 4.2).

Table 4.1

Stage of embryo treated	Number of embryos treated			No. normal embryos (%)			No. embryos with head defects (%).			No. of deaths (%).		
	Pluronic gel	Sense	Antisense	Pluronic gel	Sense	Antisense	Pluronic gel	Sense	Antisense	Pluronic gel	Sense	Antisense
7-9	5	13	14	1 (20%	1 (8%)	0 (0%)	0 (0%)	0 (0%)	3 (21%)	4 (80%)	12 (92%)	11 (79)
10-11	14	24	24	12 (86%)	17 (71%)	10 (42%)	0 (0%)	0 (0%)	9 (38%)	2 (14%)	7 (32%)	5 (23%)
12-14	12	21	21	10 (83%)	17 (81%)	7 (33%)	0 (0%)	0 (0%)	10 (48%)	2 (17%)	4 (22%)	4 (21%)
15-18	5	3	6	4 (80%)	2 (68%)	4 (67%)	0 (0%)	0 (0%)	1 (17%)	1 (20%)	1 (33%)	1 (17%)
20-24	6	9	6	5 (83%)	7 (78%)	5 (83%)	0 (0%)	0 (0%)	0 (0%)	1 (17%)	2 (22%)	1 (17%)

Incidence of normal embryos, embryos with abnormal facial primordia and deaths after administration of Connexin 43 sense or antisense oligodeoxynucleotides or pluronic gel.

Table 4.2

Stage of embryo at dosing.	Number of surviving embryos			Number of embryos with defects of facial primordia (% of surviving embryos).			Incidence of defects seen in individual primordia after antisense treatment (% of surviving embryos)		
	Pluronic gel	Sense	Antisense	Pluronic gel	Sense	Antisense	FNM/NP	Mx	Mn
7,8,9	1	1	3	0 (0%)	0 (0%)	3 (100%)	3 (100%)	2 (67%)	3 (100%)
10, 11	12	17	19	0 (0%)	0 (0%)	9 (47%)	4 (21%)	9 (47%)	3 (16%)
12-14	10	17	17	0 (0%)	0 (0%)	10 (59%)	5 (29%)	10 (59%)	3 (18%)
15-18	4	2	5	0 (0%)	0 (0%)	1 (20%)	1 (20%)	1 (20%)	1 (20%)
20-24	5	7	5	0 (0%)	0 (0%)	0 (0%)	0 (0%)	0 (0%)	0 (0%)

Incidence of growth defects in facial primordia after treatment with Connexin 43 sense or antisense oligonucleotides or pluronic gel at different embryonic stages.

Graph 4.1 Percentage of surviving embryos with facial defects after treatment with sense or antisense ODNs or pluronic gel.

Embryonic stage at time of treatment
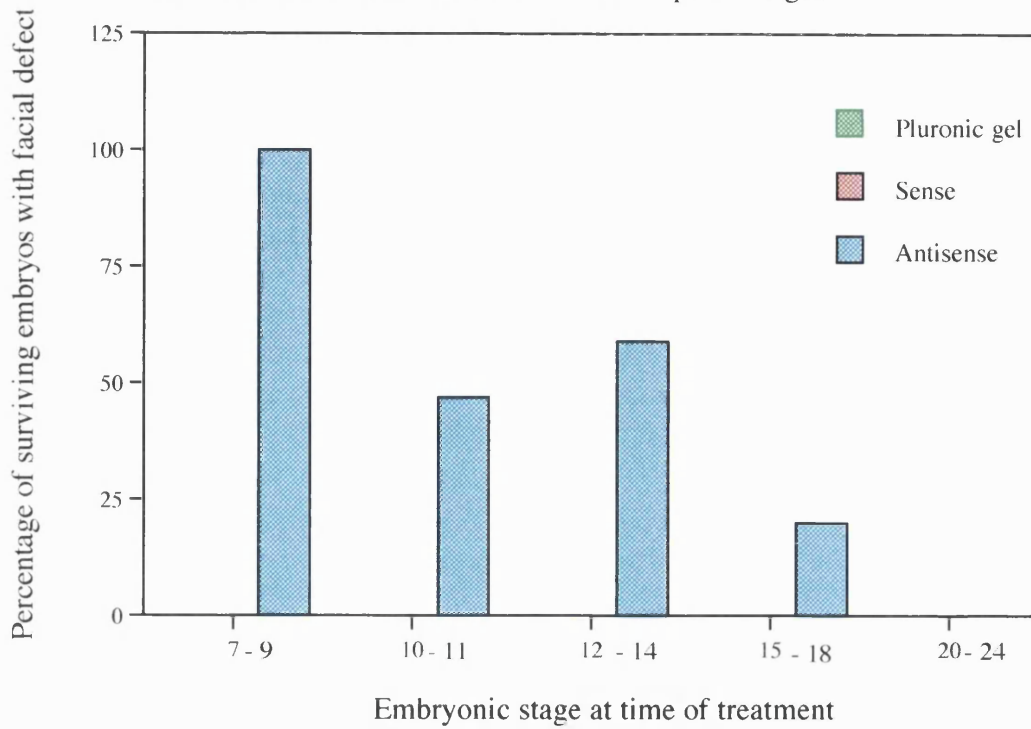
Graph 4.2 Percentage of surviving embryos treated with antisense ODNs with defects in either frontonasal mass/lateral nasal process, maxillary or mandibular primordia.

Embryonic stage at time of treatment
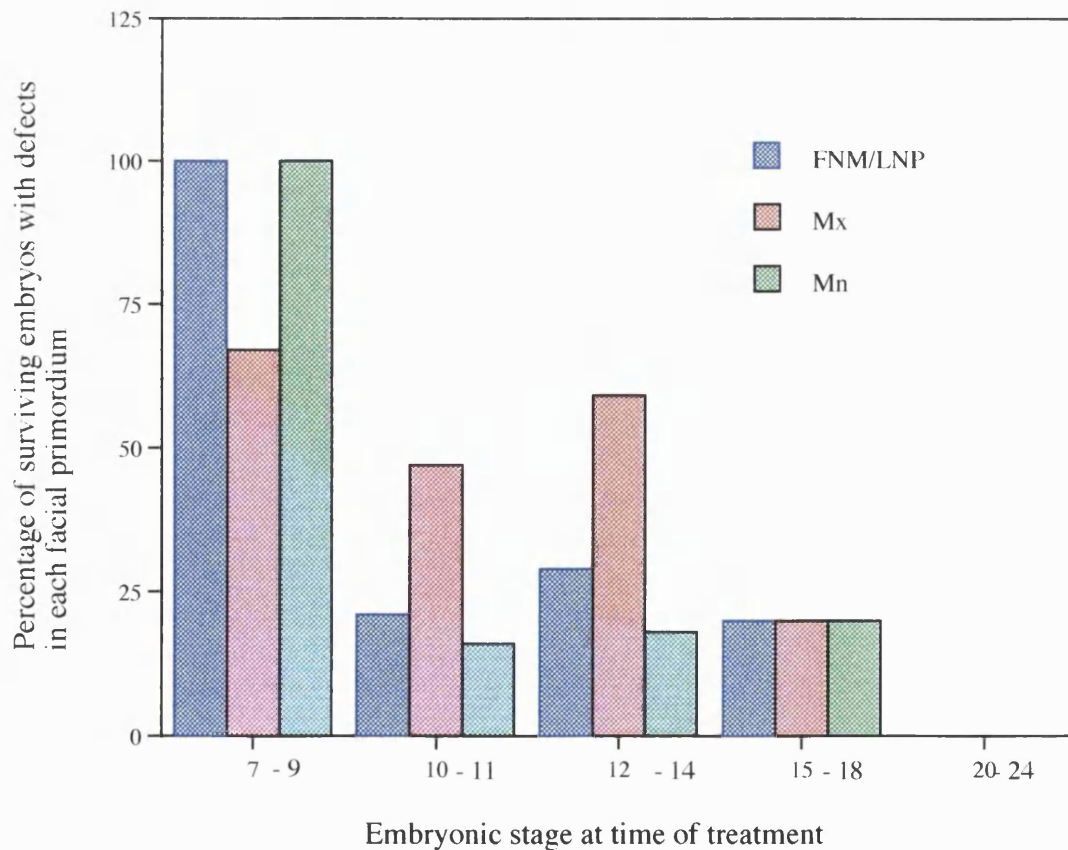
Figure 4.21 Scanning electron micrographs of facial primordia after treatment with connexin 43 antisense ODNs

A. Scanning electron micrograph (SEM) of untreated stage 23 chick head. All primordia are symmetrical. Scale bar = 500 μm.

B. SEM of chick head, stage 22, 48 hours after application of connexin 43 sense ODNs. Primordia in these embryos are also symmetrical similar to controls. Scale bar = 500 μm.

C. SEM of chick head, stage 22, 48 hours after treatment with pluronic gel. Primordia are again symmetrical in these embryos, indicating no effect. Scale bar = 500μm.

D. SEM of chick head stage 21, 48 hours after treatment with connexin 43 antisense ODNs. This embryo is affected on right and left sides of the face. The left nasal pit is wider and mis-shapen, particularly at the base (bottom white arrowhead). The left lateral nasal process is flattened compared to the control side (black arrowhead). The top of the nasal pit in the frontonasal mass region is also flattened (top white arrowhead). The right bud of the paired mandibular primordium is shorter, indicated by *. Scale bar = 500μm

E. SEM of s22/3 chick head 48 hours after treatment with connexin 43 antisense ODNs. The right maxillary primordium (indicated by *) is smaller than the contralateral control primordium in this embryo. Scale bar = 500μm

F. SEM of s23 chick head 48 hours after treatment with connexin 43 antisense ODNs. The right maxillary primordium, (*), is also shorter in this embryo. Scale bar = 500μm

G. SEM of left nasal pit on normal, contralateral control side of a connexin 43 antisense ODNs treated embryo at stage 24. The lateral (LNP) edge of the pit is normally thickened and the pit tilts towards the centre of the face. Scale bar = 50μm

H. SEM of s24 right nasal pit, 48 hours after treatment with connexin 43 antisense ODNs. (same embryo as in G). Nasal pit (NP) is wider and tilted in the wrong direction, compare to G. Surrounding tissue, particularly laterally (LNP) is also flatter. Scale bar = 50μm.

Figure labels:

FNM: Frontonasal mass.   NP: Nasal pit.

LNP: Lateral nasal process.   Mx: Maxillary primordium.

Mn: Mandibular primordium.

Figure 4.21
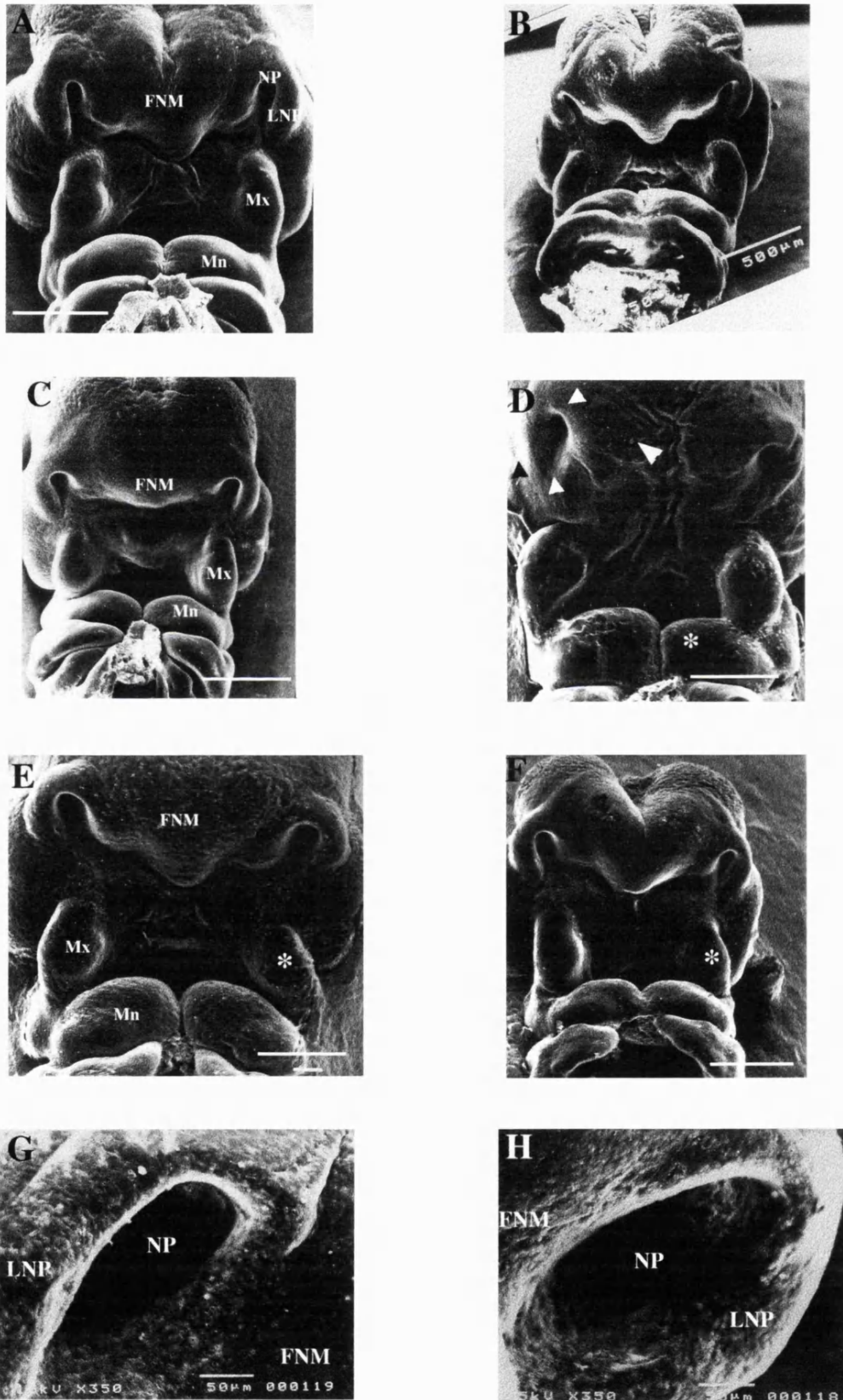
Figure 4.22 Scanning electron micrographs of stage 33/4 chick embryo heads.

A. SEM of normal stage 34/5 chick embryo head. Upper beak primordium, derived mainly from the frontonasal mass, juts out over lower beak primordium, derived from the mandibular primordia. The edge of the upper beak primordium, known as the tomium (T) is derived from the maxillary primordia. The egg tooth is an epithelial thickening found only on upper beaks. The nasal pits lie proximally on the upper beak.

B. Side view of normal s33 embryo. The thickened edge of the upper beak is more obvious from this view, as is the join between maxillary and mandibular primordia.

C. SEM of s34 embryo treated with connexin 43 sense ODNs at stage 11-12. All features are normal.

D SEM, side view, of s34 embryo treated with connexin 43 sense ODNs at stage 12. The tomium (T) is very clear in this specimen. The point where mandibular and maxillary primordia join is indicated by a white arrowhead.

E. SEM of s 34 embryo treated with pluronic gel at stage 12. Again, facial primordia of all embryos in this treatment group are normal.

F. SEM, side view, of s34 embryo treated with pluronic gel at stage 11/12. This shows clearly the mandibular/maxillary primordium join and the tomium.

Figure labels:

FNM: Frontonasal mass.   NP: Nasal pit.

LNP: Lateral nasal process.   T: Tomium.

Mn: Mandibular primordium.

Figure 4.22
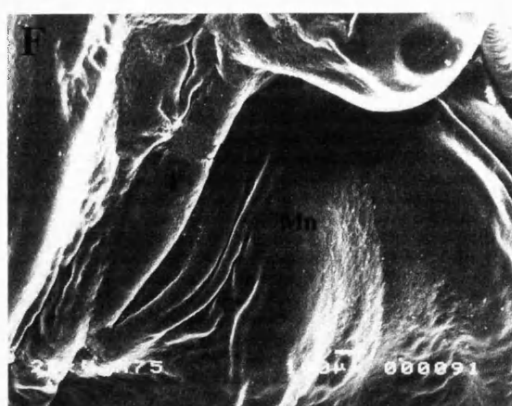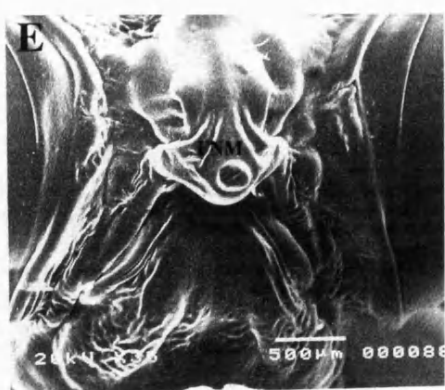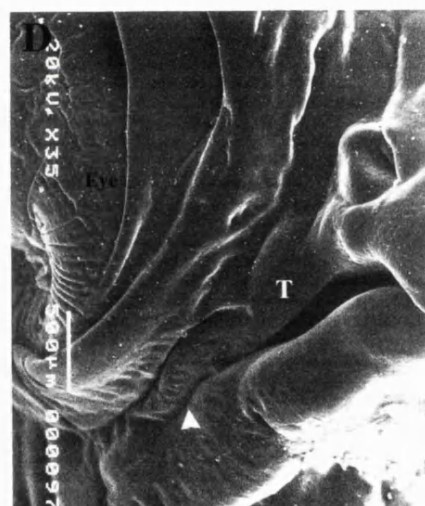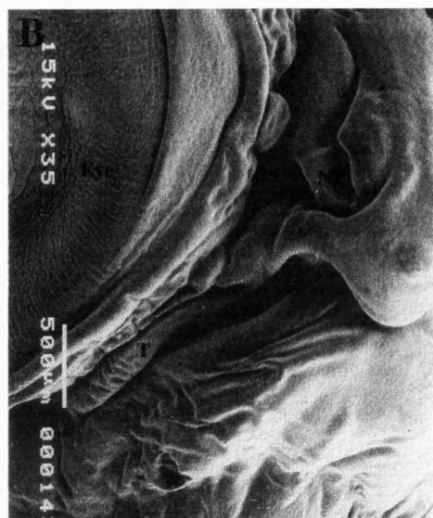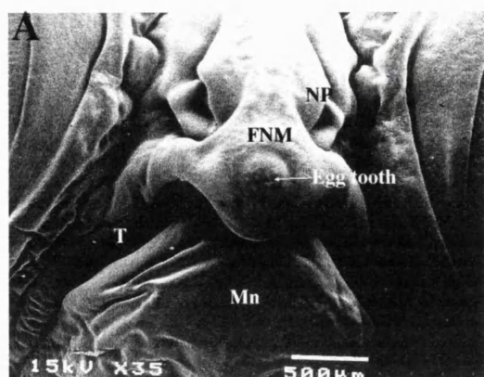
Figure 4.23 Stage 33/4 chick embryo heads treated with connexin 43 antisense ODNs.

A. SEM of s34 embryo treated with connexin 43 antisense ODNs at stage 10. This embryo has an excessively wide mouth, indicated by *, as both sides of the face have been affected. The tomium seems to be reduced/missing on both sides of the face.

B. SEM of s34 embryo treated with connexin 43 antisense ODNs at stage 12. This embryo is affected on right side of the face. The mouth gapes open and the tomium is much reduced on the right side (white arrowhead).

C. SEM of left side of embryo in B. The tomium (T) seems to have formed reasonably normally however the mouth does gape. This may be due to the defect on the opposite side of the face. The mandibular and maxillary primordia have joined normally on this side of the face as indicated by white arrowhead.

D. SEM of right side of embryo in B. Tomium is much reduced/ missing, indicated by top white arrowhead. There is also failure of fusion between the maxillary and mandibular primordia indicated by the bottom white arrowhead. The box indicates the region shown at a higher magnification in E.

E. A high power view of the failure of fusion seen in D. The tomium is missing, indicated by top arrowhead, and there is a wide gap between the mandibular and maxillary primordium, indicated by bottom arrowhead.

Figure 4.23
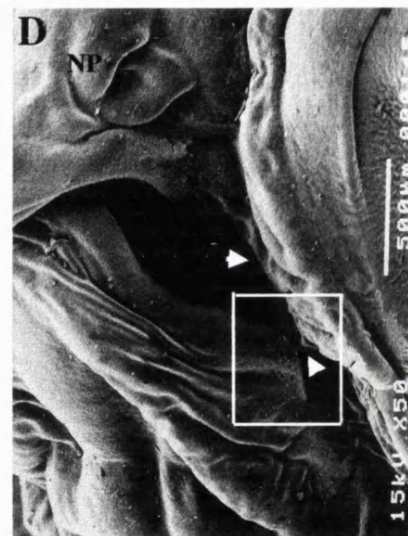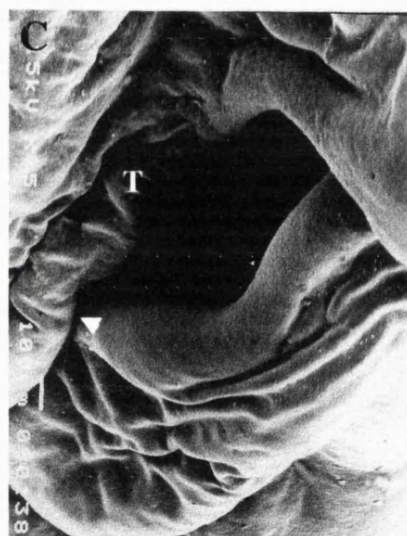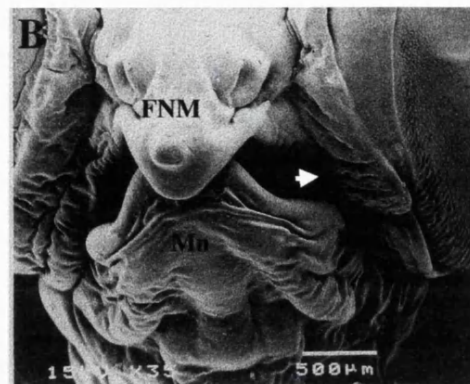
Some embryos treated with either sense or antisense oligonucleotides or pluronic gel between stages 10 and 14 were incubated up to 10 days of development (s33/4) to find out whether antisense treatment leads to alterations in final face shape. Embryos were examined by scanning electron microscopy (n=4 for each treatment group). Normal embryos examined by scanning electron microscopy at s33/4 show the developing upper beak, with egg tooth, overlapping the lower beak (Fig. 4.22A, frontal view). Both beaks have a thickened edge/lip (the tomium in the upper beak) and are joined laterally (Fig. 4.22B side view). Faces of embryos treated with sense oligonucleotides in pluronic gel (Fig. 4.22C, D) and pluronic gel only (Fig. 4.22E, F) were indistinguishable from untreated control embryos. However, all surviving embryos treated with antisense oligonucleotides against connexin 43 showed reduced or even absent posterior maxillary primordium (the tomium) (Fig. 4.23 A-E). In 3 out of 4 cases this defect was unilateral but in the remaining case was on both sides (Fig. 4.23A) resulting in an excessively wide mouth (Fig. 4.23A and B frontal views, C and D side views). In 3 out of the 4 cases, reduction in the maxillary primordium was associated with a lack of fusion between mandibular and maxillary primordium on the affected side of the face resulting in a lateral facial cleft (Figs. 4.23 D, E).

4.3.7 Effect of connexin 43 antisense ODNs on expression of *Msx-1* transcripts in facial primordia

Msx-1 is expressed in precise spatio-temporal patterns in the developing chick face (Brown *et. al.*, 1993, 1997), limb (Davidson *et. al.*, 1991) and neural tube (Suzuki *et. al.*, 1991). Interestingly, the patterns of connexin 43 protein expression in the face (this thesis), limb (Green *et. al.*, 1994) and neural tube (Ruangvoravat and Lo, 1992) correlate closely with these patterns of *Msx-1* expression.

To test the relationship between the expression of gap junctions containing connexin 43 and *Msx-1* expression in the face, antisense oligonuleotides against connexin 43 were applied to the heads of chick embryos at stage 10 and the embryos then processed for *in situ* hybridisation with the *Msx-1* riboprobe at various later times. Embryos from different time points were pooled in single tubes and in each tube, a piece of untreated tissue (stage

22-24 trunk or head) was also placed to ensure the probe was working and to act as a control for the extent of colour development. If connexin 43 expression is required for *Msx-1* expression, one would expect to see a decrease or even absence in *Msx-1* expression in antisense treated embryos.

8 hours after treatment, (approximately stage 12/13), Msx-1 expression was observed in the anterior dorsal neural tube, extending posteriorly to the level of the first few somites and also in the developing eye in sense and pluronic gel controls (Fig. 4.24A). Expression was also beginning to appear in the posterior end of the neural tube. No change in this pattern of Msx-1 expression could be detected in antisense treated embryos (Fig. 4.24B). 12 hours after treatment (approximately stage 14/5 and 4 hours after connexin 43 gap junction labelling had disappeared) *Msx-1* expression was again observed in the anterior dorsal neural tube and tail bud of sense and pluronic gel control embryos. Expression was also seen in the centre of the first branchial arch (which later splits to form maxillary primordia from the anterior part and mandibular primordium from the posterior part) in both sense and pluronic gel treated embryos (Fig. 4.24C, D). In antisense ODN treated embryos, at this stage, expression in the neural tube and first branchial arch appeared reduced (Fig. 4.24E, indicated by arrowhead) but expression was still seen in the tail bud. 24 hours after treatment with sense oligonucleotides and pluronic gel (approximately s18), *Msx-1* transcripts were abundant in the medial regions of mandibular primordium, and in the budding maxillary primordium in both pluronic gel and sense treated embryos (Figs. 4.24F, G). Slightly older control embryos also showed *Msx-1* transcript expression in the nasal pit region (Fig. 4.24G). In antisense treated embryos expression was again detected in the mandibular primordium but appeared to be very reduced (Fig. 4.24H). Expression in the maxillary primordium also appeared to be decreased in 3/3 embryos compared to the other treatment groups (Fig. 4.24H, arrowheads). Expression in the nasal pit was also very weak or even absent (Fig. 4.24H). These results show that *Msx-1* expression can still be detected in antisense treated embryos but levels of expression do appear to be reduced suggesting that connexin 43 coupling between cells may be necessary for maintenance of *Msx-1* expression.

Figure 4.24 Expression of *Msx-1* transcripts in the head and facial primordia after application of connexin 43 antisense ODNs.

A. Stage 12/13 chick embryo head, 8 hours after treatment with pluronic gel. Hybridised with the *Msx-1* riboprobe. Staining can be seen in the anterior dorsal neural tube (DNT) and also in the developing eye.

B. Stage 12/13 embryo, 8 hours after treatment with connexin 43 antisense ODNs. *Msx-1* expression is seen in the dorsal neural tube and eye primordium, as in controls. Thus treatment has had no effect on expression of *Msx-1* transcripts after 8 hours.

C. Stage 17/18 embryo, 12 hours after treatment with pluronic gel. *Msx-1* transcripts are expressed throughout the first arch primordium (1st arch).

D. Stage 18 embryo, 12 hours after treatment with connexin 43 sense ODNs. As in the previous figure, *Msx-1* expression is found in the 1st arch primordium only (1st arch).

E. Stage 18 embryo, 12 hours after treatment with connexin 43 antisense ODNs. *Msx-1* transcripts are expressed at low levels in the distal 1st arch primordium (1st arch) as indicated by arrowhead. Thus the level of *Msx-1* expression has been reduced by connexin 43 antisense ODNs treatment at this stage.

F. Stage 22/3 embryo, 24 hours after application of pluronic gel. *Msx-1* transcripts are expressed at high levels in the anterior maxillary (Mx) and mandibular (Mn) primordia.

G. Stage 24 embryo, 24 hours after application of connexin 43 sense ODNs. Expression of *Msx-1* transcripts is seen in nasal pit region in this slightly older embryo. Expression is also in anterior maxillary primordium and mandibular primordium as seen in F.

H. Stage 23 embryo, 24 hours after treatment with connexin 43 antisense ODNs. *Msx-1* transcripts are expressed at lower levels than normal in mandibular primordium, compare with F ,G. Low levels of *Msx-1* expression are seen in both maxillary primordia, (white arrowhead on the left, black arrowhead on right). Low levels of *Msx-1* are also seen in the right nasal pit, (top black arrowhead) but are absent in the left nasal pit. Thus the level of *Msx-1* transcripts are lower in all primordia in this antisense ODNs treated embryo.

Figure labels:

1st arch: 1st arch primordium	Mn: Mandibular primordium.
NP: Nasal pit.	Mx: Maxillary primordium.

Figure 4.24
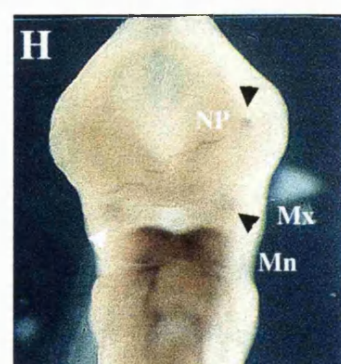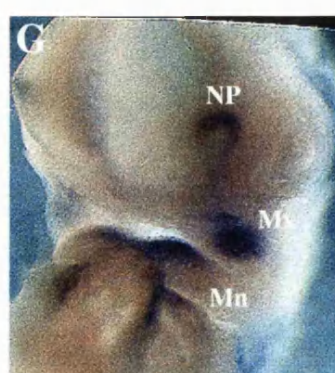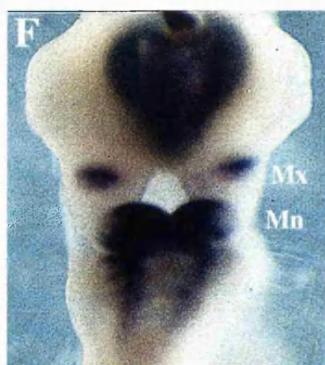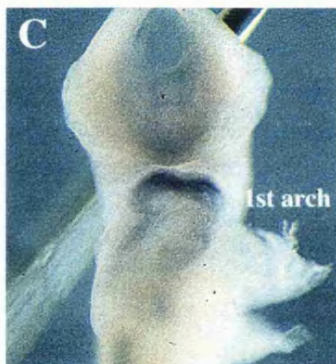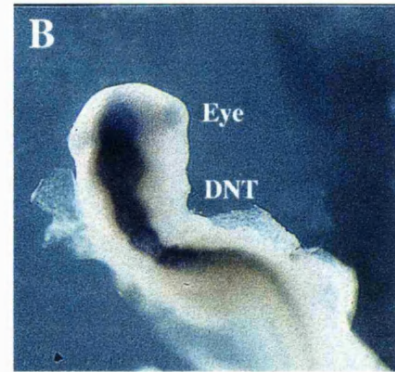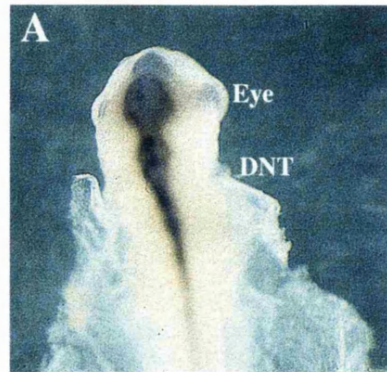
4.4 DISCUSSION

4.4.1 Gap junctions containing connexin 43 and 32 are found in regions of greatest expansion and fusion in chick facial primordia

Connexins 43 and 32 were expressed in both mesenchyme and epithelia of all facial primordia at the stages that we examined. Mesenchymal expression of both connexin 43 and 32 protein were found to be variable and spatially organised in each primordium. However, epithelial expression of both connexins tended to be more uniform.

4.4.1.1 Connexin 43 expression

Abundant Connexin 43 containing gap junctions were found in distal mesenchyme of frontonasal mass and lateral nasal process, near the nasal pits, in anterior and distal regions of the maxillary primordium, at the midline and proximal edge of the mandibular primordium and in all other regions where facial primordia fuse. Little expression was seen in the centre of the frontonasal mass, proximal maxillary primordium and lateral mandibular primordium. This pattern of expression is very similar to that described in a recent report in which the distribution of connexin 43 containing gap junctions was examined in the upper face (Minkoff *et. al.,* 1997).

Regions of facial mesenchyme in which abundant connexin 43 protein is seen at stage 20 are those that were shown, by DiI labelling, to undergo considerable expansion (chapter 3, this thesis). Furthermore the later patterns of connexin expression in the face show that, as these regions expand, cells continue to express high levels of connexin 43. Other regions in which very low levels of connexin 43 protein were found were those regions which expanded very little (compare summary diagram Fig. 4.2 and fate map chapter 3, Fig 3.6d). Experiments in chapter 3 also indicate that regions of facial primordia which expand more have the highest rates of cell proliferation while regions with low expansion have the lowest rates of cell proliferation. Thus connexin 43 protein expression correlates with regions of facial primordia that expand and grow out. This suggests that connexin 43 may play a role in controlling these processes. Higher rates of cell proliferation and connexin 43 expression were also found in regions where primordia

attach or fuse (chapter 3). Thus mesenchymal connexin 43 may also play a role in fusion of facial primordia, possibly by coordinating outgrowth so that primordia appose. This is consistent with the proposal of Minkoff *et. al.*, (1997), who also suggested a role for mesenchymal connexin 43 containing gap junctions in fusion of facial primordia.

It is interesting that, in many other systems, connexins/gap junctions have been linked to regulation of cell proliferation. However, it seems that the abundance of gap junctions can be both positively and negatively correlated with rates of cell proliferation depending on cell type. For example, growth factors TGF - beta 1 and 2 induced a high level of connexin 43 expression in 10T1/2 cells cultured *in vitro* with an associated increased in proliferation rate (Gibson *et. al.*, 1994). High levels of connexin 43 mRNA and protein were also correlated to high rates of cell proliferation in cultured human keratinocytes (Gibson *et. al.*, 1997). However other studies indicate that abundant connexin 43 expression is linked to low cell proliferation, for example in C6 glioma cells cultured *in vitro* (Zhu *et. al.*, 1991, 1992). Low connexin expression and a loss of intercellular coupling has also been linked to increased cell proliferation during tumorigenesis (see for example Lee *et. al.*, 1992).

4.4.1.2 Connexin 32 expression

Mesenchymal expression of connexin 32 protein was found to be less localised than that of connexin 43. A similar observation was reported for expression of connexin 32 in upper face primordia at similar stages (Minkoff *et. al.*, 1991). Many regions of the stage 20 chick face that subsequently undergo greater expansion express high levels of connexin 32 protein in addition to connexin 43 protein (compare Figs. 4.2 and 4.8). The exception to this being the mesenchyme around the nasal pit where, at stage 20, they are expressed in complementary patterns. This would also suggest a role for connexin 32, in addition to connexin 43, in expansion and proliferation. However, studies suggest that connexin 32 correlates, in general, with decreased cell proliferation. For example increased levels of connexin 32 expression have been linked to reduced rates of cell proliferation in the liver after partial hepatectomy (Dermietzel *et. al.*, 1987, Kren *et. al.*, 1993). Cultured thyroid epithelial cells expressing high levels of connexin 32 also have a

low rate of cell proliferation (Statuto *et. al.,* 1997). However, in C6 glioma cell lines transfected with *connexin 32* , an increase in expression of connexin 32 containing gap junctions and functional coupling, did not change the rate of cell proliferation. When these cell were transplanted *in vivo* there was a correlation between high connexin 32 expression and reduced cell proliferation (Bond *et. al.,* 1994). Thus it seems high levels of connexin 32 expression can be associated with low rates of cell proliferation.

4.4.2 Overlap of connexin 43 and connexin 32 expression domains occurs in regions of facial fusion

In chick embryos, between stages 20 and 28, mesenchymal connexin 43 and connexin 32 expression domains overlap very little in lateral nasal process while they overlap almost completely in mandibular primordia. Overlap of the expressing domains of the two connexins is also found in all regions of fusion. This overlapping expression pattern suggests that connexin 43 and 32 may be expressed in the same cells, but are they found in the same gap junctions? Only certain combinations of connexins are compatible to form functional channels when expressed in adjacent cells. Studies by Werner *et. al.,* (1989), using the *Xenopus* oocyte pairs system of expressing single connexin types in adjacent cells, indicated that heterotypic channels of connexin 43 and 32 did form and were functional. They stated that heterotypic channels had similar conductance properties to channels formed by connexins 43 and 32 alone. However, more recent reports have indicated that functional heterotypic gap junctions between connexin 43 and 32 do not form in HeLa cells *in vitro* (Elfgang *et. al.,* 1995) or in *Xenopus* oocyte pairs (White and Bruzzone 1996, Bruzzone *et. al.,* 1996). This conclusion is based on no detectable conductance or passage of fluorescent dyes. Thus there is confusion over the ability of these channels to form *in vitro* and there are no data to indicate that they form *in vivo*.

If heterotypic connexin 43 and connexin 32 gap junction channels do indeed form in the developing face *in vivo*, it is likely that they will differ in their permeability (which is not related to conductance, Veneestra 1996) and gating properties compared to homotypic connexin 43 and 32 gap junction channels and thus may have different roles to play in the

126

development of facial primordia. There is no evidence that suggests connexin 43 and 32 form heteromeric connexons.

4.4.3 The role of ectodermal connexin 43 and connexin 32 in fusion of facial primordia

Moderate levels of both connexin 43 and 32 proteins were found in facial ectoderm at all stages examined. There were, however, transient increases in protein levels at different stages in some regions where facial primordia fuse. A transient increase in gap junctions was noted at the point of primary palate fusion in the mouse (Kosaka *et. al.,* 1985). In this detailed EM study of the changes in epithelial cell morphology at the site of primary palate fusion in the mouse, a "transitional" cell type was observed which had numerous filopodia and abundant junctional complexes, including gap junctions. This transient increase in gap junction formation suggests that the presence of gap junctions between apposing epithelia may be required for fusion although we can only speculate on the exact role they may be playing in this process. For example, in primary palate fusion, they could form channels that specifically pass signals that result in epithelial cell death or epithelial migration. These are processes which may be involved in primary palate fusion. The data in this chapter imply that both epithelial and mesenchymal connexin 43 and 32 may be required for fusion of facial primordia..

The surface epithelia of the nasal pits expressed particularly high levels of both connexin proteins at all stages examined. Little staining was observed, however, in the epithelia deep in the nasal pits. The presence of abundant connexin 32 and 43 containing gap junctions in the nasal epithelia have been noted previously (Minkoff *et. al.,* 1991, 1997).

4.4.4 Gap junction channels and epithelial-mesenchymal interactions

Outgrowth of facial primordia is known to require epithelial-mesenchymal interactions (Wedden, 1987, Richman and Tickle, 1989, 1992) suggesting that there is some method of communication between the two tissues. Gap junctions have long been associated with inductive interactions during development (see for example Warner, 1985, Warner *et. al.,* 1984, Yancey *et. al.,* 1992). However, in other developing systems in which epithelial

127

mesenchymal interactions are required for outgrowth, such as the mouse limb bud (Laird *et. al.,* 1992), there is no functional gap junction coupling between ectoderm and mesenchyme.

It is striking that epithelia which express abundant connexin protein frequently overlie regions of abundant mesenchymal connexin protein expression in the developing face, but there is often a narrow region of mesenchyme, directly below the epithelia, in which no gap junctions are observed (see Figs. 4.3C, 4.6C).This mesenchymal region devoid of gap junctions was also observed by Minkoff *et. al.,* (1991). We also could not detect gap junctions between mesenchymal and epithelial cells in the face. These data would suggest that the mesenchyme and ectoderm of the face are not coupled by gap junctions.

Connexin expression may itself rely on a reciprocal interaction between tissues. This has been demonstrated in the developing chick limb bud, in which the presence of gap junction coupling in the mesenchyme has been linked to the formation of digits (Allen *et. al.,* 1990). Removal of the apical ectodermal ridge (AER) abolishes connexin 43 expression in the underlying mesenchyme while grafting of an AER induces connexin 43 expression (Green *et. al.,* 1994). This result indicates a signal from the AER maintains connexin 43 expression. A recent study has shown that, in limb mesenchymal cultures, FGF can maintain connexin 43 expression (chick and mouse) and connexin 32 (mouse) and increase coupling as shown by dye transfer (Makarenkova *et. al.,* 1997). However, the expression of FGFs, in particular FGF-2 (Richman *et. al.,* 1997) in the facial ectoderm are more widespread than in the limb, while the pattern of connexin 43 expression in facial mesenchyme is restricted. This implies that there may be alternative factors that control expression of connexins proteins in the face.

4.4.5 Retinoic acid reduces expression of connexin 43 protein in chick facial primordia.

Retinoic acid is a potent teratogen that causes clefting of the primary palate in chick embryos by reducing mesenchymal outgrowth (Tamarin *et. al.,* 1984, Wedden, 1987, Chapter 3, this thesis). A large body of work shows that the expression of gap junctions

can be affected by retinoid treatment and so it was pertinent to explore whether gap junction expression was affected in the face after retinoid treatment.

4.4.5.1 Connexin 43 expression after retinoic acid treatment

The results of the experiments in this chapter show that expression of connexin 43 was very much reduced in mesenchyme surrounding the nasal pit, particularly in regions distal and lateral to the nasal pit and in anterior maxillary primordia within 24 hours of treatment. These are regions that normally express both connexin 43 and 32 at this stage of development (stage 24, see summary diagrams Figs. 4.2 and 4.8). The regions in which connexin 43 expression was found to be most reduced were those in which expansion and cell proliferation were most affected by retinoic acid treatment (chapter 3, this thesis). This shows a correlation between reduced connexin 43 expression and reduced cell proliferation. It could simply be, however, that cells proliferating at a slower rate express less gap junction protein. Thus reduction of connexin protein expression may be consequence of reduced cell proliferation rather than the cause.

Epithelial expression of connexin 43 in upper beak primordia was less affected than mesenchymal expression. In this context, it is interesting to note that retinoic acid has an irreversible effect on facial mesenchyme, while any epithelial effects are reversible (Wedden 1987). Thus connexin 43 expression is reduced the most in tissues which are affected the most by retinoic acid. The epithelial regions most affected overlie the mesenchyme regions with large reductions in connexin 43 expression e.g. the lateral nasal process. It is possible that reduction in mesenchymal expression is affecting expression in the ectoderm, through epithelial-mesenchymal interactions.

The effect of retinoic acid upon connexin 43 protein expression seems dependent on the tissue type and the dose. Reductions in connexin 43 expression have been found in Syrian hamster embryo cell lines with concentrations 10^{-6} - 10^{-5}M retinoic acid (Rivedal *et. al.,* 1994). Neuronal cell lines treated with retinoic acid at high concentrations (10^{-5}M) show an accompanying reduction in cell coupling and differentiation (Bani-Yagoub *et. al.,* 1997). Treatment of F9 teratocarcinoma with lower doses of retinoic acid (10^{-7}M) induces connexin 43 mRNA and protein expression, increases intercellular

communication and leads to differentiation into primitive endoderm (Clairmont *et. al.,* 1996). However, treatment of a rat trophoblast cell line with retinoic acid caused no change in connexin 43 expression across a dose range 10^{-5} to 10^{-9}M (Grummer *et. al.,* 1996). Application of beads soaked in high doses of retinoic acid (1mg/ml) to the chick wing bud, causes truncation of the limb and abolishes connexin 43 expression in both ectoderm and mesenchyme (Green *et. al.,* 1994). From this evidence, it seems that the effect of retinoic acid on gap junction expression and coupling is not only dose dependant but is also cell type specific.

4.4.5.2 Connexin 32 expression after retinoic acid treatment

In contrast to the reduction in connexin 43, expression of connexin 32 in both epithelia and mesenchyme was not reduced by high doses of retinoic acid and may even have slightly increased. Unlike connexin 43, little is known about the effect of retinoic acid upon connexin 32 expression in any system.

The different sensitivities of connexin expression to retinoic acid treatment may reflect different transcriptional and translational control mechanisms. There is no indication that retinoic acid can regulate connexins at the transcriptional level but alterations in stability of connexin 43 mRNA have been reported with retinoid treatment (Clairmont *et. al.,* 1996). Decreased stability of connexin 43 mRNA may be occurring in face upon retinoic acid treatment, as it would result in reduced protein levels. Retinoic acid could also act at the post translational level by disrupting the ability of proteins to aggregate into channels (Bex *et. al.,* 1995). This is clearly not happening with connexin 43 in our studies as this would still result in protein labelling, albeit not in puncta. Studies also suggest that retinoic acid can also inhibit junctional communication by reversibly closing junctional channels (Pitts *et. al.,* 1986). We cannot rule out that connexin 32 containing gap junctions are being affected in this way in our studies. It would be very interesting to investigate dye coupling and conductance between cells in the facial primordia after retinoic acid treatment, to see if the function of the remaining connexin 32 containing gap junction channels had been affected. Differentiation between gap junctions containing connexin 43 or connexin 32 can be made with use of tracer dyes of different size and charge (Elfgang *et. al.,* 1995,

Veneestra, 1996). It would also be interesting to examine mRNA levels for connexin 43 in regions of facial primordia most affected by retinoic acid either by in situ hybridisation or RNase protection assay to see if any transcriptional changes can be detected.

4.4.6 Antisense oligonucleotides against connexin 43 are efficient tools for selectively reducing connexin 43 protein expression in chick facial primordia

Patterns of expression of connexin 43 and 32 proteins in facial primordia between stages 20 and 28 suggest a link with proliferation and fusion of primordia. Retinoic acid treatment of facial primordia at these stages selectively reduces the expression of connexin 43 protein, cell proliferation and expansion in the mesenchyme of regions involved in primary palate fusion. This suggests a possible causal role for connexin 43 in expansion and fusion of primordia and to test this possibility, connexin 43 protein expression was reduced.

The approach of functional inactivation had already been employed with *connexin 43* (Reaume *et. al.,* 1995). This mutation is not lethal, which is surprising, as blocking antibodies have indicated that connexin 43 is essential for compaction in the early mouse embryo (Lee *et. al.,* 1987, Becker *et. al.,* 1992, 1995). It was hypothesised that ectopic expression of *Connexin 45* was induced by lack of *Connexin 43* in preimplantation stages in these mice. This connexin was presumed to compensated for the lack of *Connexin 43*. The resulting phenotype of the *Connexin 43* knockout was less severe than expected as connexin 43 is expressed in a wide variety of tissues during development (Yancey *et. al.,* 1992, Ruangvoravat and Lo 1992, Green *et. al.,* 1994, Minkoff$_\wedge$ 1997). The only obvious defect is a malformation of the outflow tract of the heart which resulted in death soon after birth. No compensational increase in expression of other heart connexins, such as 40 and 45 which are normally only expressed in conducting cells of the heart, were seen. It is interesting that this phenotype is similar to that seen in humans with visceroatrial heterotaxia, some cases of which have been linked to mutations in the *Connexin 43* gene (Britz-Cunningham *et. al.,* 1995). Recently, a report of facial development in the *Connexin 43* knockout mouse indicated that there may be slight

changes in development of both mandibular and maxillary primordia (Minkoff *et. al.,* 1997). It would be very interesting to see if there are any compensatory changes in the level of expression of connexin 32 in facial primordia in these mice. Thus it seems likely that connexin 43 is important in the development of other organs and primordia but in the knockout mouse, changes may be subtle and / or increased expression of other connexins must be able to compensate for the lack of gap junctions containing connexin 43. This approach has not been sufficient to indicate a role for connexin 43 in facial development.

Connexin 32 has also been functionally inactivated in mice (Nelles *et. al.,* 1996, Anzini *et. al.,* 1997) and the phenotype is again less severe than might have been predicted from the widespread expression of this protein during development (Minkoff *et. al.,* 1991, Scherer *et. al.,* 1995, Makarenkova *et. al.,* 1997) This again may be due to compensation by other connexin proteins. Nelles and co-workers (1996) reported defective mobilisation of glucose from liver glycogen stores in response to sympathetic nerve stimulation but no other neural phenotype. Anzini *et. al.,* (1997) found a late onset, progressive peripheral neuropathy, similar to that seen in humans with X-linked Charcot-Marie-Tooth disease, a peripheral neuropathy associated with decreased nerve conductance and demyelination, which has been shown to be due to mutations in the connexin 32 gene (Bergoffen *et. al.,* 1993).

Blocking antibodies have also shown the importance of gap junction signalling in the amphibian embryo (Warner *et. al.,* 1984) and in the early mammalian embryo (Lee *et. al.,* 1987, Becker *et. al.,* 1992, 1995), without problems of compensation. However difficulties in loading sufficient antibodies into larger embryos precludes this method in studying later facial morphology.

The approach used in this study to reduce connexin 43 protein expression in the chick face is the application of antisense oligodeoxynucleotides (ODNs). Antisense oligodeoxynucleotides act at the level of translation by binding to mRNA, thus affecting the amount of protein produced in the cell. This effect is transient as the ODNs have a short half life (typically 20 minutes for unmodified ODNs, several hours for modified ODNs) due to intracellular degradation (Wagner, 1994). Thus, with this method, the gene is still active and the effect is transient, due to the short half life of ODNs. This means that

cells may not be able to adequately detect the loss of connexin 43 and therefore do not compensate, by increasing the expression of other connexins, before the antisense ODNs effects wear off.

Application of connexin 43 antisense ODNs, in pluronic gel carrier, to chick embryos *in ovo* produced a substantial reduction in connexin 43 protein expression. Subsequently, defects in development were observed in various organs, such as the facial primordia, limb, neural tube and eye, in which connexin 43 protein expression is abundant during development (Becker, Lorimer, Makarenkova, McGonnell, Tickle and Green submitted). However only the facial defects will be discussed here.

Application of connexin 43 sense ODNs and pluronic gel controls had no effect on the level of connexin 43 expression. However, unmodified connexin 43 antisense ODNs in pluronic gel resulted in a marked reduction in protein expression in the mesenchyme 8 hours after application while ectodermal expression seemed less affected. This probably reflects not only the time that it takes for the oligonucleotides to prevent protein production but also the time that it takes for the connexin 43 containing gap junction channels already present to be naturally turned over. Thus turnover of connexin 43 containing gap junctions in facial ectoderm may generally be lower than in facial mesenchyme. The use of pluronic gel, which acts as a slow, sustained release mechanism for up to 12 hours, increases the half life of the oligonucleotides substantially. A reduction in connexin 43 protein is still apparent 24 hours after application and even 48 hours in the maxillary primordium. This suggests that the antisense ODN's are effective over a substantial period of time. This may be due to a combination of factors such as sustained release of the antisense ODNs from the gel, high stability of the DNA/mRNA hybrid and possibly RNase H digestion of RNA, all of which can extend the period of effectiveness. However, we cannot be sure which, if any, are involved in prolonging the reduction of connexin 43 protein in our system. In addition to this, we also observed that recovery of protein production is variable between facial primordia. This is likely to be due to different turnover rates in each primordia. Thus our results suggest that the maxillary primordium has a lower turnover of connexin 43 protein than other facial primordia. Variability in time of recovery of connexin 43 expression between facial

primordia is consistent with results of antisense connexin 43 application to other embryonic tissues (Becker, Lorimer, Makarenkova, McGonnell, Tickle and Green, submitted).

Antisense, sense ODN and pluronic gel alone had no effect on the levels of connexin 32 expression in the facial primordia. This indicates that the antisense ODNs specifically target connexin 43 RNA in the face. Importantly, it also shows that there is no vast increase in connexin 32 protein levels which indicates that compensation is unlikely to be occurring.

4.4.7 Application of connexin 43 antisense oligonucleotides results in facial primordia defects

Treatment of chick embryo heads with antisense oligonucleotides produced defects in facial primordia at some, but not all, of the stages of development examined (stages 7-25), while treatment with sense oligonucleotides and pluronic gel only caused no facial defects. The defects were all in areas where connexin 43 is expressed during development. The number of deaths in each treatment group were similar for antisense ODN's and controls.

Treatment at early stages (7-14) produced more defects than later stages (15-25). This may be due to limitations of the method of application rather than an indication of the decreasing importance of connexin 43 expression in facial development with increasing embryonic age. The head increases in size with age thus the gel is localised to a smaller region of the face and has a greater tissue depth to diffuse through and we observed a less efficient reduction in connexin 43 protein levels in embryos treated at these later stages.

My studies indicated that connexin 43 protein is present in the chick cranial neural crest at early stages of development and that connexin 43 antisense ODNs applied very early reduce this expression substantially. Recently, connexin 43 expression and functional coupling has been reported in both migrating cranial and trunk neural crest of the mouse embryo (Lo et. al., 1997) and Ewart et. al., (1997) have proposed that disruption of neural crest migration underlies heart malformations seen in mice with Connexin 43 functionally inactivated. It is possible that disruption of cell - cell signalling may affect the

synchronised migration of these cells. If insufficient neural crest cells migrate, it can lead to defects in facial development, as shown by the disruption of neural crest migration by early treatment with retinoic acid in avian embryos (Thorogood *et. al.,* 1982, Pratt *et. al.,* 1987). It would be interesting to investigate if neural crest migration is disrupted after treatment with connexin 43 antisense ODNs, using cell lineage tracing and/or neural crest specific markers (slug or HNK-1 antibody).

The production of facial defects when embryos are treated with connexin 43 antisense ODN's later in development suggests that connexin 43 protein also plays a role in the post - migration phase of facial development. It takes 8 hours for connexin 43 protein labelling to decrease significantly after treatment. In embryos treated after stage 12, neural crest migration will have been completed before there is a reduction in connexin 43 protein levels. There must, therefore, a post neural - crest migration affect. At these developmental stages (13/14+), cell proliferation and cell rearrangement/intercalation are important processes for correct outgrowth and shaping of the face (see chapter 3 this thesis). When all these data are taken together, they suggest that loss of connexin 43 protein may reduce cell migration and cell proliferation and this leads to retarded growth of facial primordia. This hypothesis could be directly tested using S-phase labelling studies to determine rates of cell proliferation in embryos treated with antisense ODNs against connexin 43.

A retardation of maxillary primordia development was the most common defect in embryos treated with antisense ODNs against connexin 43 at the majority of stages and only defects in the development of this primordium were found at later treatment times. It may be that antisense oligonucleotides particularly affect a period when maxillary cranial neural crest migrates or affects its ability to migrate to the correct place. This could be investigated with lineage tracing dyes, such as DiI. Connexin 43 antisense ODNs might also be most effective during a period in which maxillary primordium cell proliferation is particularly important. Any changes in cell proliferation in the maxillary primordium could be investigated with S-phase labelling. It is interesting to note that we did find a higher rate of cell proliferation in the maxillary primordium in general, compared to other primordia between stages 20 and 28 and that cell populations expanded very substantially

compared to other primordia (chapter 3, this thesis). Moreover, we found that the reduction of connexin 43 expression was more sustained in the mesenchyme of the maxillary primordium compared with other primordia.

It is very interesting to note that antisense ODN's against other molecules known to be closely involved in gap junction formation have produced remarkably similar facial phenotypes to those produced by connexin 43 antisense ODN's. For example, the presence of E-cadherin adhesion molecule has been found to be essential for gap junction formation in epidermal cells *in vitro* (Jongen *et. al.,* 1991) presumably holding cells together, allowing connexons to dock. Treatment of mouse embryos with antisense ODN's against E-cadherin produced hypoplasia of facial primordia, amongst other defects (Chen and Hale 1995). Another group of molecules associated with cell adhesion are the Wnt family of secreted glycoproteins. *Wnt* genes have a wide variety of functions during development, including roles in axis formation, neural and kidney development (reviewed in Moon *et. al.,* 1997). Studies suggest that Wnt signalling may lead to changes in cell adhesion (Bradley *et. al.,* 1993, Hinck *et. al.,* 1994, Torres *et. al.,* 1996), through a down stream target, β-catenin, that associates with cadherin in the plasma membrane

(reviewed in Miller and Moon 1997). Injection of *Wnt* RNA into early *Xenopus* embryos leads to increased functional coupling of the cells (Olsen and Moon 1992) implying that Wnt signalling is closely involved in gap junction communication. Application of antisense oligonucleotides of Wnt-1 and Wnt-3a to mouse embryos results in facial hypoplasia (Augustine *et. al.,* 1993). Functional inactivation of both of these genes together results in reduction of neural crest migrating from the dorsal neural tube (Ikeya *et. al.,* 1997). It seems likely that one of the mechanism by which these antisense ODN's cause facial hypoplasia is by disruption of formation of gap junction channels. This could be tested by examining the gap junction coupling in facial primordia after treatment with E-cadherin or Wnt antisense ODNs.

Embryos examined at later stages displayed lateral facial clefts - macrostomia. This is a failure of fusion of the maxillary and mandibular primordia. This could be due to the reduced growth of either or both of the primordia, which was observed upon application of connexin 43 antisense oligonucleotides. However, fusion of the primary palate

occurred normally, which involves the maxillary primordium. It is interesting to note that retinoid treatment of hamsters on day 8 of gestation results in facial deformity including macrostomia (Irving *et. al.,* 1986). The authors suggested that this was caused by hypoplasia of the mandibular and maxillary primordia, similar to that seen in our study, rather than a failure of fusion. Cleft primary palate was not noted in these embryos either, even though growth of the maxillary primordium was much reduced, but if dosing occurred one day later, 100% of embryos displayed this defect. This showed that there is a different sensitivity for facial clefting, depending on the time of dosing. A similar mechanism may be occurring with our connexin 43 antisense ODN studies. Thus, it may be possible to affect lateral facial fusion at early stages of development and primary palate clefting at later stages, when it is difficult to achieve an effect in our experimental system due to embryo size.

4.4.8 Connexin 43 and *Msx-1* may be linked to the control of outgrowth in facial primordia.

Expression patterns of connexin 43 protein and *Msx-1* transcripts have a very similar spatiotemporal pattern in several developing systems such as the face (Brown *et. al.,* 1993, 1997 *Msx-1* and Minkoff *et. al.,* 1997 and this thesis, connexin 43) the neural tube (Suzuki *et. al.,* 1991 *Msx-1* and Ruangvoravat and Lo, 1992 connexin 43) and the limb (Davidson *et. al.,* 1991 *Msx-1* and Green *et. al.,* 1994, Makarenkova *et. al.,* 1997, connexin 43). This would suggest that they are both involved in the same developmental processes. Application of connexin 43 antisense ODNs to the head resulted in a reduction in the level of *Msx-1* mRNA transcripts found in the facial primordia. This reduction was seen within 4 hours of a reduction in connexin 43 protein and is consistent with the idea. that the expression of connexin 43 and *Msx-1* are tightly correlated. To confirm this result, quantitative RNase protection assays could be employed to detect and compare levels of *Msx-1* mRNA from individual facial primordia of treated and control embryos.

Expression of *Msx-1* has also been linked to outgrowth in the face (Brown *et. al.,* 1993,1997) and mice, in which *Msx-1* has been functionally inactivated, exhibit shorter mandibular primordia and clefting of the secondary palate (Satokata and Maas 1994),

indicating a possible role in fusion. Functional inactivation of both *Msx-1* and *Msx-2* has also been performed, resulting in an additional clefting of the primary palate, not seen in the *Msx-1* knockout (Dr. R. Maas, Boston, pers comm) which indicates that there is functional redundancy between these two genes. Recently, *Msx-1* antisense ODNs have been applied to mouse embryos cultured *in vitro* which resulted in a strikingly similar defect to that observed in our studies, namely reduced maxillary and mandibular primordia and frontonasal mass (Foerst - Potts and Sadler, 1997). Thus we may hypothesise that both connexin 43 and *Msx-1* are involved controlling outgrowth and the fusion of facial primordia. However, our data do not provide sufficiently clear evidence to indicate if they are working in the same or parallel molecular pathways that influence outgrowth of the face. Studies have shown that expression of both connexin 43 and *Msx-1* in the developing limb bud are maintained by FGFs (Vogel *et. al.*, 1995, Makarenkova *et. al.*, 1997) indicating there are common molecules controlling expression of both. Signalling via connexin 43 containing gap junctions appears to control *Msx-1* expression. It is also possible that *Msx-1* may be required for the induction of Connexin 43 expression and that there is a positive feed back loop where maintenance of *Msx-1* expression requires signalling through connexin 43 containing gap junctions. It would also be interesting to analyse expression of *Msx-1* in connexin 43 knockout mice and also connexin 43 expression in *Msx-1* knockout mice to see if there are any changes in patterns or levels of expression.

Chapter Five - The role of signaling between epithelia and mesenchyme in controlling outgrowth of maxillary primordia

5.1 Introduction

In the previous chapter, I have shown how direct cell-cell signalling between epithelial cells and between mesenchymal cells, via gap junctions, is important for growth, shaping and fusion of facial primordia. However, signalling between the epithelia and mesenchyme is also known to be important for outgrowth of facial primordia. This epithelial-mesenchymal interaction is mediated by signalling molecules, such as growth factors interacting with receptors. In this chapter, I aim to investigate how signalling between the ectoderm and mesenchyme contributes to outgrowth of the maxillary primordium, an important component of the primary palate and to discover if failure of epithelial - mesenchymal interactions leads to clefting of the primary palate. I also wish to examine which molecules mediate ectodermal signalling and to identify molecules in the mesenchyme that may be involved in responding to them.

5.1.1 Outgrowth of facial primordia is mediated by epithelial mesenchymal interaction

Growth and differentiation of many organs in the developing embryo is under the control of reciprocal signalling between epithelium and mesenchyme. Both the epithelium and the mesenchyme require signals from the opposite tissue to undergo morphological change and differentiation (reviewed in Thesleff *et. al.*, 1995). These reciprocal signals, which are the basis of epithelial mesenchymal interactions, have been shown to be important in the developing facial primordia. Experiments have been conducted in which epithelia was been removed from stage 24 chick facial primordia by enzymatic digestion, after amputation, and then re-grafted onto a host chick limb to develop in isolation. Grafts

139

of frontonasal mass mesenchyme and of mandibular primordia mesenchyme developed into truncated primordia with reduced cartilage differentiation, compared with control grafts of intact facial primordia (Wedden and Tickle 1986, Wedden, 1987, Richman and Tickle 1989). However, maxillary primordium grafts, even with intact ectoderm, did not undergo polarised outgrowth, instead forming swellings of loose connective tissue, muscle and bone cells (Richman and Tickle 1989). These experiments indicate a requirement for epithelia to establish the appropriate amount of outgrowth and also for differentiation in the developing face. They also show that maxillary primordia does not undergo normal polarised growth in isolation. It has been shown that all the facial epithelia are interchangeable (Richman and Tickle 1989) suggesting that there are common signals in the epithelium and that differences in response, e.g. amount of outgrowth and differentiation, are inherent in the mesenchyme of each primordium.

Epithelial-mesenchymal interactions occur in the developing limb and recombination of facial mesenchyme with limb ectoderm can stimulate outgrowth of frontonasal mass mesenchyme (Richman and Tickle 1992), suggesting that molecular signals are shared by at least some facial and limb ectoderm. However, structurally the limb and facial primordia differ, in that the developing limb bud has a specialised epithelial thickening at the distal tip known as the apical ectodermal ridge (AER). The AER controls outgrowth by maintaining a region of undifferentiated, rapidly dividing mesenchyme at the tip of the limb know as the progress zone (Summerbell *et. al.,* 1973). Mechanical removal of this structure is possible and this results in truncation of the limb (Saunders 1948, Summerbell 1974), similar to that seen with removal of ectoderm from facial primordia. It is also known, in the limb, that signals from the mesenchyme maintain the unique morphological and molecular nature of the ridge (reviewed by Tickle, 1991) and facial mesenchyme also has the ability to maintain the limb AER (Richman and Tickle 1992). This also suggests that there are similar signals in the face and limb mesenchyme. Considering that removal of epithelium result in truncation in both facial primordia and limb buds, evidence of common signalling pathways in both sets of primordia and the wealth of data concerning signalling in the limb, the developing limb is a useful comparison model when studying outgrowth of the face.

5.1.2 Epithelial-mesenchymal interactions in the face may be mediated by diffusible signalling molecules

The ectoderm of the limb and the face both express a variety of molecules which may play a role in the control of outgrowth. One such group of molecules is the Fibroblast Growth Factor (FGF) family of signalling molecules. Expression patterns of 3 members of the FGF family have been described in the developing chick face between stages 20 and 28, a period during which of considerable outgrowth and fusion occur. FGF-2 protein is expressed at high levels throughout the facial ectoderm of chick embryos and at lower levels in the mesenchyme (Richman *et. al.,* 1997). *Fgf-4* transcripts have been found in the distal tip ectoderm of the developing mandibular primordium in the mouse at E 9.5 (Niswander and Martin 1992) and in the chick mandible at stage 24 (Barlow and Francis-West 1997). *Fgf-8* transcripts are found around the nasal pit and at the join between the mandibular and maxillary primordium in both mouse and chick embryos (Heikinheimo *et. al.,* 1994, Ohuchi *et. al.,* 1994, Crossley and Martin 1995, Wall and Hogan 1995, Vogel *et. al.,* 1996). In chapter 3, I showed that some regions of greatest mesenchymal expansion in the face are associated with overlying ectodermal expression of *Fgf* transcripts, implying a causal role in that expansion. More recently, experiments have shown that FGF's can partially substitute for the ectoderm in grafted frontonasal mass and mandibular mesenchyme (Richman *et. al.,* 1997). Thus, there is some evidence to suggest that FGFs control outgrowth of some facial primordia.

In the developing limb, *Fgf-2*, *Fgf-4* and *Fgf-8* are expressed at high levels in the AER of the developing limb bud (Savage *et. al.,* 1993, Niswander and Martin 1992, Heikinheimo *et. al.,* 1994, Ohuchi *et. al.,* 1994, Crossley and Martin 1995, Mahmood *et. al.,* 1995, Crossley *et. al.,* 1996, Vogel *et. al.,* 1996). Studies have shown that these can maintain outgrowth of the limb bud after removal of the AER (Niswander *et. al.,* 1993, Fallon *et. al.,* 1994, Crossley *et. al.,* 1996), strongly suggesting that FGFs from the ectoderm mediate mesenchymal outgrowth.

5.1.3. Mesenchymal *Msx-1* expression is controlled by epithelial - mesenchymal interactions

Some clues to the down stream targets of FGF signalling have been provided by AER removal experiments in the limb. This results not only in truncation of the limb, but also in a reduction or abolition of the expression of some gene transcripts in the limb mesenchyme. One gene product which is abolished by ridge removal is *Msx-1* .

Msx-1 is expressed in regions of epithelial - mesenchymal interaction in the face (Mackenzie *et. al.,* 1991 a, b, Suzuki *et. al.,* 1991, Brown *et. al.,* 1993, 1997, Satokata and Maas 1994, Nishikawa *et. al.,* 1994, Mina *et. al.,* 1995, Foerst-Potts and Sadler 1997) and limb (Davidson and Hill 1991, Davidson *et. al.,* 1991, Robert *et. al.,* 1991, Brown *et. al.,* 1993) and functional inactivation of the Msx-1 gene has indicated that it is important for and outgrowth fusion and differentiation of facial primordia (Satokata and Maas 1994).

It has been shown that epithelial signals are required for the initiation and maintainance of *Msx-1* expression in the developing chick limb. Removal of the AER from the limb results in abolition of Msx-1 expression in the posterior mesenchyme i.e. the progress zone (Ros *et. al.,* 1992). Grafting of non - expressing limb proximal mesenchyme under the AER induces *Msx-1* expression (Davidson *et. al.,* 1991, Robert *et. al.,* 1991, Coelho *et. al.,* 1991, Brown *et. al.,* 1993). Thus *Msx-1* expression in limb mesenchyme is position dependent in respect to the ectoderm. In the developing face, grafting of non - expressing facial mesenchyme into anterior maxillary primordium results in *Msx-1* expression in the graft, while grafting of mesenchyme normally expressing *Msx-1* into a non-expressing region results in loss of *Msx-1* expression (Brown *et. al.,* 1993). Thus in the face, mesenchymal Msx-1 expression is also dependent on local ectodermal signals. Interestingly, if either *Msx-1* expressing or *Msx-1* non-expressing mesenchyme from the limb bud were grafted into anterior maxillary primordium, there was no Msx-1 expression (Brown *et. al.,* 1993). However, grafting of facial mesenchyme under the AER in the limb did result in maintained *Msx-1* expression (Brown *et. al.,* 1993). This would suggest the ectodermal signal that maintains Msx-1 expression in the facial mesenchyme is different to that in limb, but that the facial mesenchyme can respond to either signal.

5.1.4 Msx-1 expression is maintained by FGFs and BMPs

Evidence suggests that, in the limb, FGFs can induce and maintain the expression of *Msx-1* in the mesenchyme *in vivo* and *in vitro* . Cultures of chick posterior limb bud mesenchyme express very low levels of *Msx-1*. However, addition of bFGF (FGF-2) to culture medium increases expression (Watanabe and Ide, 1993). Mouse proximal limb mesenchymal cells cultured in FGF-2 grafted under the chick AER were found to express *Msx-1*. However, those cultured without FGF-2 did not express *Msx-1* in the same experiment (Vogel *et. al.,* 1995). Application of a bead soaked in FGF-4 to the apical tip of the limb bud after AER removal resulted in maintained *Msx-1* expression (Vogel *et. al.,* 1995). Thus it seems likely that *Msx-1* is a down - stream target of FGF signalling. There are, however, no comparable studies of the regulation of mesenchymal *Msx-1* expression in the developing face.

There is also strong evidence that another group of molecules, the Bone Morphogenetic Proteins (BMPs), can initiate and maintain the expression of *Msx-1* in the developing embryo. *Bmp-2* and *Bmp-4*, in particular, have been found to be expressed in regions of epithelial - mesenchymal interactions in the developing embryo (Lyons *et. al.,* 1990, Jones *et. al.,* 1991). *Bmp-2* and *Bmp-4* are expressed in the developing facial primordia in both mouse and chick embryos (Bennett *et. al.,* 1995, Francis-West *et. al.,* 1994, Wall and Hogan 1995). In the chick, they are expressed both in ectoderm and mesenchyme of facial primordia between stages 20 and 28. *Bmp-4* is initially expressed in the ectoderm, only appearing in the mesenchyme at stage 28 while *Bmp-2* is generally found in both ectoderm and mesenchyme throughout this period of facial development (Francis-West *et. al.,* 1994, Barlow and Francis-West 1997). *Bmp-4* expression overlies regions of mesenchymal *Msx-1* expression in the developing face (Barlow and Francis-West *et. al.,* 1997), therefore this molecule is also expressed in regions of the face that expand the most (see chapter 3, this thesis). Implantation of a bead soaked in BMP-2 to the posterior maxillary primordium resulted in bifurcation of Meckle's cartilage in the mandibular primordium and an increase in cell proliferation. Thus expression patterns and functional studies imply a role for BMPs in promoting cell proliferation and outgrowth of facial primordia. In the limb, *Bmp-2* and *Bmp-4* are both expressed in the AER (Lyons

et. al., 1990, Jones *et. al.,* 1991, Francis *et. al.,* 1994) but are thought to act in an antagonistic way to FGF, inhibiting outgrowth (Niswander and Martin 1993).

Implantation of a bead, soaked in either BMP-2 or BMP-4, into the mandibular or maxillary primordium can induce the expression of *Msx-1* (Barlow and Francis-West 1997). Different experiments, in which BMP-4 expressing cells were grafted into paraxial mesoderm, also resulted in induction of both *Msx-1* expression and ectopic cartilage formation in the region of the graft (Watanabe and Le Douarin 1996). Similarly, in the developing tooth BMP-4, normally expressed in the dental epithelium, can substitute for that epithelium, inducing both morphological change and *Msx-1* expression in the dental mesenchyme (Vanio *et. al.,* 1993). Thus there is strong evidence that BMP-4 regulates *Msx-1* expression in a number of different developing tissues.

5.1.5 Direct cell-cell signalling in the chick facial primordia

A third type of signalling in the embryo involves direct cell-cell signalling by interaction between membrane bound receptors and ligands. One group of developmentally important molecules which signal in this way are the Eph receptor protein tyrosine kinases (RTPKs).

There are 14 known members of this group (Orioli and Klein 1997) making this the largest subgroup of RPTKs. They were first isolated from an erythropoietin-producing hepatoma cell line (Hirai *et. al.,* 1987) and are well conserved throughout evolution, being found in Drosophila, mouse, chick, rat (Tuzi and Gullick 1994) and *Xenopus* (Winning and Sargent 1994) as well as humans. Under a new agreement on nomenclature (Eph nomenclature committee, 1997), which has been adopted in this thesis, Eph receptors have been divided into two subgroups, EphA and EphB, based on the amino acid homology in the extracellular domain (reviewed in Orioli and Klein 1997). Signalling occurs when an Eph receptor in the membrane interacts with an Eph ligand from a neighbouring cell. This triggers receptor dimerisation and autophosphorylation of tyrosine residues in the intracellular portion of the receptor, triggering an intracellular cascade (Schlessinger and Ullrich 1992). Eph ligands have also been re-classified into two subgroups EphrinA and EphrinB, based on whether they are anchored in the membrane

by a GPI link or a transmembrane link with a cytoplasmic tail (reviewed in Orioli and Klein 1997). Ephrin A ligands bind to EphA receptors and Ephrin B ligands bind to EphB receptors (Brambilla *et. al.*, 1995, 1996, Gale *et. al.*, 1996a) with the exception of Eph4A (also known as mSek1/Tyro1/Hek8/Cek8/Pag) which can bind both types of ligand. Thus there is promiscuity of receptor / ligand binding within a subgroup but not generally between subgroups (Gale *et. al.*, 1996a). It has recently been discovered that members of the Ephrin B subgroup of Eph ligands can also become phosphorylated on the intracellular portion upon receptor-ligand interaction and thus may also act as receptor like signalling molecules (Bruckner *et. al.*, 1997).

Many Eph receptors are expressed in the developing nervous system and studies thus far have concentrated on the role that Ephs play in neural development. A large body of work indicates that Eph receptors are involved in axonal guidance by repulsion. This has been particularly studied in the retinotectal system where neurons projecting from the temporal retina, expressing *EphA3* (Mek4) (Cheng *et. al.*, 1995, Monschau *et. al.*, 1997), project to the anterior tectum, encountering an expression boundary of *Ephrins A2* (Elf1) and A5 (RAGS) (Cheng *et. al*, 1995, Drescher *et. al.*, 1995). These receptors and ligands interact and temporal retina axons are prevented from projecting further into the posterior tectum. Expression studies have also implicated *Ephs* in the establishment of boundaries such as those seen in the hindbrain, where Eph receptors and ligands are expressed in complementary rhombomeres (Gale *et. al.*, 1996b, Bergemann *et. al.*, 1995, Becker *et. al.*, 1994). Dominant-negative *Eph4A* mRNA injected into the hindbrains of *Xenopus* and zebrafish disrupted the segmentation of the hindbrain which could be rescued with injection of *Eph4A,* (Xu *et. al.*, 1995). These experiments demonstrate directly a role in compartmentalisation of the hindbrain.

More recently, and of more interest to this thesis, Eph receptors have been implicated in the guidance of both trunk and cranial neural crest migration. In the trunk, neural crest migrates through the rostral half of the somite and is repelled from the caudal half (Rickmann *et. al.*, 1985). It has been shown that Eph ligands Ephrin B1 and B2 are expressed in the caudal somite and that they repel motor axon growth and neural crest migration in vitro (Wang and Anderson 1997, Krull *et. al.*, 1997). Similarly, migration of

hindbrain cranial neural crest occurs in a segmental manner (Lumsden *et. al.,* 1991). In *Xenopus* embryos, cranial neural crest populations migrate as 3 streams and neural crest from the 3rd stream populates arches 3 and 4. This crest population expresses *Eph4A* and *EphB1* and the receptors expressed bind to the ligand EphrinB2 expressed in arch 2. As a result of this receptor - ligand interaction, these cells are repulsed from arch 2. This restricts the neural crest population and aids in targeting the correct destination (Smith *et. al.,* 1997). Ephs may also play a role in guiding other cranial neural crest populations and this may have implications for facial development. A further study has also shown that Ephs are important for secondary palate development. Mice with both *EphB3* (mSek4) and *EphB2* functionally inactivated exhibit cleft secondary palates, not seen when these genes are inactivated singly (Orioli *et. al.,* 1996).

The chick Eph receptor *Eph4A* (*Cek-8*) was isolated in a screen of chick embryonic cDNA libraries (Sajjadi and Pasquale 1993) and is the chick homologue of *mSek1* (Gilardi-Hebenstreit *et. al.,* 1992). It has been found to be expressed in motorneurones innervating the chick limb (Fukushima *et. al.,* 1996, Ohta *et. al.,* 1996, 1997, Tanaka *et. al.,* 1997) which are repulsed by *Ephrin A5* (RAGS) and *Ephrin A2* (Elf) which are also expressed in regions the limb (Ohta *et. al.,* 1997). *Eph4A* is also expressed in the developing hindbrain of the chick, where it has been shown to be correlated with rhombomere boundary maintenance (Nittenberg *et. al.,* 1997). In the developing chick limb mesenchyme, *Eph4A* is expressed predominantly posteriorly and the levels of transcripts are rapidly reduced upon AER removal. This expression can be rescued by application of FGF (Patel *et. al.,* 1996). *Eph4A* is expressed in the chick face mainly in regions that have the greatest expansion (see results this chapter) and overlaps substantially with the domains of *Msx-1* expression.

In this chapter I also aim to investigate whether epithelial - mesenchymal interactions control *Eph4A* expression and if so, is the molecular pathway similar or different to that seen with control of *Msx-1* expression.

5.2 Materials and methods

5.2.1 Removal of facial ectoderm with 2% Nile Blue Sulphate

Nile blue sulphate (Sigma) was dissolved in sterile distilled water, 2% w/v. This was filtered using Whatman No 1 filter paper and stored at room temperature.

Stage 24 chick embryos were exposed *in ovo*, as described in section 2.1. 2% Nile blue sulphate was applied to the maxillary primordium by dipping a 2μl capacity Gilson tip into the Nile Blue Sulphate solution which was then gently touched to the maxillary primordium ectoderm. This leaves a wide "circle" of dye on the ectoderm which blisters away from the mesenchyme underneath. The edge of this circle was gently broken with the tip of a finely sharpened tungsten needle and the ectoderm was peeled away using fine forceps. Thus, no Nile Blue Sulphate solution reached the mesenchymal cells.

5.2.2 Preparation and application of FGF soaked beads to maxillary primordia.

Heparin acrylic - beads of a size 200-250μm in diameter were selected using an eyepiece graticule and stage micrometer and washed in PBS. The beads were then soaked in 1μl of either 1mg/ml FGF-2 (R+D Systems) or 0.7mg/ml FGF-4, a kind gift from J. Heath, for at least 1 hour in a humidified chamber. Control beads were soaked in PBS only.

Immediately after the ectoderm had been removed from the maxillary primordium, see above, an FGF soaked bead was placed onto the mesenchyme, in a central position. The bead was held in place by a sterile staple formed from platinum wire (0.025μm, Goodfellow).

5.2.3 Preparation and application of BMP-4 soaked beads to maxillary primordia

Affigel CM beads (Bio-Rad) of a size 200-250μm in diameter were washed twice in PBS then soaked in 100ng/ml BMP-4 (Genetics Institute, Cambridge, Massachusetts) for

at least 1 hour in a humidified chamber. Control beads were soaked in PBS only. Beads were applied to the maxillary primordium mesenchyme as described above.

5.2.4 Amputation of maxillary primordia, enzymatic removal of epithelia and grafting of maxillary mesenchyme onto the face.

The right hand side maxillary primordium from stage 24 chick embryos were removed, *in ovo*, using fine forceps. The primordium was removed along the anteroposterior axis from the join with the lateral nasal process to the point where it joins the mandibular primordium, see Fig. 5.1 as an indication. Bleeding was slight and lasted only a few minutes. If bleeding was excessive, the embryo was discarded. The amputated maxillary primordium was placed immediately in sterile, ice cold "growth medium" (see section 2.3) and the egg sealed and replaced in the incubator. Pooled maxillary primordia were washed briefly in sterile cold PBS and then incubated in sterile 2% w/v trypsin (Sigma) in PBS at 4°C for 30 minutes. Primordia were checked under a dissecting microscope to see if the ectoderm had loosened and if so, were transferred to ice cold serum containing growth medium to stop the enzymatic reaction. The medium at this point was kept cold by placing a cold block under the dish. The ectoderms were removed using a sharpened tungsten needle.

To graft maxillary primordium mesenchyme back onto the face, the tissue was transferred onto a stage 24 embryo which had undergone maxillary primordium amputation in the previous hour. The tissue was orientated, with fine forceps, so that the cut edge aligned with the cut edge of the embryo face. The tissue was pinned onto the face with a sterile platinum staple (as above). In experiments where growth factor protein soaked beads were also grafted with mesenchyme tissue, the mesenchyme was pinned onto the face first and the bead was placed centrally onto the graft and pinned with platinum staples as before.

Figure 5.1 Stage 24 chick head

Drawing of side view of stage 24 chick head, as seen *in ovo*. The maxillary primordium (Mx) is clearly visible, as are the nasal pit (NP) and frontonasal mass (FNM). Indicated on the maxillary primordium are the points where the proximodistal outgrowth (P-D) and the anteroposterior extension (A-P) are measured, in experiments contained in this chapter.

Figure 5.1

5.2.5 Preparation of the *Eph4A* (*Cek-8*) riboprobe

0.5 kb *Eph4A* DNA in pBluescript plasmid, a gift from K. Patel, was linearised with Not1, and transcribed with T3 as described in section 2.6.2 to produce a 420bp antisense RNA probe, corresponding to nucleotides 394-813. See also Patel *et. al.,* 1996.

5.3 Results

5.3.1 Role of ectoderm in outgrowth of maxillary primordia.

Grafting experiments, in which facial primordia of chick embryos were explanted to the limb bud, suggest that ectoderm is required for outgrowth of facial primordia (Wedden and Tickle, 1986, Wedden 1987, Richman and Tickle 1989). However, in this system, the maxillary primordium is unable to undergo polarised growth even in the presence of ectoderm. In order to test the role of the ectoderm in controlling outgrowth of maxillary primordium more directly, ectoderm overlying the right maxillary primordium of stage 24 chick embryos was removed *in ovo* by application of 2% Nile Blue Sulphate. The size of patch of ectoderm removed was on average 1047.9 (anteroposterior) x 460.0 (proximodistal) μm (n=80) and this more or less completely denuded the maxillary primordia mesenchyme (see section 5.3.2 below). Embryos were examined at various later times. The anteroposterior (AP) extent and the proximodistal (PD) outgrowth of each treated primordium was measured (see Fig. 5.1 for detail) as were the dimensions of the contralateral control primordium (Table 5.1, Graph 5.1, Appendix 6). It was quite clear from control measurements that maxillary primordia outgrowth is less than extension over this period, but to understand more about changes in growth between stages 24 and 30, growth curves of this data were plotted i.e. change in dimension over unit time (Table 5.2 Graph 5.2). This showed that extension (black line, Graph 5.2) and outgrowth (red line, Graph 5.2) initially increased very rapidly, both peaking at stage 24/5. They both then experienced a decelerated growth until approximately stage 26 for extension and stage 28 for outgrowth, when the growth accelerated again. Thus in both cases this growth curve was biphasic. In the second phase of accelerated growth, between stages 26 and 30, the

outgrowth (P-D) curve was steeper, suggesting that growth in this dimension was faster. However, in general the growth curves, for both dimensions (A-P and P-D) were very similar in shape. Thus growth rates in both anteroposterior and proximodistal axes seem in concert between stage 24 and 30.

Immediately after ectoderm removal, treated and control primordia showed no difference in dimensions but later, between 4 and 24 hours after ectoderm removal, when embryos were approximately stage 24-28, proximodistal outgrowth of the treated maxillary primordium was reduced compared to that of controls (Table 5.1, Graph 5.1). Comparison of data using students t-test showed that the means of the two populations were different between 4 and 24 hours after ectoderm removal (p<0.5). At stage 28, in most cases, there was a gap between maxillary primordia and frontonasal mass on the manipulated side of the face while in controls, these primordia were already in contact. By 48 hours however, outgrowth had more or less recovered and was no longer significantly different from that in controls, although treated primordia were still slightly smaller. None of these embryos displayed an obvious cleft of the primary palate, suggesting that the maxillary primordium grew sufficiently during this period to achieve fusion. The anteroposterior extent of the maxillary primordium did not differ between treated and control embryos at any time point (Table 5.1, Graph 5.1). Thus ectoderm removal transiently reduces the outgrowth (P-D) component of maxillary primordia growth. Growth curves for this experiment were also plotted and compared to control data (Table 5.2, Graph 5.2). As expected, there was no difference in the growth curves for anteroposterior extension in manipulated embryos (green line, Graph 5.2). However, in the manipulated primordium the curve indicated that the first peak of accelerated growth, between stages 24 and 25, had been lost. Surprisingly the rest of the growth curve profile was very similar to that of unmanipulated primordia (red line, Graph 5.2). Thus the rate of growth seems to have been affected for only a short time.

Table 5.1 Mean anteroposterior extension (AP) and proximodistal outgrowth (PD) of maxillary primordia with intact ectoderm (control) and after ectoderm removal wih Nile Blue Sulphate (treated).

Time after ectoderm removal (hours).	Number in data set (n).	Mean area of ectoderm removed ± S.D. (μm) (AP x PD).		Control Mean ± S.D. (μm).		Treated - Mean ± S.D. (μm).	
				Length (AP)	Width (PD)	Length (AP)	Width (PD)
0	12	855 ± 29	201 ± 89	821 ± 99	501 ± 65	820 ± 99	500 ± 62
4	12	1136 ± 416	200 ± 70	1192 ± 185	604 ± 64	1194 ± 185	521 ± 74
8	10	1321 ± 551	264 ± 22	1227 ± 348	671 ± 98	1226 ± 324	544 ± 87
12	12	1100 ±501	239 ±112	1255 ± 174	693 ± 83	1243 ± 174	572 ± 103
18	12	924 ± 446	312 ± 95	1319 ± 232	583 ± 93	1319 ± 232	708 ± 93
24	11	1090 ± 474	367 ± 88	1486 ± 251	739 ± 56	1472 ± 265	586 ± 105
48	11	949 ± 417	417.4 ± 92	1848 ± 51	1140 ± 237	1863 ± 507	1078 ± 193

Table 5.2 Increase in mean anteroposterior extension or proximodistal outgrowth (μm) between time points (hours) in intact maxillary primordia (control) and after ectoderm removal with Nile Blue Sulphate (treated).

Time (hours)	Increase in control anteroposterior extension (μm)	Increase in control proximodistal outgrowth (μm)	Increase in treated anteroposterior extension (μm)	Increase in treated anteroposterior outgrowth (μm)
4	373	103	373	20
8	33	67	32	23
12	28	22	17	29
18	65	15	77	11
24	168	31	153	35
48	361	402	390	492

Graph 5.1 Outgrowth (P-D) and extension (A-P) for the maxillary primordium with intact ectoderm and with ectoderm removed with Nile Blue Sulphate

153
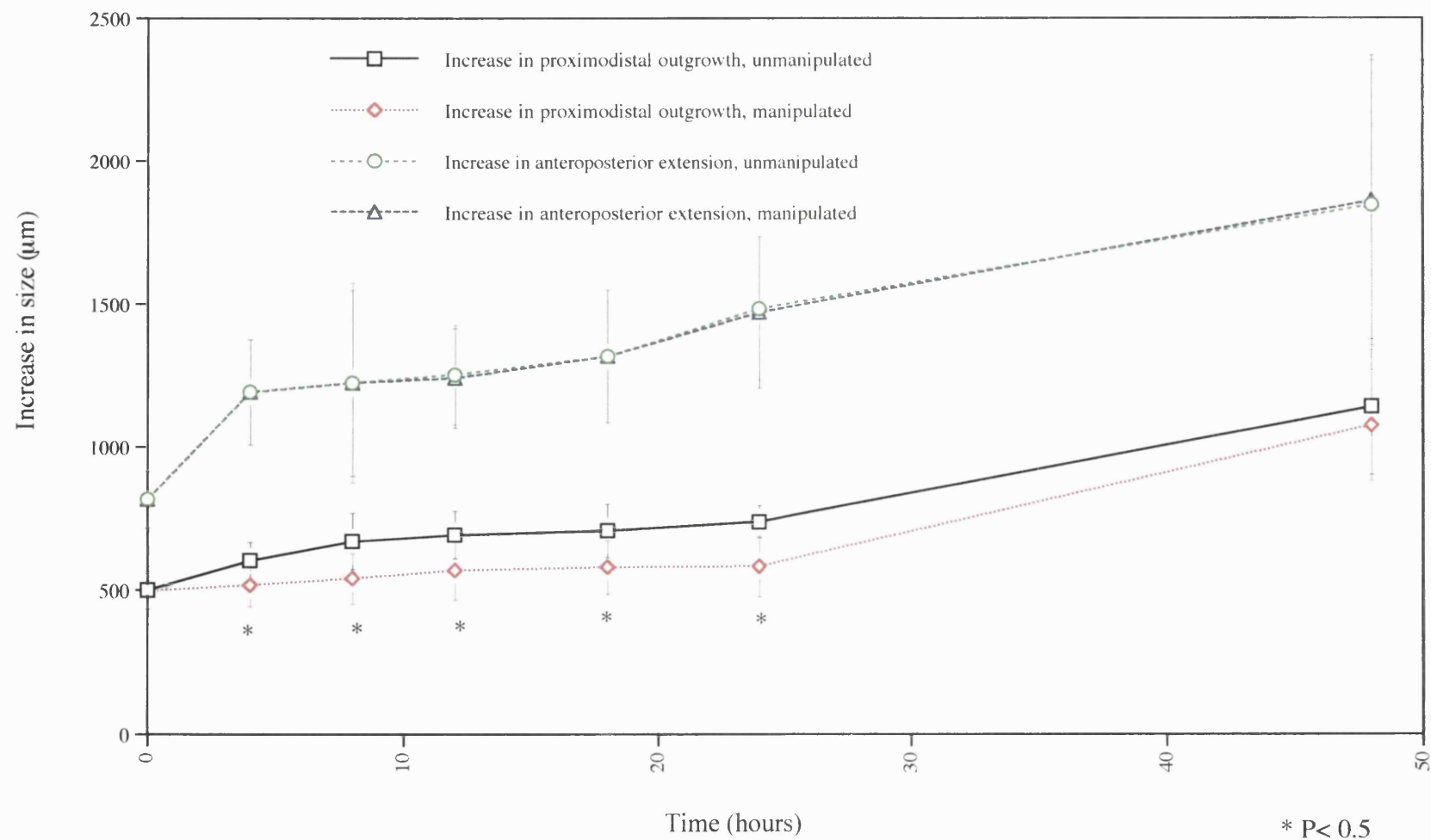
Graph 5.2 Growth curve for maxillary primordia with ectoderm and after ectoderm removal: increase in size (µm) per unit time (hours)
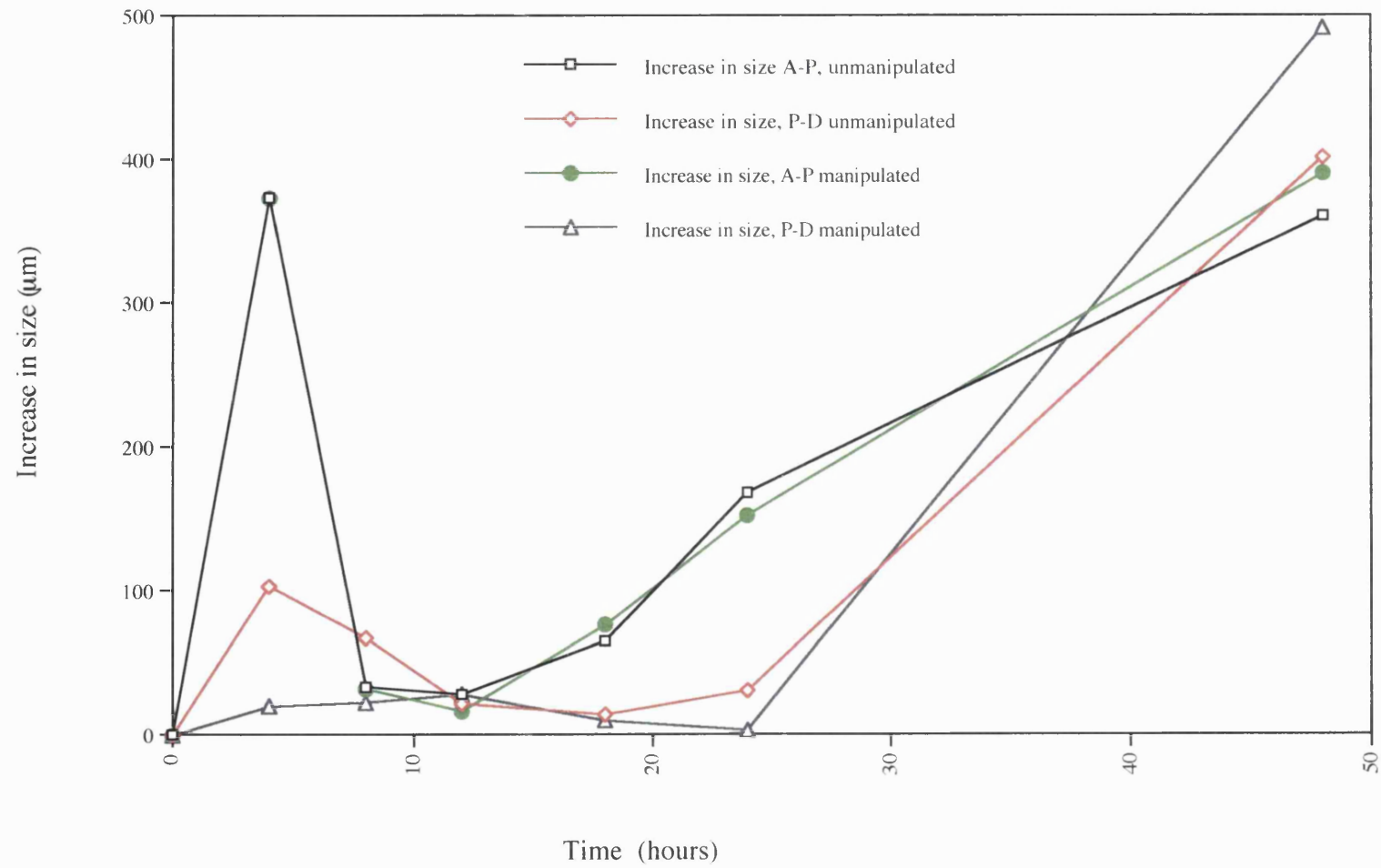
5.3.2 Maxillary primordium ectoderm re-grows after chemical removal

Resumption of outgrowth in the manipulated primordia could be due to ectoderm growing over the primordium. To investigate this possibility, the maxillary primordium was examined at various times after ectoderm removal by scanning electron microscopy. Embryos examined immediately (t = 0hrs, n=3) confirmed that most of the ectoderm had been removed from the right hand side maxillary primordium (Fig. 5.2A). However, in general, a small patch of ectoderm remained over the very distal anterior tip of the primordium (Fig. 5.2A). Small patches of tissue of the eye were also removed in two out of three cases but no other structures were affected. Ectoderm on the left hand side maxillary primordium was unaffected (Fig. 5.2B) After 2 hours, some re - growth of the ectoderm was observed at the distal edge (n=2) but a large area of maxillary mesenchyme remained exposed. After 18 hours, (n=2), ectoderm was still absent from the proximal edge of the maxillary primordium indicating that re - growth occurs in a distal to proximal direction. After 24 hours (n=2), the ectoderm of the maxillary primordium had almost fully re - grown, with only a small patch of exposed mesenchyme visible (Fig. 5.2C) thus appearing similar to the untreated maxillary primordium ectoderm (Fig. 5.2D).

5.3.3 Rescuing outgrowth of the maxillary primordium with FGF

Ectoderm overlying chick facial primordia expresses FGF-2, *Fgf-4* and *Fgf-8* (Richman *et. al.*, 1997, Barlow and Francis-West 1997, Wall and Hogan 1995, Vogel *et. al.*, 1996). To investigate if FGFs are involved in the control of outgrowth of maxillary primordia, beads soaked in either FGF - 2 or 4 protein were placed onto the exposed mesenchyme after ectoderm had been removed with Nile Blue Sulphate. The dimensions of the primordium were measured as before (Tables 5.3 and 5.4, appendicies 7, 8) at time points up to 48 hours after treatment.

Application of FGF almost completely rescued outgrowth. There was little difference in proximodistal outgrowth of mesenchyme exposed to either FGF-2 (graph 5.3) or FGF-4 (graph 5.4) and control maxillary primordia at any incubation time, although outgrowth of manipulated primordia tended to be slightly less than that of controls. Students t-test

Figure 5.2 Scanning electron micrographs of chick facial primordia after ectoderm removal by Nile Blue Sulphate *in ovo*.

A. Stage 24 maxillary primordium immediately after ectoderm removal (t = 0). Black arrowhead indicates the large patch of exposed mesenchyme.

B. Stage 24 contralateral control maxillary primordium (t = 0). Continuous ectoderm can clearly be seen in this maxillary primordium.

C. Stage 27 maxillary primordium 24 hours after ectoderm removal at stage 24. White arrowhead indicates small patch of exposed mesenchyme proximally, close to the eye.

D. Stage 27 contralateral control maxillary primordium, unmanipulated. This primodium is at a higher magnification than in C.

E. Stage 24 maxillary primordium 2 hours after ectoderm removal and application of a bead soaked in FGF. White arrow indicates position of the bead, which has fallen out during processing for SEM. The platinum staple that held the bead in can still be seen. White arrowhead indicates the ectoderm at the distal edge of the primordium, which has not been removed by Nile Blue Sulphate application. This is similar to the amount of ectoderm present on maxillary primordia in embryos which have had ectoderm removed but not treated with FGF at the same time point, see A.

F. Stage 27 maxillary primordium 24 hours after ectoderm removal and treatment with FGF. White arrow head indicates small patch of exposed mesenchyme laterally, near to the eye. This is similar to embryos with ectoderm removed but not treated with FGF at the same time point. White arrow indicates the buldge in the primordium where the bead was implanted and now covered by ectoderm.

Key:

Mx: Maxillary primordium	LNP: Lateral nasal process.
Mn: Mandibular primordium.	FNM: Frontonasal mass.
NP: Nasal pit.	

Figure 5.2
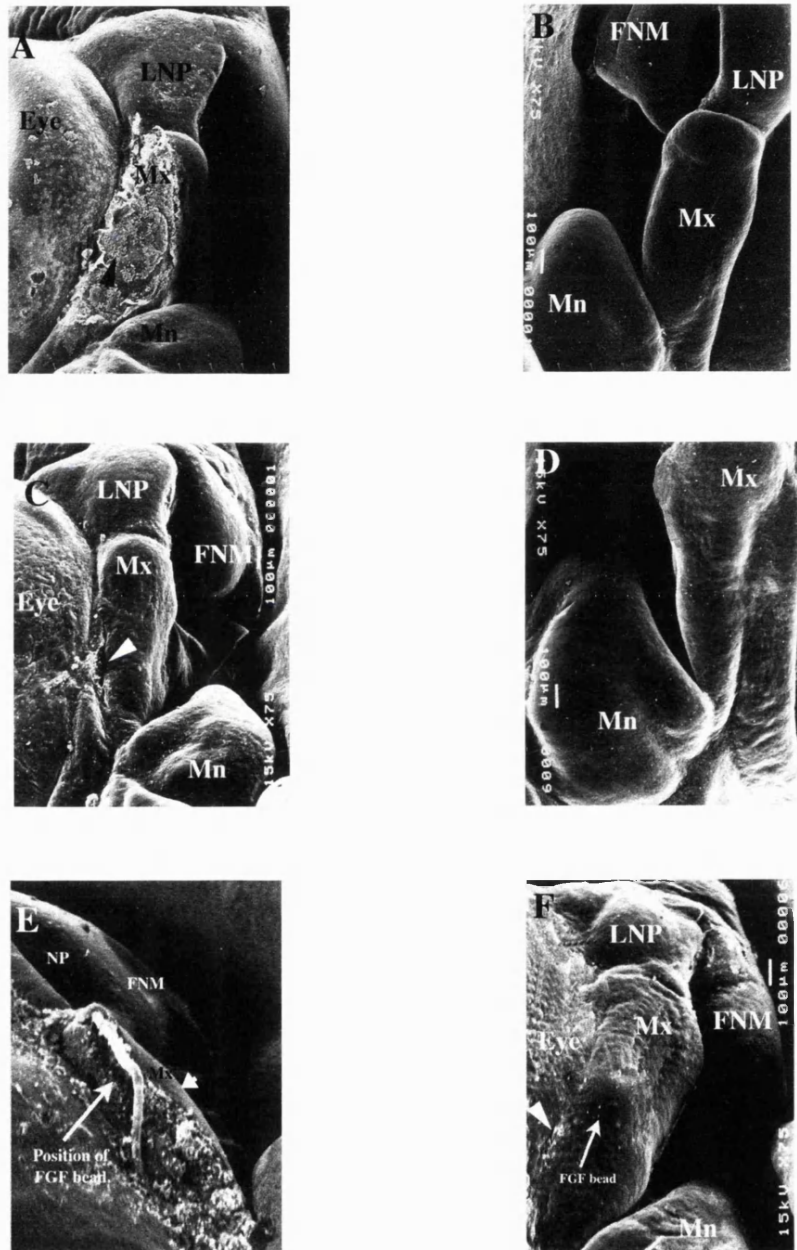
Table 5.3 Mean anteroposterior extension (AP) and proximodistal outgrowth of maxillary primordia with intact ectoderm (control) and after ectoderm removal and FGF-2 application (treated).

Time after ectoderm removal and FGF 2 treatment (hours).	Number in data set (n).	Area of ectoderm removed (μm) (AP x PD).		Control - Mean ± S.D. (μm).		Treated - Mean ± S.D. (μm).	
				Length (AP)	Width (PD)	Length (AP)	Width (PD)
4	5	818 ± 52	384 ± 91	812 ± 63	511 ± 43	812 ± 63	469 ± 61
8	3	904 ±135	376 ± 21	863 ± 47	510 ± 49	863 ± 47	488 ± 28
12	5	954 ± 107	434 ± 59	1201 ± 260	668 ± 47	1209 ± 261	651 ± 43
18	5	994 ± 212	494 ± 13	1582 ± 319	744 ± 74	1564 ± 314	717 ± 70
24	5	1043 ± 69	374 ± 19	1594 ± 58	765 ± 81	1594 ± 58	732 ± 145
48	4	1046 ± 91	385 ±81	2392 ± 408	1037 ± 48	2392 ± 408	1037 ± 48

Table 5.4 Mean anteroposterior extension (AP) and proximodistal outgrowth of maxillary primordia with intact ectoderm (control) and after ectoderm removal and FGF-4 application (treated).

Time after ectoderm removal and FGF-4 treatment (hours).	Number in data set (n).	Area of ectoderm removed (μm) (AP x PD).		Control - Mean ± S.D. (μm).		Treated - Mean ± S.D. (μm).	
				Length (AP)	Width (PD)	Length (AP)	Width (PD)
4	5	1250 ± 148	550 ± 94	911 ± 4.0	545 ± 32	902 ± 21	519 ± 57
8	6	925 ± 164	475.3 ± 112	1206 ± 130	639 ± 69	1180 ± 112	583 ± 47.3
12	4	944 ± 16	491 ± 155	1293 ± 139	666 ± 44	1267 ± 167	623 ± 26
18	5	1490 ± 198	480 ± 27	1295 ± 101	719 ± 95	1283 ± 125	716 ± 100
24	4	1156 ± 277	486 ± 138	1335 ± 61	781 ± 11	1323 ± 63	781 ± 11
48	4	1015 ± 155	632 ±297	1894 ± 71	1056 ± 43	1885 ± 79	1046 ± 51

Graph 5.3 Outgrowth (P-D) and extension (A-P) of the maxillary primordium with intact ectoderm and after ectoderm removal with Nile Blue Sulphate and application of FGF-2
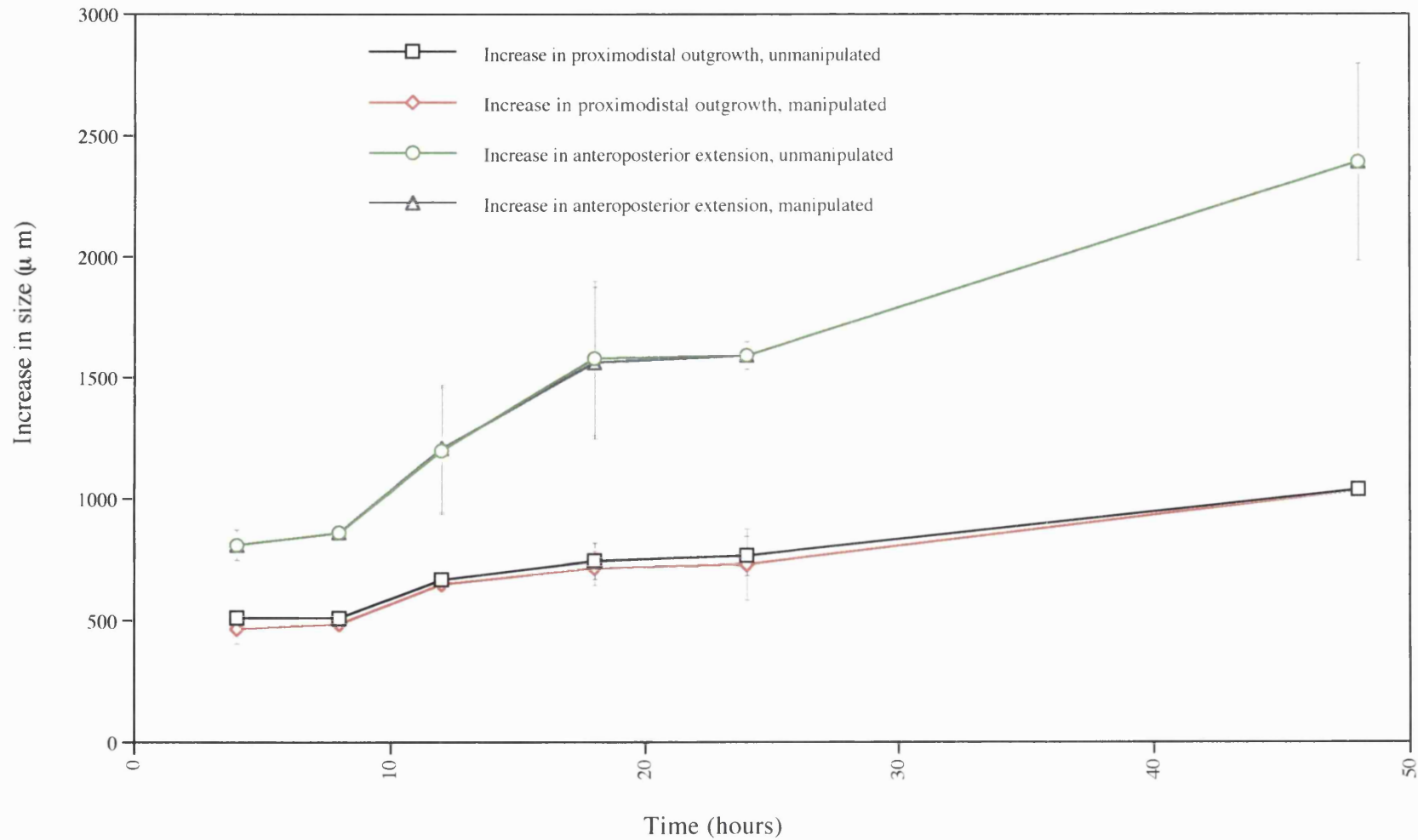
Graph 5.4 Outgrowth (P-D) and extension (A-P) of the maxillary primordium with intact ectoderm and after ectoderm removal with Nile Blue Sulphate and application of FGF-4

Increase in size (μm)

Time (hours)

Increase in proximodistal outgrowth, unmanipulated

Increase in proximodistal outgrowth, manipulated

Increase in anteroposterior extension, unmanipulated

Increase in anteroposterior extension, manipulated
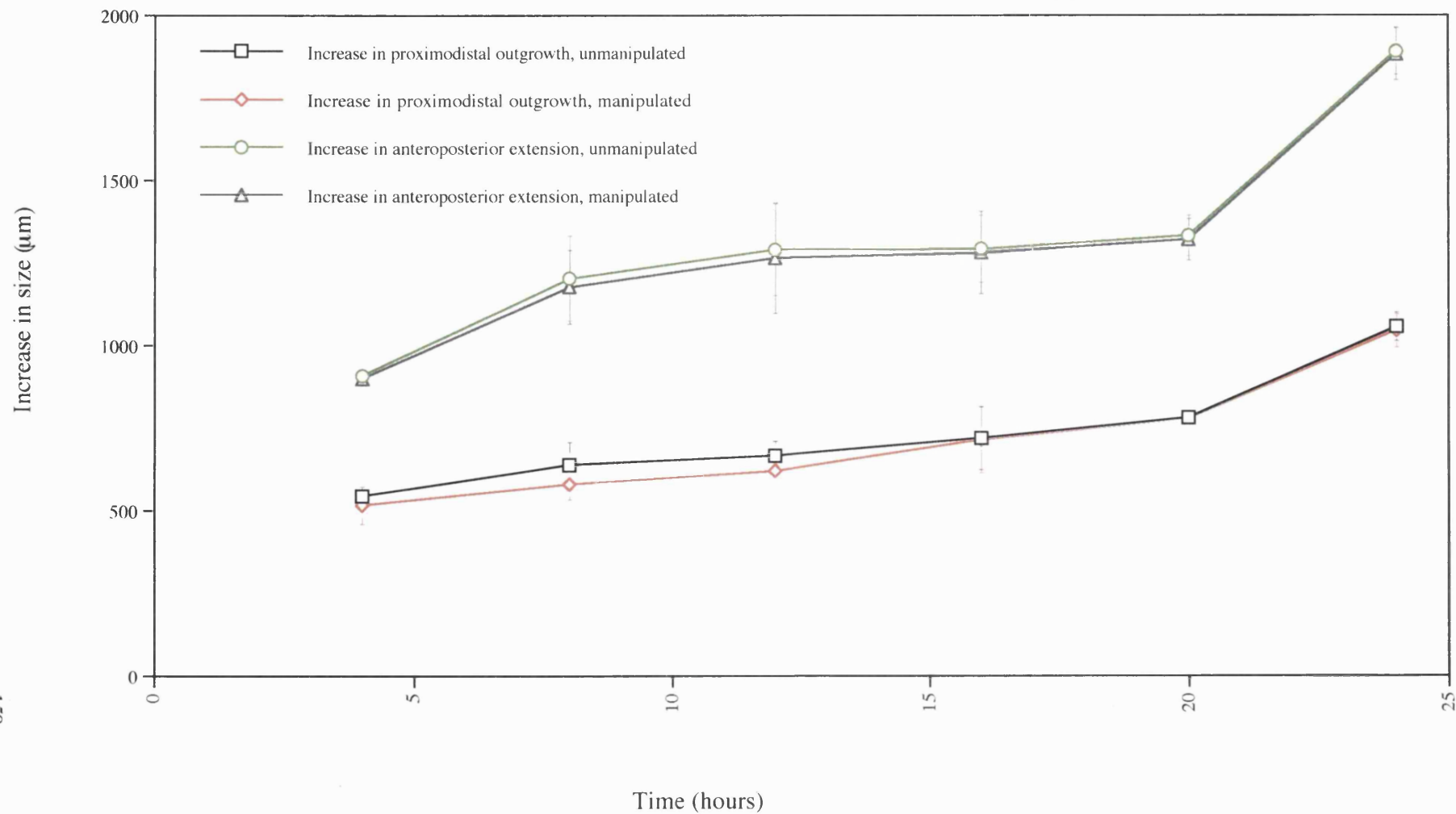
showed that there was no significant difference in the means of treated and control data. As before there was no difference in anteroposterior extent at any time point (Graphs 5.3 and 5.4).

To rule out the possibility that FGFs could simply be accelerating re-epithelisation, embryos were examined by scanning electron microscopy as before. The re-growth of the ectoderm was found to follow a similar time course in the presence of FGF, with slight anterior distal growth found after 2 hours (Fig. 5.2E) and only a small patch of exposed mesenchyme found at 24 hours (Fig. 5.2F). Therefore, maintenance of mesenchymal outgrowth is a direct effect of FGF application to the maxillary primordium, rather than secondary to accelerated epithelia re-growth.

5.3.4 Normal expression of *Msx-1* transcripts in facial primordia between stages 20 and 28 and after ectoderm removal

The mesenchymal pattern of expression of *Msx-1* in chick facial primordia is well documented (Susuki *et. al.,* 1991, Brown *et. al.,* 1993, 1997, Mina *et. al.,* 1995, see also chapters 3 and 4). Between stage 20 and 28, transcripts are found in the anterior portion of the maxillary primordium, with expression also being stronger in distal regions than in proximal regions near the eye. Transcripts are also found at the distal tips of the mandibular primordium at stage 20, extending more proximally by stage 28. Expression in the frontonasal mass and lateral nasal process does not appear until stage 22/3 and is found throughout the lateral nasal process at the distal lateral edges of the frontonasal mass, bordering the nasal pits up to stage 28.

We have shown that outgrowth of the maxillary primordium relies upon an intact ectoderm (section 5.3.1) and it has been suggested that *Msx-1* expression in the face is correlated with outgrowth (Brown *et. al.,* 1993, Satokata and Maas 1994). Therefore to investigate whether ectoderm plays a role in controlling expression of *Msx-1* transcripts in the maxillary primordia, ectoderm was removed, as before, using Nile Blue Sulphate and embryos processed for *in situ* hybridisation with chick *Msx-1* riboprobe.

Immediately upon ectoderm removal (t=0 hours), we saw no change in the expression of *Msx-1* in the treated maxillary primordium (n=3) (Fig. 5.3A). At 4 hours, outgrowth

of the maxillary primordium was noticeably reduced, as seen in previous experiments. However, there was no obvious change in expression of *Msx-1* in 2 out of 3 treated maxillary primordium (Fig. 5.3B) compared with contralateral control primordia. However in 1/3 cases, *Msx-1* expression seemed slightly increased compared to the control. At 8 and 24 hours after manipulation (n=3 each time point),when embryos had reached approximately stage 25 and stage 28, the maxillary primordium was substantially smaller. Again *Msx-1* expression in the anterior part of the primordium was not reduced and even possibly expressed at a slightly higher level (Figs. 5.3 C-E). Also, the domain of expression in the primordia without ectoderm extend proximally to the edge of the maxillary primordium near to the eye. As noted in previous experiments, outgrowth was similar between control and treated primordia 48 hours after ectoderm removal. However the level of *Msx-1* expression was still slightly increased in the treated maxillary primordium and gaps between the maxillary primordium and frontonasal mass could be seen on the manipulated side of the face (Fig. 5.3F). These results suggest that ectodermal signalling does not maintain expression of *Msx-1* transcripts in the anterior maxillary primordium. However, small patches of ectoderm from distal anterior maxillary primordia often remained after Nile Blue Sulphate removal (Fig. 5.2D) and this may have been sufficient to maintain the domain of *Msx-1* expression in the manipulated primordium. To examine this possibility, the maxillary primordium was amputated, all of the ectoderm was removed using trypsin and the mesenchyme then pinned back on to the cut edge of the maxillary primordium in other embryos.

When ectoderm is totally removed from the maxillary primordium, outgrowth is very stunted and the maxillary primordium forms a ball of tissue, as seen previously when grafted to the limb (Richman and Tickle, 1989). Four hours after the maxillary mesenchyme was totally denuded of ectoderm and pinned back onto the face, the region that had been the distal tip of the primordium continued to express *Msx-1* (3 out of 3 embryos, Fig. 5.4A). At 12 hours (n=3), the piece of grafted tissue, which could be seen attached to the posterior amputated edge of the maxillary primordium, did not express *Msx-1* transcripts (Fig. 5.4B). At 24 hours, stage 28, the tissue had not grown out or elongated and appeared as a small ball of tissue attached to the posterior region of the

161

Figure 5.3 Expression of *Msx-1* transcripts in maxillary primordia after ectoderm removal by Nile Blue Sulphate

In each case, treated primordia are on the left side of the face.

A. Stage 24 chick embryo face immediately after ectoderm removal. *Msx-1* expression is seen in the anterior regions of manipulated (black arrowhead) and unmanipulated maxillary primordia. There is no change in *Msx-1* expression in manipulated primordium.

B. Chick embryo face, 4 hours after ectoderm removal at stage 24. Level of Msx-1 expression in manipulated maxillary primordium is similar to control. However, *Msx-1* expression in manipulated primordium extends to the proximal edge (black arrowhead) while in control primordium does not extend as far proximally (white arrowhead).

C. Chick face, 8 hours after ectoderm removal. Expression of *Msx-1* is maintained in manipulated primordium, again extending to proximal edge. Expression in control primordium (white arrowhead) extends only part of the way across the primordium.

D. Chick face, 16 hours after ectoderm removal. Again Msx-1 expression is maintained in the manipulated primordium, extending to the proximal edge (black arrowhead). Control primordium is indicated by white arrowhead. Left lateral nasal process in this specimen is slightly damaged. There is a noticable gap between maxillary primordium and frontonasal mass on the left side of the face in this embryo compared to the right.

E. Chick embryo face, 24 hours after ectoderm removal. *Msx-1* expression is still strong in the manipulated maxillary primordium, extending fully to the proximal edge, (black arrowhead). As before, in the unmanipulated control maxillary primordium, Msx-1 expression only extends part of the way across the proximodistal axis.

F. Chick embryo face, 48 hours after ectoderm removal. Expression of *Msx-1* is seen in anterior part of the manipulated maxillary primordium, (black arrowhead). In control maxillary primordium, expression is seen distally, not proximally (white arrowheads). On left side of the face there is a small gap in the region where primary palate forms. On right side, the primordia are already in contact. Thus although Msx-1 expression has been maintained upon removal of ectoderm, there is a gap in the primary palate.

FNM: Frontonasal mass   LNP: Lateral nasal process

Mx: Maxillary primordium   Mn: Mandibular primordium

Figure 5.3
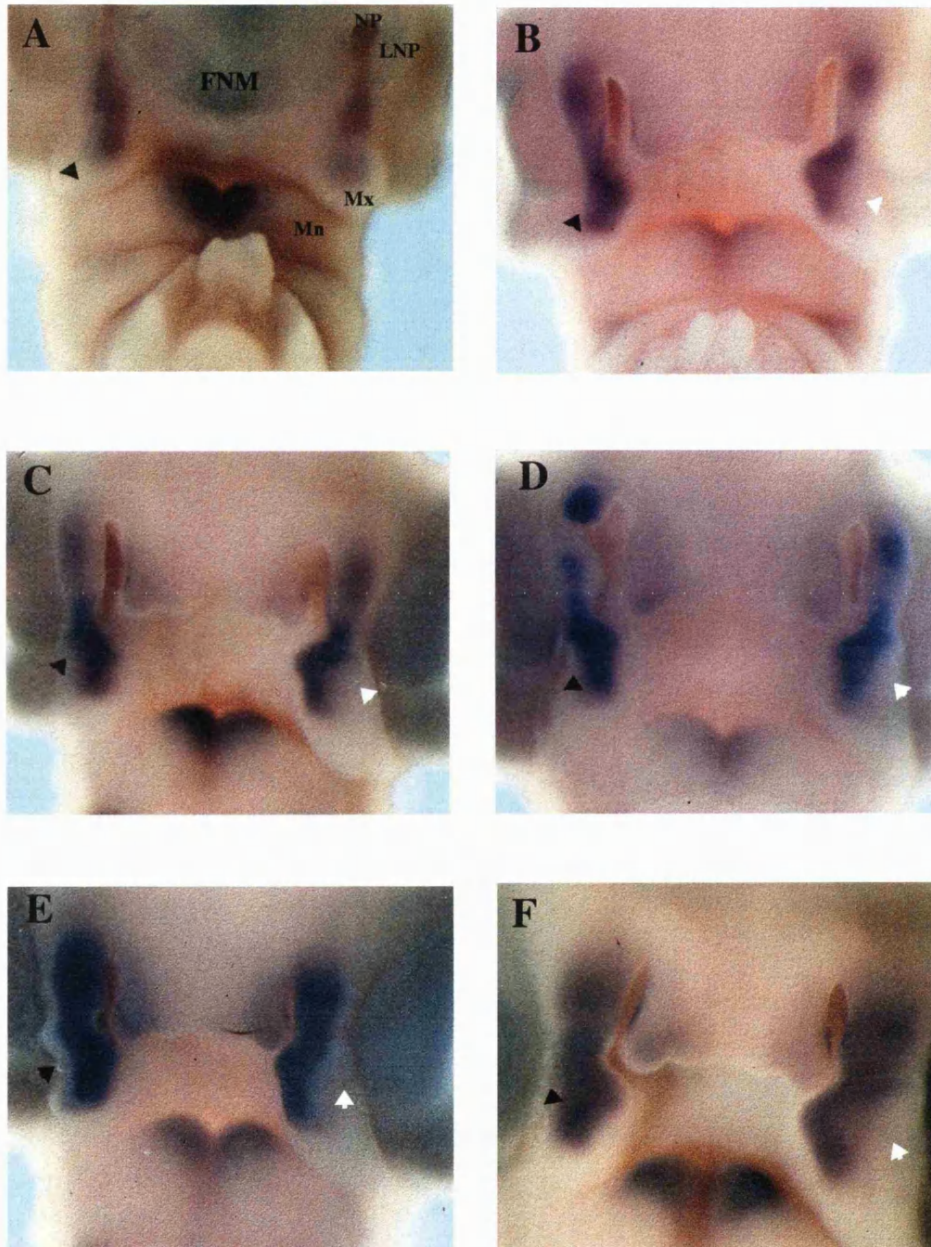
Figure 5.4 Expression of *Msx-1* in maxillary primordia after amputation and enzymatic removal of the ectoderm

A. Side view of the manipulated maxillary primordium, 4 hours after grafting of the maxillary mesenchyme. The piece of grafted mesenchyme has rounded up into a ball of tissue and can be clearly seen. *Msx-1* transcripts are expressed in a region of the grafted tissue, indicated by black arrowhead. Presumably this was the anterior part of the maxillary primordium before amputation. The rest of the grafted mesenchyme is free of *Msx-1* expression. *Msx-1* expression can be seen around the nasal pits in this embryo also.

B. Frontal view of chick embryo 12 hours after manipulation. The piece of grafted maxillary primordium mesenchyme can still clearly be seen, held by a platinum staple (black arrowhead). There is no expression of *Msx-1* in this tissue. *Msx-1* expression is seen in the anterior control maxillary primordium (right side of the face), in the distal tips of the mandibular primordium, throughout the lateral nasal process and at the distal tips of the frontonasal mass.

C. Frontal view of chick embryo 24 hours after manipulation. The graft can be seen as a small ball of tissue amalgamated into the posterior region of the maxillary primordium (black arrowhead). There is no *Msx-1* expression in this tissue. Expression of *Msx-1* is seen in the small amount of remaining maxillary primordium tissue, above the graft. However, there is clearly no contact between maxillary primordium and frontonasal mass as there is in the right, control side of this face. *Msx-1* expression is seen in the distal tips of the mandibular primordium, the anterior region of the control maxillary primordium, in the lateral nasal process and at the distal tips of the frontonasal mass.

Figure labels

NP: Nasal pit   Mn: Mandibular primordium

FNM: Frontonasal mass   LNP: Lateral nasal process

Mx: Maxillary primordium

Figure 5.4
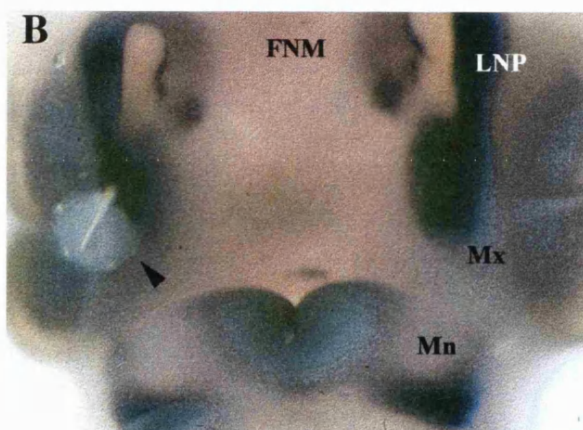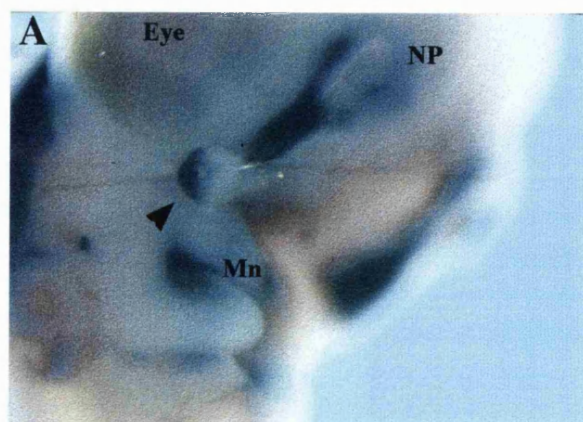
maxillary primordium. Again *Msx-1* was not expressed in this tissue (n=3 out of 3, Fig. 5.4C). Taken together, this set of experiments shows that a very small region of ectoderm is sufficient to maintain the entire region of *Msx-1* expression in the maxillary primordium and that some ectoderm is required to maintain the expression of *Msx-1* for more than 4 hours.

5.3.5 Effect of FGF upon *Msx-1* expression in the maxillary primordium.

FGFs are candidates for ectodermal signals which control outgrowth of the maxillary primordium (see section 5.4.1 above) as they have been shown to do in the limb (see section 5.1.2). Previous studies have shown that FGF induces and maintains the expression of *Msx-1* in the developing limb (Wantanabe and Ide 1993, Vogel *et. al.*, 1995). Surprisingly, application of FGF-2 to maxillary primordia, following ectoderm removal, did not enhance *Msx-1* expression but instead tended to decrease it. At 4 and 8 hours after ectoderm removal with Nile Blue Sulphate and FGF-2 application (n=3 for each time point) *Msx-1* expression in both the treated maxillary primordium and adjoining lateral nasal process was reduced compared to that in the contralateral control primordium (Fig. 5.5 A, B). This reduction in *Msx-1* expression on the right hand side of the face was more obvious 18 and 24 hours after treatment (n=3 for each time point) even if the bead was placed posterior to the *Msx-1* expressing region (Fig. 5.5C, D). 24 hours after ectoderm was removed from the maxillary primordium by Nile Blue Sulphate, *Msx-1* expression was also reduced in the frontonasal mass (Fig. 5.5D).

I also investigated whether FGF-2 could rescue *Msx-1* expression in the maxillary primordium, when the ectoderm was completely removed and mesenchyme repined onto the face. Four hours after total ectoderm removal and application of a bead soaked in FGF-2, expression of *Msx-1* transcripts was not seen in the grafted mesenchyme (Fig. 5.6A). This differed to the result found in the same experiment but without FGF application, where expression was still found in the graft at this time point (see above and Fig. 5.4A). At 12 and 24 hours after FGF-2 application there was, again, no *Msx-1* expression in the grafted mesenchymal tissue (Figs. 5.6B, C). This result indicates that FGF appears to abolish expression of *Msx-1* transcripts in the maxillary primordium both

Figure 5.5 Effect of FGF upon *Msx-1* expression in the maxillary primordium after ectoderm removal with Nile Blue Sulphate.

Manipulated primordia are on the left side of the face.

A. Frontal view of chick embryo face, 4 hours after removal of ectoderm from the maxillary primordium with Nile Blue Sulphate and application of FGF. Levels of expression of *Msx-1* in the manipulated maxillary primordium, indicated by black arrowhead, are slightly reduced but the domain of expression is similar to the control primordium on the right side.

B. Frontal view of chick face, 8 hours after ectoderm was removed from the maxillary primordium, with Nile Blue Sulphate, at stage 24, and application of FGF. The domain of *Msx-1* expression in the manipulated maxillary primordium, indicated by black arrowhead, seems smaller in this embryo compared to the control primordium on the right side of the face. The FGF soaked bead has fallen out during the *in situ* hybridisation procedure but the platinum staple that held it can be clearly seen.

C. Frontal view of chick face, 18 hours after ectoderm removal and FGF application. There is a stricking reduction in the level of *Msx-1* expression in the manipulated maxillary primordium and also the lateral nasal process which had not been treated, both indicated by arrowheads. Control levels and domains of expression can be seen on the right side of the face. The FGF soaked bead can be seen positioned quite posteriorly in this embryo, indicated by black arrow.

D. Frontal view of chick face, 24 hours after ectoderm removal and FGF application. There is a clear reduction in the level of *Msx-1* expression in the maxillary primordium, lateral nasal process and frontonasal mass (indicated by black arrowhead) on the left side of the face. The left primordium was manipulated, and the FGF soaked bead can be clearly seen, indicated by black arrow. The left lateral nasal process and frontonasal mass had not been manipulated but still showed a reduction in the levels of *Msx-1* expression.

Figure labels

NP: Nasal pit   Mn: Mandibular primordium

FNM: Frontonasal mass   LNP: Lateral nasal process

Mx: Maxillary primordium

Figure 5.5
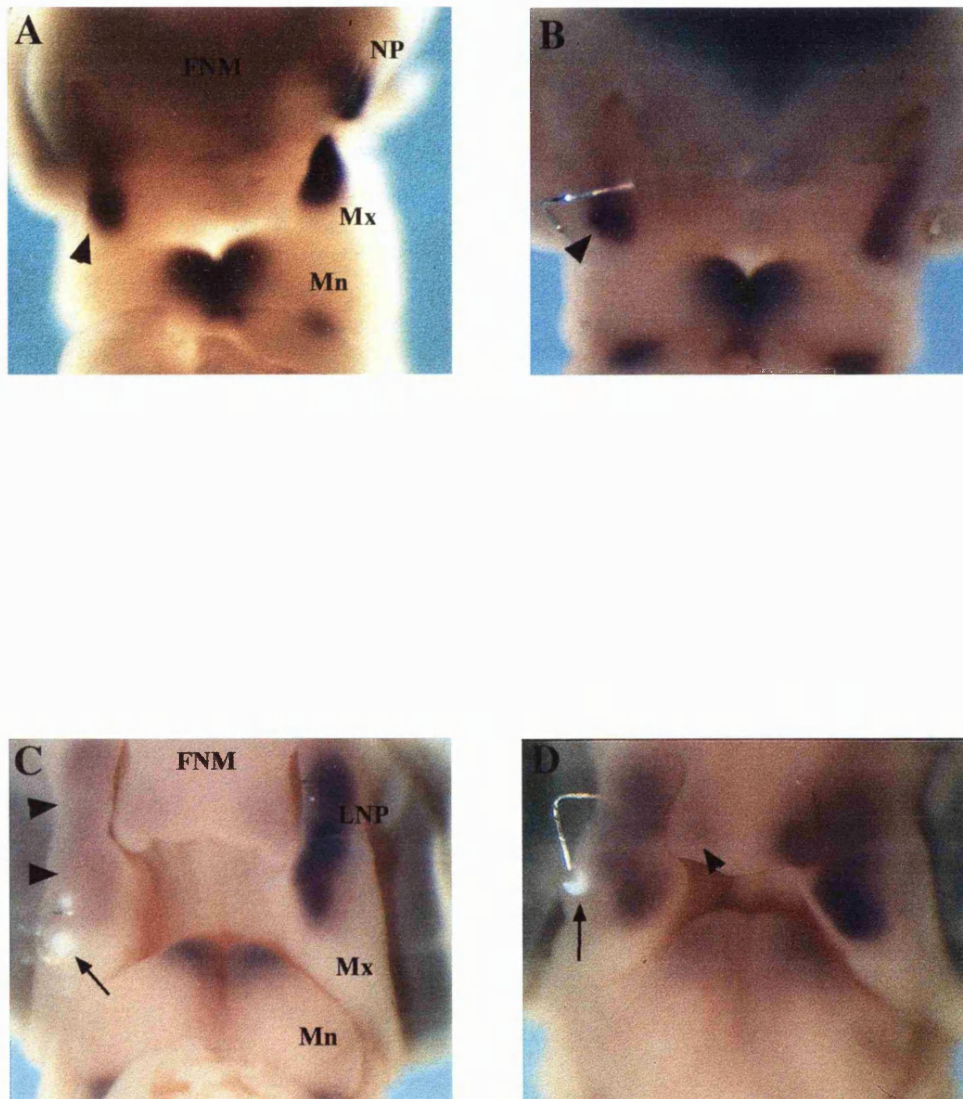
Figure 5.6 Expression of *Msx-1* in maxillary primordium after amputation, enzymatic removal of the ectoderm and application of FGF

Treated maxillary primordia, in all cases, are on the left side of the picture.

A. Side view of a chick embryo head, 4 hours after manipulation at stage 24. The grafted maxillary primordium, FGF soaked bead and platinum staple are indicated by black arrow. There is no *Msx-1* expression in this tissue. Compare this with Figure 5.4A, in which maxillary primordium mesenchyme, grafted in the same way, but without application of FGF expresses *Msx-1* transcripts.

B. Frontal view of chick embryo face 12 hours after manipulation at stage 24. The piece of grafted mesenchyme, held by platinum staples is positioned posteriorly in this embryo. There are clearly no *Msx-1* transcripts expressed in this tissue. Expression of *Msx-1* can be seen in remainder of the original maxillary primordium above the mesenchymal graft.

C. Frontal view of chick embryo face, 24 hours after manipulation at stage 24. The grafted maxillary mesenchyme, with platinum staples and FGF bead can clearly be seen in this embryo, indicated by black arrow. The grafts seems to have undergone some growth, compare with Figure 5.4 where FGF was not applied. However, *Msx-1* transcripts are not expressed in this tissue.

D. Side view of embryo shown in C. The bead soaked in FGF can be seen at the top of the graft, indicated by black arrow. This also shows that the graft has grown out considerably.

Figure labels

NP: Nasal pit   Mn: Mandibular primordium

FNM: Frontonasal mass   LNP: Lateral nasal process

Mx: Maxillary primordium

Figure 5.6
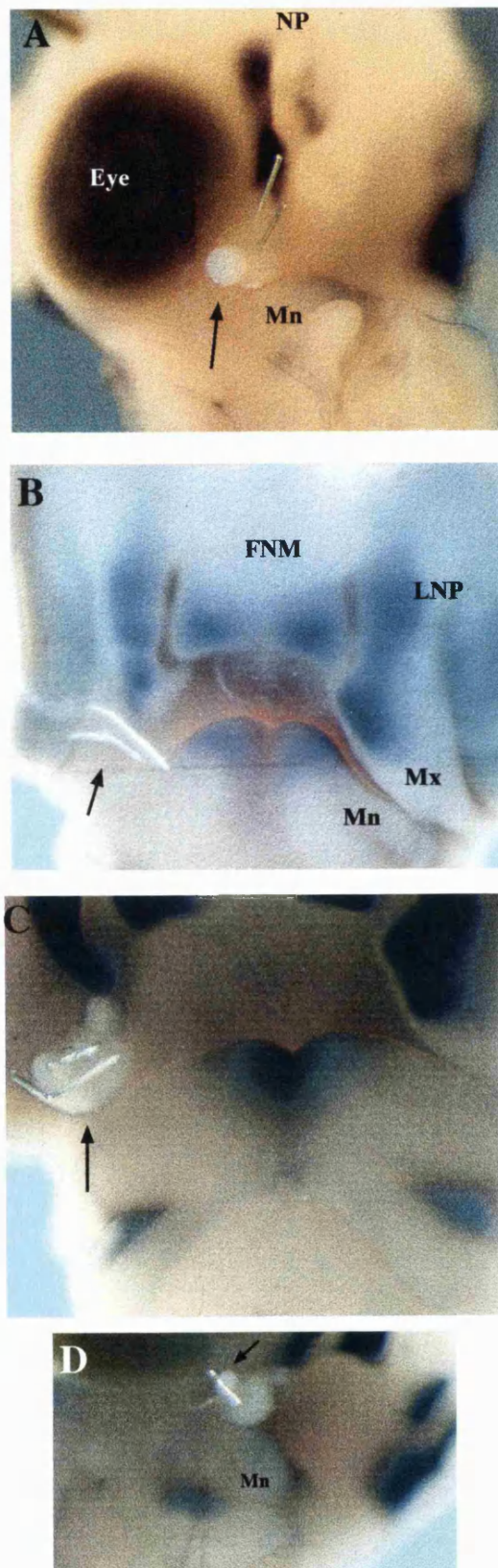
in the presence and absence of ectoderm. It is interesting to note that in this set of experiments, unlike experiments with ectoderm removed by Nile Blue Sulphate, the effect of FGF expression was confined to the maxillary primordium and we saw no effect on expression in frontonasal mass or lateral nasal process.

Taken together these data, from both sets of experiments, indicate that, although FGF can maintain outgrowth of maxillary primordia, it does not appear to be acting by maintaining mesenchymal expression of *Msx-1*.

5.3.5 The affect of BMP-4 on outgrowth of the maxillary primordium

Members of the Bone Morphogenetic Protein family (BMPs) are expressed in the ectoderm of the chick facial primordia (Francis - West *et. al.*, 1994, Wall and Hogan, 1995). BMP-2 and BMP-4 have been shown to increase mesenchymal proliferation and induce the formation of ectopic bone in chick mandibular primordia (Barlow and Francis-West 1997). To investigate whether BMPs have an affect on outgrowth in addition to differentiation of maxillary mesenchyme, ectoderm was removed *in ovo* using Nile Blue Sulphate and beads soaked in BMP-4 stapled to the mesenchyme. Outgrowth and extension were measured as before (Table 5.5, Graph 5.5, appendix 9).

At early time points, outgrowth of the treated maxillary primordium was no different to that of controls. However at 8 hours after treatment, outgrowth was noticeably reduced in the treated primordium and this difference subsequently increased with time. Statistical analysis (Students t-test) showed that there was initially no difference in the means of the treated and control populations, but after 18 hours incubation, outgrowth was significantly less in the treated population ($p<0.5$). It should be noted however, that the outgrowth of the primordium without ectoderm, but treated with BMP-4 was greater than primordia with no growth factor treatment (Graph 5.6). This indicates that, like maxillary primordia with ectoderm removed, outgrowth does not increase greatly up to stage 28 (24 hours after treatment. Thus the slope of the graph is flat. In comparison unmanipulated primordia and manipulated primordia treated with either FGF-2 or FGF-4 increase growth and have a steeper curve. This would suggest that BMP-4 has a short term ability to

Table 5.5 Mean anteroposterior extension (AP) and proximodistal outgrowth of maxillary primordia with intact ectoderm (control) and after ectoderm removal and BMP-4 application (treated).

Time after ectoderm removal (hours).	Number in data set (n).	Area of ectoderm removed (μm) (AP x PD).		Control - Mean ± S.D. (μm).		Treated - Mean ± S.D. (μm).	
				Length (AP)	Width (PD)	Length (AP)	Width (PD)
4	3	999 ± 92	498 ± 21	958 ± 132	601 ± 23	958 ± 132	601 ± 23
8	4	965 ± 64	529 ± 33	1237 ± 101	675 ± 72	1244 ± 110	608 ± 54
12	4	1037 ± 126	485 ± 54	1250 ± 96	685 ± 44	1250 ± 96	619 ± 25
18	4	1129 ± 159	584 ± 24	1335 ± 43	705 ± 32	1367 ± 75	643 ± 30
24	5	973 ± 96	521 ± 40	1747 ± 104	795 ± 60	1742 ± 109	642 ± 53

Graph 5.5 Outgrowth (P-D) and extension (A-P) of maxillary primordiua with intact ectoderm and after ectoderm removal with Nile Blue Sulphate and application of BMP-4

Legend:
- Increase in proximodistal outgrowth, unmanipulated
- Increase in proximodistal outgrowth, manipulated
- Increase in anteroposterior extension, unmanipulated
- Increase in anteroposterior extension, manipulated

Y-axis: Increase in size (μm)
X-axis: Time (hours)

$*P < 0.5$

169
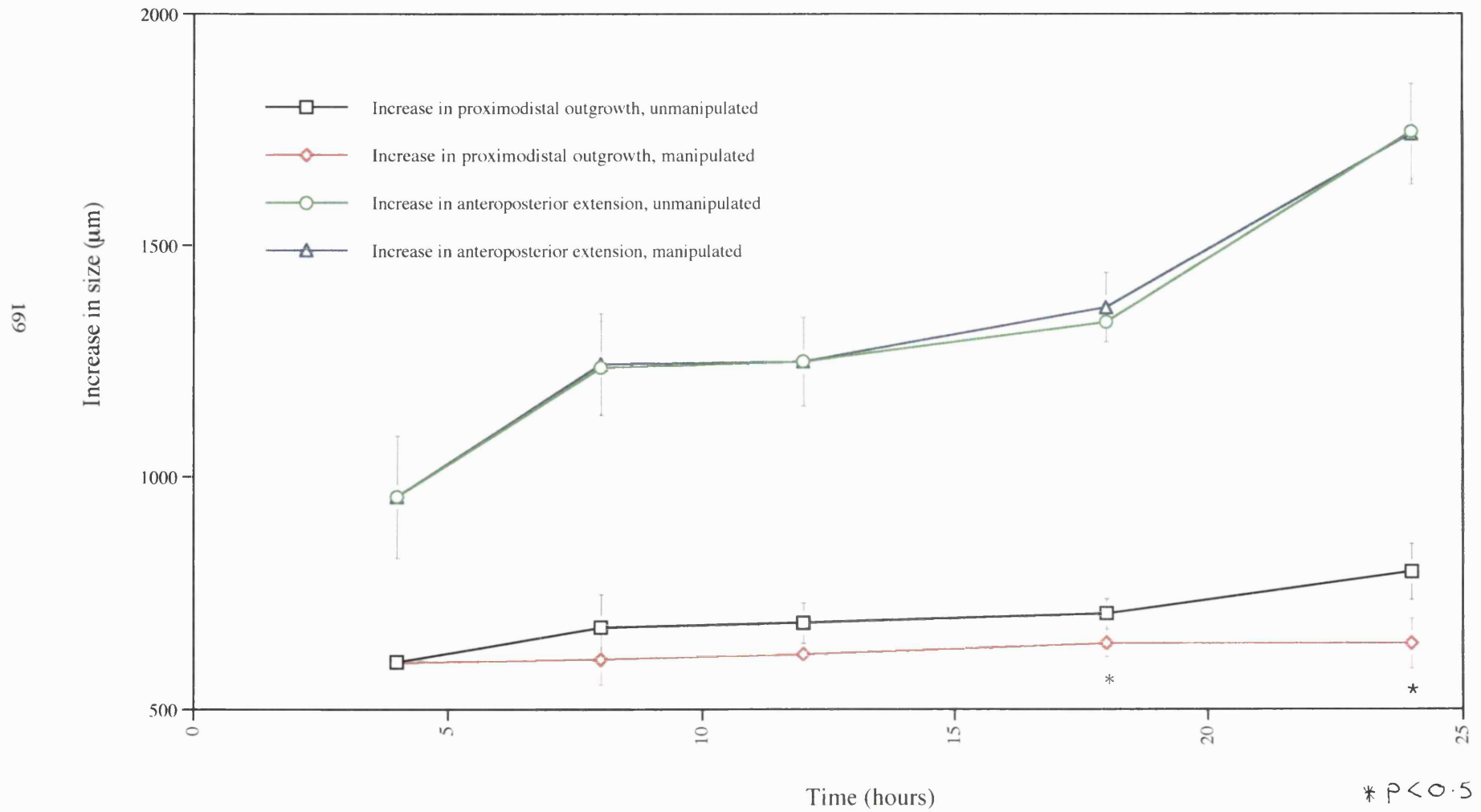
Graph 5.6 Summary of outgrowth of maxillary primordium after ectoderm removal and after ectoderm removal and treatment with either FGF-2, FGF-4 or BMP-4

Increase in outgrowth (µm)

1200

1000

800

600

400

□ Unmanipulated primordium outgrowth, experiment 5.1

◇ Outgrowth after ectoderm removal

○ Outgrowth after ectoderm removal + FGF-2

△ Ectoderm removal + FGF-4

✳ Ectoderm removal + BMP-4

0   10   20   30   40   50

Time (hours)

170

* p<0.5
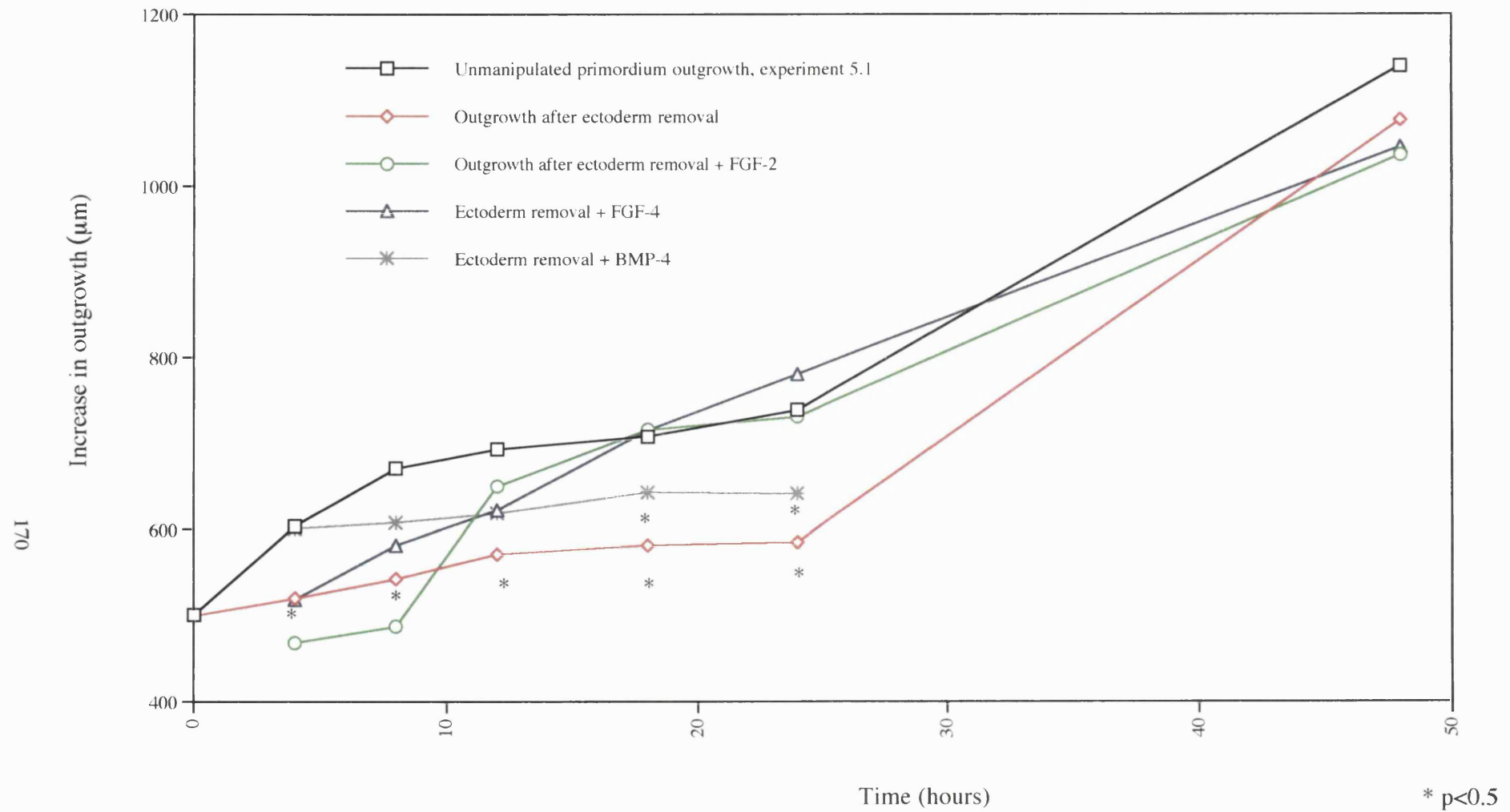
maintain outgrowth, but unlike FGFs, cannot fully maintain outgrowth of maxillary primordia over an extended period of time.

5.3.6 BMP-4 induces *Msx-1* expression in the maxillary primordium

It has recently been shown that the activity of Bmp-4 is mediated by *Msx-1* in many developmental systems such as epidermal induction in *Xenopus* embryos (Suzuki *et. al.*, 1997) and in development of facial bones in chick embryos (Barlow and Francis -West, 1997). Although BMP-4 cannot totally maintain outgrowth of the maxillary primordium, after the ectoderm has been removed, it leads to partial rescue and it is possible that this could be mediated by mesenchymal *Msx-1*. Therefore I investigated the affects of Bmp-4 on *Msx-1* expression in the maxillary primordium after ectoderm removal *in ovo* by Nile Blue Sulphate. At all time points tested (4, 8, 16, 24 hours) the level of *Msx-1* expression, i.e. the abundance of *Msx-1* transcripts, and the size of the *Msx-1* expression domain was increased in treated maxillary primordia. At earlier time points, expression was extended both posteriorly and laterally so that the whole of the treated maxillary primordium expressed *Msx-1* (Figs. 5.7A, B). At later time points (Figs. 5.7C, D) expression of *Msx-1* was extended proximally but not posteriorly. These domains of expression in the treated primordia tended to be wider than in the contralateral control primordium, even though outgrowth was reduced. Thus *Msx-1* expression   appeared to · span the whole width of BMP-4 treated primordia. However, gaps between maxillary primordia and frontonasal mass were still seen on the manipulated side of the face of these embryos at later stages (Fig. 5.7D). Expression of *Msx-1* in the lateral nasal process and frontonasal mass seemed unaffected in treated embryos.

To investigate whether BMP-4 can maintain expression of *Msx-1* in maxillary primordia when the ectoderm had been totally removed, maxillary primordia were amputated as before, treated with trypsin and repined onto a stump of a maxillary primordium with a bead soaked in BMP-4. Four hours after treatment, the whole of the grafted maxillary mesenchyme expressed low levels of *Msx-1* transcripts (n=3) (Fig. 5.8A). However at later time points the levels of *Msx-1* in the graft appeared to progressively decrease so that at 12 hours, there were very low levels of *Msx-1*

Figure 5.7 Expression of *Msx-1* in the maxillary primordium after ectoderm removal, with Nile Blue Sulphate, and application of BMP-4

Treated maxillary primordia are on the left side of the face in each figure.

A. Frontal view of stage 24 chick face, 4 hours after treatment. A considerable increase in *Msx-1* expression and extension of the expression domain occurs, indicated by the white arrow head, so that the whole maxillary expresses *Msx-1*. The contralateral control primordium (black arrowhead) shows expression in the anterior region only. The bead soaked in BMP-4 can be seen in the left maxillary primordium, indicated by white arrow.

B. Frontal view of chick embryo, 8 hours after manipulation. The domain of *Msx-1* expression is extended in the left maxillary primordium, as indicated by white arrowhead. Normal expression pattern is indicated in the right maxillary primordium (black arrowheads).

C 16 hours after manipulation. At this time point, increase in *Msx-1* expression tended to be confined to proximal regions, rather than posterior. White arrow head indicates proximal extension of *Msx-1* on treated maxillary primordium. Black arrowhead indicates proximal regions do not express *Msx-1* in untreated primordia.

D. 24 hours after manipulation. Similar to the above, the domain is expanded proximally but not posteriorly. White arrowheads indicate treated primordium, black arrowheads indicates control primordium.

Figure labels

NP: Nasal pit   Mn: Mandibular primordium

FNM: Frontonasal mass   LNP: Lateral nasal process

Mx: Maxillary primordium

Figure 5.7
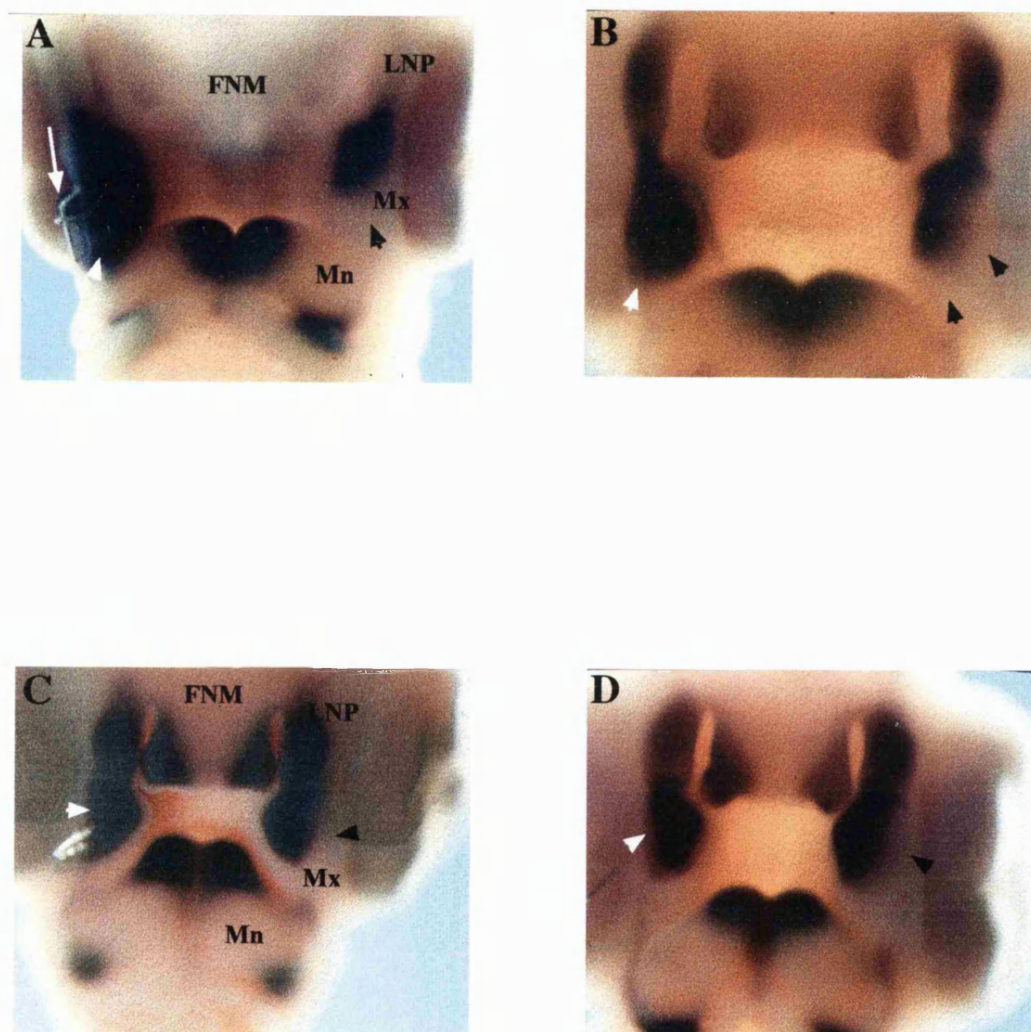
Figure 5.8 Expression of *Msx-1* in the maxillary primordium mesenchyme after amputation, enzymatic ectoderm removal, re-grafting and application of BMP-4

A. Side view of a stage 24 embryo after manipulation and BMP-4 application. Low levels of *Msx-1* expression are seen throughout the grafted tissue, indicated by black arrow. Expression can be seen as normal in the remainder of the maxillary primodium not removed, above the grafted mesenchyme, and in the distal tips of the mandibular primordium.

B. Side view of face 12 hours after manipulation and application of BMP-4. The grafted mesenchyme, with platinum staple, can be seen in the posterior region of the maxillary primordium, indicated by black arrow. There is very low level *Msx-1* expression in the graft. Expression can also be seen in the remainder of the maxillary primordium above the graft.

C. Side view of face 24 hours after manipulation and application of BMP-4. The graft with platinum staple is indicated by black arrow. Expression can be seen at the periphery of the graft but the centre of the tissue does not express *Msx-1* transcripts.

Figure labels

NP: Nasal pit   Mn: Mandibular primordium

FNM: Frontonasal mass   LNP: Lateral nasal process

Mx: Maxillary primordium

Figure 5.8
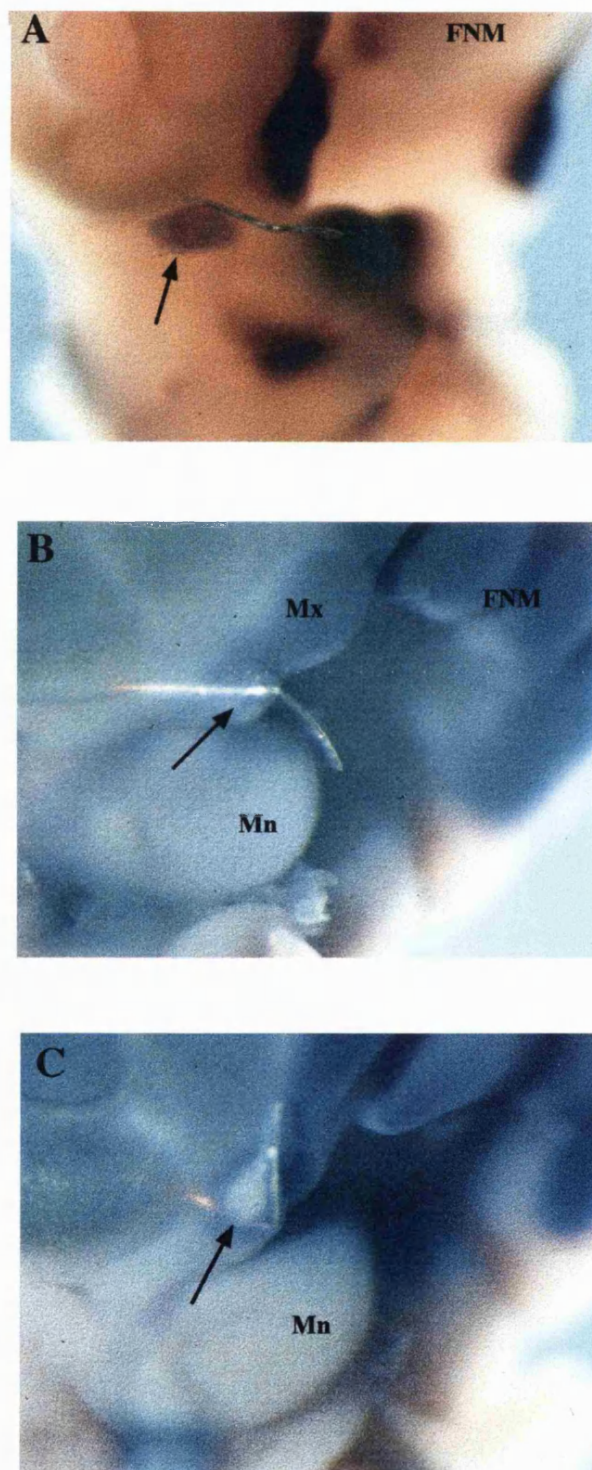
Figure 5.9 Expression of *Msx-1* in maxillary primordium after application of BMP-4 in the presence of an intact ectoderm

Treated maxillary primordia are on the left hand side in each figure.

A. Frontal view of chick face 4 hours after application of BMP-4 at stage 24. The domain of *Msx-1* expression has spread to the proximal edge of the treated maxillary primordium and also to the posterior edge, near to the mandibular primordium, indicated by black arrowhead. White arrowhead indicates the contralateral control maxillary primordium with no *Msx-1* expression posteriorly or proximally.

B. Frontal view of chick face 12 hours after BMP-4 application. *Msx-1* expression has spread proximally and posteriorly in the treated maxillary primordium, indicated by black arrowhead. Control primordium indicated by white arrowhead.

C. Frontal view of chick face 24 hours after application of BMP-4. *Msx-1* expression is only seen in the region of the bead, indicated by black arrowhead and there is only a small amount of proximal extension compared to the control primordium.

Figure labels

Mn: Mandibular primordium   Mx: Maxillary primordium

FNM: Frontonasal mass   LNP: Lateral nasal process

Figure 5.9
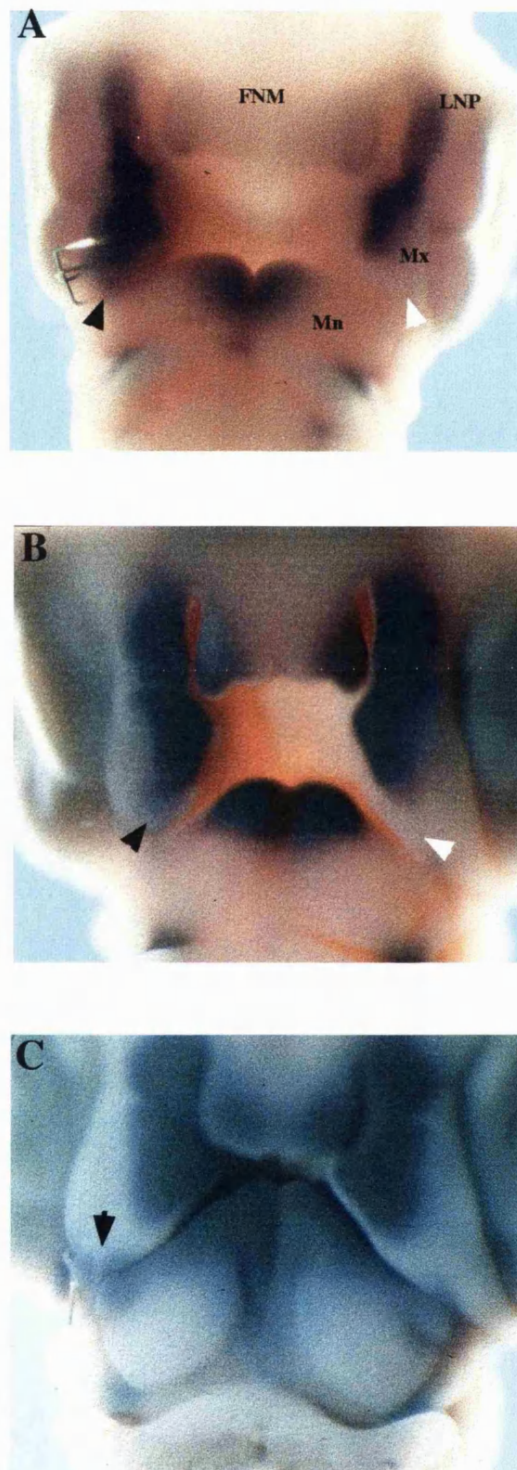
expression in the grafted mesenchyme (Fig. 5.8B). 24 hours after manipulation, only the periphery of the graft expressed *Msx-1* (Fig. 5.8C).

In view of the different effect of BMPs on maxillary primordia at later time points, depending on whether ectoderm is totally or partially removed, we explored the effects of BMP on maxillary primordium with completely intact ectoderm. The induction of expression of *Msx-1* by BMP-4 in maxillary primordia was found, in general, to follow a similar time course and pattern in the presence of an intact ectoderm to that found when most of the ectoderm was removed with Nile Blue Sulphate. 4 hours after manipulation, the *Msx-1* expression domain extended posteriorly and proximally (Fig. 5.9A) so that almost the entire maxillary primordium was expressing *Msx-1* transcripts. At later time points, 12 hours, the posterior spread was less (Fig. 5.9B). At 24 hours after BMP-4 application, only the tissue surrounding the bead showed increased *Msx-1* expression.

These findings indicate that, in the presence of a small region of ectoderm i.e. when ectoderm had been removed by Nile Blue Sulphate, the expression of *Msx-1* was increased and the domain expanded by application BMP-4 over a long period of time. However when all ectoderm is removed BMP-4 can only maintain *Msx-1* over a short period of time. This would suggest that an unknown ectodermal factor works in concert with BMP-4 to maintain long term *Msx-1* expression in the facial primordia.

5.3.7 Expression of *Eph4A* In Facial Primordia Between Stages 20 and 28.

Another gene which appears to be expressed in an overlapping pattern with *Msx-1* in the developing face is*Eph4A* (*Cek-8*) (Sajjadi and Pasquale, 1993). At stage 20 and 24, *Eph4A* transcripts were uniformly distributed throughout the maxillary primordium, restricted to distal edges of medial regions in the paired mandibular primordia and widespread throughout the lateral nasal process (Figs. 5.10A, B). In the frontonasal mass, expression of *Eph4A* transcripts was weak at stage 20, confined to the lateral distal edge, close to the nasal pit. There was also very little expression seen at stage 24 (Fig. 510B). Sections indicate that *Eph4A* was expressed in both mesenchyme and ectoderm of mandibular, maxillary primordia and lateral nasal process but only in the ectoderm of the

frontonasal mass at stage 23/4 (Fig. 5.10C). By stage 28, *Eph4A* expression in maxillary primordia became distally restricted and stronger anteriorly, near the frontonasal mass, than posteriorly, near the junction with the mandibular primordium (Fig. 5.10D). The lateral nasal process exhibited weak expression in the region adjacent to the nasal pits. The band of expression along the distal edge of the frontonasal mass was slightly stronger than in previous stages, mainly at the distal edges, close to the nasal pits. In mandibular primordia, *Eph4A* expression was seen in two broad domains with a sharp curved boundary, extending along the proximodistal axis, at some distance from the midline (Fig. 5.10D). Sections indicate that expression has become totally mesenchymal in the maxillary and mandibular primordium and lateral nasal process at stage 28 (Figs. 5.10E, F) and both ectodermal and mesenchymal expression was detected in the frontonasal mass (Fig 5.10E, F).

5.3.8 Patterns of *Eph4A* Expression in the Maxillary Primordium After Ectoderm Removal

To investigate whether mesenchymal expression of *Eph4A* transcripts depends on ectodermal signalling, ectoderm was removed from stage 24 embryos with Nile Blue Sulphate and processed for *in situ* hybridisation with the chick *Eph4A* RNA probe. Initially (t=0 hours), the levels and extent of *Eph4A* transcripts in treated primordia were similar to those in control primordia (Fig 5.11A). However, 4 hours after ectoderm removal, *Eph4A* transcripts were almost absent from the mesenchyme of the manipulated maxillary primordium (Figs. 5.11B, C, compare with contralateral controls Figs. 5.11.B, D, n=2 in each case). Typically, only a small patch of expression was seen at the anterior distal tip corresponding to the region where ectoderm tended to persist after stripping with Nile Blue Sulphate (Fig. 5.10 B, C indicated by black arrowheads). At 8 and 12 hours post treatment, when outgrowth of manipulated maxillary primordia was clearly reduced, (n=2 and 3 respectively) mesenchymal *Eph4A* expression was still reduced proximally while distally, expression was more normal (Figs. 5.11E, G, compare with contralateral controls on Figs. 5.11F, G respectively). By 18 hours post treatment (approximately stage 27) (n=2), mesenchymal expression of *Eph4A* was more extensive but still weaker

176

than normal. At 24 hours, the maxillary primordium was notably smaller and a gap between primordia forming the primary palate was noted (Fig. 5.11H, indicated by black arrowhead).

5.3.9 FGF maintains expression of *Eph4A* but does not induce it.

Eph4A is also expressed in overlapping patterns with *Msx-1* in the developing chick limb i.e. predominant expression is in the posterior distal mesenchyme. Removal of the AER also results in reduction of *Eph4A* (*Cek-8*) expression, similar to that seen in the maxillary primordium. Application of FGF after AER removal maintains *Eph4A* expression in the limb mesenchyme (Patel *et. al.,* 1996). To investigate whether FGF can maintain expression of *Eph4A* in maxillary primordia, the ectoderm was removed *in ovo* with Nile Blue Sulphate and a bead soaked in FGF-2 stapled in its place and processed for whole mount *in situ* hybridisation with the *Eph4A* RNA probe at various time points after treatment (n=2 for each time point). In every case, abundant *Eph4A* transcripts were seen in the maxillary primordium (Figs. 5.12A-C, 4, 12 and 24 hours after application respectively) and the primary palate formed as normal. Thus, unlike *Msx-1*, *Eph4A* expression in the chick maxillary primordium can be maintained by application of FGF.

In the developing limb, it has also been shown that application of FGF-2 to non *Eph4A* expressing mesenchyme results in ectopic induction of expression. To investigate whether FGF can similarly induce *Eph4A* expression in a region of facial mesenchyme which does not normally express *Eph4A* transcripts, a bead soaked in FGF-2 was placed under the ectoderm of the lateral mandibular primordium at stage 20 and 24. Embryos were examined either at 4 or 24 hours after treatment but ectopic expression of *Eph4A* was not observed at either time point (Figs. 5.13A-D).

5.3.10 Expression of *Eph4A* in facial primordia after retinoic acid treatment.

Application of retinoic acid to chicken embryos is known to cause clefting of the primary palate (Tamarin *et. al.,* 1984, Wedden 1987, Richman and Delgado 1995) and reduction of *Msx -1* expression in upper beak primordia (Brown *et. al.,* 1997). To investigate whether *Eph4A* expression is also reduced when clefting occurs, beads soaked

in 1, 5, or 10mg/ml retinoic acid were placed in the right nasal pit at stage 20 and the embryos then incubated for various periods of time. Control embryos were administered DMSO only. Treatment with 1mg/ml or 5mg/ml retinoic acid produced no detectable change in the pattern of *Eph4A* expression after 4 hours incubation (n=6) compared with controls. However, embryos incubated with 10mg/ml retinoic acid showed a slight reduction in *Eph4A* expression in the lateral nasal process near to the nasal pit, (Fig. 5.14A) n=5. By 12 hours, levels of *Eph4A* expression in the lateral nasal pit were clearly reduced (Fig. 5.14B) n=6 even with low doses of retinoic acid. Control embryos showed no change in Eph4A expression (Fig. 5.14C). 24 hours after application, when a marked morphological defect in the facial primordia could readily be detected, expression of *Eph4A* transcripts in anterior maxillary primordium was also reduced, particularly with higher concentrations of retinoic acid (Fig 5.14D). Reduced expression of *Eph4A* was observed in these regions until at least stage 28 when a cleft of the primary palate could also be observed(Fig. 5.14E) n=3. Control embryos showed no reduction of expression in the distal maxillary primordium or frontonasal mass nor did they exhibit clefting of the primary palate (Fig 5.14F). Embryos treated with different concentrations of retinoic acid at stage 24, a stage at which facial clefting is no longer induced by retinoic acid, showed no change in *Eph4A* expression at any time point. Thus retinoic acid leads to a rapid reduction in *Eph4A* expression and this reduction in *Eph4A* is correlated with clefting of the primary palate.

Figure 5.10 Expression of *Eph4A* in the chick face between stages 20 and 28

A. Expression of *Eph4A* in the stage 20 chick facial primordia. Abundant transcripts can be seen throughout maxillary primordium and lateral nasal process, at distal edges of mandibular primordium and at distal edges of frontonasal mass, next to the nasal pits.

B. Expression of *Eph4A* in the chick face at stage 24. Abundant transcripts can be seen throughout the maxillary primordium and lateral nasal process as in the previous stage. Expression is also seen at the distal tips of the mandibular primordium, in a broader domain than seen in the previous stage. Low levels of *Eph4A* expression can be seen at the distal edges of the frontonasal mass, particularly next to the nasal pits.

C. Frontal frozen section (15µm) of stage 24 chick embryo head, sectioned after whole mount *in situ* hybridisation with *Eph4A* riboprobe. Expression can be seen in both mesenchyme and epithelia of maxillary primordium. lateral nasal process and mandibular primordium. Low levels of expression can be seen in ectoderm of frontonasal mass.

D. Frontal view of stage 27/8 embryo. *Eph4A* transcripts are localised to distal edges of maxillary primordium. Expression in the lateral nasal process is much weaker than at previous stages. Expression in the mandibular primordium has extended spaning the proximodistal axis. Expression in the frontonasal mass is still only seen at distal edges.

E. Frontal frozen section of stage 28 chick head after hybridisation with *Eph4A* riboprobe. Expression can be seen localised to the distal edge of the maxillary primordium. Expression in the lateral nasal process is very weak an confined to the mesenchyme. Expression in the mandibular primordium is also mesenchymal, whlie frontonasal mass expression appears to be in both mesenchyme and ectoderm.

F. High power view of frontal frozen section of stage 28 chick head hybridised with *Eph4A* riboprobe. This shows clearly that *Eph4A* transcripts are localised to mesenchyme at this stage. Arrowhead indicates epithelium.

Mn: Mandibular primordium	Mx: Maxillary primordium
FNM: Frontonasal mass	LNP: Lateral nasal process
NP: Nasal pit	

Figure 5.10
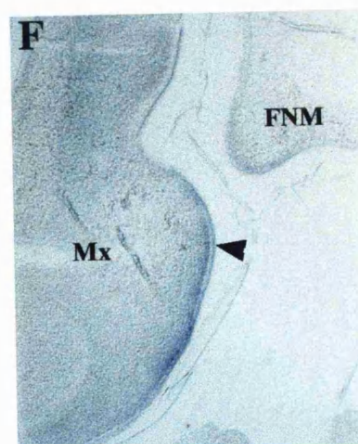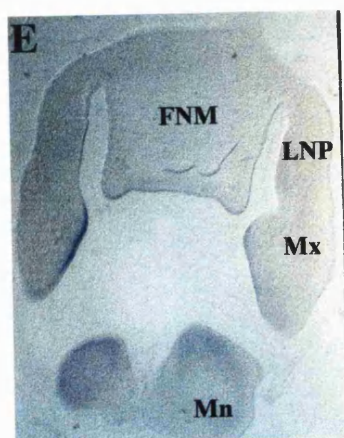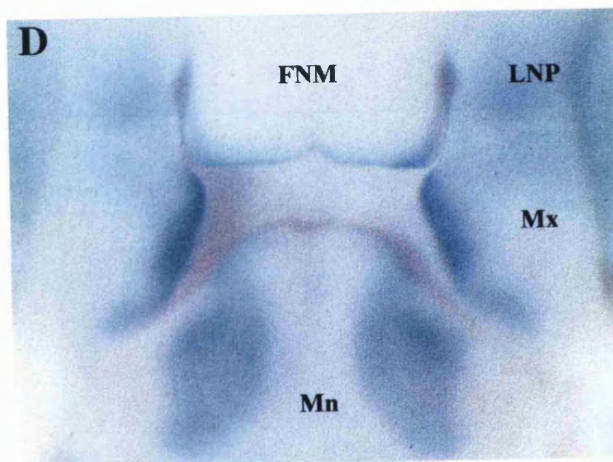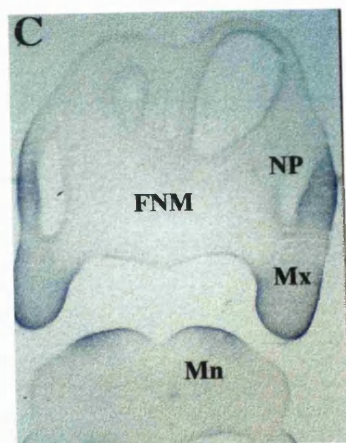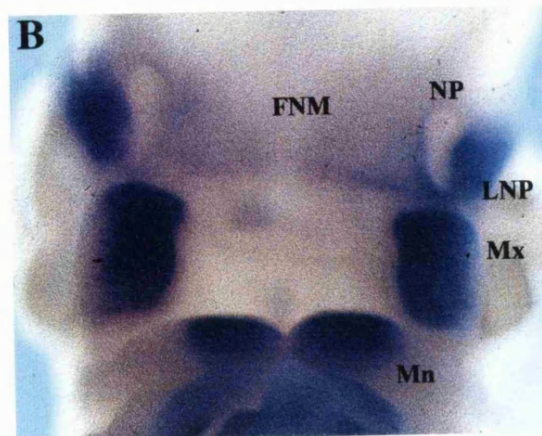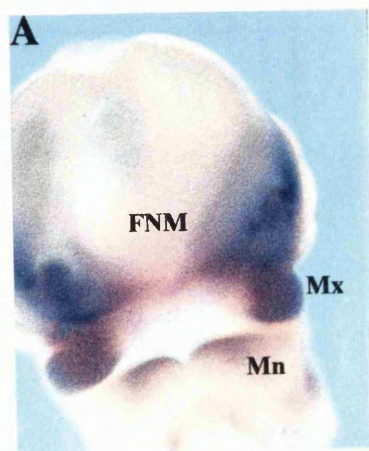
Figure 5.11 Expression of *Eph4A* in the maxillary primordium after ectoderm removal with Nile Blue Sulphate

A. Frontal view of stage 24 chick embryo immediately after removal of ectoderm. Treated primordium is on left. Expression of *Eph4A* is seen throughout the primordium, similar to the untreated maxillary primordium, right side of the figure.

B. Frontal view of chick face 4 hours after ectoderm removal. Expression of *Eph4A* is reduced in left (treated) maxillary primotrdium. Transcripts are seen in the anterior distal edge at low levels. Abundant *Eph4A* transcripts are seen in untreated (right) primordium.

C. Side view of chick embryo 4 hours after ectoderm removal. Level of *Eph4A* transcripts has been much reduced by removal of ectoderm, typically with only small patches of expression at the distal edges.

D. Side view of untreated embryo at stage 24. This shows normal, abundant expression of *Eph4A* throughout the maxillary primordium.

E. Side view of chick face, 12 hours after ectoderm removal at stage 24. *Eph4A* transcripts can be seen at the distal edge of the primodium. However more proximal regions show no expression of *Eph4A,* as indicated by blackarrowhead.

F. Side view of stage 26 chick embryo, untreated. This shows abundant *Eph4A* transcripts are expressed throughout the maxillary primordium at this stage.

G. Frontal view of chick embryo approximately stage 27, 24 hours after ectoderm removal. This shows quite abundant *Eph4A* transcripts in the maxillary primordium, concentrated towards the distal edge, as would be seen normally at this stage. Thus as the ectoderm has re-grown, *Eph4A* expression is as normal.

H. Frontal view of chick embryo face, 24 hours after ectoderm was removed from maxillary primordium. In this example, there is a clear gap between the maxillary primordium and frontonasal mass, (black arrowhead), while primordia are almost touching on control side. This indicates, although in general, the expression of *Eph4A* returns to normal at this stage, outgrowth has not fully recovered.

Figure labels

Mn: Mandibular primordium   Mx: Maxillary primordium

FNM: Frontonasal mass   LNP: Lateral nasal process

Figure 5.11
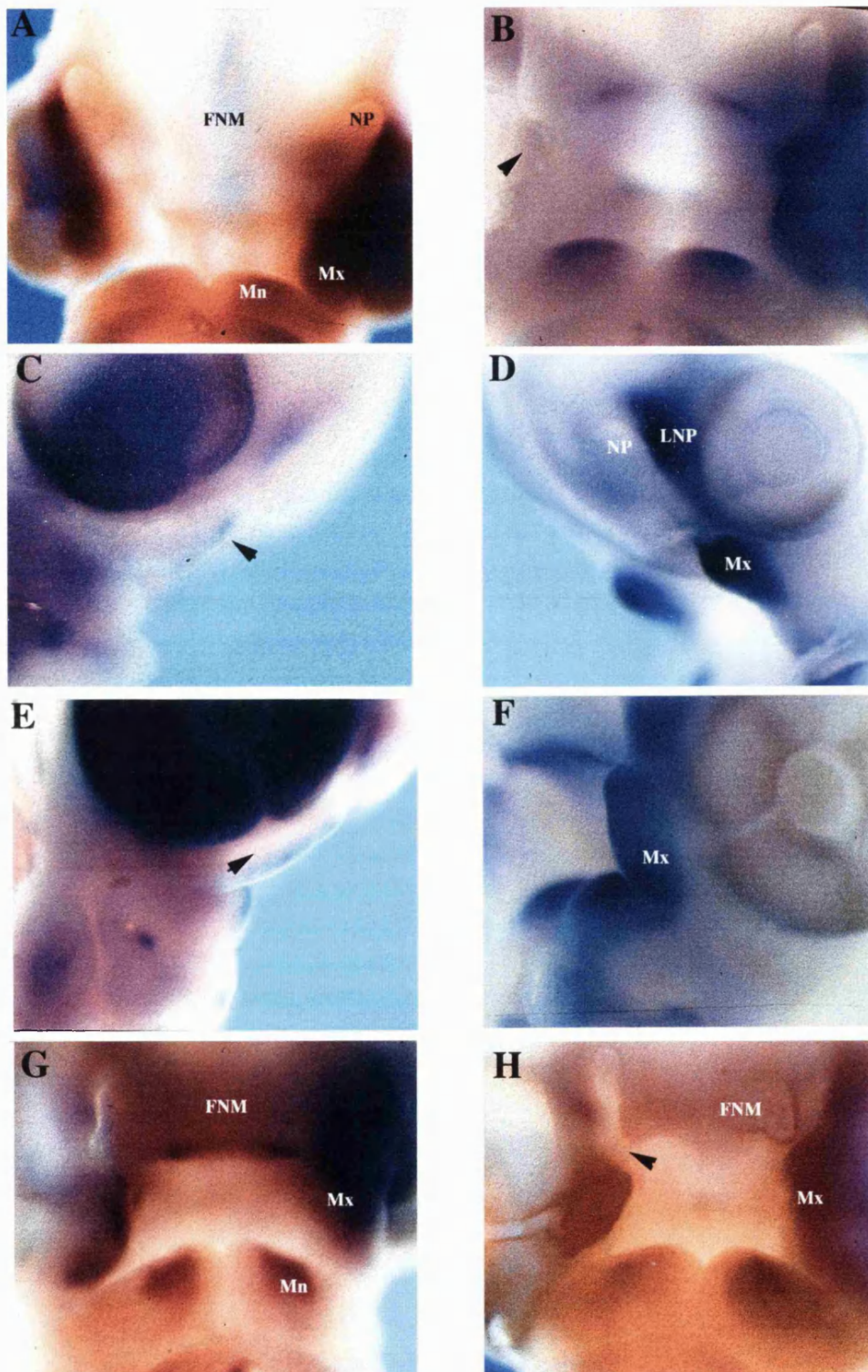
Figure 5.12 Expression of *Eph4A* in the maxillary primordium after removal of ectoderm with Nile Blue Sulphate and application of FGF

A. Frontal view of stage 24 chick embryo face, 4 hours after manipulation and application of FGF. Abundant *Eph4A* transcripts can be seen throughout the left maxillary primordium even though the ectoderm has been removed.

B. Side view of chick embryo head, 12 hours after manipulation and FGF treatment. Transcripts of *Eph4A* can be seen expressed throughout the primordium, even though the bead soaked in FGF was placed in the posterior region of the primordium.

C. Front view of chick embryo face, 24 hours after manipulation and FGF application. Eph4A transcripts are expressed, particularly at the distal edge of the maxillary primordium at this stage. The maxillary primordium and frontonasal mass have met to form the primary palate, as indicated by white arrow head.

Figure labels

Mn: Mandibular primordium   Mx: Maxillary primordium

FNM: Frontonasal mass   LNP: Lateral nasal process

NP: Nasal pit

Figure 5.12
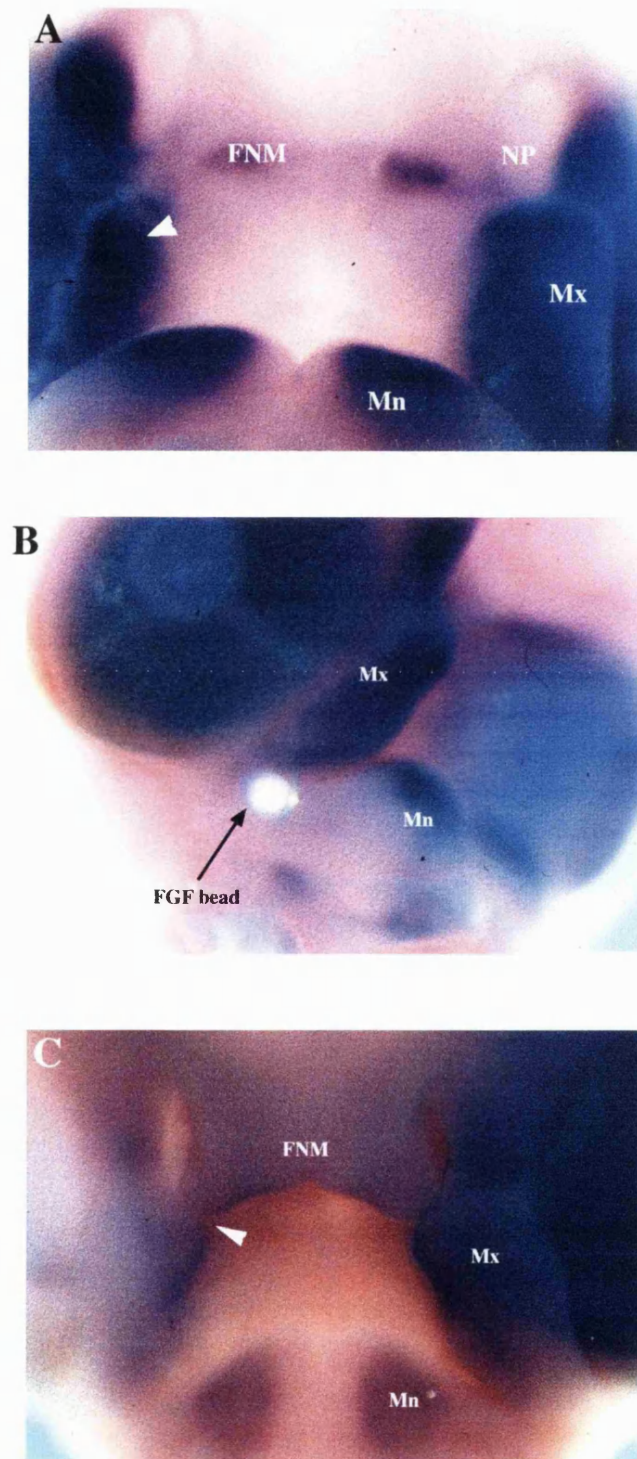
Figure 5.13 FGF application does not induce expression of *Eph4A* transcripts mandibular primordium

A. Side view of stage 21 chick embryo, 6 hours after application of FGF in the mandibular primordium. Abundant *Eph4A* transcripts can be seen in the maxillary primordium and lateral nasal process at this stage.The bead soaked in FGF can be seen in the mandibular primordium, close to the edge of the maxillary primordium, as indicated by black arrow. There are no *Eph4A* transcripts expressed in this region.

B. Opposite side of stage 21 chick embryo head as in the above picture. Abundant *Eph4A* transcripts can be seen in the maxillary primordium and frontonasal mass, as before. White arrowhead indicates that there are no *Eph4A* transcripts in the lateral mandibular primordium.

C. Side view of chick embryo face, 20 hours after FGF application to the mandibular primordium at stage 20. The bead soaked in FGF can be seen in the lateral mandibular primordium, as indicated by black arrow. However, there is no expression of *Eph4A* around the FGF bead.

D. Opposite side of chick head in the above picture. There are no *Eph4A* transcripts in the lateral mandibular primordium, as indicated by white arrowhead.

Figure labels

Mn: Mandibular primordium   Mx: Maxillary primordium

FNM: Frontonasal mass   LNP: Lateral nasal process

Figure 5.13
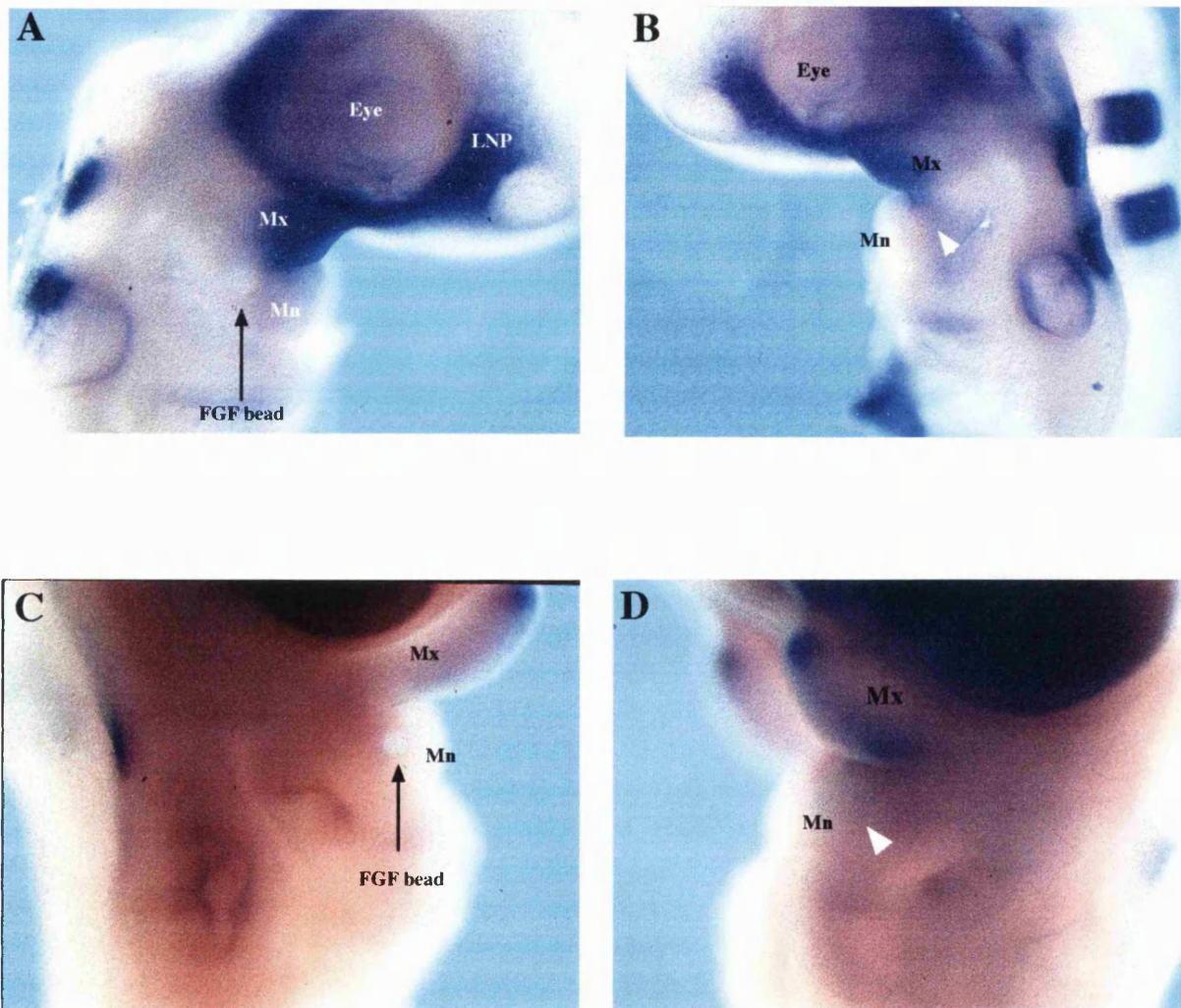
Figure 5.14 Expression of *Eph4A* in chick facial primordia after treatment with retinoic acid.

A. Frontal view of chick embryo face 4 hours after application of 10mg/ml retinoic acid at stage 20. Bead soaked in retinoic acid in the left nasal pit (black arrow). Expression of *Eph4A* transcripts in lateral nasal process are reduced (white arrowhead). Expression in right lateral nasal process is abundant (black arrowhead).

B. Frontal view of chick embryo face 12 hours after application of 1mg/ml retinoic acid at stage 20. Retinoid soaked bead in left nasal pit (black arrow). *Eph4A* expression is reduced in lateral nasal process next to the bead, (white arrowhead). Expression in contralateral control primordium is normal, (black arrowhead).

C. Frontal view of chick embryo face 12 hours after a bead soaked in DMSO was placed in nasal pit at stage 20. Expression of *Eph4A* in the left lateral nasal process is abundant and at similar levels to the control primordium (right side of the figure).

D. Frontal view of stage 24 chick embryo, 24 hours after application of 10mg/ml retinoic acid. Bead soaked in retinoic acid in left nasal pit, (black arrow). Changes in morphology are apparent. Treated nasal pit is wider and shorter than normal and maxillary primordium has become round. Expression of *Eph4A* is reduced in lateral nasal process, at the base of the nasal pit and in anterior regions of maxillary primordium (white arrowheads). Control primordia show abundant *Eph4A* expression in these regions (black arrowheads).

E. Frontal view of stage 28/9 chick embryo face, 48 hours after treatment with 1mg/ml retinoic acid at stage 20. Left nasal pit has not formed and frontonasal mass has failed to fuse with maxillary primordium, resulting in primary palate cleft (black arrow). Expression of *Eph4A* is reduced in anterior maxillary primordium (white arrowhead). Expression in frontonasal mass is also reduced (black arrow). There is no expression in left lateral nasal process. In control primordium, *Eph4A* expression is seen in tissues which have apposed to form the primary palate (black arrowhead).

F. Stage 28/9 control chick embryo head. Expression of *Eph4A* is seen in the distal edge of frontonasal mass, distal edges of maxillary primordium and regions where these primordia form the primary palate. Expression is seen in mandibular primordia also.

Figure 5.14

Scale bar = 1000μm
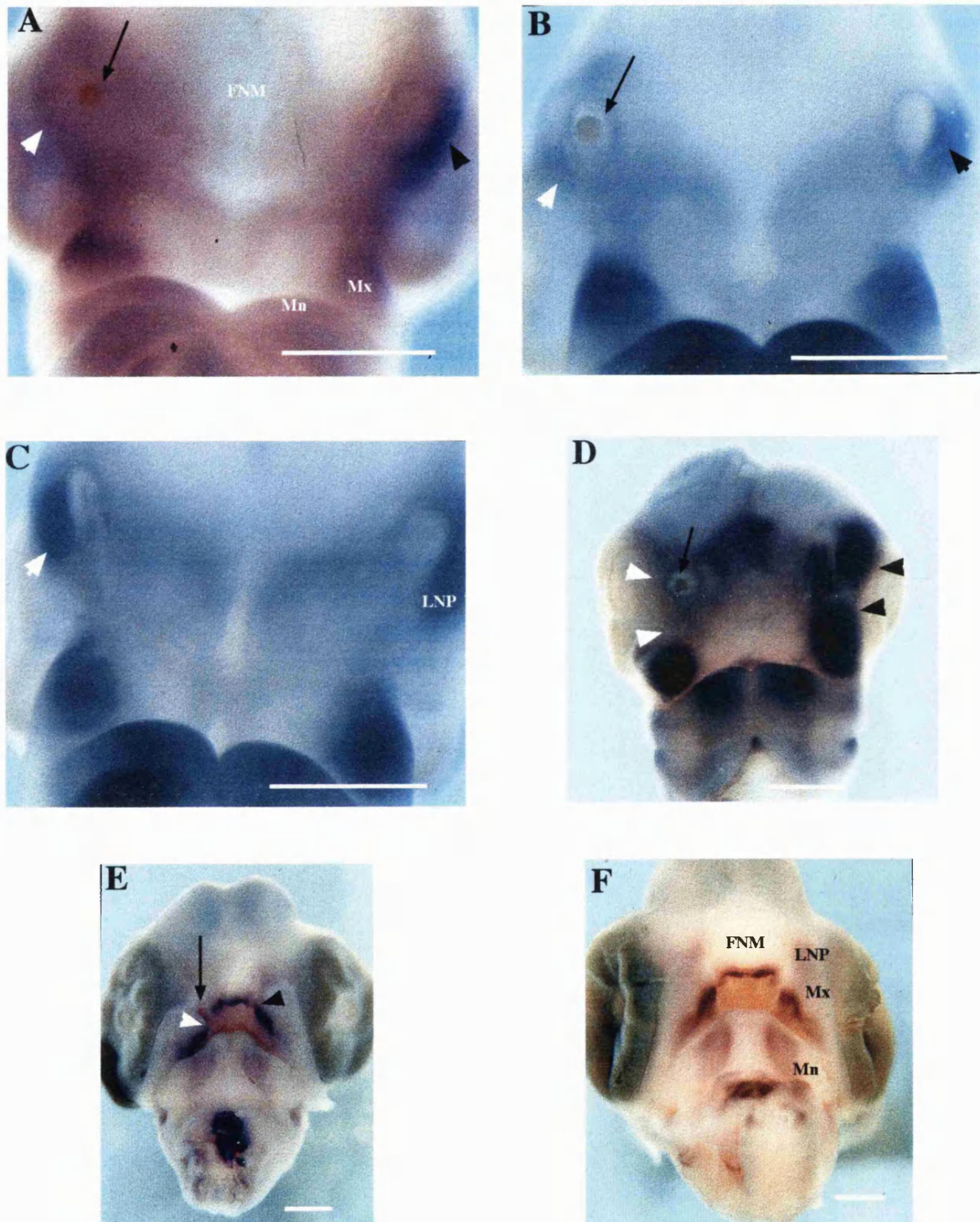
5.4 DISCUSSION.

5.4.1 Ectoderm is required for shaping and outgrowth of maxillary primordia

Previous work has shown that epithelial - mesenchymal interactions are important for the control of outgrowth and cell differentiation in developing facial primordia, (Wedden and Tickle 1986, Wedden 1987, Richman and Tickle 1989). In these experiments, pieces of facial primordia were removed and grafted onto the dorsal surface of a wing bud either with or without epithelium. This grafting method was used due to the lack of a removable, recognisable ectodermal signalling centre controlling outgrowth in facial primordia such as that seen in the developing limb bud (the AER) (Saunders 1948, Summerbell *et. al.,* 1973). These experiments showed that outgrowth and shaping of facial primordia, although a property of the mesenchyme, required an intact ectoderm. However, full outgrowth of mandibular primordium and frontonasal mass could not be recapitulated in the grafting system and outgrowth of the maxillary primordium could not be established at all even in the presence of ectoderm, instead forming a ball of tissue (Richman and Tickle 1989). As the maxillary primordium does not grow out or extend in isolation, it would appear that tension forces, which are normally exerted upon the maxillary primordium from other facial primordia, play a major role in shaping this primordium. A possible problem with the grafting method is that grafts of facial primordia mesenchyme are exposed to signals present in the dorsal ectoderm and mesenchyme of the limb bud, such as FGF-2 which has been shown to be concentrated in dorsal limb bud ectoderm and mesenchyme at the stages used for graft hosts (Savage *et. al.,* 1993) and which can initiate and promote outgrowth (Fallon *et. al.,* 1994, Cohn *et. al.,* 1995).

In our experiments, by chemically removing the ectoderm *in ovo,* with Nile Blue Sulphate, we have isolated the mesenchyme of the maxillary primordium without removing endogenous tension forces exerted upon it and without subjecting it to exogenous signalling molecules. This resulted in reduced outgrowth while there was no effect on the extension of the primordium. This shows that the outgrowth of the maxillary primordium is dependent on the presence of ectoderm. The fact that there was no effect on

the extension of the primordium in our system at any time lends weight to the idea that extension is governed by tension forces exerted by other primordia.

Within 24 hours of manipulation, there were noticeable gaps between the maxillary primordium and frontonasal mass, in the region where they join to form the primary palate, while in control embryos these primordia were already in contact. This shows the vital role that ectoderm plays in formation of the primary palate by promoting outgrowth. Scanning electron micrographs of embryos, after application of Nile Blue Sulphate, show that the removal of ectoderm is extensive but not always complete. Thus even partial ectoderm removal is sufficient to reduce outgrowth of the maxillary primordium and cause retardation in formation of the primary palate. However after 24 hours (stage 27+) outgrowth of treated primordia were not significantly different to controls and it was observed that formation of the primary palate had occurred in manipulated embryos. Scanning electron micrographs indicated that after removal of maxillary primordium ectoderm, with Nile Blue Sulphate, there was full re-growth of the ectoderm within 24 hours of treatment. The presence of a complete ectoderm 24 hours after treatment correlates with increase in outgrowth of maxillary primordia in manipulated embryos. This does not, however, explain how the manipulated primordium appear to "catchup" with the unmanipulated contralateral primordium and form normal primary palates. A hypothesis for this may be that in the normal maxillary primordium, a relatively high rate of outgrowth is maintained until contact is made with the frontonasal mass, at the time of primary palate formation, after which it begins to decrease. Thus in the manipulated primordium, after ectodem has regrown, the rate of outgrowth would remain sufficiently high to allow contact to be made with the frontonasal mass, after which it would return to normal. Growth curves constructed from my data indicate that there is an increase in the rate of outgrowth in the normal, unmanipulated, maxillary primordium at the time of primary palate formation and that in the treated primordium, the rate of outgrowth does exceed the control. However, previous studies have indicated that maxillary primordia experience a gradual decline in labelling indices i.e. proliferation between stage 24 and 30 (Minkoff and Kuntz 1977, 1978). In chapter 3, I indicated that processes other than cell proliferation contributed to expansion of cell populations, therefore cell intercalation may

play a role in maintaining outgrowth of the maxillary primordium. However, it would be interesting to investigate if there are changes in cell proliferation after ectoderm removal and regrowth in the maxillary primordia.

5.4.2 Growth factors and outgrowth of maxillary primordium.

Application of FGF-2 and FGF-4 protein fully restored outgrowth of the maxillary primordium after ectoderm had been removed. These effects of FGFs on outgrowth are not surprising, as three members of the *Fgf* family of proteins are now known to be expressed in facial primordia. FGF-2 protein has recently been shown, by immunohistochemistry, to be present at high levels in ectoderm of all facial primordia in chick embryos and at lower levels in mesenchyme (Richman *et. al.,* 1997), *Fgf-4* transcripts have been shown to be expressed in the ectoderm at the distal tips of the mandibular primordium in both mouse (Niswander and Martin 1992) and chick embryos (Barlow and Francis-West 1997), whilst *Fgf-8* transcripts are expressed in ectoderm overlying the edges of the nasal pits and at the join of mandibular and maxillary primordia in both chick and mouse embryos (Ohuchi *et al.,* 1994, Heikinheimo *et. al.,* 1994, Crossley and Martin 1995, Wall and Hogan 1995, Vogel *et. al.,* 1996). It would seem, from expression patterns in the maxillary primordium, that the most likely candidate for the endogenous ectodermal signal is FGF-2. The receptor FGFR1 is expressed ubiquitously throughout the maxillary primordia and FGFR2 and FGFR-3 are expressed in proximal and distal anterior regions of developing maxillary primordium respectively from stage 28 (Wilke *et. al.,* 1997). It has been shown that FGF-2 binds, with high affinity, to FGFR2c in vitro (Miki *et. al.,* 1992, Yayon *et. al.,* 1992, Ornitz and Leder, 1992). It has also recently been shown that FGF-2 has high mitogenic activity in cell lines transfected with FGFR1c and FGFR3c (Ornitz *et. al.,* 1996). Thus it would seem that FGF-2 may have activity with all the FGF receptors expressed in the maxillary primordium which lends weight to the idea of FGF-2 being the endogenous FGF in the maxillary primordium. Recently, the ability of FGF-2 and FGF-4 to restore outgrowth in mesenchyme of the frontonasal mass and mandibular primordium after grafting to the dorsal limb bud has been investigated (Richman *et. al.,* 1997). This study showed that

both FGFs improve the outgrowth of facial mesenchyme but do not fully restore it, even at high concentrations. It is possible that enzymatic digestion of the ectoderm, as used in the grafting system, destroys cell surface heparin sulphate proteoglycans which are required for binding of FGF proteins to receptors (Yayon *et. al.,* 1991) or CD44 which may be required to present FGF-2 to its receptors (Bennett *et. al.,* 1995), thus preventing full effect of the FGF protein.

BMP-4 was found to maintain outgrowth of the maxillary primordium for only a short time after ectoderm removal and it may be that FGFs and BMPs act together to maintain maxillary primordium outgrowth. BMP-4 and BMP-2 are expressed in the chick maxillary primordium between stages 24 and 28 and have been proposed to play a role in outgrowth (Francis-West *et al.,* 1994, see introduction section 5.1.4). Application of Bmp's to facial primordia results in a local increase in cell proliferation and ectopic bone formation (Barlow and Francis-West 1997). Although, in our experiments, application of BMP-4 to maxillary primordia after ectodermal removal could not fully restore outgrowth, we cannot total rule out the possibility that BMPs contribute to outgrowth.

Taken together, these data show that Fgf protein is likely to be an endogenous signalling molecule in the ectoderm of facial primordia which helps to control outgrowth of facial mesenchyme by interacting with FGF receptors. However, other factors such as tension forces, cell surface molecules or even other signalling molecules, such as BMPs, may also play an important role.

5.4.3 Signals from maxillary primordia ectoderm control *Msx-1* expression in mesenchyme.

It has also been shown that signals from ectoderm initiate and are required for maintenance of *Msx-1* expression in mesenchyme in the limb (Davidson *et. al.,* 1991 Robert *et. al.,* 1991, Coelho *et. al.,* 1991, Brown *et. al.,* 1993) and in the developing tooth (Vanio et. al., 1993). I hypothesised that a similar system of control may operate in the face. However, when maxillary primordium ectoderm was removed using Nile Blue Sulphate, the level of *Msx-1* expression in maxillary primordia mesenchyme was not reduced and possibly even increased and the expression domain actually expanded to the

proximal edge. This would suggest that the ectoderm is not required for *Msx-1* expression. It may even indicate that the ectoderm has a repressive influence on maxillary primordium *Msx-1* expression, particularly at the proximal edge. However, as noted in our previous experiments, this type of manipulation did not fully remove the ectoderm, typically leaving a patch of ectoderm on the distal anterior edge of the primordium which began to grow over the anterior distal part of the maxillary primordium as little as 2 hours after ectoderm was removed. It may be possible that signals from this patch of ectoderm are be sufficient to maintain *Msx-1* in the maxillary primordium. When all of the ectoderm was removed, by enzymatic digestion, not only did outgrowth and extension of the grafted mesenchyme fail but *Msx-1* expression was decreased within 12 hours. This is much less sensitive than in the limb, where Msx-1 expression is decreased within 2 hours of AER removal (Ros *et. al.,* 1992). This data would suggest that in facial primordia *Msx-1* expression is under the control of an ectodermal signal. It seems that the expression of *Msx-1* throughout the anterior maxillary primordia can be sufficiently maintained by the signal from a small piece of ectoderm at the distal edge of the primordium. This may also suggest that mesenchymal cell-cell interactions may be important for *Msx-1* expression as the mesenchyme can seemingly respond to ectodermal signals that may be situated at a distance from the expressing region. This could be further tested *in vitro* with epithelial - mesenchymal co cultures. In the limb, expression of *Msx-1* is maintained only near to the AER, not at a distance from it (Davidson *et. al.,* 1991, Brown *et. al.,* 1993).

5.4.4 *Msx-1* expression is not maintained by FGF in facial primordia

Removal of the ectoderm by Nile Blue Sulphate and application of a bead soaked in FGF-2 to the mesenchyme of the maxillary primordium resulted in a reduction of expression *Msx-1*, not only in the area surrounding the bead but also in other primordia. This is consistent with our previous observation that when ectoderm was removed from the maxillary primordium (thus removing FGF), expression increased suggesting that a repressive influence had been removed. The fact that *Msx-1* expression was also reduced

in neighbouring primordia would suggest that FGF can have a long range diffusible effect or that mesenchymal cell signalling may be "transmitting" the effect over a wide area.

When the ectoderm was totally removed by the amputation method we saw a very similar result. When an FGF2 bead was grafted with the mesenchyme, we saw an improved general growth of the tissue. However, we saw no expression of *Msx-1* transcripts at 4 hours, as we had in previous experiments. In contrast to the above experiment, the effect of FGF did not transmit to other nearby primordia which may reflect the fact that the primordia had been detached from the face.

Taken together these results would suggest that an ectodermal signal is likely to be maintaining *Msx-1* expression in the maxillary primordium, but that this signal is unlikely to be FGF-2. This is in direct contrast to the developing limb, where it has been shown that FGF -4 can maintain Msx-*1* expression in the mesenchyme (Watanabe and Ide, 1993, Vogel *et. al.*, 1995 see also introduction section 5.1.4). Thus, it is interesting to note that other studies have shown that there is a different capacity for limb and face ectoderm to maintain *Msx-1* expression in reciprocal grafts. Pieces of mouse facial mesenchyme grafted into the distal chick limb showed maintained *Msx-1* expression. However, in pieces of mouse limb mesenchyme grafted into the chick face, mesenchymal *Msx-1* expression was not maintained (Brown *et. al.,* 1993) indicating the possibility of a different ectodermal signal in the face. This implies, like our results, that *Msx-1* expression is under different control in the face and the limb. A recent study, in mouse embryos, has also indicated that there are two enhancer domains in the *Msx-1* gene. One promotes expression in the first branchial arch mesenchyme (maxillary and mandibular primordium) and nasal epithelium while the second promotes expression in the limb mesenchyme and many other tissues (Mackenzie *et. al.,* 1997). Thus it seems likely that *Msx-1* expression is maintained by different mechanisms in the face and in the limb.

5.4.5 BMP maintains Msx-1 expression in maxillary mesenchyme

Recent studies have also implicated members of the Bone Morphogenetic Protein (BMP) family of molecules in induction and control of expression of *Msx-1* and a highly related gene Msx-2 in tissues such as mouse dental mesenchyme (Vanio *et. al.*,) dorsal

1993

189

epithelia in *Xenopus* (Suzuki *et. al.,* 1997) and in subcutaneous cartilage (Wantanabe and Le Douarin 1996). *Bmp*'s are expressed in ectoderm overlying mesenchyme expressing *Msx-1* in the maxillary primordium (Barlow and Francis-West, 1997) and our results and Barlow and Francis-West (1997) show that application of ectopic BMP proteins to maxillary primordia can extend the domain of *Msx-1* expression. This shows that that BMPs induce *Msx-1* expression in the face. When ectoderm was removed either by Nile Blue Sulphate or by total amputation and BMP-4 applied, the level and extent of expression of *Msx-1* was maintained or increased. This result shows that BMP-4, normally expressed in the ectoderm, increases *Msx-1* expression in the mesenchyme. It is interesting to note that application of BMP-2 to the limb had no effect on Msx-1 expression (Patel *et. al.,* 1996) showing a further difference in the response of facial and limb mesenchymal *Msx-1* expression to growth factors.

Thus it seems that the ectoderm does control out growth of the maxillary primordium mesenchyme and this is likely to be through the action of FGF-2, although BMP-4 may also have some slight positive effect on outgrowth. *Msx-1* expression may be controlled by one or more signals of which BMP-4 is the most likely. It is interesting FGFs and BMPs seem to have an antagonistic effects upon *Msx-1* expression in the face. This is similar to an antagonistic activity between these two molecules in the developing limb where FGFs promote outgrowth and BMPs inhibit it (Niswander and Martin 1993).

5.4.6 *Eph4A* is expressed in regions of expansion of facial primordia and throughout the mesenchyme of the maxillary primordium

Transcripts of *EphA4,* are expressed extensively in tissues of the developing facial primordia between stages 20 and 28 of development. Expression is found particularly, but not exclusively, in mesenchymal regions which where found to expand the most during this period of development (see chapter 3, this thesis) namely the distal tips of mandibular primordia and around the nasal pits. In maxillary primordia, expression is initially seen throughout the primordium, but later is restricted to the distal tips. This expression pattern overlaps extensively with that of *Msx-1* in the face. This would suggest that *Eph4A* may have some role to play in the development of the face, although

this role is, as yet, not clear. Studies on the role of Eph receptors and their ligands in development implicate them cranial and trunk neural crest guidance (Wang and Anderson 1997, Smith *et. al.,* 1997) hindbrain segmentation (Xu *et. al.,* 1995) and fusion of the secondary palate (Orioli *et. al.,* 1996) indicating that they may be important molecules at many stages of face and head development from formation of neural crest to fusion.

5.4.7 *Eph4A* expression in the mesenchyme of the maxillary primordium is controlled by ectodermal FGFs

Our studies show that in the maxillary primordium, *Eph4A* expression is very rapidly reduced (within 4 hours) by removal of ectoderm with Nile Blue Sulphate. Expression returned in the mesenchyme in parallel with the regrowth of the ectoderm i.e. in a distal to proximal direction. Thus expression of *Eph4A* in the mesenchyme appears to be very sensitive to an ectodermal signal. These data also show that the ectoderm needs to be in direct contact with mesenchyme to maintain *Eph4A* expression. This is different to mesenchymal *Msx-1* expression in the maxillary primordium, which does not seem to require this direct contact. Expression of *Eph4A* has also been shown to require ectodermal signals in the developing limb as indicated by removal of the AER (Patel *et. al.,* 1996) although reduction in expression in this case was not as rapid as that seen in the face.

Application of FGF-2 protein to maxillary primordia after ectoderm removal resulted in maintenance of expression of *Eph4A* transcripts. This implies that FGF-2 is the endogenous signal in the maxillary primordium ectoderm that maintains *Eph4A* expression. Expression throughout the primordium was maintained by the bead. This suggests that diffusion of FGF from the bead is widespread in this case, as I have shown that expression of mesenchymal *Eph4A* directly require contact between ectoderm and mesenchyme (see section 5.4.9). FGF has also been shown to maintain *Eph4A* expression in the mesenchyme of the limb after removal of the AER, however expression was not maintained in all regions of the limb that expressed *Eph4A*, only those close to the FGF source (Patel *et. al.,* 1996).

When FGF beads were implanted into regions of the facial primordia that do not normally express *Eph4A* e.g. the lateral regions of the mandibular primordium, there was no ectopic expression of *Eph4A* transcripts. This suggests that either FGF alone cannot induce *Eph4A* expression and may simply act as a maintainance factor. However, it could also be that the cells in the lateral mandibular primordia are not competent to respond to FGF signal or are not competent to express *Eph4A* transcripts. It has been shown that *Eph4A* expression can be ectopically induced by FGF in non expressing regions of the limb but that there was a gradient of competency such that posterior-proximal mesenchyme could ectopically express *Eph4A* but that anterior-proximal could not (Patel *et. al.,* 1996). It would be interesting to investigate if there was a gradient of competency in the facial primordia.

These results indicate that mesenchymal expression of *Eph4A* in the face and in the limb are similarly controlled by the ectodermal signal FGF, although there are some differences in sensitivity to this signal. This is in contrast to *Msx-1* expression which I have shown is not controlled by similar mechanisms in the face and in the limb. Moreover, although *Eph4A* and *Msx-1* are expressed in overlapping patterns in the face they respond differently to signalling molecules so that *Eph4A* is maintained by FGFs whereas *Msx-1* is maintained by BMPs. It is interesting to note that application of BMP reduces Eph4A expression in the limb (Patel *et. al.,* 1996). It would be interesting to examine if this was also the case in the facial primordia. If so, it would indicate a further antagonistic activity between FGFs and BMPs in the developing face.

5.4.8 *Eph4A* expression is reduced in the facial primordia after treatment with retinoic acid.

Retinoic acid causes clefting of the primary palate in chick embryos (Tamarin *et. al .,* 1984, Wedden 1987) by causing failure of expansion of cell populations around the nasal pit (chapter 3 this thesis). *Eph4A* transcripts are expressed in regions of the face that are targets of retinoid action. Our data shows that the expression of *Eph4A* is reduced by teratogenic doses of retinoic acid in regions of facial primordia which fail to expand. This reduction is evident very rapidly, after four hours of treatment, before any morphological

defect is apparent. Interestingly, the reduced expression of *Eph4A* is first noted in the lateral nasal process, then in other primordia. The lateral nasal process is considerably flattened by retinoid treatment (Brown *et. al.,* 1997), thus a rapid reduction in *Eph4A* expression in this region may be having some effect on outgrowth. Similarly *Msx-1* has been shown to be reduced in similar regions of the facial primordia upon retinoic acid treatment, albeit not as rapidly (Brown *et. al.,* 1997). As I have shown in the experiments contained in this chapter, *Eph4A* and *Msx-1* are likely to be working in different signalling pathways. Thus it seems that retinoic acid could be affecting more than one signalling pathway in the face.

In light of evidence indicating that a functional inactivation of two Eph receptors - *EphB3* and *EphB2* results in clefting of the secondary palate (Orioli *et. al.,* 1996) which is due either to lack of outgrowth or fusion as the shelves have elevated, it is tempting to consider that *Eph4A* may normally play a role in outgrowth of facial primordia and/or in primary palate fusion and that reduction of expression may also be involved in retinoid induced clefting of the primary palate. Functional inactivation of the gene or introduction of retroviral vectors expressing dominant negative *Eph4A* receptors into the chick embryo may enable us to explore this question further.

Chapter Six - General Discussion

The general aims of this thesis were to investigate how four pairs of primordia shape and fuse to produce a face in the chick embryo. The mechanisms that I investigated were local expansion of cell populations, cell proliferation, cell death and cell intercalation. In turn, I proposed that local patterns of gene expression were responsible for these processes by encoding signalling molecules and transcription factors which influence cell behaviour. Abnormal shaping of facial primordia can lead to failure of fusion between primordia and the second major aim of this thesis was to investigate the cellular and molecular basis of this clefting.

6.1 Mechanisms that dictate shaping of the chick facial primordia

Development of the face can be considered in three phases. The first phase is the induction and migration of cranial neural crest cell populations into the ventral part of the developing head. The next phase consists budding, expansion, shaping and fusion of the primordia. The final phase involves differentiation and growth of tissues As indicated in chapter 1, phases one and three have been quite extensively investigated while phase two has largely been ignored. With the results of my investigations, I can now begin to propose some of the mechanisms by which the facial primordia shape during this phase of development.

My first specific aim was to establish how facial primordia change shape. I mapped the expansion characteristics of cell populations within each primordium to establish how this might drive the shaping of a primordia as a whole. DiI labelling of cell populations within individual primordia indicated that populations underwent non-uniform expansion, i.e. they expanded predominantly in one direction. Thus the direction of outgrowth of the whole primordium was governed by a few cell populations. Examination of the total

expansion of these populations indicated that some regions within a primordium expanded more than others. Thus each primordium acquired its characteristic shape through two types of cell behaviour- directed expansion within a cell population and local differences in expansion between cell populations.

Minkoff and co-workers had proposed that regional differences in cell proliferation between and within facial primordia was the underlying mechanism of shaping and fusion. They hypothesised that an increase in this regional difference, due to a decline in proliferation rate in one primordia, brought about the morphological changes in the facial primordia forming the primary palate (Minkoff and Kuntz, 1977, 1978, Minkoff 1984). The results of my studies have shown that regional differences in cell proliferation cannot account fully for local differences in expansion of cell populations. Cell death, cell intercalation and cell rearrangements, which have not previously been reported in the chick face, were found to play a part in maintaining regional differences in expansion. Cell death was found mainly in regions of low expansion and thus may act to reduce the size of those populations. Cell intercalation occurs in regions of high expansion and may act to magnify the size of the population. Thus, expansion of populations within a primordium, as shown by DiI labelling, is a combination of cell proliferation, cell death and cell intercalation. I propose that differences in local expansion, rather than just proliferation, underlie shaping of facial primordia.

The new observation that expansion of cell populations was directed has also given some insight into outgrowth of the facial primordia at these early stages of development. It had been observed that development of the frontonasal mass had much in common with development of the limb. Micromass cultures of stage 24 frontonasal mass mesenchyme produce sheet-like patterns of cartilage, similar to those found with micromass cultures of the progress zone mesenchyme from limb buds (Wedden *et. al.,* 1986, Archer *et. al.,* 1984). Other facial primordia produce different patterns of cartilage development in culture. Removal of the apical ectodermal ridge of the limb results in limb truncation, removal of ectoderm from the frontonasal mass results also in truncation (Wedden 1987, Richman and Tickle 1992). Wedden (1986) also proposed that a region of the ectoderm overlying the frontonasal mass was thickened, similar to the AER of the limb. Our studies

clearly demonstrate that the driving force of outgrowth in the frontonasal mass is not at the distal edge of the primordium as seen in the limb, but in more proximal regions, near the nasal pit. Thus one might look for growth promoting activity, similar to that seen in the AER of the limb bud, in the ectoderm covering this region, or even in the epithelia lining the nasal pit itself. Maxillary primordia grow out from the distal edge, particularly anteriorly and mandibular primordia grow out from the midline distal tip. Thus the latter two primordia have more in common with outgrowth in the limb.

My observations of cell expansion and movement in regions of fusion have confirmed many previous studies. My results indicate that two merging mesenchymal populations expand more than surrounding populations, as also suggested by Minkoff (1980). Different patterns of mesenchymal cell movement were found at different points of fusion. Some of these patterns had been observed by Patterson *et. al.*, (1984) however, some were also new. Thus some cell populations - the mandibular and maxillary primordia and the maxillary primordium and frontonasal mass merged together across the fusion point, exhibiting bi-directional movement. This had not previously been reported. In other cases, uni-directional movement across the fusion point was observed. Some cell populations did not move or merge at all. These cell activities are also important for shaping by establishing and maintaining fusion between adjacent primordia.

Thus in chapter 3, I established the basic cellular behaviour which produces shaping and fusion of facial primordia. But how are these cell behaviours controlled? The next specific aim was to understand how these cell behaviours were initiated and coordinated and this was further investigated in chapters 4 and 5. I proposed that the expression of genes, such as *Msx-1* and *Fgf-8*, specifically in regions of greatest expansion and fusion influenced cells to exhibit these behaviours. These genes were found to be expressed in regions of predominant expansion. Moreover, *Msx-1* and *Fgfs* are known to be important for craniofacial development through functional inactivation studies and/or human syndromes arising from mutations in these genes (see general introduction, chapter 1). This suggests that these genes do control important functions in facial development. To examine co-ordination of cell behaviour more specifically, I expanded my investigations to the function of a different type of signalling - cell-cell signalling via gap junctions.

There were reports of regional expression of gap junctions in maxillary primordia (Minkoff 1983). These regions in which gap junctions were reported to be abundant correlated with regions of high expansion in my fate map, thus overlapping with domains of *Msx-1* and *Fgf-8*, indicating they may have an important role in facial expansion. Gap junction proteins, connexins 43 and 32, were found to be expressed in regions of greatest expansion and in regions of fusion between primordia. Reducing the amount of connexin 43 expression in the facial primordia, using antisense oligodeoxynucleotides, produced a retardation in growth of all facial primordia and subsequently, lateral facial clefting. This indicates that connexin 43 which is expressed specifically in areas of high expansion and fusion, as shown by DiI fate mapping, has an important role in shaping and fusion of the face. Thus this fate map of the face may allow us to predict roles for genes expressed in the face, based on their localised expression patterns.

6.2 Shaping and outgrowth of the maxillary primordium

One important aim of this thesis was to examine how epithelial-mesenchymal interactions contribute to facial shaping. Epithelial-mesenchymal interactions are known to be required for outgrowth of facial primordia (Wedden 1987, Richman and Tickle 1989). Directed outgrowth brings primordia together for fusion and thus lack of outgrowth could have profound consequences on the final shape of the face. The exact role of epithelial-mesenchymal interactions in establishing directed outgrowth of the maxillary primordium had not been discovered due to the fact that this primordium does not develop in isolation. The maxillary primordia is an important component of the primary palate and lack of directed outgrowth of this primordium has the potential to cause clefting.

By using a chemical method for removing the ectoderm *in situ*, I was able to establish that outgrowth of the maxillary primordium requires ectoderm, but extension does not. However, this chemical ablation was not permanent and the ectoderm regenerated. I showed that FGFs can substitute for the ectoderm and re-establish outgrowth of the maxillary primordium.

Experiments in chapter 3 showed that the anterior part of the maxillary primordium expanded more than the posterior. Thus, I suggested that targets of FGF signalling may

be expressed predominantly in the anterior maxillary primordium. *Msx-1* is expressed anteriorly, however chemical removal of ectoderm, unexpectedly, did not result in a reduction of *Msx-1* expression. Total removal of ectoderm did reduce *Msx-1* expression. Furthermore, application of FGFs reduced the expression of *Msx-1*. However, *Eph4A* (*Cek-8*), a receptor protein tyrosine kinase that is expressed throughout the maxillary primordium, is reduced when the ectoderm is chemically removed and application of FGF can restore it. Further experiments indicated that BMP-4, normally expressed in the ectoderm, cannot fully re-establish outgrowth of the maxillary primordium but can positively regulate *Msx-1* expression.

From these results, I can propose a model of how these molecules may be interacting in the maxillary primordium (Figure 6.1). FGF, in the ectoderm controls outgrowth by signalling to the mesenchyme. One of its targets is *Eph4A*, although we do not know the exact role of this molecule in facial development. *Msx-1* also appears to be a target of FGF, although it is negatively regulated by it. BMP-4, in the ectoderm, contributes slightly to outgrowth and positively regulates *Msx-1* expression in the mesenchyme. Thus it would seem that FGF does not act through *Msx-1*, as it does in the limb. We cannot, however, rule out an interaction between FGF in the ectoderm and BMP-4 that would allow for indirect regulation of *Msx-1* in facial primordia.

6.3 Abnormal development of the primary palate

Establishment of the primary palate is essential for appropriate shaping of the face. Lack of fusion results in clefting which also leads to widespread changes in face shape. However, the changes in cellular behaviour leading up to primary palate clefting are not known. In this thesis, I aimed to examine how cell behaviour changed in upper beak primordia upon treatment with retinoic acid, which induces clefting of the primary palate (Tamarin *et. al.,* 1984, Wedden 1987). I found that, surprisingly, only a few populations displayed reduced expansion, with an associated reduction in cell proliferation. These regions were those that fuse to form the primary palate. However, many other populations became more uniform in shape i.e. directed expansion was lost. I proposed that this was secondary to the clefting, in other words, that normal fusion of the two

Figure 6.1 Proposed epithelial-mesenchymal interactions in the maxillary primordia.

This schematic shows the proposed signalling between ectodermal FGF-2 and mesenchymal *Eph4A* and also proposed signalling between ectodermal BMP-4 and mesenchymal *Msx-1* in the maxillary primordium.

Figure 6.1

Maxillary primordium

Mesenchyme   **Epithelium**

Eph4A ⟵ + ⟵ FGF ⟶ Outgrowth

- ? ?

Msx-1 ⟵ + ⟵ BMP-4
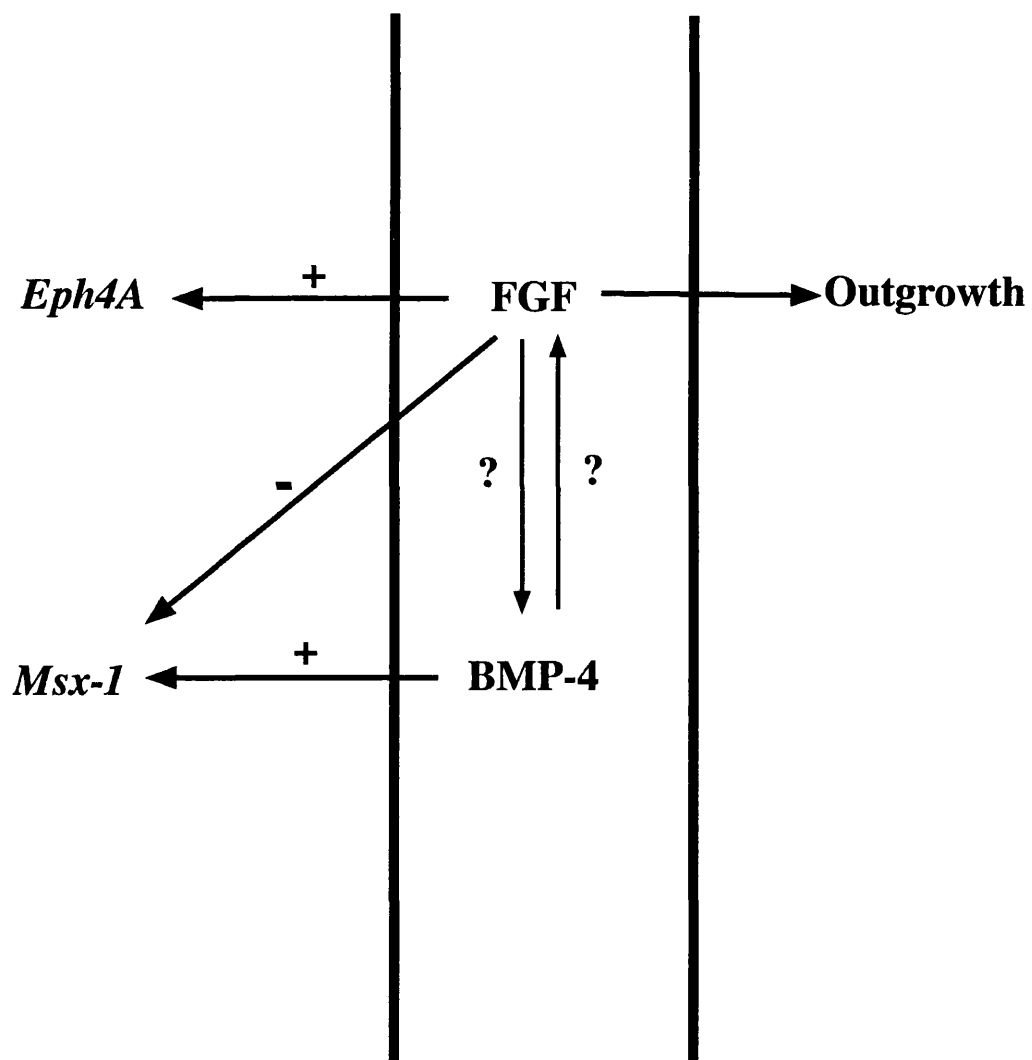
primordia created tension forces that caused stretching in a particular direction. Loss of this force causes uniform expansion. This theory is supported by findings that show removal of this tension force results in loss of shaping. Richman and Tickle (1989) showed that the maxillary primordium has no intrinsic shape in isolation. Amputation of the frontonasal mass also results in a reduced maxillary primordium, forming a rounded mass of tissue (McCann *et. al.,* 1991). Very little ectopic cell death was induced by retinoic acid, indicating that this is not a major component of its teratogenic effect. Interestingly, apoptosis still occurred in the epithelial edges of the lateral frontonasal mass and anterior distal maxillary primordium, the normal points of fusion, even though these primordia did not contact. Cell intercalation seemed somewhat reduced in the affected cell populations and one possibility is that lack of stretching is responsible. It has been suggested that the expansion of the forebrain is responsible for expansion of the frontonasal mass (Patterson and Minkoff 1985). Interestingly, the size of the forebrain is reduced in retinoic acid treated *Xenopus* (Durston *et. al.,* 1989, Ruiz-i-Altaba and Jessell, 1991) and mouse embryos (Simeone *et. al.,* 1995) with a loss of forebrain molecular markers (Lopez *et. al.,* 1995, Avantaggiato *et. al.,* 1996). Abnormal forebrain morphogenesis has also been reported in human embryos exposed to retinoic acid *in utero* (Lammer *et. al.,* 1985). Therefore, reduction in size of the forebrain, due to retinoic acid treatment, could contribute to a secondary reduction in frontonasal mass tissue. However, it is clear from previous work that retinoic acid also has direct effects upon the frontonasal mass itself because when frontonasal mass mesenchyme, exposed to retinoic acid, is grafted onto the limb bud, outgrowth is much reduced (Wedden 1987).

My results have therefore refined our knowledge of the mechanisms of retinoic acid induced clefting. They show that a small number of mesenchymal cell populations in the frontonasal mass, lateral nasal process and maxillary primordium undergo reduced expansion and that changes in cell behaviour in these particular populations have global consequences in the shaping of the face. However, what makes these populations targets? It is known that the retinoic acid receptor *RARβ* is expressed in the anterior maxillary primordium mesenchyme, lateral nasal process and lateral frontonasal mass (Rowe *et. al.,*

1992) and thus may mediate the effect in these regions only. But what are the downstream targets? Expression of *Msx-1* and of *Msx-2* are specifically reduced in the targeted cell populations after retinoic acid treatment (Brown *et. al.,* 1997) and functional inactivation of both of these genes results in clefting of the primary palate (R. Maas, pers. comm.). I have shown, in chapter 4, that expression of connexin 43, but not 32, was also reduced by treatment with retinoic acid. Again, this reduction was specifically seen in those mesenchymal cell populations which experience a reduction of expansion and cell proliferation upon retinoid treatment. Thus I hypothesised that a reduction in cell-cell signalling was part of the mechanism that leads to facial clefting. Evidence consistent with this idea was obtained using connexin 43 antisense oligodeoxynucleotides which produced facial clefts. Finally, *Eph4A* expression in these regions was found to be particularly sensitive to retinoic acid treatment (chapter 5). It will be interesting to see if functional inactivation of this gene leads to facial clefting.

Therefore, from my results, I propose that part of the molecular mechanism by which retinoic acid causes facial clefting is as follows: Retinoic acid interacts with receptor RARβ, expressed in specific mesenchymal regions of the developing face. This, in turn, interacts with genes or proteins such as *Msx-1, Msx-2*, connexin 43 and *Eph4A*, reducing their expression in these regions. This leads to a change in cell behaviour i.e. reduced cell proliferation and possibly intercalation and a subsequent decrease in expansion in regions of facial primordia that normally grow out and fuse. As these regions do not appose, they do not fuse and secondary changes in shape occur as a result of lack of tension. It is interesting to note that these are all mesenchymally expressed genes or that expression is specifically disrupted in the mesenchyme. This is consistent with the findings that the effects of retinoic acid treatment of chick frontonasal mass mesenchyme are irreversible, while effects on the ectoderm are reversible (Wedden 1987).

6.4 General mechanisms of primary palate clefting

This thesis has examined the mechanism of one type of chemically induced primary palate clefting i.e. retinoic acid induced clefting by reducing expansion of frontonasal

mass mesenchymal cell populations. However, primary palate clefting can occur by other mechanisms, which are targeted by different types of teratogens, such as a reduced outgrowth of maxillary primordia or disruption of the fusion process between the primordia that form the primary palate.

Hypoplasia of either the maxillary primordia or the lateral nasal process can also result in clefting of the primary palate. Smith and Monie (1969) indicate that administration of methyl salicylate, trypan blue or 9-methyl PGA to pregnant rats results in underdevelopment of the maxillary primordia and clefting of the primary palate. Hypoplasia of the lateral nasal processes occurs after administration of phenytoin to pregnant mice also resulting in primary palate clefting (Sulik et. al., 1979). This hypoplasia may be due, for example, to reduced migration of neural crest populations early in development, reduced cell proliferation or increased cell death.

Fusion of the primary palate may require epithelial cell death in the regions of the frontonasal mass and maxillary primordium that come into apposition. Apoptosis was seen in these regions in the chick (chapter 3) and has also been reported in mammalian embryos (Pellier and Astic 1994). It is possible that teratogenic compounds could interfere with this process and thus prevent the breakdown of this epithelial seam between primordia forming the primary palate. Maternal hypoxia can induce clefting of the primary palate in the mouse embryo. In this case, increased cell death was seen at the base of the olfactory placode. This increases the distance between median and lateral nasal processes, thus decreasing the possibility of fusion (Bronsky et. al., 1986). In regions of fusion in the face, other than the primary palate, the fate of the epithelial seam is more certain. Fusion of the paired mandibular primordium in the mouse involves migration of epithelial cells to oral surfaces (Chai et. al., 1997). In the fusing edges of the secondary palate, epithelial cells have been observed to undergo apoptosis (Ferguson 1988, Mori et. al., 1994), epithelial to mesenchymal transformation (Fitchett and Hay, 1989, Schuler et. al., 1991, 1992) and migration to oral and nasal surfaces (Carette and Feurguson 1992). Any combination of the processes may be occurring in the region of the primary palate and would be susceptible to disruption. By developing an organ culture system of the primordia that form the primary palate, similar studies to the above may be performed.

This may be able to indicate the fate of epithelial cells and movement of mesenchymal cells, thus providing us with more information about cellular behaviour during primary palate fusion and how this may be disrupted.

6.5 Genetic involvement in clefting and facial malformations

There is also a genetic component to primary palate clefting and facial malformation in general. Several strains of mice have been bred that have a predisposition to facial clefting, mainly due to changes in shape of the frontonasal mass and position and orientation of the nasal pits (for example, Trasler, 1968, Juriloff and Trasler 1976, Millicovsky et. al., 1982). Genetic analysis of some of these strains of mice suggests that one major gene is involved (Juriloff 1986). Several genes have been linked to the manifestation of sporadic cleft primary palate in the human population. However, unlike the mouse model, it is thought that a combination of genes may be involved. Genetic linkage maps of affected humans and also susceptible mice strains have lead to identification of candidate genes. One such candidate is TGF-α (Ardinger et. al., 1989, Juriloff 1993) which has also been shown to be specifically expressed in the fusing regions of the mammalian primary palate (Iamaroon et. al., 1996). However, functional inactivation of TGF-α has not resulted in mice with primary palate clefts (Luetteke et. al., 1993, Mann et. al., 1993). RAR - α, (Chenevix et. al., 1992, Juriloff 1993) Msx-1 (Hibbert and Field, 1996) and $Bcl3$ (Stein et. al., 1995) have also been implicated. Functional inactivation of RAR-α does not cause any facial clefts (Lufkin et. al., 1993) while multiple RAR isoform knockouts display median facial clefts and secondary palate clefts, but not primary palate clefts (Lohnes et. al., 1994). Functional inactivation of Msx-1 results in secondary palate clefting and functional inactivation of Msx-1 and Msx-2 is reported to result in cleft primary palate (R. Maas pers. comm). This confirms the view that there may be several genes involved in predisposing humans to facial clefting, probably by altering the shape of primordia. Moreover, a link between genetic susceptibility and environmental factors has been established, such as with mutations in

the TGF-α locus and maternal cigarette smoking (Shaw *et. al.,* 1996). Thus it seems that in humans at least, that there are multiple causes of sporadic clefting of the primary palate that involve a combination of genetic and non genetic factors.

These reports also confirm my observations that indicate *Msx-1* is important in facial shaping and fusion. My results suggest that mutation in *Connexin 43* may also predispose towards clefting. Furthermore, investigations of epithelial-mesenchymal interactions indicate that *Bmp-4* could play a role in clefting, through the regulation of *Msx-1* expression, and I would predict that functional inactivation of *BMP-4* in the face might result in clefts. Similarly, *Eph4A* may also be interesting to look at, especially because of its sensitivity to retinoic acid treatment. Finally, several human craniofacial malformation syndromes have been linked to mutations in the FGF receptor family. All have craniosynostosis (premature fusion of the cranial sutures) and a variety of other facial defects. Crouzon and Jackson - Weiss syndromes cause mid facial hypoplasia and are both associated with mutations in *FGFR-2* (Reardon *et. al.,* 1994, Jabs *et. al.,* 1994). Pfeiffer syndrome is associated with mutations in *FGFR-1* and is characterised by midfacial hypoplasia and small nose (Muenke *et. al.,* 1994). Saethre-Chotzen syndrome is linked to the TWIST gene, an upstream regulator of FGFR signalling (El Ghouzzi *et. al.,* 1997, Howard *et. al.,* 1997), and results in facial asymmetry, maxillary hypoplasia and deviated nasal septum. Thus my results are consistent with these reports, in that I have found that disruption of FGF signalling results in reduced outgrowth and shaping of facial primordia. My studies have identified genes which are expressed in regions of fusion of facial primordia and are implicated in primary palate formation. I have shown that a reduction in expression of these genes is associated with facial clefting. Therefore they may be good indicators for assessing potential teratogens.

References

Allen, F., Tickle, C. and Warner, A. (1990). The role of gap junctions in patterning of the chick limb bud. Development 108, 623-634.

Anzini, P., Neuberg, D. H. H., Schachner, M., Nelles, E., Willecke, K., Zielasek, J., Toyka, K. V., Suter, U. and Martini, R. (1997) Structural abnormalities and deficient maintenance of peripheral nerve myelin in mice lacking the gap junction protein connexin 32. J. Neurosci. 17, 4545-4551.

Archer, C. W., Cottrill, C. P., and Rooney, P. (1984) Cellular aspects of cartilage differentiation and morphogenesis. In "Matrices and Cell Differentiation" (R.B. Kemp and J. R. Hinchliffe, eds), pp-409-426. Liss. New York.

Ardinger, H. H., Buetow, K. H., Bell, G. I., Bardach, J., VanDermark, D. R. and Murray, J. C. (1989) Association of genetic variation of the transforming growth factor-alpha gene with cleft lip and palate. Am. J. Hum. Genet. 45, 348-353.

Augustine, K., Liu, E. T. and Sadler, T. W. (1993) Antisense attenuation of Wnt-1 and Wnt-3a expression in whole embryo culture reveals roles for these genes in craniofacial, spinal cord and cardiac morphogenesis. Dev. Genet. 14, 500-520.

Avantaggiato, V., Acampora, D., Tuorto, F. and Simeone, A.(1996) Retinoic acid induces stage-specific repatterning of the rostral central nervous system. Dev. Biol. 175, 347-57

Baker, J. C. and Harland, R. M. (1997) From receptor to nucleus: the Smad pathway. Curr. Biol. 7, 467-473.

Bani-Yagoub, M., Bechberger, J. F. and Naus, C. A. (1997) Reduction of connexin 43 expression and dye coupling during neuronal differentiation of human NTera/2clone D1 cells. J. Neurosci. Res. 49, 19-31.

Barlow, A. J. and Francis-West, P.H. (1997) Ectopic application of recombinant BMP-2 and BMP-4 can change patterning of developing chick facial primordia. Development **124**, 391-398.

Baroffio, A, Dupin, E., and LeDouarin, N. M. (1991) Common precursors for neural and mesectodermal derivatives in the cephalic neural crest. Development, **112**, 301-305.

Barrio, L. C., Suchyna, T., Bargiello, T., Xu, L. X., Roginski, R. S., Bennett, M. V. L. and Nicholson, B. J. (1991) Gap junctions formed by connexins 26 and 32 alone and in combination are differently affected by applied voltage. Proc. Natl. Acad. Sci. USA **88**, 8410-8414.

Becker, D. L., Leclerc-David, C. and Warner, A. (1992) The relationship of gap junctions and compaction in the preimplantation mouse embryo. Development, **103?** (suppl), 113-118.

Becker, N., Seitanidou, T., Murphy, P., Mattei, M. G., Topiko, P., Nieto, M. A., Wilkinson, D. G., Charnay, P. and Gilardi-Hebenstreit, P. (1994) Several receptor tyrosine kinase genes of the Eph family are segmentally expressed in the developing hindbrain. Mech. Dev. **47**, 3-17.

Becker, D. L., Evans, W. H., Green, C. R. and Warner, A. (1995). Functional analysis of amino acid sequences in connexin 43 involved in intercellular communication through gap junctions. J. Cell Sci. **108**, 1455-1467.

Becker, D. L., Lorimer, J., Makarenkova, H. P., McGonnell, I. M., Tickle, C. and Green, C. (1998) Developmental defects resulting from spatiotemporal regulation of gap junction expression. Submitted.

Bennett, M. V. L, Barrio, L. C., Bargiello, T. A., Spray, D. C., Hertzberg, E. and Saez, J. C. (1991) Gap junctions : New tools, new answers, new questions. Neuron **6**, 305-320.

Bennett, J. H., Hunt, P. and Thorogood, P. (1995) Bone morphogenetic protein 2 and 4 expression during murine orofacial development. Arch. Oral Biol. **40**, 847-854.

Bennett, K. L.; Modrell, B., Greenfield, B., Bartolazzi, A., Stamenkovic, I., Peach, R., Jackson, D. G., Spring, F. and Aruffo, A. (1995) Regulation of CD44 binding to hyaluronan by glycosylation of variably spliced exons. J. Cell Biol. 1995 131, 1623-33

Bergemann, A. D., Cheng, H. J., Brambilla, R., Klein, R. and Flanagan, J. G. (1995) ELF-2, a new member of the Eph ligand family is segmentally expressed in mouse embryos in the region of the hindbrain and newly forming somites. Mol. Cell. Biol. 15, 4921-4929.

Bergoffen, J., Scherer, S. S., Wong, S., Scott, M. O., Bone, L. T., Paul, D. L., Chen, K., Lensch, M. W., Chance, P. F. and Fishbeck, K. H. (1993) Connexin mutations in x-linked Charcot-Marie-Tooth disease. Science 262, 3039-3042.

Bex, V., Mercier, T., Chaumonet, C., Gillard-Sanchez, I., Flechon, B., Mazet, F., Traub, O. and Martel, P.(1995) Retinoic acid enhances connexin 43 expression at the post-transcriptional level in rat liver epithelial cells. Cell Biochem. Func. 13, 69-77.

Beyer, E. C., Paul, D. L and Goodenough, D. A. (1987) Connexin 43: a protein from rat heart homologous to a gap junction protein from liver. J. Cell Biol. 105, 2621-2629.

Birgbauer, E., Sechrist, J., Bronner-Fraser, M. and Fraser, S. (1995) Rhombomeric origin and rostrocaudal reassortment of neural crest cells revealed by intravital microscopy. Development 121,935-945.

Blake, K. R., Murakami, A., Spitz, S. A., Glave, S. A., Reddy, M. P., Ts'o, P. O. P. and Miller, P. S. (1985) Hybridisation arrest of globin synthesis in rabbit reticulocyte lysates and cells by oligodeoxyribonucleoside methylphosphonates. Biochemistry 24, 6139-6145.

Bond, S. L., Bechberger, J. F., Khoo, N. K. and Nows, C. C., (1994). Transfection of C6 glioma cells with Connexin 32: the effects of expression of a non endogenous gap junction protein. Cell Growth Diff. 5, 179-186.

Bradley , R. S., Cowin, P. and Brown, A. M. C. (1993) Expression of Wnt-1 in PC12 cells results in modulation of plakoglobin and E-cadherin and increased cellular adhesion J. Cell Biol. 123, 1857-1865.

Brambilla, R., Schnapp, A., Casagranda, F., Labrador, J. P., Bergemann, A. D., Flanagan, J. G., Pasquale, E. B. and Kline, R. (1995) Membrane bound LERK2 ligand can signal through three different Eph-related receptor protein tyrosine kinases. EMBO J. 14, 3116-3126.

Brambilla, R., Bruckner, K., Orioli, D., Bergemann, A. D., Flanagan, J. G., Kline, R. (1996) Similarities and differences in the way transmembrane type ligands interact with the Elk subclass of Eph receptors. Mol. Cell. Neurosci. 8, 199-209.

Bronsky, P.T., Johnston, M. C. and Sulik, K. (1986) Morphogenesis of hypoxia-induced cleft lip in CL/Fr mice. J. Craniof. Genet. Dev. Biol. 2 (supp) 113-128.

Britz-Cunningham, S. H., Shah, M. M., Zuppan, C. W. and Fletcher, W. H. (1995) Mutations of connexin 43 gap junction gene in patients with heart malformations and defects of laterality. N. Eng. J. Med. 332, 1323-1329.

Bronner-Fraser, M. (1995) Origins and developmental potential of the neural crest. Exp. Cell Res. 218, 405-417

Brown, J.M., Wedden, S.E., Millburn, G.H., Robson, L.G., Hill, R.E., Davidson, D.R. and Tickle, C. (1993) Experimental analysis of the control of expression of the homeobox-gene *Msx-1* in the developing limb and face. Development 119, 41-48.

Brown, J.M., Robertson, K.E., Wedden, S.E. and Tickle, C. (1997) Alterations in *Msx-1* and *Msx-2* expression correlate with inhibition of outgrowth of chick facial primordia induced by retinoic acid. Anat. Embryol. 195, 203-207.

Bruckner, K., Pasquale, E. B. and Klein, R. (1997) Tyrosine phosphorylation of transmembrane ligands for Eph receptors. Science. 275, 1640-3

Bruzzone, R., White, T. W. and Paul, D. L. (1996) Connections with connexins : the molecular basis of direct intercellular signalling. Eur. J. Biochem. 238, 1-27.

Burglin, T. R (1994) In Dubole D. (ed) Homeobox genes, Oxford University Press. Oxford, pp27-71.

Carette, M. J. M. and Ferguson, M. W. L. (1992) The fate of medial edge epithelial cells during palate fusion *in vitro*: An analysis of DiI labelling and confocal microscopy. Development **114**, 379-388.

Chai, Y., Sasano, Y., Bringas, P., Mayo, M., Kaartinen, V., Heisterkamp, N., Groffen, J., Slavkin, H. and Shuler, C. (1997) Characterisation of the fate of midline epithelial cells during the fusion of mandibular prominences in vivo. Dev. Dyn. **208**, 526-535.

Chambon, P. (1996) A decade of molecular biology of retinoic acid receptors. FASEB J. **10**, 940-954.

Chen, B. and Hale B. F. (1995) Antisense ODNs down regulation of E-cadherin in the yolk sac and neural tube malformations. Biol. Reprod. **53**, 1229-1238.

Chenevix, G. T., Jones, K., Green, A. C., Duffy, D. L. and Martin, N. G. (1992) Cleft lip with or without cleft palate: associations with transforming growth factor α and RAR loci. Am. J. Hum. Genet. **51**, 1377-85.

Cheng, H. J., Nakamoto, M., Bergemann, A. D. and Flanagan, J. G. (1995) Complementary gradients in expression and binding of ELF-1 and Mek4 in development of the topographic retinotectal projection map. Cell **82**, 371-381.

Ch'ng, J., Mulligan, R., Schimmel, P. and Holmes, E. (1989) Antisense RNA complementary to 3' coding and non coding sequences of creatine kinase is a potent inhibitor of translation in vivo. Proc. Natl. Acad. Sci. USA, **86**, 10006-10010.

Clairmont, A., Tessmann, D. and Sies, H. (1996) Analysis ofCx*43* gene expression induced by retinoic acid in F9 teratocarcinoma cells. FEBS Letts. **397**, 22-24.

Coelho, C. N. D., Krabbenhof, K. M., Upholt, W. B., Fallon, J. F. and Kosher, R. A. (1991) Altered expression of the chicken homeobox-containing genes *GHox-7* and *GHox-8* in the limb buds of limbless mutant chick embryos. Development **113**, 1487-1493.

Cohn, M. J., Izpisua-Belmonte, J. C., Abud, H., Heath, J. K. and Tickle, C. (1995) Fibroblast growth factors induce additional limb development from the flank of chick embryos. Cell, 80, 739-746.

Cole, W. C. and Garfield, R. E. (1986) Evidence for a physiological regulation of myometrial gap junction permeability. Am. J. Physiol. 251, C411-C420.

Colige, A., Sokolov, B. P., Nugent, P., Baserga, R. and Prockop, D. J. (1993) Use of antisense oligonucleotides to inhibit expression of a mutated human procollagen gene (COL1A1) in transfected mouse 3T3 cells. Biochemistry 32, 7-11.

Conlon, R. A. and Rossant, J. (1992) Exogenous retinoic acid rapidly induces anterior ectopic expression of murine Hox-2 genes in vivo. Development 116, 357-68

Couly, G. and Le Douarin, N. (1985) Mapping of the early neural primordium in quail-chick chimeras. I Developmental relationships between placodes, facial ectoderm and prosencephalon. Dev Biol 110, 422-439.

Couly, G. F. and Le Douarin, N. (1987) Mapping of the early neural primordium in Quail-Chick chimeras. II The prosencephalic neural plate and neural folds: implications for the genesis of cephalic human congenital abnormalities. Dev. Biol. 120, 198-214.

Couly, G. and Le Douarin, N. (1990) Head morphogenesis in embryonic avian chimeras: evidence for a segmental pattern in the ectoderm corresponding to the neuromeres. Development 108, 543-558

Couly, G. F., Coltey, P. M. and Le Douarin, M. (1992) The developmental fate of the cephalic mesoderm in chick -quail chimeras. Development 114, 1-15.

Couly, G. F., Coltey, P. M. and Le-Douarin, N. M. (1993) The triple origin of skull in higher vertebrates: a study in quail-chick chimeras. Development 117, 409-29

Crossley, P.H. and Martin, G.R. (1995) The mouse *Fgf-8* gene encodes a family of polypeptides and is expressed in regions that direct outgrowth and patterning in the developing embryo. Development 121, 439-451.

Crossley, P. H., Minowada, G., MacArthur, C. A., and Martin, G. R. (1996) Roles for FGF8 in the induction, initiation and maintenance of chick limb development. Cell, 84, 127-136.

Dahl, G., Werner, R., Levine, E. and Rabadan-Diehl, C. (1992) Mutational analysis of gap junction formation. Biophys. J 62, 172-182.

Dahl, G., Nonner, W. and Werner, R. (1994) Attempts to define functional domains of gap junction proteins with synthetic peptides. Biophys. J. 67, 1816-1822.

Davidson, D.R. and Hill, R.E. (1991) Msh-like genes: a family of homeobox genes with wide-ranging expression during vertebrate development. Sem. Dev. Biol. 2, 405-412.

Davidson, D.R., Crawley, A., Hill, R.E. and Tickle, C. (1991) Positional-dependent expression of two related homeobox genes in developing vertebrate limbs. Nature 352, 429-431.

Davis, A. P. and Cappechi, M. R. (1994) Axial homeosis and appendicular skeleton defects in mice with targeted disruption of Hoxd11. Development 120, 2187-2198.

Davis, A. P., Witte, D. P., Hsieh-Li, H. M., Potter, S. S. and Capecchi, M. R. (1995) Absence of radius and ulna in mice lacking Hox a11 and Hoxd11 . Nature 375, 791-795

Dermietzel, R., Hwang, T. K. and Spray, D. S. (1987) The gap junction family : structure, function and chemistry. Anat. Embryol. 182, 517-528.

Dersch, H. and Zile, M. H (1993) Induction of normal cardiovascular development in the Vitamin A deprived quail embryo by natural retinoids. Dev. Biol. 160, 424-433

Dickman, E. D., Thaller, C. and Smith, S. (1997) Temporally-regulated retinoic acid depletion produces specific neural crest ocular and nervous system defects. Development 124, 3111-3121.

Drescher, U., Kremoser, C., Handwerker, C., Loscinger, J., Noda, M. and Bonhoeffer (1995) In vitro guidance of retinal ganglion cell axons by RAGS, a 25kDa tectal protein related to ligands for Eph RPTKs . Cell, 82, 359-370.

Durston, A. J., Timmermans, J. P. M., Hage, W. J., Hendriks, H.F. J., de Vries, N. J., Hedeveld, M. and Nieuwkoop, P. D. (1989) Retinoic acid causes an anteroposterior transformation in developing central nervous system. Nature 340, 140-143.

Ebner, R., Chen, R. H., Shum, L., Lawler, S., Zioncheck, T. F., Lee, A., Lopez, A. R. and Derynck, R. (1993) Cloning of a TGFbeta receptor and its affect on TGFbeta binding to the type II receptor. Science 260, 1344-1348.

Eichele, G., Tickle, C. and Alberts, B.M. (1984) Microcontrolled release of biologically active compounds in chick embryos: Beads of 200μm diameter for the local release of retinoids. Anal. Biochem. 142, 542-555.

Elfgang, C. , Reiner, E., Lichtenberg-Frate, Butterweck, A., Traub, O., Klein, R., Hulser, D., Willecke, K. (1995) Specific permeability and selective formation of gap junction channels in connexin-transfected HeLa cells. J. Cell Biol. 129, 805-817.

El Ghouzzi, V., Le Merrer, M., Perrin-Schmitt, F., Lajeunie, E., Benit, P., Renier, D., Bourgeois, P., Bolcato-Bellemin, A. L., Munnich, J. B. (1997) Mutations of the TWIST gene in the Saethre-Chotzen syndrome. Nat. Gen. 15, 42-46.

Eph Nomenclature Committee (1997) Unified nomenclature for Eph family receptors and their ligands, the ephrins. Cell 90, 403-4

Ewart, J. L., Cohen, M. F., Meyer, R. A., Huang, G. Y., Wessels, A., Gourdie, R. G., Chin, A. J., Park, S. M. J., Lazatin, B. O, Villabon, S. and Lo, C. W. (1997) Heart and neural tube defects in transgenic mice overexpressing the Cx43 gap junction gene. Development 124, 1281-1292.

Fallon, J. F. and Saunders, J.W. (1968) In vitro analysis of the control of cell death in zone of prospective necrosis from the chick wing bud. Dev. Biol. 18, 553-570.

Fallon, J. F., Lopez, A., Ros, M. A., Savage, M. P., Olwin, B. B. and Simandl, B. K. (1994) FGF-2: apical ectodermal ridge growth signal for chick limb development. Science 264, 104-107.

Ferguson, M.W. (1988). Palate development. Development. 103 (suppl), 41-60.

Fichett, J. E. and Hay, E. D. (1989) Medial edge epithelium transforms to mesenchyme after embryonic palatal shelves fuse. Dev. Biol. 131, 455-474.

Fisher, T. L., Tierhorst, T., Cao, X. and Wagner, R. W. (1993) Intracellular disposition and metabolism of unmodified and modified antisense oligodeoxynucleotides microinjected into mammalian cells. Nuc. Acid Res. **21**, 3857-65

Flagg-Newton, J., Simpson, I. and Lowenstein, W. R. (1979) Permeability of the cell-cell membrane channels in mammalian cell junction. Science, **205**, 404-407.

Foerst - Potts, L. and Sadler, T. W. (1997) Disruption of *Msx-1* and *Msx-2* reveals roles s in craniofacial, eye and axial development. Dev. Dyn. **209**, 70-84.

Francis, P. H., Richardson, M. K., Brickell, P. M. and Tickle, C. (1994) Bone morphogenetic proteins and a signalling pathway that controls patterning in the developing chick limb. Development **120**, 209-218.

Francis-West, P.H., Tatla, T and Brickell, P.M. (1994) Expression patterns of the bone morphogenetic protein genes *Bmp-4* and *Bmp-2* in the developing chick face suggests a role in outgrowth of the primordium. Dev. Dyn. **201**, 168-178.

Freid, K. A. J., Mitsiadis, T. A., Guerrier, A. and Meister, B. (1996) Combinatorial expression patterns of the connexins 26, 32 and 43 during development, homeostasis and regeneration of rat teeth. Int. J. Dev. Biol. **40**, 985-995.

Fukushima, M., Nakamura, M., Ohta, K., Okamura, R., Negi, A. and Tanaka, (1996) Regional specification of motorneurons along the A-P axis is independent of the notochord. Development **122**, 905-914.

Gale, N. W., Holland, S. J., Valenzuela, D. M., Flenniken, A., Pan, Li., Ryan, T. E., Henkemeyer, M., Strebhardt, K., Hirai, H., Wilkinson, D. G., Pawson, T., Davis, S. and Yancopoulos, G. D. (1996a) Eph receptors and ligands comprise two major specificity subclasses and are reciprocally compartmentalised during embryogenesis. Neuron, **17**, 9-19.

Gale, N. W., Flenniken, A., Compton, D. C., Jenkins, N. A., Gilbert, D. J., Davis, S., Wilkinson, D. G. and Yancopoulos, G. D. (1996b) Elk-L3, a novel transmembrane ligand for the Eph family of RPTKs, expressed in the embryonic hindbrain, floor plate and roof plate. Oncogene **13**, 1343-1352.

Ganan, Y., Macias, D., Duterque-Coquillaud, M., Ros, M. A. and Hurle, J. M. (1996). Role of TGF betas and BMPs as signals controlling the position of the

digits and the areas of interdigital cell death in the developing chick limb autopod. Development. **122,** 2349-57.

Gibson, D. F., Hossain, M. Z., Goldberg, G. S., Acevedo, P. and Bertran, J. S. (1994) Mitogenic effects of TGFs β1 + β2 in C3H/10T1/2 cells occur in the presence of enhanced gap junctional communication. Cell Growth Diff. **6,** 687-96.

Gibson, D. F., Bikle, D. D., Herns, J. and Goldberg, G. S., (1997) The expression of the gap junction protein connexin 43 is restricted to proliferating and non differentiated normal and transfected keratinocytes. Exp. Dermat. **4,** 167-74.

Gilardi-Hebenstreit, P., Nieto, M. A., Frain, M., Mattei, M. G., Chestier, A., Wilkinson, D. G. and Charnay, P. (1992) An Eph related receptor protein tyrosine kinase gene segmentally expressed in the mouse developing hindbrain. Oncogene **7,** 2499-2506.

Goodenough, D. A. (1974) Bulk isolation of mouse hepatocyte gap junctions. Characterisation of the principal protein connexin. J. Cell Biol. **61,** 557-563.

Gospodarowicz, D. (1974) Localisation of a fibroblast growth factor and its effects alone and with hydrocortisone on 3T3 cell growth. Nature **249,** 123-127.

Goulding, E. H. and Pratt, R. M. (1986) Isotretinoin teratogenicity in mouse whole embryo culture. J. Craniof. Genet. Dev. Biol. **6,** 99-112.

Green, C. R., Bowles, L., Crawley, A. and Tickle, C. (1994). Expression of the Cx43 gap junction protein in tissues at the tip of the chick limb bud is related to the epithelial-mesenchymal interactions that mediate morphogenesis. Dev. Biol., **161,** 12-21.

Grummer, R., Hellmann, P., Traub, O., Soares, M. J., El-Sabban, M. E. and Winterhager, E. (1996) Regulation of connexin 31 gene expression upon retinoic acid treatment in rat choriocarcinoma cells. Exp. Cell Res. **227,** 23-32.

Guthrie, S. C. (1984) Patterns of junctional communication in the early amphibian embryo. Nature, **311,** 149-151.

Guthrie, S. and Gilula, N. B. (1989) Gap junctional communication and development. TINS **12,** 12-16.

Hamburger V. and Hamilton H.L. (1951) A series of normal stages in the development of the chick embryo. J. Morphol **88,** 49-92.

Hanson, J. W. and Smith, D. W. (1975) The fetal hydantoin syndrome. J. Pediatr. **87**, 285-90.

Harris, A. L., Spray, D. C. and Bennett, M. V. L. (1981) Kinetic properties of a voltage - dependent junctional conductance. J. Gen. Physiol. **77**, 95-117.

Heath, L., Wild, A. and Thorogood (1992) Monoclonal antibodies raised against pre-migratory neural crest reveal population heterogeneity during crest development. Differentiation **49**, 151-165.

Heikinheimo, M., Lawshe, A., Shackleford, G.M., Wilson, D.B. and MacArthur, C.A. (1994) *Fgf-8* expression in post-gastrulation mouse suggests roles in development of the face, limbs and central nervous system. Mech. Dev. **53**, 129-138.

Heine, U. I., Roberts, A. B., Munoz, E. F., Roche, N. S. and Sporn, M. B. (1985) Effects of retinoid deficiency on the development of the heart and vascular system of the quail embryo. Virchows Arch **50**, 135-152.

Helms, J.A., Kim, C. H., Hu, D., Minkoff, R., Thaller, C., and Eichele, G., (1997) Sonic hegehog participates in craniofacial morphogenesis and is down regulated by teratogenic doses of retinoic acid. Dev. Biol. **187**, 25-35.

Hennemann, H., Suchyna, T., Lichtenberg-FratÇ, H., Jungbluth, S., Dahl, E., Schwarz, J., Nicholson, B. J. and Willecke, K. (1992) Molecular cloning and functional expression of mouse connexin 40 a second gap junction gene preferentially expressed in lung. J. Cell Biol. **117**, 1299-1310.

Hibbert, S. A. and Field, J. K. (1996) Molecular basis of familial cleft lip and palate. Oral Dis. **2**, 238-41.

Hill, R. E., Jones, P. F., Rees, A. R., Sime, C. M., Justice, M. J., Copeland, N. G., Jenkins, N. A., Graham, E. and Davidson, D. R. (1989) A new family of mouse homeobox containing genes. Genes Dev. **3**, 26-37.

Hinck, L., Nathke, I. S., Papkoff, J. and Nelson, W. J. (1994) Wnt-1 modulates cell-cell adhesion in mammalian cells by stabilising β-catenin binding to the cell adhesion molecule cadherin. J. Cell Biol., **124**, 729-741.

Hirai, H., Maru, Y., Hagiwara, K., Nishida, J. and Takaku, F. (1987) A novel putative tyrosine kinase receptor encoded by the *eph* gene. Science **238**, 1717-1720.

Hoke, G. D., Draper, K., Freier, S. M., Gonzalez, C., Driver, V. B., Zounes, M. C. and Ecker, D. J. (1991) Effects of phosphorothioate capping on antisense oligonucleotides stability, hybridisation and antiviral efficacy versus herpes simplex virus infection. Nucleic Acids Res. **19**, 5743-8.

Horton, C. and Maden, M. (1995) Endogenous distribution of retinoids in normal development and teratogenesis in the mouse embryo. Dev. Dyn. **202**, 312-323.

Howard, T. D., Paznekas, W. A., Green, E. D., Chiang, L. C., Ma, N., De Luna, R., Delgado, C. G., Gonzalez-Ramos, M., Kline, A. D. and Jabs, E. W. (1997) Mutations in TWIST, a basic helix-loop-helix transcription factor in Saethre-Chotzen syndrome. Nat. Genet. **15**, 36-41.

Howell, J.Mc. C., Thompson, J. N. and Pitt, G. A. (1963) Histology of the lesions produced in the reproductive tract of animals fed a diet deficient in vitamin A alcohol but containing vitamin A acid. I The male rat. J. Reprod. Fert. **5**, 159-167.

Iamaroon, A., Tait, B. and Diewert, V. M. (1996) Cell proliferation and expression of EGF, TGF-alpha, and EGF receptor in the developing primary palate. J. Dent. Res. **75**, 1534-9.

Ikeya, M., Lee, S. M. K., Johnson, J. E., McMahon, A. P., Takada, S., (1997) Wnt signalling is required for expansion of neural crest and CNS progenitors. Nature **389**, 966-971.

Irving D.W., Willhite, C.C. and Burk, D.T., (1986) Morphogenesis of isotretinoin - induced microcephaly and micrognathia studied by scanning electron microsopy. Teratology **34**, 141-153.

Jabs, W. E., Muller, U., Li, X., Ma, L., Luo, W., Haworth, I. S., Klisak, I., Sparkes, R., Warman, M. L., Mulliken, J. B., Snead, M. L. and Maxson, R. (1993) A mutation in the homeodomain of the human MSX2 gene in a family affected with autosomal dominant craniosynostosis. Cell, **75**, 443-450.

Jabs, W. E., Jabs, W. E., Li, X., Scott, A. F., Meyers, G., Chen, W., Eccles, M., Mao, J., Charnas, L. R., Jackson, C. E. and Jaye, M. (1994) Jackson-Weiss and Crouzon syndromes are allelic with mutations in fibroblast growth factor receptor 2. Nat. Genet. **8**, 275-279.

Jelinek, R. and Kistler, A. (1981) Effect of retinoic acid upon the chick embryonic morphogenetic systems. I. The embryotoxicity dose range. Teratology **23**, 191-195.

Jiang, J. X. and Goodenough, D. A. (1996) Heteromeric connexons in lens gap junction channels. PNAS. **93**, 1287-1291.

Johnston M.C. (1966) A radioautographic study of the migration and fate of cranial neural crest cells in the chick embryo. Anat. Rec. **156**, 130-143.

Jones, C. M., Lyons, K. M. and Hogan, B. L. M (1991) Involvement of *BMP-4* and *Vgr-1* in morphogenesis and neurogenesis in the mouse. Development, **111**, 531-542.

Jongen, W. M. F., Fitzgerald, D. J., Asamoto, M., Piccoli, C., Slaga, T. J., Gros, D., Takeichi, M.. and Yamasaki H. (1991) Regulation of connexin 43-mediated gap junctional intercellular communication by Ca^{2+} in mouse epidermal cells is controlled by E-cadherin. J. Cell Biol. **114**, 545-555.

Juriloff, D. M. and Trasler, D. G (1976) Test of the hypothesis that embryonic face shape is a causal factor in genetic predisposition to cleft lip in mice. Teratology **14**, 35-42.

Juriloff, D. M. (1986) Major genes that cause cleft lip in mice: progress in construction of a congenic strain and linkage map. J. Craniof. Genet. Dev. Biol. **supp 2**, 55-66.

Juriloff, D. M. (1993) Current status of genetic linkages studies of a major gene that causes CL(P) in mice exclusion map. J. Craniofac. Genet. Dev. Biol. **13**, 223-9.

Kastner, P., Mark, M. and Chambon, P. (1995) Nonsteroid nuclear receptors: what are genetic studies telling us about their role in real life. Cell **83**, 859-869.

Keller, R. and Danilchick, M. (1988) Regional expression, pattern and timing of convergence and extension during gastrulation of *Xenopus laevis*. Development **103**, 193-209.

Kelsell, D. P., Dunlop, J., Stevens, H. P., Lench, N. J., Liang, J. N., Parry, G., Mueller, R. F and Leigh, I. M. (1997) Connexin 26 mutation in hereditary non syndromic sensoneurial deafness. Nature **387**, 80-83.

Kosaka, K., Hama, K. and Kazuhiro, E. (1985) Light and electron microscopic study of fusion of facial prominences. Anat. Embryol. **173**, 187-201.

Kosaka, K and Eto, K. (1986) Appearance of a unique cell type in the fusion sites of facial processes. J. Craniofac. Genet. Dev. Biol. **2** (suppl), 45-52.

Köntges, G. and Lumsden A. (1996) Rhombencephalic neural crest segmentation is preserved throughout craniofacial ontogeny. Development **122**, 3229-3242.

Kren, B.T., Kumar, N.M., Wang, S., Gilula, N.B. and Steer, C.J. (1993) Differential regulation of multiple gap junction transcripts and proteins during rat liver regeneration. J. Cell Biol. **123**, 707-718.

Krull, C. E., Lansford, R., Gale, N. W., Collazo, A., Marcelle, C., Yancopoulos, G. D., Fraser, S. E. and Bronner-Fraser, M. (1997) Interactions of Eph-related receptors and ligands confer rostrocaudal pattern to trunk neural crest migration. Curr. Biol. **7**, 571-580.

Krumlauf, R., Marshall, H., Studer, M., Nonchev, S., Sham, M. H. and Lumsden, A. (1993) Hox homeobox genes and regionalisation of the nervous system. J. Neurobiol. **24**, 1328-40.

Kumar, N. M. and Gilula, N. B (1996) The gap junction communication channel. Cell **84**, 381-388.

Laird, D. W., Yancey, BS. B., Bugga, L. and Revel, J.P. (1992) Connexin expression and gap junction communication compartments in the developing mouse limb. Dev. Dyn. **195**, 153-161.

Lammer, E. J., Chen, D.T., Hoar, R. M., Agnish, N. D., Benke, P. J., Braun, J.T., Curry, C., Fernhoff, P.M., Grix, A. W., Lott, I.T., Richard, J. M. and Sun, S. C. (1985) Retinoic acid embryopathy. N. Engl. J. Med. **313**, 837-41

Le Douarin, N. (1973) A biological cell labelling technique and its use in experimental embryology. Dev. Biol. **30**, 217-222.

Le Douarin, N. M., Ziller, C. and Couly, G. (1993) Patterning of neural crest derivatives in the avian embryo: *In vivo* and *in vitro* studies. Dev. Biol. **159**, 24-29.

Lee, S., Gilula, N.B. and Warner, A.E. (1987) Gap junctional communication and compaction during preimplantation stages of mouse development. Cell **51**, 851-860.

Lee, S. W., Tomasetto, C., Paul, D., Keyomarsi, K. and Sager, R. (1992) Transcriptional down regulation of gap junction proteins blocks junctional communication in human mammary tumor cell lines. J. Cell Biol. **118**, 1213-1221.

Leid, M., Kastner, P. Lyons, R., Nakshatri, N., Saunders, M., Zacharewski, T., Chen, J. Y., Staub, A., Gardiner, J. M., Mader, S. and Chambon, P. (1992) Purification, cloning and RXR identity of HeLa cell factor with which RAR or TR heterodimerises to bind target sequences efficiently. Cell 68, 377-395.

Le Lièvre C.S. (1978) Participation of neural crest-derived cells in genesis of the skull in birds. J. Embryol. exp. Morph. **47**, 17-37.

Le Lièvre, C.S. and Le Douarin N. (1975) Mesenchymal derivatives of the neural crest: analysis of chimaeric quail and chick embryos. J. Embryol. exp. Morph. **34**, 125-154.

Li, E., Sucov, H. M., Lee, K. F., Evans, R. M. and Jaenisch, R. (1993) Normal development and growth of mice carrying a targeted disruption of the $\alpha 1$ retinoic acid receptor gene. Proc. Natl. Acad. Sci. USA **90**, 1590-1594.

Lo, C. W. and Gilula, N. B. (1979) Gap junction communication in the preimplantation mouse embryo. Cell **18**, 399-409.

Lo, C. W., Cohen, M. F., Huang, G. Y., Lazatin, B. O., Patel, N., Sulivan, R., Pauken, C. and Park, S. M. J. (1997) *Cx43* gap junction gene expression and gap junctional communication in mouse neural crest cells. Dev. Genet. **20**, 119-132.

Lohnes, D., Kstner, P., Dierich, A., Mark, M., LeMeur, M. and Chambon, P. (1993) Function of RARγ in the mouse. Cell **73**, 643-658.

Lohnes, D., Mark, M., Mendelsohn, C., Dolle, P., Dierich, A., Gorry, P., Gansmuller, A. and Chambon, P. (1994) Function of the retinoic acid

receptors (RARs) during development (I) Craniofacial and skeletal abnormalities in RAR double mutants. Development **120**, 2723-2784.

Loke, S. L., Stein, C. A., Zhang, X. H., Mori, K., Nakonishi, M., Subasinghe, C., Cohen, J. S. and Neckers, L. M. (1989) Characterisation of oligonucleotides transport into living cells. Proc. Natl. Acad. Sci. USA **86**, 3474-3478.

Lopez, S.L., Dono, R., Zeller, R. and Carrasco, A. E. (1995) Differential effects of retinoic acid and a retinoid antagonist on the spatial distribution of the homeoprotein Hoxb-7 in vertebrate embryos. Dev. Dyn. **204**, 457-71

Lowenstein, W. R. (1981) Junctional intercellular communication: the cell-cell membrane channel. Phys. Rev. 61, 829-913.

Lu, H. C., Eichele, G. and Thaller, C. (1997) Ligand bound RXR can mediate retinoid signal transduction during embryogenesis. Development **124**, 195-203.

Luetteke, N. C., Qiu, T H., Pfeiffer, R. L., Oliver, P., Smithies, O. and Lee, D. C. (1993) TGFα deficiency results in hair follicle and eye abnormalities in targeted and Waved -1 mice. Cell **73**, 263-278.

Lufkin, T., Lohnes, D., Mark, M., Dierich, A., Gorry, P., Gaub, M. P., LeMeur, M., and Chambon, P. (1993) High postnatallethality and testis degeneration in RAR α mutant mice. Proc. Natl. Acad. Sci.USA **90**, 7225-7229.

Lumsden, A. Sprawson, N. and Graham, A. (1991) Segmental origin and migration of neural crest in the hindbrain region of the chick embryo. Development **113**, 1281-1291.

Luo, J., Pasceri, P., Conlon, R. A., Rossant, J. and Giguere, V. (1995) Mice lacking all isoforms of retinoic acid receptor beta develop normally and are susceptible to the teratogenic effects of retinoic acid. Mech. Dev. **53**, 61-71.

Lyons, K. M., Pelton, R. W. and Hogan, B. L. M. (1990) Organogenesis and pattern formation in the mouse: RNA distribution patterns suggest a role for *BMP-2A*. Development **109**, 833-844.

Mackenzie, A., Leeming, G.L., Jowett, A.K., Ferguson, M.W.J. and Sharpe, P.T. (1991a) The homeobox gene *hox 7.1* has specific regional and temporal

expression patterns during early murine craniofacial embryogenesis, especially tooth development in vivo and in vitro. Development **111**, 269-285.

Mackenzie, A., Ferguson, M.W.J. and Sharpe, P.T (1991b) *Hox-7* expression during murine craniofacial development. Development **113**, 601-611.

Mackenzie, A., Ferguson, M.W.J. and Sharpe, P.T. (1992) Expression patterns of homeobox gene, *Hox 8*, in the mouse embryo suggest a role in specifying tooth initiation and shape. Development **115**, 403-420.

Mackenzie, A., Purdie, L., Davidson, D., Collinson, M., and Hill, R. E. (1997) Two enhancer domains control early aspects of the complex expression pattern of *Msx-1*. Mech. Dev. **62**, 29-40.

Mahmood, R., Bresnick, J., Hornbruch, A., Mahony, C., Morton, N., Colquhoun, K., Martin, P., Lumsden, A., Dickson, C. and Mason, I. (1995) A role for FGF-8 in the initiation and maintenance of vertebrate limb bud outgrowth. Curr. Biol. **5**, 797-806.

Makarenkova, H., Becker, D.L., Tickle, C. and Warner, A.E. (1997) Fibroblast growth factor 4 directs gap junction expression in the mesenchyme of the vertebrate limb bud. J. Cell Biol. **138**, 1125-1137.

Mann, G. B., Fowler, K. J., Gabriel, A., Nice, E. C., Williams, L. and Dunn, A. R. (1993) Mice with a null mutation of the TGFα gene have abnormal skin architecture, wavy hair and curly whiskers and often develop corneal inflammation. Cell **73**, 249-261.

Marshall, H., Nonchev, S., Sham, M. H., Muchamore, I., Lumsden, A. and Krumlauff (1992) Retinoic aicd alters hindbrain HOX code and induces transformation of rhombomeres 2/3 into a 4/5 identity. Nature **360**, 737-741.

Marshall, H., Studer, M., Popperl, H., Aparicio, S., Kuroiwa, A., Brenner, S. and Krumlauf, R. (1994) A conserved retinoic acid response element required for early expression of the homeobox gene Hoxb-1. Nature. **370**, 567-71

Marshall, H., Morrison, A., Studer, M., Popperi, H. and Krumlauf, R. (1996) Retinoids and *Hox* genes. FASEB J. **10**, 969-978.

McCann, J. P., Owens, P. D. A. and Wilson, D. J. (1991) Chick frontonasal mass excision significantly affects mid-facial development. Anat. Emb. **184**, 171-178.

Mege, R. M., Matsuzaki, F., Gallin, W. J., Goldberg, J. I., Cunningham, B. A. and Edleman, G. D. (1988) Construction of epithelioid sheets by transfection of mouse sarcoma cells with cDNAs for chicken cell adhesion molecules. Proc. Natl. Acad. Sci. USA, **85**, 7274-7278.

Mehta, P. P., Bertram, J. S. and Lowenstein, W. R. (1989) The actions of retinoids on cellular growth correlate with their actions on gap junction communication. J. Cell Biol. **108**, 1053-1065.

Mendelsohn, C., Lohnes, D., Decimo, D., Lufkin, T., LeMeur, M., Chambon, P. and Mark, M. (1994) Function of the retinoic acid receptors (RARs) during development (II) Multiple abnormalities at various stages of organogenesis in RAR double mutants. Development **120**, 2749-2771.

Miki, T., Tottaro, D. P., Fleming, T. P., Smith, C. L., Burgess, W. H., Chan, A. M. and Aaranson, S. A. (1992) Determination of ligand binding secificity by alternative splicing: two distinct growth factor receptors encoded by a single gene. Proc. Natl. Acad. Sci. USA **89**, 246-250.

Miller, J. R. and Moon, R. T. (1997) Signal transduction through β-catenin and specification of cell fate during embryogenesis. Genes Dev. **10**, 2527-2539.

Millicovsky, G., Ambrose, J. H., and Johnston, M. C. (1982) Developmental alterations associated with spontaneous cleft lip and palate in CL/Fr mice. Am. J. Anat., **164**, 29-44.

Milligan, J. F., Matteucci, M. D. and Martin, J. C. (1993) Current concepts in antisense drug design. J. Med. Chem. **36**, 1923-1937.

Milks, L. C., Kumar, N. M., Houghten, R., Unwin, N. and Gilula, N. B. (1988) Topology of the 32 kD gap junction protein determined by site directed antibody localisation. EMBO J. **7**, 2967-2975.

Mina, M., Gluhak, J., Upholt, W.B., Kollar, E.J. and Rogers, B. (1995) Experimental analysis of *Msx-1* and *Msx-2* gene expression during chick mandibular morphogenesis. Dev. Dyn., **202**, 195-214.

Minkoff, R. (1980) Regional variation of cell proliferation within the facial processes of the chick embryo: a study of the role of 'merging' during development. J. Embryol. exp. Morph. **57**, 37-49.

Minkoff, R. (1983) Distribution of gap junctions in mesenchyme during primary palate formation. J. Dent. Res. **236**. abstr. 602

Minkoff, R. (1984) Cell cycle analysis of facial mesenchyme in the chick embryo I Labelled mitoses and continuous labelling studies. J. Embryol. exp. Morphol. **81**, 49-59.

Minkoff, R. and Kuntz, A. (1977) Cell proliferation during morphogenetic change: analysis of frontonasal morphogenesis in the chick embryo employing DNA labelling indicies.J. Embryol. Exp. Morphol. **40,** 101-113.

Minkoff, R. and Kuntz, A. (1978) Cell proliferation and cell density of mesenchyme in the maxillary primordium and adjacent regions during facial development in chick embryos. J. Emb. exp. Morph. **46,** 65-74.

Minkoff, R., Parker, S. B. and Hertzberg, E. L. (1991) Analysis of distribution patterns of gap junctions during development of embryonic chick facial primordia and brain. Development **111**, 509-522.

Minkoff, R., Parker, S. B., Rundus, V. R. and Hertzberg, E. L. (1997) Expression patterns of CX 43 during facial development in chick embryos. Anat. Rec. **248,** 279-290.

Monschau, B., Kremoser, C., Ohta, K., Takana, H., Kaneko, T., Yamada, T., Handwerker, C., Hornberger, M. R., Loschinger, J., Pasquale, E. B., Siever, D. A., Verderame, M. F., Muller, B., Bonhoffer, F. and Drescher, U. (1997) Shared and distinct functions of RAGS and ELF-1 in guiding retinal axons. EMBO J. **16**, 1258-1267.

Moon, R. T., Brown, J. D. and Torres, M. (1997) Wnts modify cell fate and behaviour during vertebrate development. TIG **13**, 157-162.

Mori, C., Nakamura, N., Okamoto, Y., Osawa, M., and Shiota, K. (1994) Cytochemical identification of programmed cell death in the fusing fetal mouse palate by specific labelling of DNA fragmentation. Anat. Embryol. Berl. **190**, 21-8.

Morris, G. M. (1972) Morphogenesis of the malformations induced in rat embryos by maternal hypervitaminosis A. J. Anat. **113,** 241-250.

Morris, G. M. (1973) The ultrastructural effects of excess maternal vitamin A on the primitive streak stage rat embryo. J. Embryol. exp. Morphol. **30,** 219-242.

Morris Kay, G. M. (1993) Retinoic acid and craniofacial development: molecules and morphogenesis. Bioessays **15,** 9-15.

Morris-Kay, G. M., Murphy, P., Hill, R. and Davidson, D. (1991) Effects of retinoic acid excess on expression of Hox 2.9 and Krox 20 and on morphological segmentation of the hindbrain of mouse embryos. EMBO J. **10,** 2985-2995.

Morris-Kay, G., Ruberte, E. and Fukiishi, Y. (1993) Mammalian neural crest and neural crest derivatives. Ann. Anat. **175,** 501-507.

Morris - Kay, G. M. and Sokolova, N (1996) Embryonic development and pattern formation. FASEB J. **10,** 961-968.

Muenke, M., Schell, U., Hehr, A., Robin, N. H., Losken, H. W., Schinzel, A., Pulleyn, L. J., Rutland, P., Reardon, W., Malcolm, S. and Winter, R. M. (1994) A common mutation in the fibroblast growth factor receptor gene in Pfeiffer syndrome. Nat. Genet. **8,** 269-273.

Napoli, J. L. (1996) Retinoic acid biosynthesis and metabolism. FASEB J. **10,** 993-1001.

Nelles, E., Bützler, C., Jung, D., Temme, A., Gabriel, H. D., Dahl, U., Traub, O., Stümpel, F., Jungermann, K., Zielasek, J., Toyka, K. V., Dermietzel, R. and Willecke, K. (1996) Defective propagation of signals generated by sympathetic nerve stimulation in the liver of connexin 32 deficient mice. Proc. Natl. Acad. Sci. USA **93,** 9565-9570.

Nicholson, S.M. and Bruzzone, R. (1997) Gap junctions : getting the message through. Curr. Biol. **7,** R340-R344

Nishikawa, K., Nakanishi, T., Aoki, C., Haltori, T., Takahashi, K. and Taniguchi, S. (1994) Differential expression of homeobox - containing genes *Msx-1* and *Msx-2* and homeoprotein MSX-2 expression during chick craniofacial development. Biochem. Mol. Biol. Int. **32,** 763-71.

Niswander, L. and Martin, G.R. (1992) Fgf-4 expression during gastrulation, myogenesis, limb and tooth development in the mouse. Development 114, 755-768.

Niswander, L. and Martin, G.R. (1993) FGF-4 and BMP-2 have opposite effects on limb growth. Nature 361, 68-71.

Niswander, L. A., Tickle, C., Vogel, A., Booth, I. and Martin, G. R. (1993) FGF-4 replaces the apical ectodermal ridge and directs outgrowth and patterning of the limb. Cell 75, 579-587.

Nittenberg, R., Patel, K., Joshi, Y., Krumlauf, R., Wilkinson, D. G., Brickell, P. M., Tickle, C. and Clarke, J. D. (1997) Cell movements, neuronal organisation and gene expression in hindbrains lacking morphological boundaries. Development 124, 2297-306

Noden, D.M. (1975) An analysis of the migratory behavior of avian cephalic neural crest cells. Dev. Biol. 42, 106-130.

Noden, D.M. (1978a) Control of avian cephalic neural crest cytodifferentiation. I . Skeletal and connective tissues. Dev. Biol. 67, 296-312.

Noden, D. M. (1978b) Control of avian cephalic neural crest cytodifferentiation. II Neural tissues. Dev. Biol. 67, 313-329.

Noden D. M. (1983a) The embryonic origins of avian cephalic and cervical muscles and associated connective tissues. Am. J. Anat. 168, 257-276.

Noden D. M. (1983b) The role of the neural crest in patterning of avian cranial skeletal, connective and muscle tissues. Dev. Biol. 96, 144-165.

Noden, D. M. (1988) Interactions and fates of avian craniofacial mesenchyme. Development 103 (suppl.) 121-140.

Ohta, K., Nakamura, M., Hirowaka, K., Tanaka, S. Iwamaa, A., Suda, T., Ando, M. and Tenaka, H. (1996) The receptor tyrosine kinase Cek-8 is transiently expressed on subtypes of motorneurons in the spinal cord during development. Mech Dev. 54, 59-69.

Ohta, K., Iwamasa, H., Drescher, U., Terasaki, H. and Tenaka, H. (1997) The inhibitory effect on neurite outgrowth of motoneurones exerted by the ligands ELF-1 and RAGS. Mech. Dev. 64, 127-135.

Ohuchi, H., Yoshioka, H., Tanaka, A., Kawakami, Y., Nohno, T. and Noji, S. (1994) Involvement of androgen-induced growth factor (*FGF-8*) in mouse embryogenesis and morphogenesis. Biochem. Biophys. Res. Comm. 204, 882-888.

Orioli, D., Henkemeyer, M., Lemke, G., Klein, R. and Pawson, T. (1996) Sek-4 and Nuk receptors cooperate in guidance of commissural axons and in palate formation. EMBO J. 15, 6035-6049.

Orioli, D. and Klein, R. (1997) The Eph receptor family: Axonal guidance by contact repulsion. TIG 9, 354-359.

Ornitz, D. M. and Leder, P (1992) Ligand specification and heparin dependence of fibroblast growth factor receptors 1 and 3. Biol. Chem. 267, 16305-16311

Ornitz, D. M., Xu, J., Colvin, J. S., McEwen, D. G., MacArthur, C. A., Coulier, F., Gao, G., and Goldfarb, M. (1996) Receptor specificity of the fibroblast growth factor family. J. Biol. Chem. 271, 15292-15297.

Olsen, D. J. and Moon, R. T. (1992) Distinct effects of ectopic expression of *Wnt-1*, Activin B and bFGF on gap junction permeability in 32-cell *Xenopus* embryos. Dev. Biol., 151, 204-212.

Osumi-Yamashita, N., Ninomiya, Y., Doi, H. and Eto, K. (1994) The contribution of both forebrain and midbrain crest cells to the mesenchyme in the frontonasal mass of mouse embryos. Dev. Biol. 164, 409-419.

Pardanaud, L., Altmann, C., Kitos, P., Dieterlen-Lievre, F. and Buck, C. A. (1987) Vasculogenesis in the early quail blastodisc as studied with a monoclonal antibody recognising endothelial cells. Development 100, 399-349.

Patel, K., Nittenberg, R., D'Souza, D., Burt, I. D., Wilkinson, D. G. and Tickle, C. (1996) Expression and regulation of Cek-8, a cell-cell signaliing receptor in developing chick limb buds. Development 122, 1147-1155.

Patten, B.M. (1961) Human Embryology, McGraw-Hill, New-York.

Patterson, S.B., Johnston, M.C., and Minkoff, R. (1984) An implant labeling technique employing sable hair probes as carriers for ^{3}H-thymidine: Applications to the study of facial morphogenesis. Anat. Rec. 210, 525-536.

Patterson, S.B. and Minkoff, R. (1985) Morphometric and autoradiographic analysis of frontonasal development in the chick embryo. Anat. Rec. **212**, 90-99.

Pellier, V. and Astic, L. (1994) Detection of apoptosis by electron microscopy and in situ labelling in the rat olfactory pit. NeuroReport, **5**, 1429-1432.

Perez, J. R., Li, Y., Stein, L. A., Majumder, S. and Naraganan, R. (1994) Sequence independant induction of Sp1 transcription factor activity by phosphorothioate ODNs. Proc. Natl. Acad. Sci. USA **91**, 5959-5961.

Pitts, J. D., Hamilton, A. E., Kam, E. Burk, R. R. and Murphy, J. P. (1986) Retinoic acid inhibits junctional communication between animal cells. Carcinogenesis **7**, 1003-1010.

Pratt, R. M., Goulding, E. H. and Abbot, B. D. (1987) Retinoic acid inhibits migration of cranial neural crest cells in the cultured mouse embryo. J. Craniofac. Genet. Dev. Biol. **7**, 205217.

Reardon, W., Winter, R. M., Rutland, P., Pulleyne, L. J., Jones, B. M. and Malcolm, S. (1994) Mutations in the FGF2 receptor gene causes Crouzon syndrome. Nature Genet. **8**, 98-103.

Rathbone, M. P., Middlemiss, P. J., Kim, J. K., Gysbers, J. W., DeForge, S. P., Smith, R. W. and Hughes, D. W. (1992) Adenosine and its nucleotides stimulate proliferation of chick astrocytes and human astrocytoma cells. Neurosci-Res. **13**, 1-17

Reaume, A. G., Sousa, P. A., Kulkarni, S., Langille, B. L., Zhu, D., Davies, T. C., Juneja, S. C., Kidder, G. M., Rossant, J. (1995) Cardiac malformation in neonatal mice lacking connexin43. Science **267**, 1831-1833.

Richman, J.M. and Delgado J.L. (1995) Locally released retinoic acid leads to facial clefts in the chick embryo but does not alter the expression of receptors for fibroblast growth factor. J. Craniofac. Dev. Biol. **15**, 190-204.

Richman, J.M. and Tickle, C. (1989) Epithelia are interchangeable between facial primordia of chick embryos and morphogenesis is controlled by the mesenchyme. Dev. Biol. **136**, 201-210.

Richman, J.M. and Tickle, C. (1992) Epithelial-mesenchymal interactions in outgrowth of limbs and facial primordia in chick embryos. Dev. Biol. **154**, 299-308.

Richman, J. M., Herbert, M., Matovinovic, E. and Walin, J. (1997) Effect of FGFs on outgrowth of facial mesenchyme. Dev. Biol. **189**, 135-147.

Rickmann, M., Fawcett, J. W. and Keynes, R. J. (1985) The migration of neural crest cells and the growth of motor axons through the rostral half of the chick somite. J. Embryol. exp. Morphol. **90**, 437-455.

Rivedal, E., Yamasaki, H. and Sanner, T. (1994) Inhibition of gap junction intercellular communication in Syrian hamster embryo cells bt TPA, retinoic acid and DDT. Carcinogenesis **15**, 689-694.

Robert. B., Sassoon, D., Iacq, B., Gehring, W. and Buckingham, M. (1989) Hox-7, a mouse homeobox gene with a novel pattern of expression during embryogenesis. EMBO J. **8**, 91-100.

Robert, B., Lyons, G., Simandl, B. K., Kuroiwa, A. and Buckingham, M. (1991) The apical ectodermal ridge regulates *Hox-7* and *Hox-8* gene expression in developing chick limb buds. Genes Dev. **5**, 2363-2374.

Robinson, S. R., Hampson, E. C. G. M., Munro, M. N. and Vaney, D. I. (1993) Unidirectional coupling of gap junctions between neuroglia. Science **262**, 1072-1074.

Ros, M. A., Lyons, G., Kosher, R. A., Upholt, W. B., Coelho, C. N. D. and Fallon, J. F. (1992) Apical ridge dependent and independent mesodermal domain and GHox-8 expression in chick limb buds. Development **116**, 811-818.

Rowe, A., Richman, J.M. and Brickell, P.M. (1992) Development of the spatial pattern of retinoic acid receptor - beta transcripts in embryonic chick facial primordia. Development, **114**, 805-813.

Ruangvoravat, C. P. and Lo, C. W. (1992) Connexin 43 expression in the mouse embryo: localisation of transcripts within developmentally significant domains. Dev. Dyn. **194**, 261-281.

Ruiz-i-Altaba, A. and Jessell T. (1991) Retinoic acid modifies the pattern of cell differentiation in the central nervous sytem of neurula stage Xenopus embryos. Development **112**, 945-958.

Saez, J. C., Spray, D. C., Nairn, A. C., Hertzberg, E., Greengard, P. and Bennett, M. V. (1986) cAMP increases junctional conductance and stimulates phosphorylation of the 27-kDa principal gap junction polypeptide. PNAS, **83**, 2473-2477.

Sajjadi, F. G. and Pasquale, E. B. (1993) Five novel avian Eph-related tyrosine kinases are differentially expressed. Oncogene **8**, 1807-1813.

Satokata, I and Maas, R. (1994) Msx-1 deficient mice exhibit cleft palate and abnormalities of craniofacial and tooth development. Nat. Genet. **6**, 348-356.

Saunders, J. W. (1948) The proximo-distal sequence of origin of the parts of the chick wing and role of the ectoderm. J. exp. Zool. **108**, 363-403.

Savage, M. P., Hart, C. E., Riley, B. B., Sasse, J., Olwin, B. B. and Fallon, J. F. (1993) Distribution of FGF-2 suggests it has a role in chick limb bud growth. Dev. Dyn. **198**, 159-170.

Searls, R.L. and Janners, M.Y. (1971) The initiation of limb bud outgrowth in the embryonic chick. Dev. Biol. **24**, 198-213.

Sechrist, J., Serbedzija, G. N., Scherson, T., Fraser, S. E. and Bronner-Fraser, M. (1992) Segmental migration of the hindbrain neural crest does not arise from its segmental generation. Development **118**, 691-703.

Scherer, S. S., Deschànes, S. M., Xu, Y., Grinspan, J. B., Fischbeck, K. H. and Paul, D. L. (1995) Connexin 32 is a myelin related protein in the PNS and CNS. J. Neurosci. **15**, 8281-8294.

Schlessinger, J. and Ullrich, A. (1992) Growth factor signalling by receptor tyrosine kinases. Neuron, **9**, 383-391.

Schuler, C. F., Guo, Y., Majumder, A and Luo, R. (1991) Molecular and morphological changes during the epithelial-mesenchymal transformation of palatal shelve medial edge epithelia in vitro. Int. J. Dev. Biol. **35**, 463-472.

Stein, C.A., Mori, K., Loke, S. L., Subasinge, C., Shinozuka, K.,

Cohen, J. S. and Neckers, L. M. (1988) Phosphorothioate and normal

deoxyribonucleotides with 5'-linked acridine: characterisation and preliminary kinetics of

cellular uptake. Gene **72**, 333-341.

Schuler, C. F., Halpern, D. E., Guo, Y. and Sank, A. C. (1992) Medial edge epithelia fate traced by cell lineage analysis during epithelial-mesenchymal transformation in vivo. Dev. Biol. **154,** 318-330.

Shaw, G. M., Wasserman, C. R., Lammer, E. J., O'Malley, C. D., Murray, J. C., Basart, A. M. and Tolarova, M. M. (1996) Orofacial clefts, parental cigarette smoking and TGFα gene variants. Am. J. Hum. Genet. **58,** 511-61.

Shuttleworth, J. and Coleman, A. (1988) Antisense oligonucleotides-directed cleavage of mRNA in Xenopus oocytes and eggs. EMBO J. **7,** 427-434.

Simeone, A., Avantaggiato, V., Moroni, M. C., Mavilio, F., Arra, C., Cotelli, F., Nigro, V. and Acampora, D. (1995) Retinoic acid induces stage-specific antero-posterior transformation of rostral central nervous system. Mech-Dev. **51,** 83-98

Simon, A. M., Goodenough, D. A., Li, E. and Paul, D. L. (1997) Female infertility in mice lacking Cx37. Nature **385,** 525-529.

Simpson, I., Rose, B. and Lowenstein, W. R. (1977) Size limit of molecules permeating the junctional membrane channels. Science, **195,** 294-296.

Small, K. M., and Potter, S. S. (1993) Homeotic transformations and limb defects in *Hox a11* mutant mice. Genes Dev. **7,** 2318-28

Smith, S. C. and Monie, I. W. (1969) Normal and abnormal nasolabial morphogenesis in the rat. Teratology **2,** 1-12.

Smith, A. L., Robinson, V., Patel, K. and Wilkinson, D. G. (1997). The Eph4A and EphB1 receptor tyrosine kinases and ephrin-B2 ligand regulate targeted migration of branchial neural crest cells. Curr. Biol. **7,** 561-570.

Statuto, M., Audebet, C., Tonoli, H., Selmi, S. R., Rousset, B.and Muriarisilem, Y. (1997) Restoration of cell-cell communication in thyroid cell lines by transfection with and stable expression of Cx32 gene. J. Bio. Chem. **39,** 24710-24716.

Stein, C. A., Subasinghe, C. and Cohen, J. S. (1991) Physicochemical properties of phosporothioated ODNs. Nuc. Acid Res. **16,** 3209-3221.

Stein, C. A. and Cheng, Y. C. (1993) Antisense oligonucleotides as therapeutic agents - is the bullet really magical ? Science 261, 1004-1012.

Stein, J., Mulliken, J. B., Stal, S., Gasser, D. L., Malcolm, S., Winter, R., Blanton, S. H., Amos, C., Seemanova, E and Hecht, J. T. (1995) Nonsyndromic cleft lip with or without cleft palate: evidence of linkage to Bcl3 in 7 multigeneration families. Am. J. Hum. Genet., 57, 257-72.

Stevenson, M. and Iversen, P. L. (1989) Inhibition of HIV type 1 mediated cytopathic effects by poly(L)lysine conjugatedsynthetic antisense ODNs. J. Gen. Virol. 70, 2673-2682.

Streeter, G.L. (1948) Developmental horizons in the human embryo. Contr. Embryol. Carn. instn. Washington. 32, 133-203.

Sucov, H. M., Izisua-Belmonte, J. C., Ganan, Y and Evans, R. M. (1995) Mouse embryos lacking RXRα are resistant to retinoic acid-induced limb defects. Development, 121, 3997-4003.

Sulik, K. K., Johnston, M. C., Ambrose, L. J. H. and Dorgan, D. (1979) Phenytoin (Dilantin)- induced cleft lip and palate in A/J mice: A scanning and transmission electron microscopic study. Anat. Rec. 195, 243-256.

Summerbell, D., Lewis, J. H. and Wolpert, L. (1973) Positional information in chick limb morphogenesis. Nature 244, 492-496.

Summerbell, D. (1974) A quantitative analysis of the effect of excision of the AER from the chick limb-bud. J. Embryol. exp. Morphol. 32, 651-660.

Suzuki, H.R., Padanilam, B.J., Vitale, E., Ramirez, F. and Solursh, M. (1991) Repeating developmental expression of G-Hox 7, a novel homeobox-containing gene in the chicken. Dev. Biol. 148, 375-388.

Suzuki, A., Ueno, N. and Hemmati-Brivaniou (1997) Xenopus msx1 mediates epidermal induction and neural inhibition by BMP4. Development 124, 3037-3044.

Tamarin, A., Crawley, A., Lee, J., and Tickle, C. (1984) Analysis of upper beak defects in chicken embryos following treatment with retinoic acid. J. Embryol. exp. Morph. 84, 105-123.

Tan, S. S. and Morris-Kay, G. M. (1985) The development and distribution of te cranial neural crest in the rat embryo. Cell. Tissue. Res. **240,** 403-416

Tanaka, H., Fukushima, M., Ohta, K., Sudo, A., Shirabe, K. and Takeshita, M. (1997) Commitment of motorneurone progenitors of chick embryo along the A-P axis. Dev. Neurosci.**19,** 106-111.

Thesleff, I., Vaahtokari, A. and Partananen, A. M. (1995) Regulation of organogenesisi. Common molecular mechanisms regulating the development of teeth and other organs. Int. J. Dev. Biol. **39,** 35-50.

Thomas, J. T., Kilpatrick, M. W., Lin, K., Erlacher, L., Lembessis, P., Costa, T., Tsipouras, P. and Luyten, F., P. (1997) Disruption of human limb morphogenesis by a dominant negative mutation in CDMP1. Nat. Gen. **17,** 58-64.

Thompson, N. J., Howell, J. M., Pitt, G. A. J. and McLaughlin C. I. (1969) The biological activity of retinoic acid in the domestic fowl and the effects of vitamin A deficiency on the chick embryos. Br. J. Nutr. **23,** 471-490.

Thorogood, P., Smith, L., Nicol, A., McGinty, R. and Garrod, D. (1982) Effects of Vitamin A on the behaviour of migratory neural crest cells *in vitro*. J. Cell Sci. **57,** 331-350.

Tickle, C. Alberts, B., Wolpert, L. and Lee, J. (1982) Local application of retinoic acid to limb bud mimics action of the polarising region. Nature **296,** 564-566.

Tickle, C. (1991) Retinoic acid and chick limb bud development. Development (suppl.) **1,** 113-21.

Torres, M. A., Yang-Snyder, J., Purcell, S. M., DeMarais, A. A., McGrew, L L. and Moon, R. T. (1996) Activities of the *Wnt-1* class of secreted signaling factors are antagonised by the *Wnt*-5A class and by a dominant negative cadherin in early *Xenopus* development. J. Cell Biol. **133,** 1123-1137.

Trasler, D. (1968) Pathogenesis of cleft lip and its relation to embryonic face shape in A/J and C57BL mice. Teratology **1,** 33-50

Turin, L. and Warner, A. (1977) Carbon dioxide reversibly abolishes ionic communication between cells of early amphibian embryo. Nature, **270,** 56-57.

Turin, L. and Warner, A. E. (1980) Intracellular pH in early Xenopus embryos: its effect on current flow between blastomeres. J. Physiol **300**, 489-504.

Tuzi, N. L. and Gullick, W. J. (1994) *eph*, the largest known family of putative growth factor receptors. Br. J. Cancer **69**, 417-421.

Unwin, P. N. T. and Zampighi, G. (1980) Structure of the junction between communicating cells. Nature **283**, 545-549.

Urist, M. R. (1965) Bone: formation by autoinduction. Science, **150**, 893-899.

Vanio, S., Karavanova, I., Jowett, A. and Thesleff, I. (1993) Identification of BMP-4 as a signal mediating secondary induction between epithelial and mesenchymal tissues during early tooth development. Cell, **75**, 45-58.

Veneestra, R. D. (1996) Size and selectivity of gap junction channels formed from different connexins. J. Bioen. Biomemb. **28**, 327-337.

Vogel, A., Roberts-Clarke, D., Niswander, L. (1995) Effect of FGF on gene expression in chick limb bud cells *in vivo* and *in vitro*. Dev. Biol. **171**, 507-520.

Vogel, A., Rodriguez, C. and Izpisua-Belmonte, J. C. (1996) Involvement of FGF-8 in initiation, outgrowth and patterning of the vertebrate limb. Development **122**, 1737-1750.

Wagner, R., Matteucci, M., Lewis, J., Gutierrez, A., Moulds, C. and Froehler, B. (1993) Antisense gene inhibiton by oligonucleotides containing C-5 propyne pyrimidines. Science **260**, 1510-1513.

Wagner, R.W. (1994) Gene inhibition using antisense oligodeoxynucleotides. Nature **372**, 333-335.

Wall, N.A. and Hogan, B.L.M. (1995) Expression of bone morphogenetic protein-4 (*Bmp-4*), bone morphogenetic protein-7 (*Bmp-7*), fibroblast growth factor-8 (*Fgf-8*) and sonic hedgehog (*Shh*) during branchial arch development in the chick. Mech. Dev. **53**, 383-392.

Wang, K. Y., Juriloff, D. M. and Diewert, V. M. (1995) Deficient and delayed primary palatal fusion and mesenchymal bridge formation in cleft lip liable strains of mice. J. Craniof. Genet. Dev. Biol. **15**, 99-166.

Wang, H. U. and Anderson, D. J. (1997) Eph family transmembrane ligands can mediate repulsive guidance and motor axon outgrowth. Neuron **18**, 383-396.

Warner, A. E. (1985) The role of gap junctions in amphibian development. J. Embryol. exp. Morphol. **89** (suppl), 365-380.

Warner, A. E., Guthrie, S. C., Gilula, N. B. (1984) Antibodies to gap-junction protein selectively disrupt junctional communication in the early amphibian embryo. Nature, *311*, 127-131.

Warner, A., Clements, D. K., Parikh, S., Evans, W. H. and DeHaan, R.L. (1995) Specific motifs in the external loops of connexin proteins can determine gap junction formation between chick heart myocytes. J. Physiol. **488**, 721-728.

Watanabe, A. and Ide, H. (1993) Basic FGF maintains some characteristics of the progress zone of the chick limb bud in cell culture. Dev. Biol. **159**, 223-231.

Watanabe, Y. and Le Douarin, N. (1996) A role for *BMP-4* in the development of subcutaneous cartilage. Mech. Dev. **57**, 69-78.

Wedden, S., (1986) Pattern formation and the effects of retinoids on chick facial morphogenesis. PhD thesis. University of London.

Wedden, S. E. (1987) Epithelial-mesenchymal interactions in the development of chick facial primordia and the target of retinoid action. Development **99**, 341-351.

Wedden, S.E. and Tickle, C. (1986) Quantitative analysis of the effects of retinoids on facial morphogenesis. J. Craniofac. Genet. Dev. Biol. (suppl) **2**, 169-178.

Wedden, S. E., Lewin-Smith, M. R. and Tickle, C. (1986) The patterns of chondrogenesis of cells from facial primordia of chick embryos in micromass culture. Dev. Biol. **117**, 71-82.

Weiss, B., Davidkova, G., and Zhang, S. P. (1997) Antisense strategies in neurobiology. Neurochem. Int **31**, 321-348.

Werner, R., Levine, E., Rabadon-Diehl, C. and Dahl, G. (1989) Formation of hybrid cell-cell channels. Proc. Natl. Acad. Sci. USA, **86**, 5300-5384.

White, T. W. and Bruzzone, R. (1996) Multiple connexin proteins in single intercellular channels : Connexin compatibility and functional consequences. J. Bioen. Biomemb. **28**, 339-350.

Wilke, T. A., Gubbels, S., Schwartz, J. and Richman, J. (1997) Expression of FGFRs (FRGR1, FGFR2, FGFR3) in the developing head and face. Dev. Dyn. **210**, 41-52.

Will, L. A. and Meller, S. M. (1981) Primary palate development in the chick. J. Morph. **169**, 185-196.

Wilson, J. G., Roth, C. and Warkany, J. (1953) An analysis of the syndrome of malformation induced by maternal vitamin A deficiency. Effects of restoration of vitamin A at various times during gestation. Am. J. Anat. **92**, 189216.

Winning, R. S. and Sargent, T. D. (1994) Pagliaccio, a member of the Eph family of reeceptor tyrosine kinases has localised expression in a subset of neural crest and neural tissues in Xenopus laevis embryos. Mech Dev. **46**, 219-229.

Winograd, J., Reilly, M., Roe, R., Lutz, J., Laughner, E., Xu, X., Asakura, T., vander Kolk, C., Strandberg, J. D. and Semenza, G. L. (1997) Perinatal lethality and multiple craniofacial malformations in *Msx-2* transgeneic mice. Hum. Mol. Genet. **6**, 369-379.

Wood, H., Pall, G. and Morris-Kay, G. (1994) Exposure to retinoic acid before or after the onset of somitogenesis reveals separate effects on rhombomeric segmentation and 3' HoxB gene expression domains. Development **120**, 2279-2285.

Woolf, T. M., Melton, D. A. and Jennings, C.G.B (1992) Specificity of antisense oligonucleotides *in vivo*. PNAS **89**, 7305-7309.

Wrana, J. L., Attisano, L., Wieser, R., Ventura, F. and Massague, J.(1994) Mechanism of activation of the TGFbeta receptor. Nature **370**, 341-347.

Xu, Q., Alldus, G., Holder, N. and Wilkinson, D. G. (1995) Expression of truncated *Sek-1* receptor tyrosine kinase disrupts the segmental restriction of gene expression in the *Xenopus* and zebrafish hindbrain. Development **121**, 4005-4016.

Yancey, S. B., Biswal, S. and Revel, J. P. (1992) Spatial and temporal patterns of distribution of the gap junction protein connexin 43 during mouse gastrulation and organogenesis. Development **114**, 203-212.

Woolf, T. M., Jennings, C. G. B., Rebagliati, M. and Melton, D. A. (1990) The stability, toxicity and effectiveness of unmodified phosphorothioate antisense oligodeoxynucleotides in *Xenopus* oocytes and embryos. Nucleic Acids Research **18**, 1763-1769.

Yayon, A., Klagsbrun, M., Esko, J. D., Leder, P. and Ornitz, D. M. (1991) Cell surface heparin like molecules are required for binding of basic FGF to its high affinity receptor. Cell, **64**, 841-848.

Yayon, A., Zimmer, Y., Guo-Hang, S., Avivi, A., Yarden, Y and Givol, D. (1992) A confined variable region confers ligand specificity on FGF receptors. EMBO J. 11, 1885-1890.

Yee, G. W. and Abbott, U. K. (1978) Facial development in normal and mutant chick embryos. Exp. Zool **206**, 307-322.

Yokouchi, Y., Oshugi, K., Sasaki, H. and Kuroiwa, A. (1991) Chicken homeobox gene *Msx-1* : Structure, expression in limb buds and effects of retinoic acid.

Zhang, H. and Bradley, A. (1996) Mice deficient for BMP2 are nonviable and have defects in amnion/chorion and cardiac development. Development **122**, 2977-2986.

Zhu, D., Caveney, S., Kidder, G.M. and Naus, C. C. G. (1991) Transfection of C6 glioma cells with connexin 43 cDNA : analysis of expression, intercellular coupling and cell proliferation. PNAS **88**, 1883-1887.

Zhu, D., Kidder, G. M., Caveney, S. and Naus, C. C. G. (1992) Growth retardation in glioma cells cocultured with cells overexpressing a gap junction protein. PNAS, **89**, 10218-10221.

Appendices

Appendix 1. Expansion of DiI labelled cell populations in mandibular primordia.

POSITION ON PRIMORDIUM	DiI SPREAD PD x ML (μm)	DIMENSIONS OF PRIMORDIA PD x ML (μm)	AREA OF DiI SPREAD ON PRIMORDIUM (μm²)	AREA OF PRIMORDIUM (μm²)	% AREA OF PRIMORDIUM COVERED BY DiI
C4	352 x 192	400 x1200	67584	480000	14
	720 x 80	1120 x 2320	57600	2598400	2
	528 x 160	960 x 1920	84480	1843200	5
average	533 x 144	827 x 1813	69888 (± 13587)	1640533 (± 107364)	7 (± 6)
B4	577x 1026	1474 x 2436	592002	3590664	17
	480 x 720	1360 x 2160	345600	2937600	12
	625 x 400	1125 x 2000	250000	2250000	11
average	486 x 790	1320 x 2218	395867 ± 176455	2926088 (± 670406)	13 (± 3)
A4	321 x 513	769 x 1538	164673	1182722	14
	350 x 520	890 x 1520	182000	1352800	12
	321 x 513	1282 x 1923	164673	2465286	8
average	331 x 515	980 x 1660	170449 (± 10004)	1666936 (± 696602)	11 (±4)
C3	560 x 80	1200 x 1600	44800	1920000	2
	520 x 50	970 x 1770	26000	1716900	2
	480 x 48	880 x 2000	23040	1760000	1
average	520 x 59	1017 x 1810	23480 (± 21103)	1798967 (±107010)	2 (± 0.5)
B3	272 x 320	768 x 2160	246849	1710342	5
	410 x 290	1200 x 2210	118900	2652000	5
	500 x 250	1750 x 2975	125000	5206250	2
average	394 x 287	1239 x 2448	163583 (± 72175)	3189531 (± 1808880)	4 (± 2)
A3	577 x 833	1795 x 2436	480641	4372620	11
	510 x 890	1720 x 2330	453900	3956000	11
	192 x 641	641 x 1667	123072	1068547	12
average	426 x 788	1385 x 2144	352538 (± 199172)	2581710 (± 1448727)	12 (± 0.5)
C2	192 x 240	1200 x 1760	46080	2112000	2

	210 x 170	1000 x 1920	35700	1920000	1
	192 x 112	800 x 2160	21504	1728000	1
average	198 x 174	1000 x 1947	34428 (±12357)	1920000 (± 1920000)	1 (± 0.6)
B2	320 x 320	720 x 2080	102400	1497600	7
	340 x 250	810 x 2000	85000	1620000	5
	320 x 176	896 x 1920	56320	1720320	3
average	327 x 249	809x 2000	81240 (± 23269)	1612640 (± 111542)	5 (± 2)
A2	115 x 769	1282 x 1795	88435	2301190	4
	120 x 720	672 x 1728	86400	1161216	7
	80 x 320	1600 x 2080	25600	3328000	1
	192 x 800	1280 x 2560	153600	3276800	5
average	127 x 652	1209 x 2041	88509 (± 52278)	2516802 (± 1019762)	5 (± 2)
C1	128 x 513	1026 x 2051	65664	2104326	3
	167 x 420	1110 x 2101	70140	2332110	3
	160 x 240	1280 x 2000	38400	2560000	2
average	152 x 391	1339 x 2051	58068 (± 17179)	2332145 (±227837)	3 (± 0.6)
B1	64 x 192	1090 x 1923	12288	2096070	1
	90 x 244	641 x 1538	21960	985858	2
	240 x 560	1440 x 2240	134400	3225600	4
average	131 x 332	1057 x 1900	56216 (± 67882)	2102509 (± 1119885)	2 (± 1)
A1	160 x 560	1056 x 200	89600	2112000	4
	180 x 600	1270 x 2111	108000	2680970	4
	160 x 640	1120 x 2400	102400	2688000	4
average	167 x 600	1149 x 2170	100000 (± 9432)	2493657 (±330543)	4 (± 0.3)
D1	449 x 513	897 x 2051	230337	1839747	13
	577 x 128	769 x 1667	73856	1281923	6
	513 x 321	950 x 1885	164673	1790557	9
	400 x 240	1200 x 1600	96000	1920000	5
average	485 x 301	1017 x 1730	141217 (± 70886)	1708057 (±289055)	9 (± 3)

Appendix 2. Expansion of DiI labelled cell populations in maxillary primordia.

POSITION ON PRIMORDIUM	DiI SPREAD AP x PD (μm)	DIMENSIONS OF PRIMORDIA AP x PD (μm)	AREA OF DiI SPREAD ON PRIMORDIUM (μm^2)	AREA OF PRIMORDIUM (μm^2)	% AREA OF PRIMORDIUM COVERED BY DiI
I1	288 x 320	1600 x 640	92160	1024000	9
	240 x 544	1392 x 880	130560	1224960	11
	160 x 1040	1280 x 1760	166400	2252800	7
average	229 x 635	1424 x 1093	129707 (± 37127)	1500587 (± 659139)	9 (±2)
H1	641 x 103	1538 x 641	66023	985858	7
	520 x 80	1390 x 700	41600	973000	4
	385 x 64	1410 x 641	24640	903810	3
average	515 x 82	1446 x 661	44088 (± 20803)	954223 (± 44129)	5 (± 2)
H2	385 x 513	1218 x 769	197505	936642	21
	409 x 552	1471 x 740	225768	1088540	21
	500 x 625	1625 x 750	312500	1218750	26
average	431 x 563	1438 x 753	245258 (± 59924)	715684 (± 519836)	23 (±3)
G1	321 x 64	1410 x 577	20544	813570	3
	880 x 160	1680 x 1120	140800	1881600	8
	480 x 192	1600 x 960	92160	1536000	6
average	560 x 139	1563 x 886	84501 (± 60493)	1410390 (± 544982)	6 (±2)
G2	321 x 385	1200x 513	123585	615600	20
	300 x 350	1111 x 454	105000	504394	21
	272 x 320	1040 x 384	87040	399360	22
average	289 x 352	1117 x 450	105208 (± 18273)	506451 (± 108135)	21 (± 1)
F1	103 x 64	962 x 256	6592	246272	3
	250 x 90	1600 x 700	22500	1120000	2
	400 x 48	1520 x 880	19200	1337600	1

average	217 x 67	1361x 612	16097 (± 8396)	901291 (±577602)	2 (± 0.7)
F2	77 x 128	962 x 256	9856	172224	6
	210 x 170	1288 x 400	35700	515200	7
	352 x 240	1584 x 960	84480	1520640	6
average	213 x 179	1278 x 539	43345 (± 37894	738241 (± 698132)	6 (± 0.7)
E1	240 x 240	20 x 15	57600	1920000	3
	352 x 240	1920 x 1120	84480	2150400	4
	256 x 26	1923 x 1154	6656	2219142	0.3
	128 x 577	769 x 1667	73856	1281923	6
	800 x 160	1520 x 1040	128000	1580800	8
average	355x 248.6	1466 x 1316	70118 (± 44030)	1830453 (± 395182)	4 (±3)

Appendix 3. Expansion of DiI labelled cell populations in frontonasal mass and lateral nasal process

POSITION ON PRIMORDIUM	DiI SPREAD PD x ML (μm)	DIMENSIONS OF PRIMORDIA PD x ML (μm)	AREA OF DiI SPREAD ON PRIMORDIUM (μm²)	AREA OF PRIMORDIUM (μm²)	% AREA OF PRIMORDIUM COVERED BY DiI
M2	304 x 224	592 x 1120	68096	663040	10
	560 x 80	800 x 800	44800	640000	7
	416 x 240	832 x 1680	99840	1397760	7
average	427 x 181	741 x 1200	70912 (± 27628)	900267 (± 430996)	8 (± 2)
M3	240 x 224	784 x 1360	53760	1066240	5
	319 x 124	807 x 1191	39556	961137	4
	480 x 80	960 x 1360	38400	1305600	3
average	250 x 143	850 x 1304	43905 (± 8554)	1110992 (± 176538	4 (± 1)
L1	320 x 112	800 x 480	35840	384000	9
	397 x 127	920 x 510	50419	469200	11
	380 x 160	960 x 560	60800	537600	11
average	366x 133	893 x 517	49020 (± 12539)	463600 (± 76953)	10 (±1)
L3	475 x 244	950 x 1282	115900	1217900	10
	352 x 320	704 x 1120	112640	788480	14
	444 x 300	824 x 1109	133200	913816	14
average	424 x 288	826 x 1170	120580 (±11050)	180295 (± 220816)	12 (± 2)
L4	256 x 13	1282 x 950	3328	1217900	0.3
	192 x 18	719 x 521	3456	374599	0.8
	64 x 13	600 x 449	832	269400	0.3
average	171x 15	867x 640	2339 (± 1479)	743650 (± 670691)	0.5 (± 0.03)
K1	80 x 592	592 x 720	47360	426240	11
	109 x 629	597 x 844	68561	503868	13

	112 x 720	520 x 950	80640	494000	16
average	100 x 647	570 x 838	65520 (± 16847)	474703 (± 42259)	14 (± 3)
K2	224 x 300	75 x 17	67200	537600	13
	96 x 720	1520 x 1040	69120	1580800	4
	510 x 160	720 x 1432	81600	1031040	8
average	277 x 393	1195 x 957	72640 (± 7819)	1049813 (± 521853)	8 (± 4)
K3	160 x 384	960 x 1520	61440	1459200	4
	189 x 244	812 x 1447	46116	1174964	4
	240 x 160	720 x 1360	38400	979200	4
average	196x 263	831 x 1442	48652 (± 11727)	1204455 (± 241355)	4 (± 0.1)
K4	64 x 256	641 x 1154	16384	739714	2
	224 x 192	640 x 1280	43008	819200	5
	112 x 320	800 x 800	35840	704000	5
average	133 x768	694 x 1078	31744 (± 13777)	721857 (± 58970)	4 (± 2)
J1	51 x 244	769 x 705	12444	542145	2
	39 x 127	810 x 754	4953	610740	1
	13 x 51	1023 x 962	663	984126	0.1
average	34 x 141	867 x 807	6020 (± 237862)	712337 (± 237862)	1 ± 1

Appendix 4. Expansion of DiI labelled cell populations in maxillary primordia after retinoic acid treatment.

POSITION ON PRIMORDIUM	DiI SPREAD AP x PD (μm)	DIMENSIONS OF PRIMORDIA AP x PD (μm)	AREA OF DiI SPREAD ON PRIMORDIUM (μm²)	AREA OF PRIMORDIUM (μm²)	% AREA OF PRIMORDIUM COVERED BY DiI
I1	320 x 480	1472 x 800	153600	1177600	13
	397 x 416	1291 x 708	16512	914028	18
	384 x 400	1155 x 660	153600	762300	20
average	367 x 432	1306 x 723	107904 (± 79148)	969950 (± 210145)	17 (± 4)
H1	256 x 240	1275 x 659	61440	840225	7
	277 x 251	126 x 600	69527	832920	8
	304 x 200	1173 x 663	60800	777699	8
average	279 x 230	1237 x 661	63922 (± 4864)	816948 (±34186)	8 (± 0.6)
H2	368 x 752	1037 x 610	276736	632570	44
	128 x 560	1092 x 600	71680	655200	11
	282 x 617	1111 x 621	173994	689931	25
average	259 x 643	1062 x 630	174137 (± 102528)	659234 (± 28892)	26 (±16)
G1	321 x 64	1410 x 577	20544	813570	3
	880 x 160	1680 x 1120	140800	1881600	8
	480 x 192	1600 x 960	92160	1536000	6
average	560 x 139	1563 x 886	84501 (± 60493)	1410390 (± 544982)	6 (± 3)
G2	240 x 592	1200 x 513	142080	1449770	10
	320 x 400	1360 x 880	128000	1196800	11
	224 x 720	1040 x 384	161280	944640	17
average	261 x 571	1354x 881	143787 (± 16706)	1197070 (± 252565)	13 (± 4)

F1	368 x 240	1565 x 680	88320	246272	2.7
	176 x 128	736 x 464	22528	1120000	2.0
	240 x 144	1248 x 960	34560	1337600	1.4
average	261 x 171	1183 x 701	48469 (± 35032)	901291 (± 577602)	2 (± 0.7)
F2	272 x 400	1520 x 640	108800	972800	11
	112 x 160	1280 x 800	17920	1024000	2
	400 x 304	1360 x 960	121600	1305600	9
average	261 x 288	1387 x 800	82773 (±56528)	1100800 (± 179200)	7 (±5)

Appendix 5. Expansion of DiI labelled cell populations in frontonasal mass and lateral nasal process after retinoic acid treatment

POSITION ON PRIMORDIUM	DiI SPREAD PD x ML (μm)	DIMENSIONS OF PRIMORDIA PD x ML (μm)	AREA OF DiI SPREAD ON PRIMORDIUM (μm²)	AREA OF PRIMORDIUM (μm²)	% AREA OF PRIMORDIUM COVERED BY DiI
M2	80 x 320	480 x 1040	25600	499200	5
	240 x 336	800 x 1920	80640	1536000	5
	161 x 351	670 x 1710	56511	1145700	5
average	160 x 336	650 x 1557	54250 ($\pm$ 27590)	1060300 ($\pm$ 523649)	5 ($\pm$ 0.1)
M3	160 x 240	640 x 1600	38400	1024000	4
	224 x 320	1088 x 1504	71680	1636350	4
	182 x 277	921 x 1520	50414	1399920	4
average	189 x 279	883 x 1541	53498 ($\pm$ 16853)	1353423 ($\pm$ 308812	4 ($\pm$ 0.2)
L1	400 x 240	1073 x 827	96000	887371	11
	208 x 160	700 x 510	33280	357000	9
	316 x 199	929 x 620	62884	575980	11
average	308 x 200	900 x 652	64055 ($\pm$ 131376)	606784 ($\pm$ 266524)	10 ($\pm$1)
L3	348 x 360	850 x 1200	1252800	1020000	12
	336 x 400	720 x 1360	134400	1183200	11
	362 x 380	861 x 1310	137560	1127910	12
average	349 x 380	810 x 1290	132413 ($\pm$6376)	1110370 ($\pm$ 83002)	12 ($\pm$ 1)
L4	128 x 288	720 x 1888	36864	1359360	3
	80 x 240	880 x 1200	19200	1056000	2
	129 x 237	800 x 1572	30573	1257600	2
average	112 x 255	800 x 1553	28879	1224520	3

				(± 8953)	(±154394)	(± 0.5)
K1	112 x 400	1280 x 800	44800	1024000	4
	192 x 192	528 x 512	36864	270336	14
	320 x 128	750 x 400	40960	300000	14
average	208 x 240	853 x 571	40875	531445	11
			(± 3969)	(±426823)	(± 5)
K2	256 x 352	720 x 1760	90112	1267200	7
	64 x 224	880 x 1280	14336	1126400	1
	364 x 369	1182 x 1297	51216	1275180	4
average	165 x 289	801 x 1543	51888	1222927	4
			(± 37892)	(± 83690)	(± 3)
K3	400 x 480	1040 x 1680	192000	1747200	11
	320 x 288	1040 x 1200	92160	124800	7
	364 x 369	1182 x 1297	134316	1533054	9
average	361 x 379	1087 x 1392	139492	1135018	9
			(± 50121)	(± 881402)	(± 2)
K4	256 x 240	480 x 1520	61440	729600	8
	336 x 288	656 x 1360	96768	892160	11
	320 x 254	510 x 1419	81280	723690	11
average	304 x 261	549 x 1433	79829	781817	10
			(± 17709)	(± 95606)	(± 2)
J1	560 x 640	1520 x 912	358400	1386240	26
	384 x 560	1264 x 886	215040	1119904	19
	576 x 320	1395 x 888	184320	1254105	15
average	34 x 141	1393 x 899	252587	1253416	20
			(± 92915)	(± 133169)	(± 6)

Appendix 6. Outgrowth and extension of control maxillary primordia and primordia after ectoderm removal with Nile Blue Sulphate (treated).

TIME AFTER ECTODERM REMOVED (hours)	AREA OF ECTODERM REMOVED (μm) (AP x PD)	RESULTS Dimensions of Primordia (μm).	
		Control (AP x PD)	Treated (AP x PD)
0	900 x 240	625 x 438	625 x 438
0	900 x 420	750 x 438	750 x 438
0	887x 450	938 x 594	937 x 594
0	900 x 500	938 x 625	938 x 594
0	767 x 410	938 x 531	938 x 563
0	656 x 459	720 x 400	720 x 400
0	833 x 433	800 x 480	800 x 480
0	740 x 370	870 x 522	870 x 522
0	759 x 379	833 x 467	833 x 467
0	741 x 444	781 x 500	781 x 500
0	735 x 412	758 x 485	758 x 485
0	1438 x 625	895 x 526	895 x 526
4	1333 x 533	938 x 625	938 x 438
4	1188 x 513	875 x 563	875 x 500
4	1053 x 368	1350 x 600	1350 x 550
4	882 x 353	1190 x 476	1190 x 429
4	1000 x 353	1591 x 500	1591 x 409
4	941 x 353	1217 x 609	1174 x 522
4	882 x 353	1227 x 682	1227 x 636
4	1250 x 400	1227 x 636	1227 x 545
4	1053 x 421	1194 x 645	1194 x 613
4	1500 x 500	1250 x 656	1250 x 594
4	1176 x 471	1250 x 667	1250 x 542
4	1368 x 368	1059 x 588	1059 x 471
8	1800 x 333	875 x 625	875 x 438
8	1133 x 666	938 x 563	938 x 438
8	1467 x 600	895 x 579	895 x 474
8	1286 x 476	1667 x 600	1667 x 467
8	962 x 462	1800 x 867	1733 x 667
8	1200 x 450	1500 x 667	1500 x 556
8	1042 x 292	1300 x 650	1300 x 600
8	1333 x 1000	917 x 792	1033 x 633
8	1318 x 818	1375 x 738	1318 x 636
8	1667 x 417	1000 x 632	1000 x 526
12	1020 x 660	850 x 563	850 x 375
12	1333 x 333	1333 x 583	1250 x 500
12	833 x 444	1515 x 788	1515 x 667
12	1111 x 556	1176 x 765	1176 x 647
12	789 x 474	1176 x 765	1176 x 647
12	1063 x 563	1235 x 765	1176 x 588
12	1000 x 440	1471 x 765	1471 x 706

12	938 x 438	1136 x 636	1136 x 545
12	1250 x 500	1395 x 698	1395 x 651
12	1200 x 667	1222 x 611	1222 x 528
12	1000 x 600	1296 x 630	1296 x 593
12	1666 x 333	1250 x 750	1250 x 417
18	792 x 417	1294 x 824	1235 x 706
18	833 x 375	1471 x 706	1471 x 647
18	857 x 381	1294 x 706	1235 x 588
18	769 x 385	1320 x 680	1320 x 600
18	667 x 333	1560 x 640	1460 x 560
18	1059 x 474	1320 x 840	1200 x 720
18	1389 x 500	1600 x 720	1600 x 600
18	556 x 389	1190 x 667	1190 x 571
18	882 x 353	1400 x 800	1400 x 480
18	1667 x 600	1571 x 786	1571 x 642
18	840 x 540	875 x 563	875 x 438
18	780 x 600	938 x 563	938 x 438
24	824 x 412	1250 x 679	1250 x 464
24	667 x 381	1474 x 789	1368 x 684
24	1190 x 571	1647 x 706	1647 x 588
24	1000 x 467	1714 x 800	1714 x 571
24	833 x 444	1667 x 714	1667 x 476
24	1063 x 438	1458 x 750	1458 x 625
24	957 x 565	1818 x 682	1818 x 591
24	833 x 500	1667 x 857	1667 x 809
24	1316 x 632	1467 x 733	1467 x 600
24	1316 x 474	1200 x 667	1200 x 600
24	2000 x 333	1000 x 750	938 x 438
48	1200 x 400	3200 x 1667	3200 x 1467
48	1067 x 467	2056 x 1500	2056 x 1389
48	1000 x 600	1667 x 1111	1667 x 1111
48	1250 x 563	1765 x 1118	1765 x 1118
48	1250 x 313	2000 x 1154	2000 x 1000
48	952 x 429	1250 x 938	1250 x 875
48	714 x 333	1778 x 1111	1778 x 1056
48	625 x 375	1889 x 889	1994 x 889
48	1000 x 333	1667 x 1000	1722 x 944
48	556 x 389	1667 x 1056	1667 x 1056
48	833 x 389	1389 x 1000	1389 x 944

Appendix 7 Outgrowth and extension of control maxillary primordia and primordia after ectoderm removal with Nile Blue Sulphate and FGF-2 application.

TIME AFTER ECTODERM REMOVED AND FGF-2 TREATMENT (hours)	AREA OF ECTODERM REMOVED (μm) (AP x PD)	RESULTS Dimensions of Primordia (μm). Control (AP x PD)	Treated (AP x PD)
4	871 x 286	714 x 476	714 x 476
4	800 x 300	812 x 531	812 x 490
4	750 x 500	882 x 545	882 x 500
4	800 x 400	806 x 455	806 x 364
4	870 x 435	845 x 548	845 x 516
8	1056 x 370	856 x 459	856 x 459
8	856 x 359	820 x 557	820 x 492
8	800 x 400	914 x 514	914 x 514
12	800 x 400	870 x 696	870 x 652
12	914 x 357	1087 x 609	1087 x 609
12	970 x 435	1191 x 681	1234 x 638
12	1087 x 478	1579 x 632	1579 x 632
12	1000 x 500	1277 x 723	1277 x 723
18	1250 x 500	1304 x 783	1304 x 696
18	800 x 500	1682 x 819	1591 x 819
18	800 x 500	1406 x 625	1406 x 625
18	1182 x 471	2095 x 762	2095 x 714
18	938 x 500	1423 x 731	1423 x 731
24	1077 x 385	1538 x 667	1538 x 564
24	1000 x 400	1661 x 870	1661 x 957
24	950 x 350	1629 x 710	1629 x 710
24	1864 x 364	1529 x 762	1529 x 762
24	1126 x 370	1611 x 815	1611 x 667
48	1600 x 400	2100 x 1100	2100 x 1100
48	1182 x 273	2850 x 1000	2850 x 1000
48	1000 x 400	2619 x 1048	2619 x 1048
48	1000 x 467	2000 x 1000	2000 x 1000

Appendix 8. Outgrowth and extension of control maxillary primordia and primordia after ectoderm removal with Nile Blue Sulphate and FGF-4 application.

TIME AFTER ECTODERM REMOVED AND FGF-4 TREATMENT (hours)	AREA OF ECTODERM REMOVED (µm) (AP x PD)	RESULTS Dimensions of Primordia (µm).	
		Control (AP x PD)	Treated (AP x PD)
4	1176 x 500	917 x 500	917 x 417
4	1176 x 582	909 x 590	909 x 545
4	1471 x 582	909 x 545	864 x 545
4	1176 x 624	909 x 545	909 x 545
4	1176 x 412	909 x 545	909 x 545
8	786 x 357	1400 x 600	1350 x 550
8	720 x 450	1176 x 588	1178 x 512
8	830 x 545	1000 x 593	1000 x 583
8	1071 x 500	1200 x 750	1200 x 600
8	1071 x 357	1200 x 700	1200 x 650
8	1071 x 643	1260 x 600	1150 x 600
12	1063 x 625	1500 x 683	1500 x 600
12	1000 x 357	1136 x 690	1136 x 646
12	714 x357	1136 x 690	1136 x 645
12	1000 x 625	1200 x 600	1096 x 600
16	1500 x 450	1287 x 696	1287 x 652
16	1350 x 500	1150 x 609	1087 x 609
16	1250 x 500	1304 x 696	1304 x 739
16	1600 x 450	1435 x 725	1435 x 713
16	1750 x 500	1301 x 870	1301 x 870
24	1176 x 529	1316 x 789	1316 x 789
24	1125 x 622	1167 x 783	1167 x 783
24	824 x 294	1176 x 788	1176 x 788
24	1500 x 500	1087 x 765	1087 x 765
48	1176 x 882	1975 x 1100	1975 x 1100
48	882 x 882	1866 x 1000	1841 x 989
48	1118 x 294	1922 x 1048	1922 x 1020
48	882 x 471	1811 x 1076	1800 x 1076

Appendix 9 Outgrowth and extension of control maxillary primordia and primordia after ectoderm removal with Nile Blue Sulphate and BMP-4 application.

TIME AFTER ECTODERM REMOVED AND BMP-4 TREATMENT (hours)	AREA OF ECTODERM REMOVED (μm) (AP x PD)	RESULTS Dimensions of Primordia (μm).	
		Control (AP x PD)	Treated (AP x PD)
4	920 x 497	882 x 588	882 x 588
4	1100 x 520	882 x 588	882 x 588
4	978 x 478	1111 x 627	1111 x 627
8	876 x 549	1323 x 588	1353 x 529
8	922 x 480	1309 x 649	1309 x 649
8	1026 x 556	1207 x 755	1207 x 617
8	1011 x 550	1107 x 707	1107 x 636
12	882 x 422	1333 x 667	1333 x 593
12	1090 x 500	1333 x 733	1333 x 667
12	1177 x 549	1158 x 632	1158 x 626
12	1000 x 467	1176 x 706	1176 x 588
18	920 x 472	714 x 1379	647 x 1429
18	1091 x 511	714 x 1349	665 x 1429
18	1290 x 605	733 x 1333	600 x 1333
18	1240 x 599	660 x 1277	660 x 1277
24	891 x 490	1875 x 750	1875 x 625
24	981 x 571	1647 x 882	1647 x 588
24	1026 x 532	1786 x 786	1786 x 714
24	1100 x 541	1680 x 760	1660 x 640

Appendix 9 Outgrowth and extension of control maxillary primordia and primordia after ectoderm removal with Nile Blue Sulphate and BMP-4 application.

TIME AFTER ECTODERM REMOVED AND BMP-4 TREATMENT (hours)	AREA OF ECTODERM REMOVED (μm) (AP x PD)	RESULTS Dimensions of Primordia (μm).	
		Control (AP x PD)	Treated (AP x PD)
4	920 x 497	882 x 588	882 x 588
4	1100 x 520	882 x 588	882 x 588
4	978 x 478	1111 x 627	1111 x 627
8	876 x 549	1323 x 588	1353 x 529
8	922 x 480	1309 x 649	1309 x 649
8	1026 x 556	1207 x 755	1207 x 617
8	1011 x 550	1107 x 707	1107 x 636
12	882 x 422	1333 x 667	1333 x 593
12	1090 x 500	1333 x 733	1333 x 667
12	1177 x 549	1158 x 632	1158 x 626
12	1000 x 467	1176 x 706	1176 x 588
18	920 x 472	714 x 1379	647 x 1429
18	1091 x 511	714 x 1349	665 x 1429
18	1290 x 605	733 x 1333	600 x 1333
18	1240 x 599	660 x 1277	660 x 1277
24	891 x 490	1875 x 750	1875 x 625
24	981 x 571	1647 x 882	1647 x 588
24	1026 x 532	1786 x 786	1786 x 714
24	1100 x 541	1680 x 760	1660 x 640